Alyona Lovska

DYNAMICS AND STRENGTH OF RAIL CARS IN FERRY TRANSPORTATION

Monograph

IZDEVNIECĪBA
BALTIJA
PUBLISHING
2023

UDK 629.463.004.4:656.211.7
Lo886

Reviewers:
G. L. Vatulia – Doctor of Technical Sciences, Professor, Deputy Director for Research, Educational and Scientific Institute of Construction and Civil Engineering, O.M. Beketov National University of Urban Economy in Kharkiv;
S. V. Myamlin – Doctor of Technical Sciences, Professor, Laureate of the State Prize of Ukraine in Science and Technology, Honored Worker of Science and Technology of Ukraine, Deputy Director of Ukrtransinvest

Recommended for publication of the Academic Council
of Ukrainian State University of Railway Transport
(Minutes No. 4 dated the 21.06.2023)

Alyona Lovska. Dynamics and strength of rail cars in ferry transportation : Monograph. Riga, Latvia : Baltija Publishing, 2023. 288 p.

ISBN 978-9934-26-346-0

DOI: 10.30525/978-9934-26-346-0

The book provides results and peculiarities of the research into dynamics and strength of basic types of freight and passenger cars transported by train ferries. The authors focus on the theoretical concepts, methodological basics and practical solutions to determination of accelerations and forces exerting in the oscillation systems (train ferry – rail car – container).

The book will be of interest for specialists in science and engineering who are concerned with development and research into the freight and passenger railcar design. It will also be of considerable use for research scientists, designers, developers and doctoral students.

The results presented will be of considerable use for anyone concerned with development and operation of containers and train ferries.

The book can be used as an educational aid for graduate and post-graduate students of the related specialties.

Pictures – 318, Tables – 43, References – 165.

UDC 629.463.004.4:656.211.7

© Alyona Lovska, 2023
ISBN 978-9934-26-346-0
© Izdevniecība “Baltija Publishing”, 2023

ABSTRACT

A rapid development of economic relations between European countries has required reforms in the transport industry. And one of the most promising ways is introduction of combined transport systems; therefore, maritime countries are developing train ferry transport. A particular feature of such transit is a possibility to transport rail cars by sea on specially equipped vessels – train ferries.

Stability of rail cars on the deck is ensured by a complex of reusable devices. Among them are chain binders with turnbuckles (eight per car), support jacks (four per car), and brake shoe holders under the rolling surface of wheels. The cars are hold from longitudinal displacements by joining the end cars in batches with bumping posts.

It should also be mentioned that the car body structure does not have any special fasteners for fixation on the train ferries decks. Therefore, the car bodies transported by sea are fastened with any available structural elements.

Besides, a typical fixation patterns for a car on the deck does not relieve dynamic loads on the car body through the fasteners. The chain binder transfers loading to the body with consideration of the initial tension force (50–60 kN), as well as the force exerted by train ferry oscillations.

This causes damage of the carrying structure of the rail cars transported by sea, and requires off-schedule repairs.

Analysis of the literature sources devoted to the research into dynamics and strength of rail cars has made it possible to conclude that the determination of dynamic loads and strength of cars transported by train ferries has not been intently studied. Some peculiarities about determination of the forces on the car body in transportation by train ferries were presented in works by Central Research Institute of the Ministry of Railways (Soviet Union) with determination

of the accelerations occuring at the location zones of cars on the deck with differentiation of the law of sea wave motion. The calculation was made for the train ferry Soviet Azerbaijan operated on the route between Baku (Azerbaijan) and Makhachkala (Dagestan) and between Baku (Azerbaijan) and Türkmenbaşy (Turkmenistan) [86].

The intensive development of train ferry transportation, construction of new ferries and a variety of hydro meteorological characteristics of the cruising areas urgently require additional engineering research. Besides, the issue of strength determination of the rail cars in ferry transportation has not been studied yet. Therefore, there is a need to obtain enough data in the field.

The authors present the results and details of their research into dynamics and strength of the main types of freight and passenger cars transported by train ferries. Particularly, the book provides the theoretical concepts, methodological basics and practical solutions to determination of accelerations and loading in complex oscillation systems (train ferry – rail car – (tank) container).

The following tasks were set during the research:

– to analyze the present state of the train ferry transportation, such as historical aspects of operation, research into statistical data on damage of train cars, features of freight turnover and prospects to develop this transport for Ukraine;

– to study existing systems and fasteners for train cars on ferries;

– to refine the values of accelerations occurring in the train cars during their transportation by ferries across oceans and seas;

– to determine stresses in structural components of the train cars transported by ferries with application of existing fixation patterns and lashing devices;

– to develop the structural component for fixation of cars on the ferry decks;

– to design the concept of a device for fixation of rail cars on the ferry decks. One of them is the device with a viscous link for fixation of rail cars on the ferry decks, and another is the device for fixation of passenger car bodies.

The subject matter of the research is the loading of the carrying structure of rail cars transported by train ferries.

The scope of the research is the carrying structure of a rail car.

The book is of interest for scientists and engineers concerned with development and research into the design of freight and passenger rail cars. It can also be of considerable use for research scientists, designers, developers and doctoral students.

The findings presented in the book will be of use for anyone concerned with design and operation of containers and train ferries.

The book can be used as an educational aid for graduate and post-graduate students of the related specialties.

Key words: transport mechanics; railway transport; dynamics and strength of rail cars; train ferries.

CONTENTS

INTRODUCTION

Integration of Ukraine to the international transport corridor system stipulates Ukraine's participation in the transport system of European countries. An increased volume of freight transported across the territory of Ukraine, being a link between European and Asian countries, has resulted in growing popularity of combined transportation systems. One of the most promising systems is the rail/ferry transport.

The statistical data on transportation of rail cars by ferries made it possible to conclude that each year about 10 % of cars out of the total railcar turnover in the international rail/sea transportation of Ukraine by the route Chornomorsk (Ukraine) – Varna (Bulgaria), one of the most promising, require uncoupling repairs. The greatest percentage of damage is in open car and boxcars. During last years the amount of damage in open cars in the international rail/sea transportation accounts for about 30 % out of the total damaged cars, or over 10 % out of the total number of the open cars operated on the route.

The main defects of the cars are deformations and tear-offs in the structural elements used for fastening on the ferry deck; they are caused, first of all, by structural inadaptability of cars for tight interaction with fasteners.

In order to substantiate the improved carrying structure of a car for transportation by train ferries the authors made the strength calculation for basic types of rail cars. The calculation included actual fixation patterns used for rail cars during the full-scale research on the decks of Ukrainian train ferries. The results of the calculation proved that high stresses occur in the location areas of rail cars on the deck; the numerical values of these stressed exceed the admissible ones.

Therefore, the authors propose some measures to improve the carrying structure of a rail car to ensure the required strength for

ferry transportation. The results of the strength calculation confirmed the efficiency of the solutions proposed.

Besides, the study deals with higher efficiency of container transportation included in combined trains carried by ferries. The research involved the admissible tilt angles for the train ferry that can ensure the stability of containers relative to the flat cars.

The study focuses on the peculiarities of experimental determination of the strength characteristics of the carrying structure of an open car as one of the most popular types of cars for international rail/sea transportation. The results of the research proved the theoretical results obtained.

The research will encourage the specialists to ensure the strength of the carrying structure of a rail car transported by a ferry and increase the operation efficiency of rail/ferry routes.

PART 1
FEATURES OF TRAIN FERRY TRANSPORTATION

1.1 Historical aspects of evolution and operation of train ferry transport

The world's first train ferry service was launched in 1851; it operated across the Firth of Forth from Granton and Burntisland [1].

In Germany the first train ferry service was put into operation in 1882; it was a 25-km route which linked Stralsund and Altefähr.

In 1905 Italy started a train ferry service across the Strait of Messina. It was an 8-km route with ten ferries in operation and the distance between the ports Villa San Giovanni and Messina was covered in 40 min [29].

Later on, in 1961 a train ferry across the Tyrrhenian Sea was launched; it connected mainland Europe and the Island of Sardinia [1].

In 1983 Italy built the double-deck ferry *Garibaldi* for this route. Apart from rail cars it transports wheeled vehicles. It also has some passenger cabins. Rail cars and wheeled vehicles are rolled on through the stern doors equipped with a ramp. The ferry has two elevators which can simultaneously lift 40-ton rail cars to the upper or to the hold decks in 30 sec. The rail cars are distributed across the hold width with a special platform moving along the transverse axis of a ferry.

The ferry is also equipped with a crane with capacity of 25 tons for elevating 24 containers to the upper deck.

The displacement length of the ferry is 137.8 m, the breadth – 18.9 m, the draft – 5.7 m, and capacity – 80 rail cars. The ferry speed is 20.3 knots [35].

In 1909 a train ferry service started between Sassnitz (Germany) and Trelleborg (Sweden). The route was serviced by the ferries *Rügen*, *Rostock*, *Trelleborg* and others [1].

The ferry *Rügen* was built in 1972 and it could place 37 freight cars. The automobile deck accommodated 12 freight cars or 73 passenger cars. The ferry speed was 20.3 knots [1, 29]. Cars were rolled on/off horizontally through the stern ramp. The ferry was equipped with stabilization devices against sea disturbance [13].

The ferry *Rostock*, built in 1977, could transport 49 freight cars located on its five tracks. The motorcar deck capacity was 21 vehicles. The ferry speed was 20.5 knots [1, 29].

The ferry *Trelleborg* was put into operation in 1982 and it had five tracks for rail cars. The full ferry length was 170.1 m and the breadth – 22.5 m. Its speed was 19 knots. The total length of the tracks accounted for about 700 m. The ferry could accommodate 55 rail cars. It could also transport 800 passengers. The train ferry Gotland (Sweden) also had five rail tracks [29].

In 1959 the ferry *Saßnits* was built. Its length was 137.5 m and the beam – 18.8 m. The four tracks on the 380-m deck could accommodate 30 freight cars. The ferry speed was 18 knots [29].

The ferry *Sea Wind* (former name *Saga Wind*, built in 1972) was re-equipped by Blohm & Voss, German shipbuilding and engineering company, and put into operation from Stockholm (Sweden) to Turku (Finland). The ferry transports rail cars located on the main deck, trucks and automobiles on the upper and boat decks; it also carries passengers. The ferry is equipped with facilities to roll on wheeled vehicles. They include a stern hydraulic ramp and an inter-deck ramp on the left side to link the upper and boat decks, and a stem gangway on the right side for light vehicles. The ferry length is 154 m, the breadth – 21 m, and the draft – 5 m [34].

In 1920 the shipbuilding company Bell began to build special ships for sea transportation of bulky cargo including rail cars.

The ship *Bell Vu* transported 22 cars for an electrified railway and two steel barges from England to Buenos Aires. Each car weighed 37 tons. In order to save space, the eight cars were located above the barges on the special wooden platforms at a height of 12 feet

and thoroughly adjusted for the barges well in advance before they were loaded on the ship.

One of the ships *Beldjan* transported simultaneously 24 rail cars for the underground railway, 20 locomotives, 2 small river tow-boats and engine barges with length of up to 27 m and mass of 100 tons each. The rail cars were located at two levels (behind the mid-ship superstructure). The height of this construction was the same as the height of the bridge.

The upper raw of rail cars was mounted on the specially built metal frame.

Besides, some types of heavy freight cargo were accommodated in the hold; it compensated an elevated center of gravity [62].

In 1923 in order to transfer the steam ships of the series $Э^{ш}$ and $Э^{ш2}$ from Sweden and Germany to Russia across the Baltic Sea, a ferry service was launched [55].

The ferry service between Great Britain and mainland Europe has been in operation since 1924. And the first line across the Channel was from Harwich (Great Britain) to Zeebrugge (Belgium). The ferry service with France has been in operation since 1936. In 1967 the second ferry service from Harwich (Great Britain) and Dunkirk (France) was launched. However, it was closed due to the construction of the English Channel Tunnel [1].

The ferry service from Hirtshals (Denmark) to Kristiansand (Norway) was launched in 1958 with the ferry *Skagen* of the length 80.9 m, the breadth – 13.8 m and the speed – 18 knots. The journey time was 4 hours [3].

The ferry could carry seven rail cars, 40 automobiles, and 600 passengers on its one 69-m track.

Later on, Germany built the train-motor-passenger-electric ferry *Teodor Heus* intended for service in ice conditions.

The ferry had three tracks for 30 rail cars. The middle deck could accommodate 100 automobiles. The passenger capacity of the ferry was 600 passengers with their luggage. The maximum length of the ferry was 135.9 m, the breadth – 17.7 m, the hull height – 7.35 m,

the draft – 4.79 m at the water displacement 6 438 tons, the traffic speed – 16.6 knots [3].

The ferry service between Travemünde (Germany) and Hanko (Finland) was put into operation in 1975. It was a three-deck ferry intended for transportation of 65 rail cars. In 1979 the ferry length was extended, thus, its capacity was increased by 30 %. And in 1984 the route obtained one more ferry [1].

Ferry transportation was also introduced in America. The loaded freight cars are transported by the tugboats *Dalzell* and *Transfer* [3]. The tugboats transport rail cars from station to station along the river Hudson, and also to New Haven. Two ferries loaded with 20 rail cars each are simultaneously towed.

An 18-km route in the Strait of Georgia is serviced by two ferries. They transport both passengers and freight. The journey time is 55 min. One ferry is in operation between Matane and Baie-Comeau (45 km). It transports freight cars. The journey time is 2 hours [29].

In 1964 the longest ferry service in the Pacific Ocean region was introduced between Canada and Alaska (over 2000 km). Double-deck ferries are in service on the route.

The ports Goose Bay and Lewisport in the Atlantic Ocean are linked by a 615-km ferry service. The journey time is 30 hours. The ports Sydney and Port aux Basque are also linked by ferry service. The route length is 164 km. The journey time is 6 hours. The length of the ferry service from Cape Tormentine and Borden is 14 km. The ferry transports passengers and freight. The journey time is 45 min. [29].

Japan operates ferry service between the islands Honshu, Hokkaido, Shikoku and Kyushu. The ferry route between Hakodate (Hokkaido) and Aomori (Honshu) is 103.7 km, between Tamano (Honshu) and Takomatsu (Shikoku) is 17 km, between Niigata and Oarai is 34.8 km, and between Simonesi (Honshu) and Moji (Kyushu) is 3.4 km [3].

The route from Somory to Hakodate was serviced by a passenger ferry which could accommodate 1 200 passengers and 19 rail cars, and a freight / passenger ferry was intended for 300 passengers and 45 rail cars.

In 1962 the rolling stock from Baku to the northern coast of the Caspian Sea was transported by the seaborne barge *Ishimbay* which was re-equipped for this purpose. It was a dry-cargo one-deck non-self propelled double-bottom barge and it could transport containers, timber, cotton, and grain in the cabins and on the deck [15].

It had 16 rail tracks on the specially designed platforms for rolling stock on the main desk above the hatch covers across the width and perpendicular to the center line plane.

The platform length was chosen according to the largest dimension of a rolling stock unit with consideration of rolling on/off on the left side.

The vehicles were rolled on the stem and moved to the stern. The rail tracks of the ferry were joined to the port tracks with pads and screws.

The first vehicle was rolled on the stem track with a diesel locomotive and a buffer wagon.

There were two variants to fasten a rolling stock unit on the barge deck. The first one supposed chain binders (a 17-mm chain gauge) with a special spring turnbuckle to damp dynamic jerks from sea disturbance. The binders were fixed with brackets to special eye plates welded to the frames of rolling stock units, decks and hatch covers on the barge.

The second variant provided for application of rigid buckles made of fabricated wagon buckles intended for 30 tons. Wooden wedges were used as supports hammered between the wheel bogie and the frame.

Due to lack of time the second variant was chosen as less labour-intensive.

The deck of the barge *Ishimbay* turned out to be reliable and efficient in transportation.

Shipment across the Caspian Sea was conducted by the ferry *Soviet Azerbaijan* manufactured by the shipyard Krasnoye Sormovo (Figure 1.1).

The ports Baku and Krasnovodsk (160 miles) were connected by the ferries *Soviet Azerbaijan* and *Hamid Sultanov* built from 1962 to 1968 [17]. The journey time was 12 hours with 3-hour stops in the destination ports [22].

Figure 1.1 – Train ferry *Soviet Azerbaijan*

All rail cars were located on one deck. The ferry length was 133.8 m, the beam – 18.32 m, the maximum draft – 4.4 m. The ferry could accommodate about 30 rail cars [4].

Later on the train ferries *Soviet Dagestan* (Figures 1.2, 1.3 [23]), *Soviet Tajikistan* (Figure 1.4) and *Soviet Kalmykia* were built in Yugoslavia for servicing the route between Baku and Krasnovodsk. The ferries had a closed rail car deck along the whole length with tracks for cars and the hold for light vehicles. The rolling-on and rolling-off were conducted across the stem water-proof doors. The bottom deck was equipped with a ramp for rolling-on automobiles to the hold.

The ferry length was 154.4 m, the beam – 18.3 m, the maximum draft – 4.5 m, and the speed – 17 knots. The ferry could accommodate about 30 rail cars [5].

The cars were fastened on the decks with chain binders, which passed through deck eye plates and car frames, and a tension mechanical device Speed Lash (with a link length of about 2.5 m, the operating tension – 80 kN). Similar devices are used for automobiles and trailers. The automobiles are fastened with soft lashing ropes and deck eye plates with the braking strength 12 kN. The stem part of the lower deck is equipped with four end buffers with the SA-3 automatic

coupler. The cars are maintained on the brake by the compressed air system connected to them [21, 166].

The sea disturbance is reduced with the active disturbance control system equipped with the side steering wheels. The system decreases the disturbance amplitude from 19° to 4° at the speed 17 knots and sea disturbance of 7 points [23].

Such ferries operated on the ferry route from Baku to Aktau were introduced in 1985 [18].

Figure 1.2 – Train ferry *Soviet Dagestan*

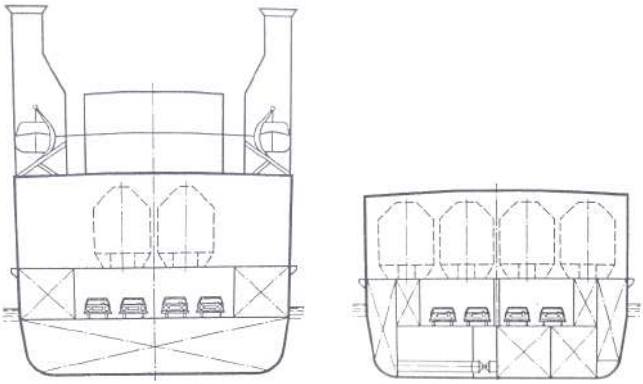

Figure 1.3 – Ferry section

Figure 1.4 – Train ferry *Soviet Tajikistan*

The ferries *Soviet Kazakhstan* and *Soviet Turkmenistan* were built to link Krasnovodsk and Bekdash [19]. The journey time was 9 hours.

With time the number of ferries operated across the Caspian Sea totaled thirteen [20]. Among them were *Soviet Nakhchivan*, *Soviet Kirgizia*, *Soviet Uzbekistan* and others.

Besides, the Caspian Sea was serviced by the ferry *Mercuri-2* (Figure 1.5). But in 2002, due to loss of stability by the tank cars on its deck, it sank. It carried 16 tank cars with petroleum products, one car with consumer goods, 8 passengers and 42 crew members. The tank cars detached from the fasteners due to the wave impact and slipped to the slope side; thus, it capsized [6].

In 2008 the train ferry *Akademik Zarifa Aliyeva* was put into operation (Figure 1.6). It was built at the shipbuilding company Uljanik (Croatia). The ferry length is 154.5 m, the breadth – 17.5 m, the capacity – 52 rail cars [7].

Figure 1.5 – Train ferry *Mercuri-2*

Figure 1.6 – Train ferry *Akademik Zarifa Aliyeva*

The innovative technology of that time was used to allocate rail cars on the ferry which was equipped with special devices and elevators [8].

Uljanik shipyard also built the train ferries *Makhachkala* for operation across the Caspian Sea from Makhachkala to Aktau and Turkmenbashi (Figure 1.7). The ferry length is 154.5 m, the breadth – 18.3 m, the draft – 4.67 m, and the capacity – 52 rail cars. The ferry speed is 14 knots [9]. It can transport up to 52 rail cars [26, 166].

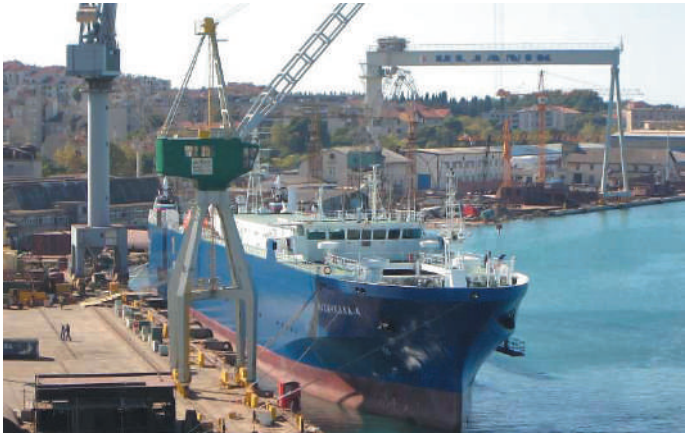

Figure 1.7 – Train ferry *Makhachkala*

The ferry service Vanino – Kholmsk connects mainland Russia and the island Sakhalin. It was launched in 1973. The rail cars were carried by the ferry icebreaker *Sakhalin* (Figure 1.8). The ferry length is 127 m, the breadth – 19.8 m, the draft – 6.2 m, and the speed – 18 knots. The ferry has a rail car (main) deck with four rail tracks for rolling stock. The cars were located by batch on two middle and two side tracks.

Figure 1.8 – Train ferry *Sakhalin*

Loading and unloading were conducted across the ramp rested on the stern step of the deck. The rail cars were loaded with locomotives simultaneously on two tracks, and automobiles were rolled on with their own power [11, 12, 166]. At present there exist a great number of such ferries.

The ports Borden (Prince Edward Island) and Cape Tomentine (New Brunswick) in Canada were connected with the ice breaking train ferry. The ferry length was 106 m, the breadth – 18.6 m, the draft – 5.8, the speed – 16.5 knots. The ferry could accommodate 19 freight cars, 60 automobiles and 900 passengers [10].

The diesel ferry Malmohus connected Copenhagen and Malmo. The ferry length was 94.1 m, the breadth – 16 m, the draft – 4.1 m, and the speed – 17 knots. It was intended for transportation of up to 3100 passengers and freight cars [10].

Poland also began to develop the ferry transportation. After WWII the train ferry service was launched between Świnoujście and Sweden with only one ferry. In 1953 the ferry service suspended for some period. And in the mid 1960s the ferry service was resumed with passenger-automobile ferries.

The ferry route from Świnoujście to Ystad is serviced by the ferries *Nikolaus Copernicus* and *Johannes Hevelius* manufactured in Norway in 1973 and 1975 respectively. The train ferries transport rail cars and trucks. They make several runs per day by necessity [25].

In October 1986 the ferry service between Klaipeda (USSR) and Mukran (GDR) was introduced. The length 540 km was serviced by the train ferries *Klaipeda* and *Mukran* (Figure 1.9). The ferry length was 190 m and the breadth – 28 m. The ferry speed was 16 knots [27, 28, 30].

They were double-deckers and could transport 103 rail cars. For the first time the revolutionary loading/unloading technology of that period was used for the route. With its two decks the ferry joined to a 45-m suspension double-deck ramp (Figure 1.10).

The ramp is the front part of a 175-m platform. Each level has five rail tracks similar to those on the decks. Two decks cannot be loaded simultaneously due to possible loss of stability.

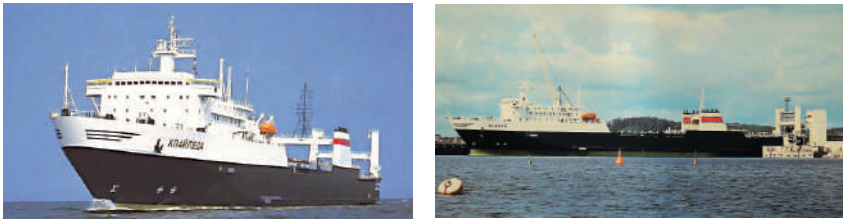

a) b)

Figure 1.9 – Train ferries for the route Klaipeda – Mukran:
a) Klaipeda; b) Mukran

Figure 1.10 – Double-deck ramp

The speed of the locomotive during loading/unloading operations is 1 m/sec.

An automated anti-tilting system is used for maintaining stability within a range of 3° during freight operations [31]. At present these ferries are not in operation.

In 1989 the new Ro-Ro/Rail/Passenger ferry *Kaunas* was put into operation (Figure 1.11). The vessel is supervised by the Lloyd's shipping

registry. The full length of the ferry is over 190 m and the breadth – 28 m. Two freight decks can simultaneously accommodate 49 universal rail cars and 50 overweight vehicles TIR [32].

Figure 1.11 – Train ferry *Kaunas*

In 2006 the ferry service between Ust-Luga and Baltiysk was put into operation. The route is serviced by the train ferry *Baltiysk* (Figure 1.12). The ferry length is 187.36 m and the breadth – 22 m. The total length of the rail tracks is 1943 m. The ferry capacity is 135 rail cars (the length over pulling faces of couplers is 12020 m) or 92 rail cars (the length over pulling faces of couplers is 16 970 m). Besides, the ferry can carry 76 automobiles on the open upper deck. The ferry speed is 18.5 knots.

The ferry has three cargo decks with five rail tracks each. The loading of the middle deck is made across the stern doors. Rail cars and wheeled vehicles are lifted up and put on the upper and bottom decks with a double-deck elevator with freight capacity of 94 tons. The upper and lower elevator's platforms have freight areas of the length 28 m equipped with clamping grips for car wheels and holes for fixing lashing ropes.

The cars are transferred on the decks with rotating hands installed in the stem part of the upper and bottom decks. The ferry is also equipped with seven shipboard trailers.

Figure 1.12 – Train ferry *Baltiysk*

The rolling-on/off of cargo in the ports without dock ramps is made across special removable ramps mounted on the stern area through special holes for lashing ropes of hydraulic winches which are mounted on the middle deck to the left and to the right. A set of removable ramps can be stored in the ports or on the ferries [33, 61].

Later on the ferries *Ambal* (Figure 1.13) and *Petersburg* (Figure 1.14) were put into operation on the route.

Figure 1.13 – Train ferry *Ambal*

Figure 1.14 – Train ferry *Petersburg*

The ferry services from Romania to Turkey and from Romania to Georgia, which have shortened the journey distance by 340 km and 1075 km respectively, operate the three-deck ferries *Mangalia* and *Eforie* belonging to the state-owned freight railway business of Romania CFR Marfă. These ferries can carry 85–100 rail cars located on the deck rail tracks with a distance between the running edges of rail heads of 1435 mm, and of the total length of 1680 m [58].

The ferries have a lift for transferring rail cars from the middle deck to the upper or bottom decks and a deck crane. Their five rail tracks are used for joining to the on-land rail track infrastructure. To transfer rail cars from one track to another the ferry decks are equipped with one movable platform. Besides, the ferries have a switch for shunting operations.

Across the Black Sea the ferry service was launched in the middle of the 20th century. In 1958 the European and Asian shores of Turkey across the Bosporus Strait were connected between the ports Sirkeli and Haydar [36].

In March 1955 the ferry service connected the Ukrainian and the Russian Republics of the former Soviet Union [37–40, 166].

Two train ferry complexes between the stations of Crimea and Caucasus were built to shorten a journey time for mass freight transportation between the republics. This rail/ferry service shortened the distance up to 1 000 km, and relieved the Rostov Railway junction [166].

Due to a short distance of about 4 kilometers, the ferry service across the Taman Bay is considered to be rather safe for rolling stock, despite the harsh climatic conditions in that region.

As far as Kerch has always been the cross-road of great merchant routes from Europe to Asia, from the Varangians to the Greeks and that of the Great Silk road, the train ferry service Crimea-Caucasus is an important link in the transport corridor connecting Ukraine with Russia, Kazakhstan, countries of Caucasus and Central Asia by sea rail ferry routes in the Caspian Sea: from Makhachkala to Aktau and from Makhachkala to Turkmenbashi [39]. At first the route was serviced by four train diesel electric ferries: *Yuzhny* (Figure 1.15), *Vostochny* (Chulym and Nadym respectively [41]), *Severny* and *Zapoliarny*. Such ferries were intended for transportation of 16 freight cars.

Figure 1.15 – Diesel electric ferry *Yuzhny*

After the collapse of the Soviet Union in 1986, the volume of transportation on the route considerably decreased and later on it was closed. And only in October 2004, due to combined efforts of Ukraine and Russia the ferry service was resumed [42, 43]. And now the ferry service operates the one-deck ferries *Petrovsk* and *Annenkov* (Figure 1.16) with combined capacity of 25 rail cars.

a) b)

Figure 1.16 – Train ferries on the route Crimea – Caucasus:
a) Annenkov; b) Petrovsk

The ferry decks have four rail tracks. The ferry length is 110.5 m, the breadth – 16.0 m and the draft – 3.2 m. The ferry speed is 10 knots [49].

Due to a steady increase in the freight turnover during the recent years, there is a need to raise the freight traffic capacity of the ferry routes. In 2007 the one-deck ferries *SMAT* and *FERUZ* (Figure 1.17) with capacity of 50 tank cars 1-T with five tracks on the deck were built for the ferry routes Caucasus – Samsun (Russia – Turkey) and Caucasus – Poti (Russia – Georgia) [44, 48].

The special feature of them is narrow and broad gauge rail tracks on the deck.

The ferry length is 150.32 m, the breadth – 22 m and the draft – 3.8 m. The ferry speed is 10 knots [48].

a) b)

Figure 1.17 – Train ferry *SMAT*:
a) loaded with open cars; b) loaded with traction rolling stock

On the analysis of positive results on the existing rail/ferry routes and due to the strategic targets, on 23rd April 1975 the Soviet Union and Bulgaria signed a Treaty on organization of ferry service between the ports Illichovsk (now Chornomorsk) and Varna in 1978 [45, 59, 60].

The Chornomorsk port infrastructure was built by the construction company Chernomorhydrostroy and the rail infrastructure facilities were build by the construction company Odessatransstroy. One of the specific features of the port is its advantageous position on the cross-road of main transport routes between Europe and Asia, North and South, Central and Eastern Europe, industrial regions of Russia and Ukraine, and communications across the Mediterranean Sea to the Atlantic and Indian Oceans.

The following international transport corridors run across the port Chornonorsk:

– TRASEKA (the transport system Europe – Caucasus – Asia);
– Crete Corridor IX;
– Corridor Baltic – Black Sea.

The ferry route was serviced by four train ferries: *Geroi Shipki* and *Geroi Plevny* (Soviet Union) and *Geroi Odessy* and *Geroi Sevastopolia* (Bulgaria), each could accommodate up to 108 cars 1–T, 0–T and

01–T (Figure 1.18). These ferries had 13 rail tracks (five tracks on the upper and main decks each and three tracks on the hold deck) [50].

a) b)

Figure 1.18 – Rail cars on upper decks of ferries:
a) Geroi Shipki; b) Geroi Odessy

The ferry length is 184.5 m, the breadth – 26.49 m and the draft – 6.5 m. The ferry speed is 19.5 knots [51].

The ferry routes Chornomorsk – Poti (opened in 1994) and Chornomorsk – Batumi (opened in 1996) are serviced by the Ro-Ro/passenger ferry *Greifswald* (Figure 1.19) supervised by the Lloyd's shipping registry.

The ferry was built by VEB Mathias Thesen Werft in Wismar (Germany) in 1988 and they serviced the route Rostok (Germany) – Klaipeda (Lithuania) [46].

The ferry length is 190.8 m, the breadth – 26 m and the draft – 6 m. The ferry speed is 16 knots [52].

In 1996 the ferry was re-equipped and a passenger complex was added. The ferry has two cargo decks which can accommodate 103 rail cars, but due to structural features of the loading facilities in the ports of Chornomorsk and Poti/Batumi, only 50 cars can be put on the main deck. Besides, it can accommodate 50 heavyweight trailers on the deck, thus offering possibilities for bimodal, contrailer and other combined transport systems [47].

a) b)

Figure 1.19 – Train ferry *Greifswald*:
a) side view; b) main deck

Since 2001 the ferry route Chornomorsk (Ukraine) – Derince (Turkey) has been in operation with the ferries *Geroi Shipki* and *Geroi Plevny*.

Since 2013 the rail/ferry route between Ukraine and Georgia has been serviced by the ferry *Vilnius Seaways* (Figure 1.20), early operated across the Baltic Sea. Two freight decks can simultaneously accommodate 50 universal rail cars and 50 heavyweight trucks. The ferry has cabins for 110 and seats for 24 passengers.

Figure 1.20 – Train ferry *Vilnius Seaways*

The ferry has the certificate of the Guinness World Records on being the biggest world passenger/Ro-Ro/railway ferry [53].

In 2009 the group of companies *AnRussTrans* built the train ferries Avangard for 45 rail cars (Figure 1.21) and *Slavianin* for 50 rail cars (Figure 1.22) by the project of the Marine Engineering Bureau.

Figure 1.21 – Train ferry *Avangard*

The train ferry *Avangard* is intended for operation on the route Caucuses (Russia) – Varna (Bulgaria) – Samsun (Turkey) – Poti (Georgia). The ferry length is 133.67 m, the breadth – 22 m and the draft – 4.8 m. The ferry speed is 12 knots.

Figure 1.22 – Train ferry *Slavyanin*

The train ferry *Slavyanin* has the length 149.95, the breadth – 22 m and the draft – 4.5 m. The ferry speed is 12 knots.

In 2010 the train ferry *Ulfat* was built (Figure 1.23). The ferry can transport 45 rail cars and it is intended for the route Caucuses – Varna – Samsun – Poti. The ferry length is 133.82 m, the breadth – 22 m and the draft – 5 m. The ferry speed is 12 knots [36].

Train ferries transporting passenger cars can offer seamless transportation for passengers accommodated in the cabins. And today this type of transportation is very popular. For example, the train ferries operating across the Baltic Sea can offer this service [63–65].

Figure 1.23 – Train ferry *Ulfat*

In the early days, passenger cars were loaded from the port tracks on the deck with hoisting machines (Figure 1.24). Today they roll on/off across the ramp which considerably shortens the loading/unloading operations.

It should be mentioned that safe transportation of rail cars by ferries is ensured by strong fixation of rail cars on the deck, as far as the forces during sea transportation considerably differ from those during rail transportation. Therefore, it is crucially important to research the dynamic loading and strength of rail cars transported by ferries, and the technical adaptation of the rail car structure to interaction with fasteners on the deck.

Figure 1.24 – Loading of passenger cars on the train ferry

Besides, train ferries have become popular for river transportation. For example, in 1892 a ferry service across the river Desna was launched [2]. It was a crossover route with traffic capacity of 88 car pairs; the ferry capacity was six cars. The loading/unloading operations were made manually. A track cable was stretched across the 100-m river through blocks mounted on the ferry. The ferry was transferred with four hand winches.

From 1896 to 1935 there was a ferry service across the Volga River near Saratov of the Ryazan-Ural Railway [2] with the ferry *Saratovskaya Pereprava* (Figure 1.25 [54]). The ferry was built by the British manufacturing company Sir W.G. Armstrong Mitchel in 1896 [14]. The ferry had a hydraulic elevating mechanism to convey cars from the ramp to the deck. During navigation seasons the ferry transported 160 cars per day rolled on its deck. In winter seasons it transported 120 cars at shuttle service (28 cars per run [2].

Later on the ferry *Pereprava Vtoraya* (Second) built in 1909 was put into service on the route (Figure 1.26 [54]). It was built at the Nizhny Novgorod Machine Factory. During the best shipping periods the route traffic capacity was 200 rail cars. In 1926 the ferry *Stalin* was put into operation on the route.

Figure 1.25 – Train ferry *Saratovskaya Pereprava*

Figure 1.26 – Train ferry *Pereprava Vtoraya (Second)*

The route was also serviced by the ferry *Saratovskiy Ledokol* to break ice and transport passengers and freight [54].

From 1903 to 1915 between the harbors Baikal and Tankhoy there was a ferry service across Lake *Baikal* on the Trans-Siberian route. The icebreaker ferry Baikal transported 27 rail cars. Its average speed was 18 km/h in summers, and less than 11 km/h in winters. The ferry design was similar to that of the American icebreaker operating on Lake Michigan.

It was built in 1896 and had the biggest water displacement among the existing then icebreakers [10].

The year 1918 saw the last voyage of the icebreaker *Baikal* (Figure 1.27). By its decision the Irkutsk Council established the Red Baikal Fleet to fight against the counter-revolutionary movement. The icebreaker *Baikal* was damaged by field artillery fire, burnt and sank during a battle [24].

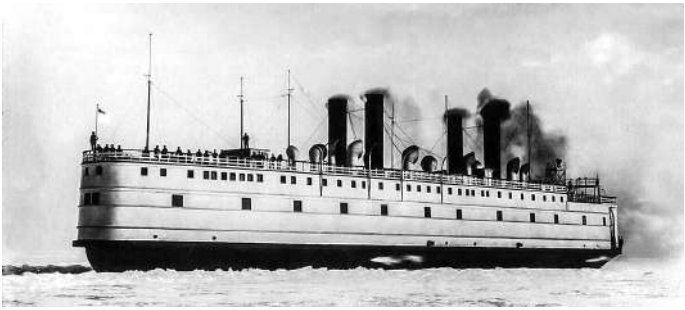

Figure 1.27 – Ice breaking train ferry *Baikal*

In the period 1926–1936 there was a ferry service from Gorky (now Nizhny Novgorod) to Kotelnich. The ferry had a reinforced concrete body intended for breaking ice [14].

Later, on the section Komsomolsk – Pivan across the Amur River a 7-km ferry service was put into operation with the train ferries *Volga* (Figure 1.28), *Don* (built in 1951), and *Amur* and *Komsomolsk* (both built in 1951). They were river ferries with an open deck and a rail car hoist in the stern section. The cars were located in four lines and lifted by a device with capacity of 80 tons and hoist height of up to 5 m. The wagons were transferred on the deck with trailer bogies, ropes and winch generators installed at the end of each track [14].

In 1939 across the Danube River the cities Ruse and Giurgiu were connected by the ferry service carried automobiles and rail cars. This route is now in operation thought it is not used [56, 57].

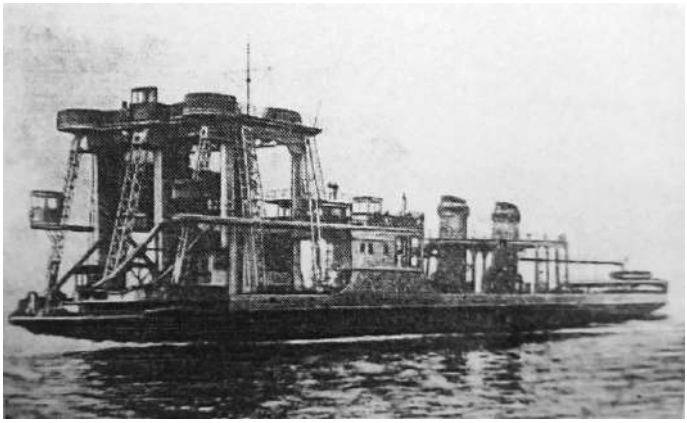

Figure 1.28 – Train ferry *Volga*

In 1941 during World War II there was built a ferry route across the River Volga. A twin-hulled ferry transported rail cars. The cars were rolled on simultaneously from two port tracks by gradually transferring the ferry along the port side with two 5-ton wrenches installed on the dock at a distance of 100 m. The ferry had 18 tracks. Each track could accommodate three double-axle or two four-axle rail cars, or a steam locomotive with a tender. The cars were rolled on through two suspension linkspans installed on the pier [16].

In 1909 Norway had a train ferry across Lake Tinshe between Tinnuset and Mel. Its length was 28 km. The journey time was 1 hour 20 minutes.

Since 1964 Turkey has operated a train ferry between the ports Tatvan and Van. Its length is 90 km with two train ferries in service.

A train ferry is in service between the ports Thunder Bay (Canada) and Superior (US) across Lake Superior. The route length is 285 km. The journey time is 14 hours [29].

There are two train ferry routes across Lake Michigan (US): Ludington – Kewaunee (105 km) and Ludington – Manitowoc (104 km). Each line has one ferry; the journey time of each is 4 hours.

Since 1971 South American countries Peru and Bolivia have been connected with a ferry service across Lake Titicaca [29].

Since 1983 a ferry service has been in operation across Lake Victoria between Uganda and Tanzania in Africa. Its length is 400 km. In 1985 the line was supplied with two ferries. Their length is 92.13 m and the breadth – 16.5 m each. Each carries 22 freight cars and 5 containers. They can also carry passengers and cargo.

Apart from Uganda, Tanzania and Kenya operate ferry routes across Lake Victoria [29].

The historic overview conducted makes it possible to conclude that, economically, transportation of rail cars by sea is an important aspect. It should be noted that most of vessel types considered in this section are not in operation anymore; however a positive experience gained in terms of their operation and maintenance can be used while introducing new train ferry routes with ferries servicing them.

1.2 Mechanical appliances of train ferries and fasteners for rail cars

The issue of freight transportation by sea, including rail cars, is a very urgent and important problem both economically and ecologically.

The main causes of shipwrecks are technical failures, human errors, delivery problems, and those connected to the freight transported. Besides, natural factors, such as wind, waves, and sea currents greatly influence the safety of movement of sea vessels. All these factors can cause a loss of stability and lead to shipwreck.

The wrecks of ships including train ferries cause human and financial losses, as well as danger to the environment.

It is known that accidents with ships account for 14 % of oil pollution in the environment. The oil slick and spills on the sea surface can keep up to several months. Besides, oil spills can move at large

distances due to the wind and sea currents. The bulk freight transported by sea can also be hazardous. Besides, during accidents with ships the heavy metals and other materials transported can pollute the sea.

The research into the causes for wrecks of the ships transported vehicles demonstrated that stability loss was resulted from freight displacement.

Therefore, the problem of the stable securing of the rail cars on the ferry deck is of primary importance.

Let us consider the technology used for handling the cars transported by Ukraine's train ferries [12, 13] by an example of the ferry *Geroi Shipki*.

Car batches are formed in the sorting yard; then they are transferred to a rail yard by shunting locomotives. After customs procedures the car batches are delivered to the main deck across the special ramp (Figures 1.29 and 1.30).

Rail cars can be rolled on the main deck of a ferry with two or three railcar movers (uniloks) capable of travelling both on deck and rail tracks (Figure 1.31). The movers are coupled to the cars with a standard automatic coupler, and, if needed, they can supply air to the cars' brake systems. At the admissible trim of a ferry (not exceeding 1.2° on the stern), the railcar mover can move two four-axle cars of any freight capacity.

a) b)

Figure 1.29 – Ramp:
a) station Chornomorsk; b) station Crimea

a) b)

Figure 1.30 – Rolling-on of cars:
a) station Chornomorsk; b) station Crimea

a) b)

Figure 1.31 – Railcar mover (uniloc):
a) in free state; b) in interaction with a car

There is a hydraulic elevator with freight capacity of 170 tons equipped with two 30-m platforms between the ferry decks (Figure 1.32, a). Each platform can sustain two standard 14.7-m cars.

The cars move horizontally between the tracks across the upper and hold decks with rotating sectors actuated by a hydraulic drive from the platform: the upper deck (for two cars) with loading capacity of 175 tons and a rotation radius of 35 m, and the hold deck (for one car) with loading capacity of 90 tons and a rotation radius of 22 m (Figure 1.32, b).

a) b)

Figure 1.32 – Devices for transferring cars on the ferry deck:
a) hydraulic elevator; b) rotating sector

The car stability in ferry transportation is ensured by fixation on the deck with a set of disposable fasteners (Figure 1.33). Besides, the car's braking system is connected to the special hoses supplying compressed air to the wheelsets.

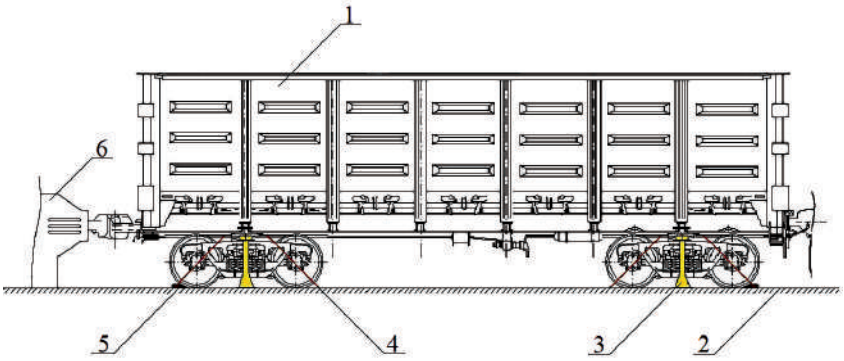

Figure 1.33 – Diagram of fastening a car on the ferry deck:
1 – car; 2 – deck; 3 – mechanic support jack; 4 – chain binder; 5 – braking shoe; 6 – buffer stop

Chain binders with bottle screws (Figure 1.34), which connect the car frame and the rings (Figure 1.35) located along the tracks on the ferry deck, are intended to prevent longitudinal and vertical movements of cars [12, 14, 117].

They can be of various structures. Each binder usually has a bottle screw with a hook on one end, and a hole on the other; an enlarged chain without knots and a chain section with knots are joined to this hole. The free end of the chain section has a clamping hook.

a) b)

Figure 1.34 – Chain binders in operation:
a) fixation of tank car; b) fixation of boxcar

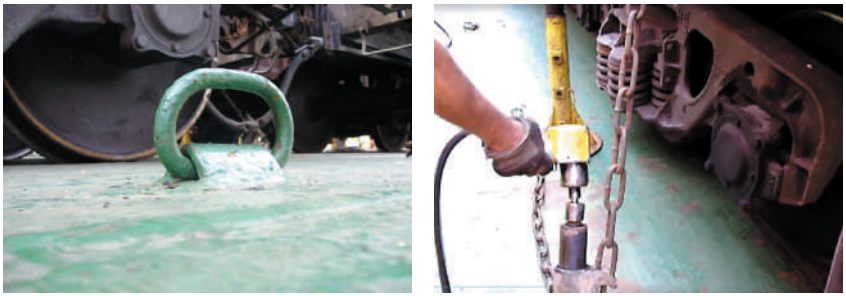

a) b)

Figure 1.35 – Fastening of a chain binder:
a) deck ring; b) pneumatic hammer

Japan's ferries are equipped with open binders with hooks for fixation of cars on the deck. The hooks of a bottle screw (with right-handed and left-handed threads with a diameter of 28 mm at the ends) can travel, thus, regulating the length of a binder from 800 to 1300 mm [14, 117].

It is possible to apply binders with an 11-mm chain without knots. Such a binder has a hook on one end for coupling to the car; its other end passes through the chain gear with the crown wheel rotating with the click. The binder can move parallel to the midship line with a special bogie.

Expending portable support jacks used for unloading the spring suspension of cars under rail/ferry transportation (Figure 1.36).

a) b)

Figure 1.36 – Expending portable support jack:
a) on the ferry Greifswald; b) on the ferry Petrovsk

The device consists of the upper and bottom ball seats connected by the body with cartridge, guide tube and screw. The upper surface of the cartridge has three longitudinal and two ring grooves. The travelling

nut of the upper support can move along the longitudinal grooves and at the rotation angle 60° it engages in the ring grooves with its supports. The upper and bottom supports have plates with notches on the support surfaces. The upper plate has two support planes for interaction with the car frame in the horizontal and vertical planes; the bottom plane has a flat support surface.

A spiral spring is embedded in the upper support; thus it keeps the contact with the car frame during the rolling motion of a ferry.

Buffer stops are mounted on the car batch's end equipped with an automatic coupler which is used for joining to the automatic coupler of an end car. They are used to soften impact loads when the cars are rolled on the ferry, and retain them on the track (Figure 1.37). They are divided into stationary and collapsible ones. The former ones are mounted in the stern or stem parts of a ferry on the side opposite to that loaded with cars.

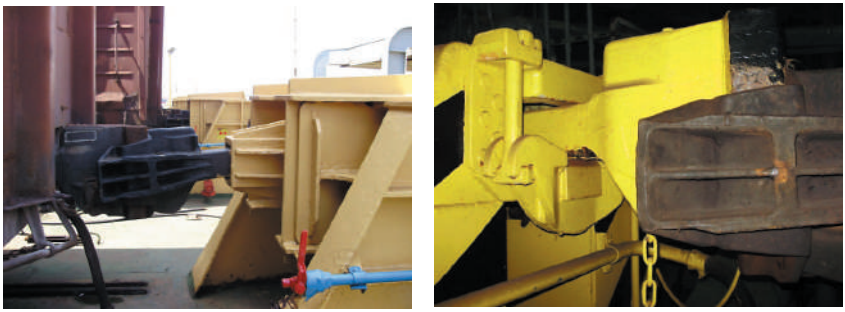

a) b)

Figure 1.37 – Buffer stops:
a) the ferry Geroi Odessy; b) the ferry Greifswald

The collapsible stops restrict displacements of cars along the tracks. They consist of a folding part and a base-plate mounted on the ferry deck with the pad eyes for fixation of the folding part axle.

The train ferry *Sakhalin* servicing the route Vanino-Kholmsk across the Sea of Japan uses hydraulic drive supports. Cars are rolled

on across the stern part. Each track end in the stern part of a ferry has stationary supports with automatic couplers. When all the cars are rolled on, a hydraulic drive support is connected to the end car from the stern. During the rolling-on of cars, this support is hidden in a special place (recess).

The support rests on the platform travelling along the guides located in the recess. The coupler's head is fixed in the upper part of the support mounted on the platform, and during the rolling-on it is stored in the recess. The platform and the support's sections move with the hydraulic cylinders.

Automatic couplers are divided into couplers for rail cars, couplers with shock springs, and locomotive couplers (without shock springs). The most popular ones are standard SA-3 couplers.

Brake shoes. Ukraine's train ferries use standard brake shoes to avoid longitudinal displacements of cars due to a trim (Figure 1.38).

a) b)

Figure 1.38 – Brake shoes:
a) in free state; b) under the car wheel

The ferry *Soviet Azerbaijan* operating on the route Aktau (Azerbaijan) – Türkmenbashi (Turkmenistan) uses special shoes. Such a shoe consists of foot rested on the rail, support and clamp to fasten the shoe to the rail. One clamp jaw is welded to the foot and

the support, the other one rotates about the axle and presses the shoe to the rail with a trapezoidal screw [117].

Special supports consisting of two parts connected with a chain can be used instead of brake shoes (Figure 1.39).

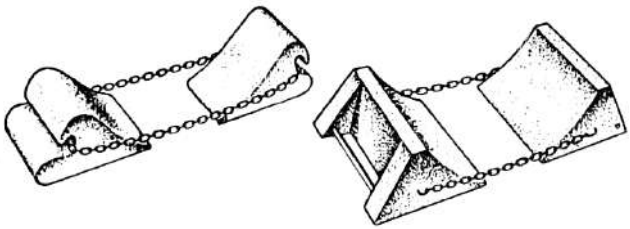

Figure 1.39 – Supports against longitudinal displacements of transport vehicles

Brake system. For sea transportation the brake air lines of cars are connected to the valves on the buffer stops for braking wheelsets.

The compressed air from the tank located in the engine room is supplied to the valves through the driver's brake controller located on the car deck. The compressed air, supplied to the driver's air controller, is regulated with a manometer and a reducer.

The rolling-on and rolling-off of railcars and their fastening on the decks are similar to those used on Ukraine's train ferries.

The ferry *Greifswald* has only two loading decks with five tracks. Rolling on the upper deck is conducted through the main (bottom) deck across the ramp (Figure 1.40).

Besides, there is a space reserve for loading wheeled automatic equipment. The above-mentioned lashing devices are used for railcars. The structural peculiarity of turnbuckles of chain binders is their small length and different gauge.

a) b)

Figure 1.40 – Train ferry *Greifswald*:
a) roll-on ramp; b) upper deck

1.3 Analysis of statistical data on damage of freight cars in train ferry transportation

The most frequent defects of rail cars transported by ferries were studied on the data taken from the Book on Technical Maintenance of Freight Cars.

Figure 1.41 demonstrates a diagram of defect distribution for freight cars after interaction with reusable lashing devices on the ferry under sea disturbance. The diagram makes it possible to conclude that the most serious defects in rail/sea transportation are bodies of open cars and boxcars as being the most vulnerable. The greatest percentage of defects by the data of recent years is 18 % and 54 % out of the total number of the cars under study, respectively. The least percentage of defects was identified in flat cars when they were fastened on the ferry deck by the reinforced side beams.

A quantitative ratio of the most frequent defects in the bodies of open cars and boxcars out of the total number of defects is given in Figures 1.42 and 1.43.

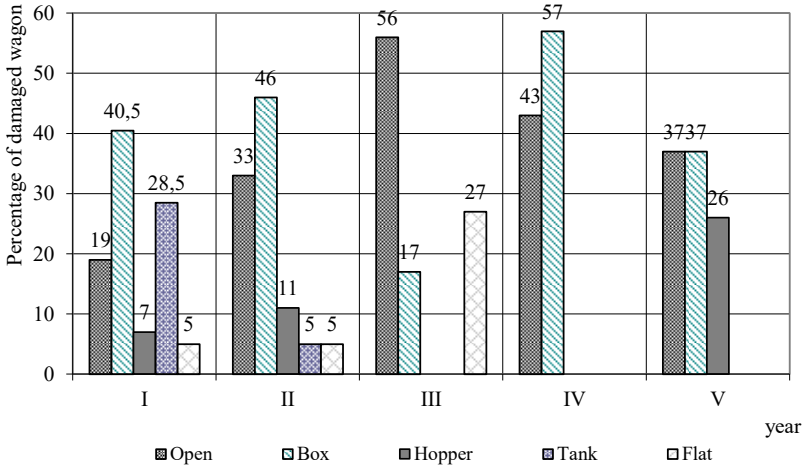

Figure 1.41 – Percentage of damaged freight cars carried by ferries in recent years

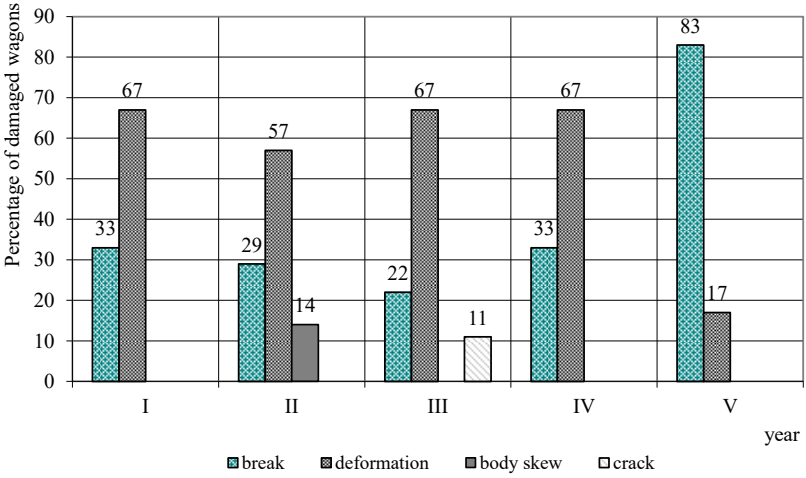

Figure 1.42 – Most frequent defects in open cars transported by train ferry

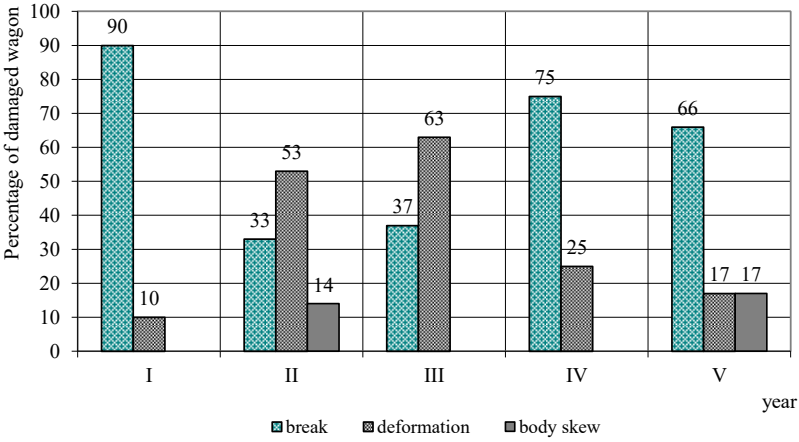

Figure 1.43 – Most frequent defects in boxcars transported by train ferry

According to the research conducted the authors can conclude that the basic types of defects in the cars are deformations and tears of the structural body elements used for fastening on the ferry decks. Besides, due to sea disturbance the cargo transported can move on the deck, it may cause lead to distortion of the body.

A percentage ratio of the most frequent defects in the bodies of open cars and boxcars in international rail/sea transportation in recent years is given in Figures 1.44 and 1.45, respectively.

The given diagram demonstrates that the most frequent defects in open cars in international rail/sea transportation are found in the body lining.

The most vulnerable elements of a boxcar in international rail/sea transportation are a bottom cord and towing shackles, i.e. the structural elements used for fixation on the deck.

The Wagon Department of the Odessa Railway Division and the Safety Inspection registered an accident when an open car transported by the ferry was damaged due to a collision with a steel support truss; it caused the tear of the car body, deformation of two beams and

the cord belt. A similar accident was with a boxcar, when, due to breakage of chain binders the rail car lost stability, but did not turn over owing to the pillar of the deck superstructure (Figure 1.46). The car was recognized as unserviceable; the cargo was completely damaged and disposed from the ferry deck.

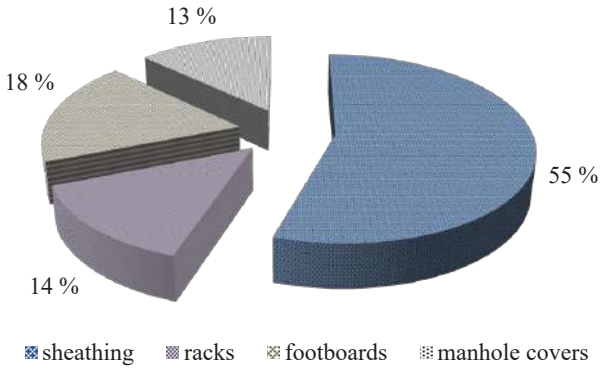

Figure 1.44 – Percentage ratio of the most frequent defects in the body elements of an open car in international rail/sea transportation

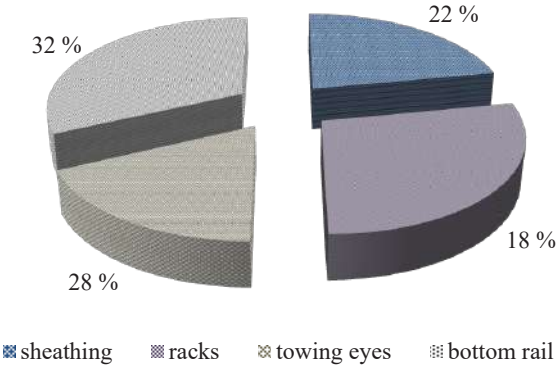

Figure 1.45 – Percentage ratio of the most frequent defects in body elements of a boxcar in international rail/sea transportation

a) b)

Figure 1.46 – Loss of stability by a boxcar on the train ferry deck due to breakage of chain binders during sea disturbance:
a) side view; b) view from above

The full-scale investigation into typical schemes used for fixation of rail cars on the ferry decks at the station Chornomorsk determined the car bodies' structural elements used for fixation. The choice of such structural zones is of sporadic nature, which is a negative factor. Let us distinguish the car elements most frequently used for fixation; they are hatch covers, locking devices, brackets for holding cars during shunting operations, bolster beams of the frame, etc.

Therefore, it is important and necessary to improve the carrying structure of freight cars to ensure the stable interaction with lashing devices on the deck.

Conclusions to Part 1

1. The research analyzed historical aspects of evolution and operation of ferry transportation, and studied the peculiarities of rail/ferry transportation on seas and rivers. The authors studied today's main rail/ferry routes and technical peculiarities of the ferries;

2. The research also deals with mechanical aids and lashing devices used for fixation of cars on the ferry decks. The authors analyzed peculiarities of their work and studied typical schemes applied for fixation of cars on the decks of Ukraine's train ferries. They determined structural elements used for fixation of cars on the decks. On the basis of the above-mentioned analysis it was established that the carrying structures are not suitable for interaction with lashing devices on the deck; therefore it causes damage in the body elements used for such fixation during sea disturbance;

3. The authors analyzed statistical data on damage of freight cars in train ferry transportation. It was determined that the most vulnerable elements of the car's carrying structure are the hands used to tighten the hatch covers, holding devices, hooks for drawing cars during shunting operations, bolster beams of frames, pillars, etc.

The analysis conducted demonstrates a need to define loading on the carrying structure of the cars transported by ferries and to research into the strength factors during interaction with lashing devices.

PART 2
DETERMINATION OF FORCES ON CAR BODY IN FERRY TRANSPORTATION

2.1 Analysis of the basic forces on the car body in ferry transportation

The oscillations of a train ferry loaded with rail cars during sea disturbance can be regarded as the oscillations of a solid body with attached masses. The forces exerted by these oscillations are proportional to the values of displacements of a ferry relative to its initial position. These forces are presented as additional buoyancy forces to the ferry body [70–72]. Therefore, a train ferry is regarded as a solid body with several degrees of freedom:

– vertical translational displacements along the axle Z;

– angular displacements around the transverse axle Y at an angle of φ;

– angular displacements around the longitudinal axle X at an angle of θ.

The other three potential displacements (advance displacement in the longitudinal direction along the axle X, angular displacement around the axle Z at an angle of ψ, advance displacement in the transverse direction relative to the axle Y) are not of oscillatory nature, as they do not change the size and form of the underwater part of a train ferry [71, 72].

The most critical displacements causing a loss of stability by the rail cars located on the deck are the angular displacements of a train ferry along the transverse and longitudinal axles (Figure 2.1).

During sea disturbance the oscillations of a train ferry loaded with cars can cause not only rotary movements around the transverse

and longitudinal axles which run through the center of gravity, but also travels of the axles along some trajectories similar to a circle. The period of these displacements equals to a wave cycle. A radius of the trajectory of displacements of a train ferry loaded with cars can be taken in calculation as equal to the wave amplitude [71, 72].

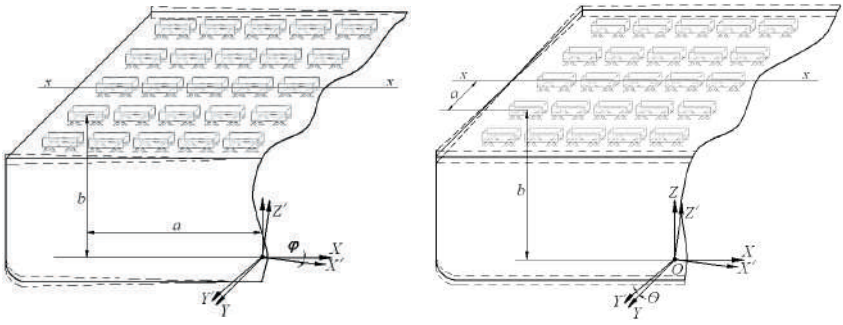

Figure 2.1 – Displacements of a car body in ferry transportation:
a) angular about the transverse axle; b) angular about the longitudinal axle

Figure 2.2 presents the force diagram for a ¼ open car body during sea disturbance. The diagram is based on the design diagram given in [80] and complemented with additional forces typical for these operation conditions.

The basic forces on the car body in ferry transportation are vertical static forces, vertical dynamic forces, wind forces, inertia forces, pressure from bulk and liquid freight, and tensile forces through the chain binders. It should be noted that due relieve of the spring suspension of a car bogie, the vertical dynamic force is rather small therefore, in estimation of the strength and stability of a car body on the deck of a train ferry during sea disturbance it can be neglected.

The above-mentioned forces are reduced to the following groups by direction of action [80]:

– vertical;

– side (transverse);
– longitudinal.

The layout of rail cars on the deck has a significant effect on forces to the car bodies during sea disturbance. Thus, the cars located on the farthest tracks from the bulwark are under the greatest forces at the angular displacements of a train ferry around the transverse axle than the cars located on the nearest tracks to the diameter plane.

The similar situation is observed at angular displacements of a train ferry about the longitudinal axle; the cars farthest from the sternpost have to sustain larger forces than the cars located on the tracks nearest to the middle transverse section [68–70].

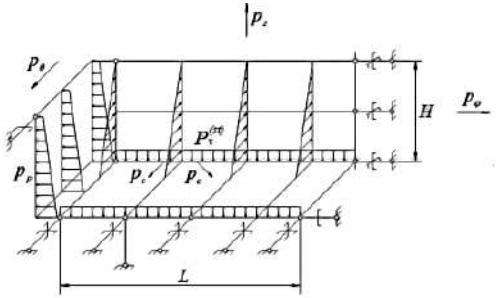

Figure 2.2 – Diagram of forces on the open car body during sea disturbance: P_z, P_φ, P_θ – inertia forces on the open car body during vertical displacements around the longitudinal and transverse axles, respectively; $P_v^{(st)}$ – intensity of the vertical static force; P_p – pressure forces from the bulk freight; P_c – forces to the open car body through the chain binders when it travels as relative to the initial position; L – ½ car body length; H – car body height

The vertical static force $P_v^{(st)}$ on the car body can be defined by the formula:

$$P_v^{(st)} = P_{gw} - P_w, \tag{2.1}$$

where P_{gw} – car gross weight, kN;
P_w – weight of car's gearing parts, kN.

– During vertical advance displacements of a train ferry the vertical static force equals:

$$P_v^{(st)} = P_g^b.$$

– During angular displacements of a train ferry about the transverse axle:

$$P_{v\ x}^{(st)} = P_g^b \cdot \sin\varphi,$$

$$P_{v\ z}^{(st)} = P_g^b \cdot \cos\varphi, \qquad (2.2)$$

where φ – angle of a transverse displacement of a ferry loaded with cars on the deck, deg.

– During angular displacements of a ferry about the longitudinal axle:

$$P_{v\ y}^{(st)} = P_g^b \cdot \sin\theta,$$

$$P_{v\ z}^{(st)} = P_g^b \cdot \cos\theta, \qquad (2.3)$$

where θ – longitudinal displacement angle of a ferry, deg.

By approaching the dockside a ferry turns around for docking the ramp and rolling-off the rail cars.

The following forces are applied to the ferry as it turns around:

– forces and moments appearing in the ferry's engines;

– forces to the steering equipment;

– forces and inertia moments among which are those from the attached water masses;

– hydraulic mechanic forces and moments on the ferry body.

Besides, as a ferry turns around, the following forces affect it: an inertia force applied in the gravity center of a ferry and directed along an instantaneous radius of curvature, as well as an inertia force along a tangential line to the trajectory of the center of gravity towards the instantaneous traffic speed [89].

The centered force on the ferry (Figure 2.3), and thus, on the cars located on it, can be defined by the following formula [68–70]:

$$C = \frac{D \cdot \vartheta^2}{R}, \tag{2.4}$$

where D – water displacement of a ferry;
R – turning radius;
ϑ – turning rate.

Or, as is known from theoretical mechanics, the centered force can be defined by the formula:

$$C = D \cdot \omega^2 \cdot \rho, \tag{2.5}$$

where ω – angular speed;
ρ – turning pole.

When a ferry turns around two stern screws together with one front screw begin to work, the stern screws act in the opposite directions and form the moment which facilitates a turn of a ferry. The centered force and the forces through the chain binders affect the cars located on the ferry decks [68–70].

The diagram of forces to the car body through the chain binders when the ferry turns around is given in Figure 2.4.

The approximate turning rate of the ferry Geroi Plevny equals ϑ = 1,3 km/h = 0,36 m/s. For the car body farthest from the sternpost R = 79 m.

Thus, considering D = 23 744 tons, the centered force is C = 39 kN.

The centered force components are:

$$C = \int_0^{180} C \cos\rho d\rho = C(\sin 180 - \sin 0) = 0,$$

$$C_y = \int_0^{180} C \sin\rho d\rho = -C(\cos 180 - \cos 0) = 98 \text{ kN}.$$

The force to the car body through the chain binder is $F = \frac{C}{4}$.

Therefore, the force components in the longitudinal and transverse directions are defined as:

$$F_x = F\cos\beta; \quad F_x = F\sin\beta \cdot$$

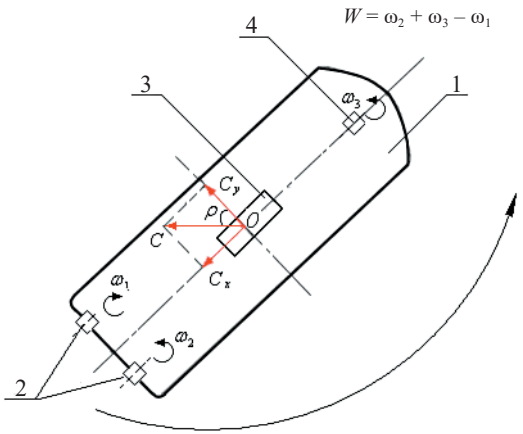

Figure 2.3 – Diagram of the centered force on a ferry with a conditional car on the deck when the ferry turns around:
1 – ferry; 2 – stern engines; 3 – rail car; 4 – stem engine

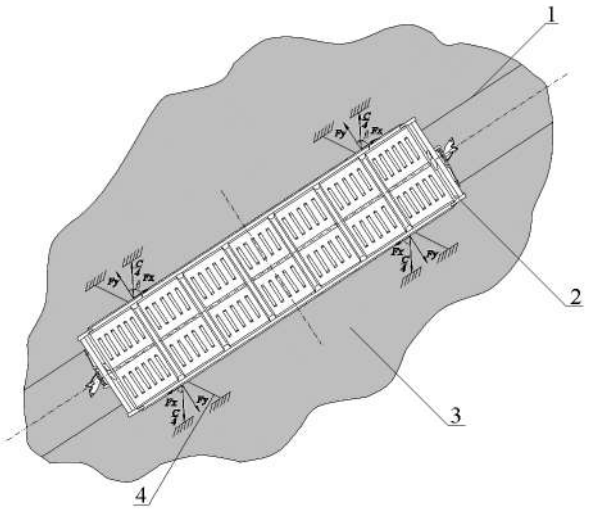

Figure 2.4 – Diagram of forces on the car body through chain binders when the ferry turns around:
1 – rail track; 2 – car; 3 – ferry deck; 4 – chain binder;
F_x, F_y, – projections of forces to the car body through chain binders

As far as the centered force value obtained is relatively small, for estimation of the force value on the car body it can be disregarded.

The location of chain binders used for fastening a car relative to the body planes also impacts the car strength.

Non-symmetrical fixation of chain binders by the carrying structure of a car causes irregular force impact on the body and results in residual deformations and even damage of the body elements [68–70].

Therefore, chain binders have spatial location relative to the body for effective fixation of a car body on the ferry deck. The location of chain binders and the space diagram of forces are presented in Figure 2.5.

The location angles of chain binders relative to the car body planes for the symmetrical fixation according to [49, 51, 52] are presented in Table 2.1.

Thus, at angular displacements of a train ferry about the longitudinal and transverse axles we can obtain the following notations [68–70]:

$$\begin{aligned} p_v^{(st)}{}_y &= \frac{p_v^{(st)}}{8}\sin\alpha, \quad p_v^{(st)}{}_x = \frac{p_v^{(st)}}{8}\cos\beta, \quad p_v^{(st)}{}_x = \frac{p_v^{(st)}}{8}\cos\gamma, \\ p_v^{(st)}{}_z &= \frac{p_v^{(st)}}{8}\cos\alpha, \quad p_v^{(st)}{}_y = \frac{p_v^{(st)}}{8}\sin\beta, \quad p_v^{(st)}{}_z = \frac{p_v^{(st)}}{8}\sin\gamma. \end{aligned} \tag{2.6}$$

The wind force on the car body wall is defined by the formula:

$$p_e = p' \cdot S_c, \tag{2.7}$$

where p' – wind force per surface unit, kN/m^2;

S_c – area of a corresponding car body wall, m^2.

Table 2.1 – The location angles of chain binders relative to the car body planes

Angle	Numerical value
α	<30°
β	30° – 60°
γ	<60°

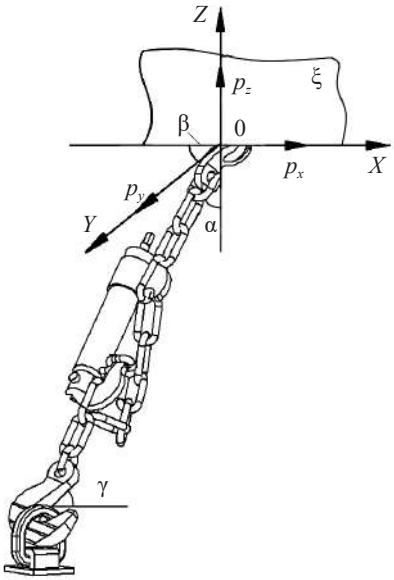

Figure 2.5 – Spatial location of a chain binder relative to the car body:
p_x, p_y, p_z – projections of the force from a chain binder applied to the fixation area on the body along the coordinate axle; α, β, γ – location angles of a chain binder relative to the car body planes

On the basis of research into fixation patterns of rail cars on the train ferry decks at the station Chornomorsk the authors made a selection of such fixation areas (Table 2.2), determined analytical dependencies, obtained the coefficients which take into account uneven fixation of chain binders relative to the car body planes and compare the actual locations of chain binders relative on the car body with those prescribed by the normative documents [68–70, 90].

By using the dependencies of mathematical statistics and probability theory we can state that the number of the selected elements (chain binders) was sufficient for obtaining a realistic estimate [91–95].

The irregularity coefficients of fixation of chain binders relative to the car body planes are given in Table 2.3.

Table 2.2 – Statistical data on location of chain binders relative to the car bodies

156	**Open car**	**310**	**Boxcar**	**304**	**Autonomous refrigerated car converted to boxcar**
n	***class***	***n***	***class***	***n***	***class***
4	85–100	1	53	3	90–95
8	100–105	22	85–90	43	95–100
0	105–110	103	90–95	195	100–105
2	110–115	84	95–100	36	105–110
5	115–120	87	100–105	27	110–115
25	120–125	9	105–110	–	–
57	125–130	1	110–115	–	–
9	130–135	1	115–120	–	–
11	135–140	1	120–125	–	–
18	140–145	1	125–130	–	–
15	145–150	1	130–135	–	–
2	150–155	–	–	–	–

Table 2.3 – Irregularity coefficients of fixation of chain binders on the car body

Type of car	**Irregularity coefficient for chain binders by the height of car body**		**Irregularity coefficient for chain binders from deck ring to car body's vertical plane**	
	Calculation based on measurement	**Calculation based on normative documents**	**Calculation based on measurement**	**Calculation based on normative documents**
Open car	1.17	1.09	1.2	1.1
Boxcar	0.97	0.91	1.36	1.27
Autonomous refrigerated car converted to boxcar	1.04	0.97	1.24	1.15
Tank car	0.96	1.02	1.08	1.1

The selection included the following types of cars: 21 open cars, 41 boxcars, 39 autonomous refrigerated cars converted to boxcars, and 13 tank cars; the number of the chain binders used for fixation: 156 for open cars, 310 for boxcars, 304 for autonomous refrigerated cars converted to boxcars, and 104 for tank cars [68–70].

Table 2.3 demonstrates that a difference between the coefficients which involve irregular location of chain binders with respect to the car body planes, obtained through measurements and the normative documents was about 1 %.

The evaluation of the forces to the car body through chain binders requires tolerance coefficients which involve the location angles of the chain binders relative to the car body planes, and, therefore, the forces they transfer to the carrying structure of a car [68–70].

Thus, we can obtain:

$$p = p_c \cdot k_h \cdot k_b, \tag{2.8}$$

where p_c – force through a chain binder to the car body;

k_h, k_b – coefficients which involve the location irregularity of a chain binder along the car body height and from the deck ring to the vertical plane of a car body.

2.2 Mathematical modelling of forces on car bodies in ferry transportation

The design forces on the car body in ferry transportation were determined through studying the hydrometeorological characteristics of the Black Sea [66]; the maximum roll angles and trims [67] were defined for the condition of sea disturbance, which accounted for 12,2° and 2,5°, respectively [68–70]. The roll was determined for the static action of wind to the topside projection of a ferry loaded with cars on the upper deck.

It was taken into account that the car body was rigidly fixed on the deck and travelled the same path as the deck. An impact force of sea waves to the train ferry loaded with rail cars on the deck was neglected [68–70, 83].

The model assumed the trochoidal law of disturbing motion (sea waves) to the train ferry loaded with car bodies on the deck.

$$\left(0{,}07\frac{0{,}8}{g}D\cdot L^2\right)\ddot{q}_1+\left(\beta_\phi\cdot\frac{L}{2}\right)\dot{q}_1=p'\cdot\frac{h}{2}+\Lambda_\phi\cdot\frac{L}{2}\cdot\dot{F}(t); \tag{2.9}$$

$$\left(\frac{D}{12\cdot g}(B^2+4z_g{}^2)\right)\ddot{q}_2+\left(\beta_\theta\cdot\frac{B}{2}\right)\dot{q}_2=p'\cdot\frac{h}{2}+\Lambda_\theta\cdot\frac{B}{2}\cdot\dot{F}(t), \tag{2.10}$$

where $q_1=\varphi, q_2=\theta$ – generalized coordinates corresponding to: φ – angular displacement of a body around the transverse axle which runs through the mass center, θ – angular displacement around the longitudinal axle. The initial point of the coordinate system was located in the mass center on the train ferry;
D' – mass water displacement;
D – weight water displacement;
L, B – length and breadth of a train ferry, respectively;
h – moulded depth, m;
β_1 – oscillation damping coefficient;
z_g – weight center coordinate, m;
p' – wind force;
$F(t)$ – law of force actuating the movement of a train ferry loaded with cars on the decks.

The profile of a wave moving by the trohoidal law is described by equation (2.11) [73]:

$$\begin{aligned} x &= a+\mathrm{Re}^{kb}\sin(ka+\omega t),\\ z &= b-\mathrm{Re}^{kb}\cos(ka+\omega t), \end{aligned} \tag{2.11}$$

where a and b – horizontal and vertical coordinates of the trajectory center along which a particle with the coordinates x and z moves for the time being;
R – radius of the trajectory along which a particle rotates;
ω – sea wave frequency;
k – frequency of an excitation force trajectory.

The technical characteristics of a train ferry, a car body and the hydro meteorological characteristics of the cruising area were taken as the input parameters of the mathematical model.

The equations were solved by the method of variations of free constants [74]:

$$q_i = C_i^*(t)\tilde{q}_i^* + C_i^{**}(t)\tilde{q}_i^{**}, \tag{2.12}$$

where $C_i^*(t), C_i^{**}(t)$ – functions to be determined;

$\tilde{q}_i^*, \tilde{q}_i^{**}$ – solutions to equations (2.1), (2.2) with consideration of their reduction to homogeneous equations.

The displacement of the system at angular oscillations around the transverse axle, as the general solution, has the form

$$q_2 = \left[-\frac{R \cdot e^{kb}\omega\beta_\phi}{2I_y\nu} \left(-\frac{1}{\omega-\nu}\cos(t(\omega-\nu)+ka) + \frac{1}{\omega-\nu}\cos ka - \frac{1}{\omega+\nu}\cos(t(\omega+\nu)+ka) + \right.\right.$$

$$+\frac{1}{\omega+\nu}\times\cos\kappa a - \frac{1}{\omega-\nu}\sin(ka-t(\omega-\nu)) + \frac{1}{\omega-\nu}\sin ka - \frac{1}{\omega+\nu}\sin(ka+(t(\omega+\nu)) +$$

$$\left.\left. + \frac{1}{\omega+\nu}\sin ka) \right] + \frac{p'\frac{h}{2}}{I_y\nu^2}(\cos\nu t+1) \right]\cos\nu t + \left[\frac{R \cdot e^{kb}\omega\beta_\phi}{2I_y} \left(\frac{1}{\omega-\nu}\sin(ka+t(\omega-\nu)) - \right.\right.$$

$$- \frac{1}{\omega-\nu}\sin ka + \frac{1}{\omega+\nu}\sin(ka+t(\omega+\nu)) - \frac{1}{\omega+\nu}\sin ka - \frac{1}{\omega-\nu} \times$$

$$\times \cos(ka + t(\omega-\nu)) + \frac{1}{\omega-\nu}\cos ka - \frac{1}{\omega+\nu}\cos(ka+t(\omega+\nu)) +$$

$$\left.\left. + \frac{1}{\omega+\nu}\cos ka \right) + \frac{p'\frac{h}{2}\sin\nu t}{I_y\nu} \right] \times \times \nu\sin\nu t, \tag{2.13}$$

where ν – frequency of free oscillations of a train ferry loaded with car bodies on the decks;

I_Y – inertia moment of train ferry mass relative to the transverse axle.

Displacements of the system at angular oscillations around the longitudinal axle are defined by formula (2.5) with consideration of the corresponding numerical parameters of a train ferry and an excitation force.

The general acceleration of a car body includes the location component and the component of free fall acceleration.

The improved acceleration values based on the location of cars on the train ferry deck involved wave angles in reference to the deck (0° – 180°) [49, 75, 76].

Differential equations (2.9) and (2.10) were also solved in MathCad software with the Runge–Kutta method [77, 78]. The oscillation damping coefficients were found by the technique presented in [67, 76]. The wind force was taken equal to 1.47 kN/m^2 [79].

The results of the calculation are given in Figure 2.6.

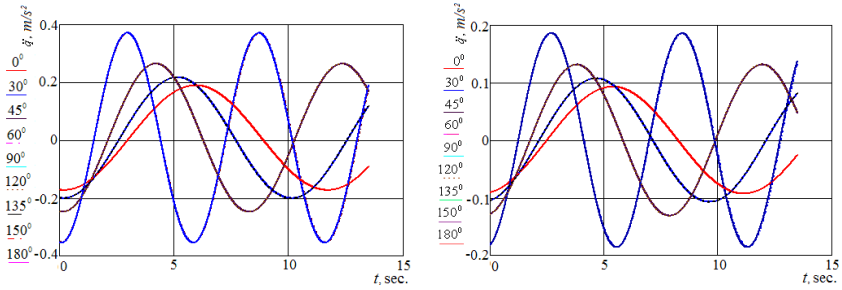

a) b)

Figure 2.6 – Accelerations on the car body during train ferry oscillations:
a) at angular displacements around the transverse axle;
b) at angular displacements around the longitudinal axle

The research into the fixation patterns used for cars on Ukraine's train ferries passing via the station Chornomork of the Odessa Railway

demonstrated that the car bodies can move on the deck during sea transportation. These displacements can be caused by:

– deck irregularity;
– inoperable state of lashing devices;
– deflections in the geometry of bodies and their deformations;
– non-symmetric loading of a car body with freight, etc.

The accelerations to the car body in ferry transportation with consideration of their potential displacements on the deck during sea disturbance were defined by means of the mathematical model designed (2.14).

The authors took into account the angular displacements of a train ferry loaded with cars along the longitudinal axle, as a case of the maximum forces.

The first equation of the mathematical model describes the train ferry displacements caused by sea disturbance, and the other one describes the displacements of a car body relative to the deck.

$$\begin{cases} \left(\frac{D}{12\cdot g}(B^2+4z_g{}^2)\right)\ddot{q}_1+\left(\Lambda_\theta\cdot\frac{B}{2}\right)\dot{q}_1=p'\cdot\frac{h}{2}+\Lambda_\theta\cdot\frac{B}{2}\cdot\dot{F}(t), \\ I_y^\kappa\cdot\ddot{q}_2=p'_\kappa\cdot\frac{h_\kappa}{2}+M_в, \end{cases} \tag{2.14}$$

where $q_1 = \theta_1$, $q_2 = \theta_2$ – generalized coordinates corresponding to
θ_1 – angular displacement of a train ferry relative to the longitudinal axle running through the center of masses;
θ_2 – angular displacements of a car body relative to the longitudinal axle running through the center of masses.

Train ferry characteristics: D – weight water displacement; B – breadth; z_g – weight center coordinate; h – moulded depth; Λ_θ – oscillation damping coefficient.

Car characteristics: I_y^κ – inertia moment of a car body relative to the longitudinal axle; p'_κ – wind force to the side wall of a car body located on the upper deck; h_κ – car body height; $M_в$ – moment of forces between the car and the deck.

Parameters of excitation force: p' – wind force to the topside of a train ferry; $F(t)$ – law of force action actuating the movement of a train ferry loaded with rail cars on the deck;

The initial displacement and speed of a train ferry were taken equal to zero. For the car the initial displacement was conditioned by the potential flexibility of its assembly units relative to the deck (axle-box unit relative to the wheelset axle, bogie frame relative to the box unit axle, friction wedge relative to the center of the side axle, body central beam relative to the friction wedge, body central plate relative to the bogie central plate [80]); it accounted for 31 mm. The initial speed was taken equal to zero.

The mathematical model designed did not involve the impact force of sea waves to the body of the train ferry loaded with rail cars.

The results of the calculation are given in Figure 2.7. The total value of acceleration on the car body farthest from the bulwark was 0.3 g, on the car body located on the second track from the bulwark – 0.24 g, on the car body located on the middle track – 0.22 g.

The results obtained made it possible to conclude that these acceleration values exceeded the accelerations on the car body rigidly fastened on the deck by about 20 %, and those on the car body in operation on the trunk lines – by 40 % [81, 82].

The authors investigated into the basic rail/ferry routes in Europe and Asia in order to determine accelerations on the car body in sea transportation. The hydro meteorological characteristics of cruising areas of the train ferries were determined by the data presented in [66]. The accelerations by specific locations of rail cars on the decks for different ferry types were calculated according to the developed model [83, 50, 17, 31, 33, 48, 84, 85, 49, 44, 58]. The parameters taken for determining accelerations on the car bodies and the results are given in Table 2.4 [86].

Dependencies of the accelerations on the car bodies (with the component of free fall acceleration) located on the train ferry decks are given in Figures 2.8 and 2.9.

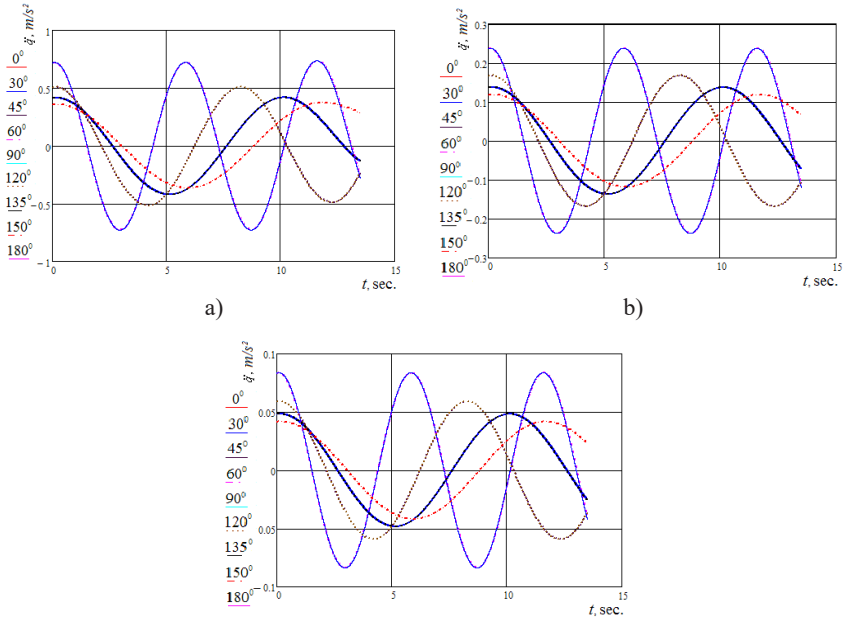

Figure 2.7 – Accelerations on the car body during train ferry oscillations:
a) car body located on the farthest track from the bulwark; b) car body located on the second track from the bulwark; c) car body located on the middle track

The case of spontaneous sea disturbance was also taken into account in the research. Besides, it involved the actual hydro meteorological characteristics of sea disturbance recorded during the storm in the Black Sea [87, 88]. As far as the storm affected area II of the Black Sea (Figure 2.10), the calculation involved the ferry route length across this area, i.e. Chornomorsk (Ukraine) – Poti (Georgia) and Chornomorsk – Batumi (Georgia).

The research presents the results of calculation for the Chornomorsk – Poti route, the journey time across the stormy area in the Black Sea was about four hours at a design speed of 18.6 knots (9.6 m/s).

Table 2.4 – Accelerations on the car body in train ferry transportation

Parameter	Train ferry									
	Geroi Shipki	**Soviet Azerbaijan**	**Mukran**	**Baltiysk**	**SMAT (FERUZ)**	**Sakhalin**	**Avangard (Slavyanin)**	**Annenkov (Petrovsk)**	**Greifswald**	**Ambal**
1	2	3	4	5	6	7	8	9	10	11
Length, m:										
maximum	184.25	135	190.5	187.36	150.32	127.3	133.7	110.5	190.94	187.7
Breadth, m	26	18.4	28	22	22	19.8	21	16	28	21.6
Moulded depth, m:										
to upper deck	15.2	6.2	15.2	18.95	7.15	8.8	8.0	6.25	15.2	18.95
Water displacement, t	23744	8530	22404	20077	9863	5485	9863	9863	22255	20077
Draft, m	7.42	4.06	7.2	6.5	3.8	6.2	4.8	4.8	6.6	6.5
Speed, knots	18.6	16	16	18.5	10	16.5–18	10	10	16–17	18.5
Car capacity, pcs	108	30	103	135	50	28	45	25	103	135
Operation area	the Black Sea	the Caspian Sea	the Baltic Sea	the Baltic Sea	the Azov Sea	the Tatar Strait	the Black Sea	the Azov Sea	the Black Sea	the Baltic Sea
Roll angle, deg.	12.2	5.54	10.2	9.1	7.97	4.0	5.1	3.6	18.8	9.1

End of the table

1	2	3	4	5	6	7	8	9	10	11
Sea wave characteristics										
Height, m	8	6	6	6	3.5–4	8–10	8	3.5–4	8	6
Length, m:	126.5	76.54	39	39	10–15	126.5	126.5	10–15	126.5	39
Period, s	9	7	5	5	5	9	9	5	9	5
Accelerations on the specific locations of cars on the train ferry decks										
For farthest car from bulwark	0.38	0.25	0.04	0.084	0.03	0.1	0.03	0.021	0.02	0.102
Horizontal component of free fall acceleration at set roll angle	2.1	0.95	1.74	1.6	1.4	0.7	0.87	0.62	3.2	1.6
Total acceleration value, m/s^2	2.48	1.2	1.78	1.68	1.43	0.8	0.9	0.64	3.22	1.7
Total acceleration value in fractions g, m/s^2	0.25	0.1	0.2	0.2	0.15	0.08	0.1	0.07	0.33	0.2

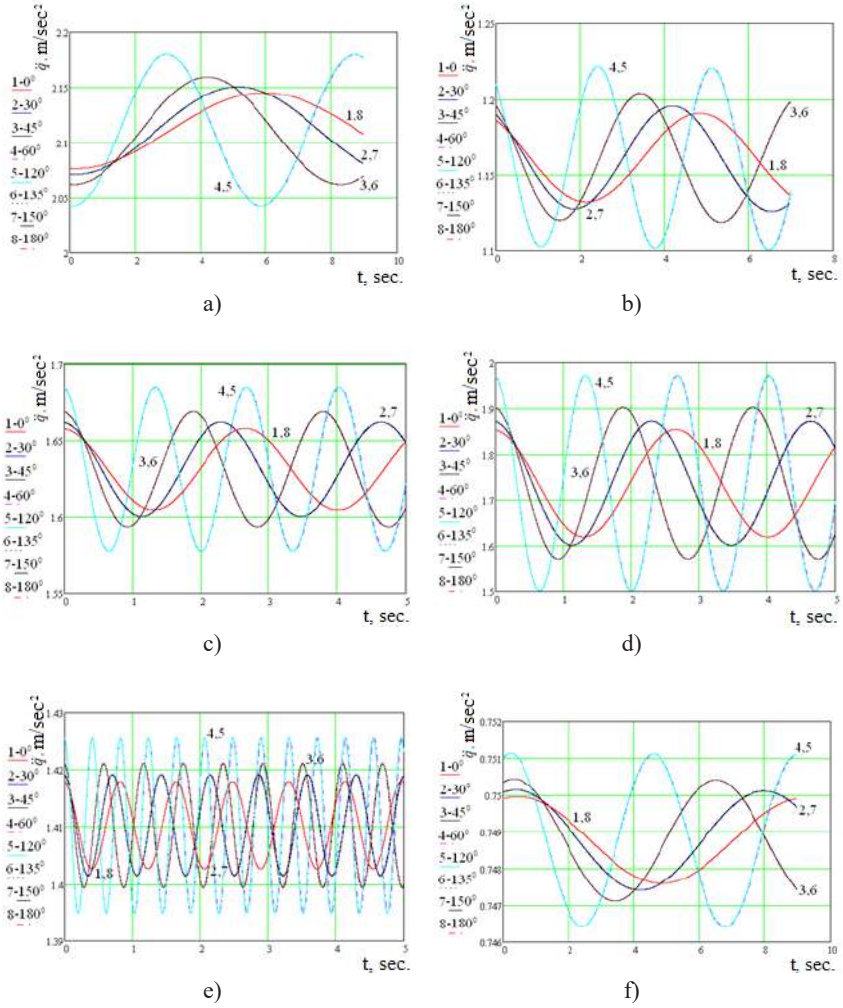

Figure 2.8 – Accelerations of car bodies in train ferry transportation:
a) Geroi Shipki (the Black Sea); b) Soviet Azerbaijan (the Caspian Sea); c) Mukran (the Baltic Sea); d) Baltiysk (the Baltic Sea); e) SMAT/FERUZ (the Azov Sea); f) Sakhalin (the Tatar Strait)

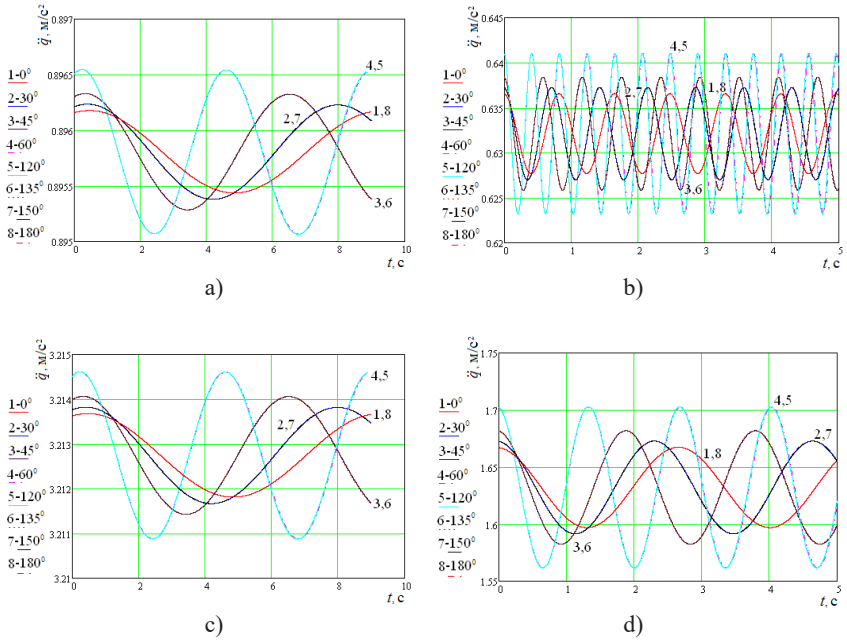

Figure 2.9 – Accelerations of car bodies in train ferry transportation:
a) Avangard/Slavyanin (the Black Sea); b) Annenkov/Petrovsk (the Azov Sea); c) Greifswald (the Black Sea); d) Ambal (the Baltic Sea)

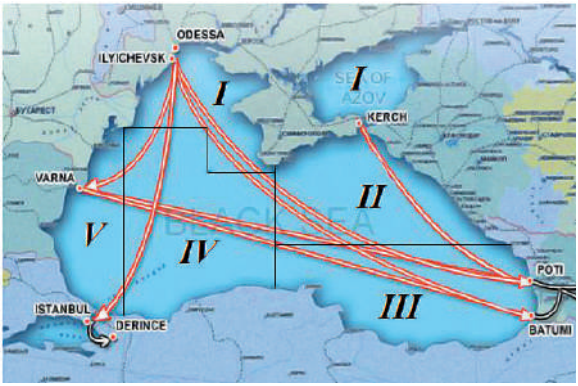

Figure 2.10 – Ukrainian rail/ferry routes in the Black Sea divided by areas

The variables of disturbing action were factored in the F-series [76]:

$$F(t)=\frac{a_0}{2}+\sum_{i=1}^{\infty}C_i\cos(\omega_i t+\beta_i)=\frac{a_0}{2}+\sum_{i=1}^{\infty}a_i\cos(\omega_i t)+\sum_{i=1}^{\infty}b_i\sin(\omega_i t); \quad (2.15)$$

$$\frac{a_0}{2}=\frac{1}{T}\int_0^T F(t)dt; \quad (2.16)$$

$$a_i=\frac{2}{T}\int_0^T F(t)\cos(\omega_i t)dt; \quad (2.17)$$

$$b_i=\frac{2}{T}\int_0^T F(t)\sin(\omega_i t)dt. \quad (2.18)$$

After the appropriate calculation we can obtain:

$$F(t)=a-\frac{2R\cdot e^{k\cdot b}}{\omega\cdot t}\left(\cos\left(k\cdot a+\omega\cdot t\right)-1\right)+2b-\frac{2R\cdot e^{k\cdot b}}{\omega\cdot t}\sin\left(k\cdot a+\omega\cdot t\right)+$$
$$+\sum_{i=1}^{n}\left(\frac{2a}{t\cdot\omega}\sin\omega t+\frac{R\cdot e^{k\cdot b}}{t}\left(t\cdot\sin\left(k\cdot a\right)-\frac{1}{2\omega}\left(\cos\left(k\cdot a+2\omega\cdot t\right)-\cos\left(k\cdot a\right)\right)\right)+\right.$$
$$\left.+\frac{2b}{t\cdot\omega}\sin\left(\omega\cdot t\right)-\frac{R\cdot e^{k\cdot b}}{t}\left(t\cdot\cos\left(k\cdot a\right)+\frac{1}{2\omega}\left(\sin\left(k\cdot a+2\omega\cdot t\right)-\sin\left(k\cdot a\right)\right)\right)\right)+$$
$$+\sum_{i=1}^{n}\left(-\frac{2a}{t\cdot\omega}\left(\cos\left(\omega_i\cdot t\right)\right)+\frac{R\cdot e^{k\cdot b}}{t}\left(t\cdot\cos\left(k\cdot a\right)-\frac{1}{2\omega}\left(\sin\left(k\cdot a+2\omega\cdot t\right)\right)\right)-\right.$$
$$\left.-\frac{2b}{t\cdot\omega}\left(\cos\left(\omega_i\cdot t\right)\right)+\frac{R\cdot e^{k\cdot b}}{t}\left(t\cdot\sin\left(k\cdot a\right)-\frac{1}{2\omega}\left(\cos\left(k\cdot a+2\omega\cdot t\right)\right)\right)\right). \quad (2.19)$$

On the basis of the calculation the authors determined the accelerations on the car bodies in train ferry transportation, which involved various wave angles to the body of a train ferry. The results of the calculation are given in Figure 2.11.

Figure 2.11 demonstrates that the maximum acceleration values were about 0.11 m/s^2 (with a horizontal component of free fall

acceleration of 2.2 m/s^2 (0.22 g)); it corresponds to wave angle values of $\chi = 45°$; 60°; 150° and 180°.

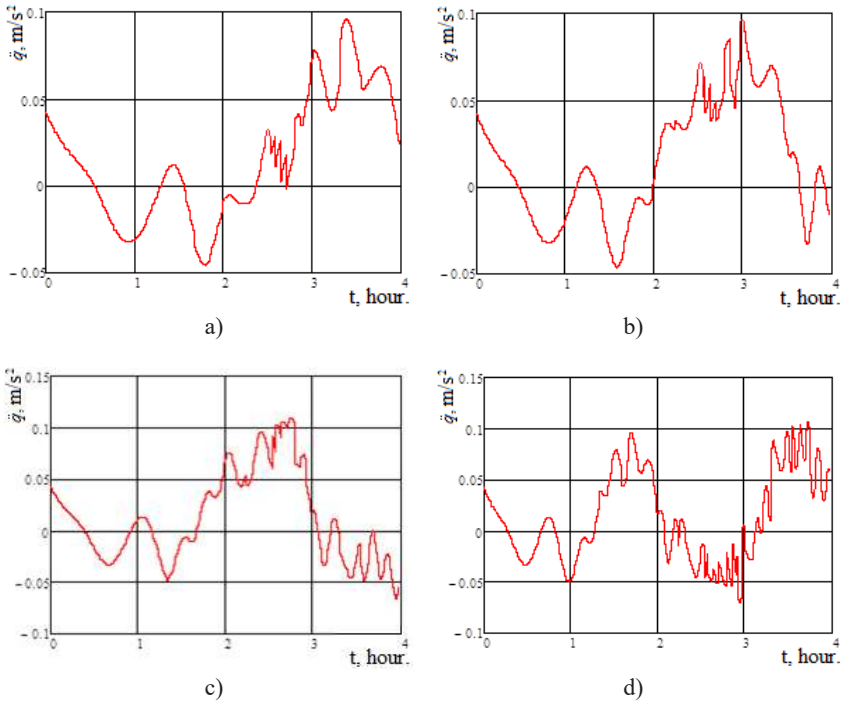

Figure 2.11 – Accelerations to the end car body (from the bulwark) on the upper deck of a ferry:
a) at χ = 0° and 120°; b) at χ = 30° and 135°; c) at χ = 45° and 150°; d) at χ = 60° and 180°

The dynamic loading on the tank car in ferry transportation was determined by a mathematic model (2.20). It involved the absence of displacements of a tank car relative to the deck during the ferry oscillations, i.e. it implied that only liquid freight was engaged in the oscillation process. The case of angular displacements of a train ferry relative to the longitudinal axle was taken into account.

$$\begin{cases} \left(\frac{D}{12\cdot g}\left(B^2+4z_g{}^2\right)\right)\ddot{\theta}_1+\left(\Lambda_\theta\cdot\frac{B}{2}\right)\dot{\theta}_1=p'\cdot\frac{h}{2}+\Lambda_\theta\cdot\frac{B}{2}\cdot\dot{F}(t), \\ I_{ij}\cdot\ddot{\theta}_2-m_{ij}\cdot c_{ij}\cdot l_{ij}\cdot\ddot{\theta}_1+g\cdot m_{ij}\cdot l_{ij}\cdot\theta_2=0, \end{cases} \quad (2.20)$$

where I_{ij} – inertia moment of a pendulum;
m_{ij} – pendulum mass in the tank car's barrel;
c_{ij} – distance from the plane $z_i = 0$ to the point where the pendulum was fixed in the tank car's;
l_{ij} – pendulum length;
I_θ – reduced inertia moment of a barrel with liquid freight which did not move relative to the barrel;
z_{ci} – height of the weight center of a tank car;
m_i – mass of the body equivalent to the barrel with part of the liquid freight which did not move relative to the barrel.

The movement of the liquid freight in the barrel was described according to [114]. The hydrodynamic characteristics of the liquid freight were determined by the technique presented in [115]. The research used petrol as the liquid freight. The calculation was based on the maximum admissible loading of a tank with liquid freight according to [116].

The results of the calculation are given in Figure 2.12. The total value of acceleration on the tank car farthest from the bulwark was 0.31 g.

The values of accelerations obtained differ from those given in [81, 82], where the acceleration at a roll angle of for the Caspian Sea was 1g. Therefore, there is a need to improve and complement the normative values of the forces on the cars in train ferry transportation.

The above-mentioned mathematic models can use the input parameters for determining the dynamic loads on the body of a passenger car in sea transportation [118].

Thus, for the case of displacements of a passenger car body relative to the deck the accelerations obtained are presented in Figure 2.13.

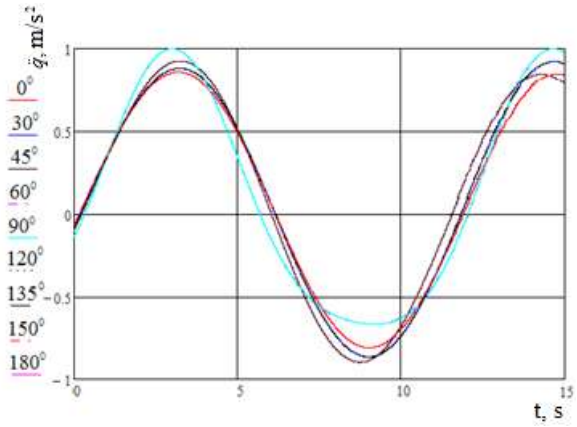

Figure 2.12 – Accelerations to the tank car farthest from the bulwark

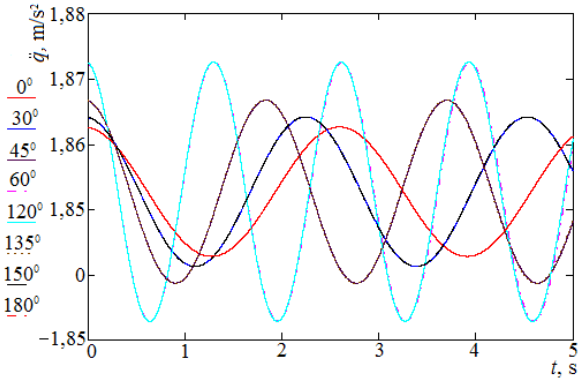

Figure 2.13 – Accelerations on the passenger car body in train ferry transportation

The study established that the maximum acceleration to the car body at wave angles of 60° and 120° to the train ferry body accounted for about 1.9 m/sec^2. It implies that it exceeded the value of accelerations on the passenger car body in operation on the main tracks by 20 % (at a satisfactory estimation of motion of an empty car) [81, 82].

2.3 Computer modelling of dynamic loads on the freight car body in train ferry transportation

The computer modelling of dynamic loads on the car bodies located on the train ferry under the sea disturbance conditions is based on the spatial model of a fragment of the ferry *Geroi Shipki* [105]. The basic structural elements were included in the model. The length of the model was 39.6 m, and the breadth – 26 m [50].

The research was made for a 12-757 open car manufactured at Kryukiv Railway Car Building Works.

The spatial model of a train ferry fragment with open cars on the deck is given in Figure 2.14.

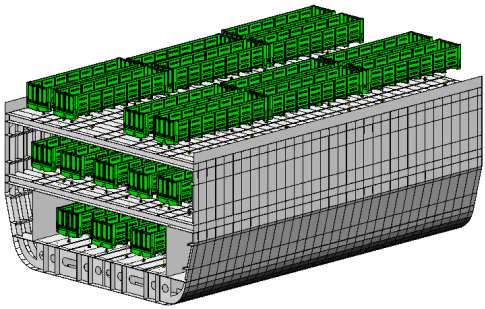

Figure 2.14 – Spatial model of a train ferry fragment with cars on the decks

The research involved the building of the spatial model of a mechanical support jack, taken from the Album of drawings of reusable lashing devices, to provide supports for the carrying structures of car bodies (Figures 2.15).

On the basis of this spatial model the authors designed a model for determination of the accelerations of the cars located on the train ferry.

The calculation was made with the finite element method [96–98] in CosmosWorks software (version 2015) [99–102].

The finite element model (Figure 2.16) was built with spatial isoparametrical tetrahedrons (Figure 2.16). The number of nodes in a mesh was 149 223, and the number of elements – 500 354. The maximum size of an element was 1 000 mm, and the minimum size – 200 mm. The minimum number of elements in a circle was 15; the element size gain ratio in a mesh was 1.8. The maximum side ratio was $9{,}5 \cdot 10^5$, the percentage of elements with a side ratio less than three was 6.96 and more than ten was 81.5.

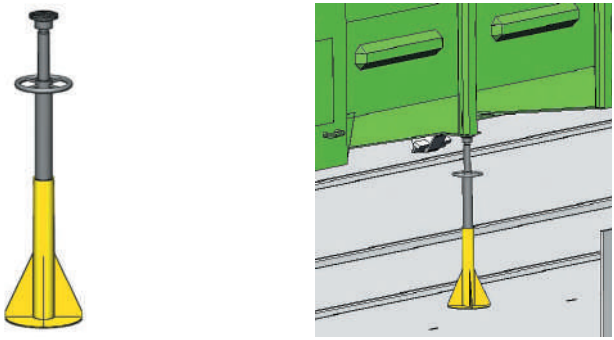

a) b)

Figure 2.15 – Modelling of interaction between the open car body and the mechanical support jack:
a) in free state; b) during interaction with a car body

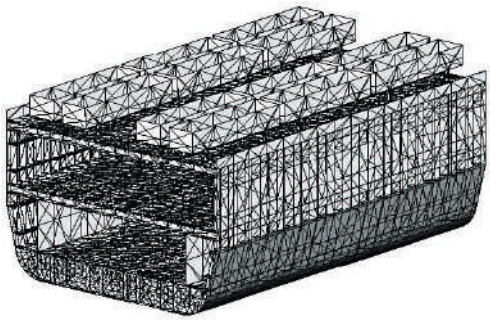

Figure 2.16 – Finite element model of a fragment of the train ferry *Geroi Shipki* loaded with car bodies

The model considered the following forces on the train ferry: vertical static P_v^{st}, conditioned by gross weight of ferry, wind force P_w, hydrostatic force P_h on the underbody of the ferry, buoyancy force P_b, forces on the ferry deck through the rail cars both vertical P_{bv} and horizontal P_{hv}, and also forces on the deck through the multiple-use lashing devices, i.e. chain binders P_{cb} and mechanical support jacks P_j.

Figure 2.17 presents a design diagram of a train ferry loaded with car bodies on the decks during angular displacements relative to the longitudinal axle as the case of the largest loading on the carrying structure of car bodies during sea disturbance.

As far as the calculation involved only a train ferry fragment, in order to take into account the rest, vertical, longitudinal and transverse forces were applied in the appropriate sections. The numerical values of these forces were defined by the method of sections.

The determination of forces on the deck through the cars involved the roll angle of a train ferry; the horizontal force from the wheel flanges to the rails on the internal side of the excitation force included the free fall acceleration component, wind and inertia forces.

The determination of the wind force on the topside projection of a train ferry loaded with car bodies on the upper deck included the wind force which is typical of the Black Sea, the value of which is equal to 1.47 kN/m^2 [79].

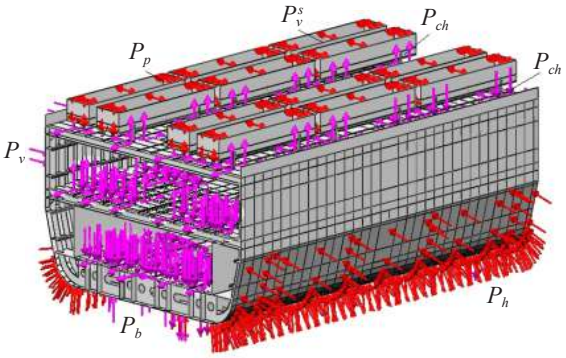

Figure 2.17 – Design diagram of a train ferry fragment loaded with car bodies

The force on the train ferry deck through chain binders was modeled with the pads the geometry of which was similar to that of the area where a ring was fastened to the deck. Due to the spatial location of chain binders, the force on the deck through them was decomposed with consideration of spatial angles of the chains (Figure 2.18). The pads were also installed in the areas where mechanical support jacks rested on the deck; their geometry was similar to the geometry of the support jack foundation. The forces on the pads were determined with consideration of the roll angle of a train ferry. They were smaller on the external side of the disturbing force, and larger on its internal side.

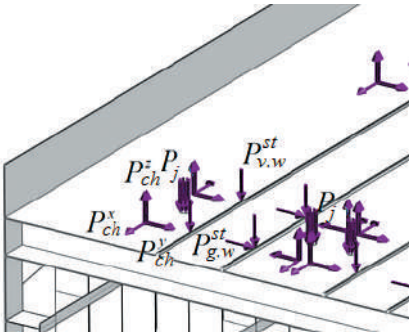

Figure 2.18 – Diagram of forces on the ferry deck from cars and reusable lashing devices

Steel Grade D was used for the train ferry; the ultimate strength is $\sigma_s = 440 – 590$ MPa and the creep stress $\sigma_c = 315$ MPa, Steel 09G2S with $\sigma_s = 490$ MPa and $\sigma_c = 345$ MPa was used for the carrying structure of a car.

The research involved the following forces impacting the carrying structure of an open car (Table 2.5): vertical static force P_v^{st} conditioned by the gross weight of a car, wind force P_v on the car farthest from the bulwark and located from the wind force, pressure from the bulk freight (black coal), and forces on the open car body through the chain binders P_{ch}^i.

Table 2.5 – Forces on the open car body symmetrically fixed on the deck in train ferry transportation

Car body displacements	Forces on open car body				Force components on open car body through chain binders									
	Vertical static force, kN	Wind force, kN	Pressure (from tilt side of body), kPa	Tension force through chain binders, kN	Dynamic force, kN			Wind force, kN			Tension force through chain binders, kN			
					XY	YZ	XZ	XY	YZ	XZ	XY	YZ	XZ	
Angular forces relative to transverse axle	p_x=53.2 p_z=829.13	10.96	7.47	54	p_x=6.65 p_y=11.52	p_y=6.65 p_z=11.52	p_x=6.65 p_z=11.52	p_x=1.37 p_y=2.37	p_y=1.37 p_z=2.37	p_x=1.37 p_z=2.37	p_x=27 p_y=47	p_y=27 p_z=47	p_x=27 p_z=47	
Angular forces relative to longitudinal axle	p_y=209.22 p_z=811.18	41.61	15.5	54	p_x=26.16 p_y=45	p_y=26.16 p_z=45.3	p_x=26.16 p_z=45.3	p_x=5.2 p_y=9.0	p_y=5.2 p_z=9.0	p_x=5.2 p_z=9.0	p_x=27 p_y=47	p_y=27 p_z=47	p_x=27 p_z=47	

The open car body was fixed according to the diagrams given in [49, 51, 52]. As far as a chain binder had spatial location, the forces to the body through it were decomposed into three elements. The results of research into the accelerations on the car bodies located on the train ferry are given in Figure 2.19. The research consisted of three stages in order to shorten the computation time. The open cars were located on the upper deck for the first stage, on the main deck for the second stage, and on the hold deck for the third stage.

The adequacy of the model was checked with an F-test.

$$F_p = \frac{S_{ad}^2}{S_{sq}^2}. \tag{2.21}$$

The dispersion of adequacy was calculated by the formula:

$$S_{ad}^2 = \frac{\sum_{i=1}^{n}\left(y_i - y_i^p\right)}{f_i}, \tag{2.22}$$

where y_i^p – design value of the variable obtained in modelling;
f_i – number of degrees of freedom.

$$f_i = N - q, \tag{2.23}$$

where N – number of tests in the planning matrix;
q – number of equation coefficients.

The error mean square was defined by the formula:

$$S_{sq}^2 = \frac{1}{N}\sum_{i=1}^{n} S_i^2, \tag{2.24}$$

where S_i^2 – dispersion in each line with parallel tests.

Let us consider that the model under study was linear, therefore it was one-factor and characterized a change in accelerations of the open car bodies, which took into account the location of the bodies on the deck. The number of degrees of freedom at $N = 5$ was $f_1 = 3$.

At angular displacements of a train ferry loaded with cars relative to the transverse axle, the value of error mean square was $S^2_{sq} = 0.002$ and the value of dispersion of adequacy was $S^2_{ad} = 0.0007$. The actual value of an F-test was $F_1 = 2,86$, i.e. lower than the tabular value of the criterion $F_1 = 5,41$. It implied that the hypothesis on adequacy was not rejected. The approximation error at this case was about 10 %.

a)

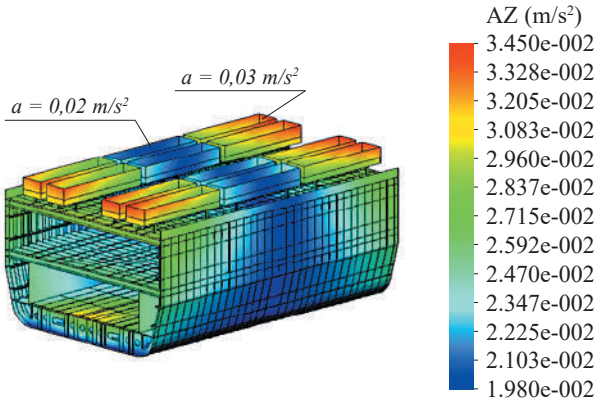

b)

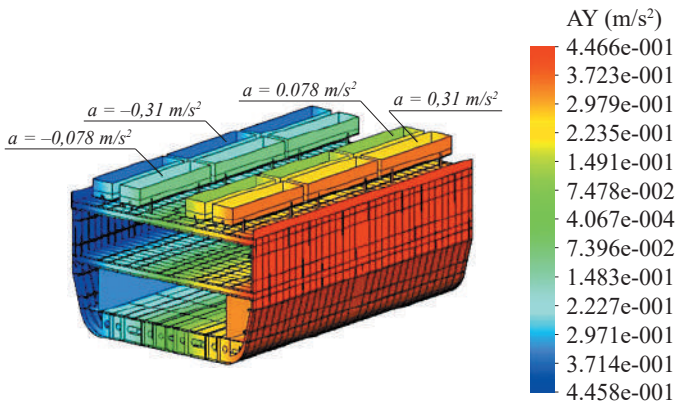

Figure 2.19 – Accelerations to the car bodies located on the upper deck of a train ferry:
a) at angular displacements relative to the transverse axle;
b) at angular displacements relative to the longitudinal axle

At angular displacements of a train ferry loaded with car bodies relative to the longitudinal axle the following values were obtained: the value of error mean square $S_{sq}^2 = 0.07$ and the value of dispersion of adequacy $S_{ad}^2 = 0.017$ at $f_2 = 5$, therefore it was established that the actual value of an F-test was $F_p = 5{,}24$, which was lower than the tabular value $F_t = 5{,}41$. It implies that the hypothesis on adequacy was not rejected. The approximation error in that case was about 6 %.

2.4 Determination of strength characteristics for the carrying structure of a car body in ferry transportation

2.4.1 Determination of strength characteristics for the carrying structure of an open car body in ferry transportation

A 12-757 model was used for determination of the strength characteristics of the carrying structure of an open car in ferry transportation.

The four-axle universal open car (Figure 2.20) is intended for transportation of bulk, bulky, piece (including long items), block and other types of freight which do not require protection from weather.

Figure 2.20 – Universal open car

An open car had all-steel body which consisted of side walls, frame, end doors, floor with 14 unloading hatches, automatic coupler, gear part, automatic and parting brakes.

All the basic carrying elements of an open car body were made of low-carbon Steel 09G2D.

The side wall framing consisted of top and bottom cords, angular and middle posts. The boxed top cord was made up of two special profiles folded out of a 6-mm sheet and an angular hot-rolled profile with a folded flange. The bottom cord was made up of an angular 160 × 100 × 10-mm profile. The components of a locking mechanism for the unloading hatch covers were mounted on the bottom cord.

The angular posts were made of a pressed 10-mm sheet of constant section; they were reinforced with a line in the high-stress zone. Higher strength of the angular posts was achieved by their installation at 390 mm lower than the bottom cord triangle. The stepping boards and rails were mounted diagonally to the angular posts.

The middle posts were made of a hot-rolled special profile. The bottom inside part of the posts was reinforced with strips; these strips were joined to the transverse beams of the frame.

The side wall lining consisted of two roll-formed corrugated overlap-welded profiles. The upper sheet of the size 1300 × 12075 × 3.6 mm had two rows of corrugation; the lower sheet of the size 815 × 12075 × 4.5 had one row of corrugation. Steel 10CrNiCuP was used as the lining material.

The frame consisted of a center sill, two end beams, two bolster beams and four middle transverse beams. Couplers, brake equipment, and unloading hatch covers with locking and elevating mechanisms were installed on the frame.

The main bearing element of the frame was the center sill consisted of three hot-rolled profiles: two reinforced Z-profiles № 31 and a special T-profile (190 mm in height) welded to each other. The hands of hatch covers were fastened to the T-profile. Standard front and rear coupler's supports were mounted on the center sill ends. The contact areas of the center sill and the bolster beams were reinforced with

welded boxes. The contacts between the middle transverse beams and the center sill were also reinforced with diaphragm plates.

The end beam of welded structure consisted of a front plate, two rear plates, two bottom plates and four diaphragm plates. The front sheet had reinforced under-buffer plates used for installation of typical buffer devices. The diaphragm plates had oval gaps in the bottom part for tightening screws while mounting the buffers. The hatch cover supports and lines were mounted on the end beam to protect the bogies from fine fractions of bulk freight during unloading through the floor hatches.

The bolster beams were box-section welded structures of variable rigidity, they consisted of the upper cord of form-rolled profile, four vertical sheets, gussets and the bottom cord. A distance between vertical sheets of the bolster beam in the transverse section was increased from 128 to 150 mm. In comparison with those of old-design open cars, the width of bottom and upper sheets of the beam was increased by 20 mm. Besides, a distance from the folding of a lower sheet to the flange of a Z-profile of the center sill was increased by 40 mm.

The bottom sheets of bolster beams had side slides and center plates which provided interaction of the body and the bogies.

The middle transverse beams were composed of the top cord of form-rolled profile, two vertical and two lower sheets. The hatch cover supports were welded to the vertical sheets of the transverse beams. The vertical sheets of the middle beams were of constant height.

The end doors of the body in the closed state acted as the end walls of an open car. Their structure and the locking mechanism were similar to those of old-design cars.

With open doors the body could hold and transport long freight (timber, pipes) with length exceeding the inner body length, and wheeled equipment.

The floor of an open car body was formed by the vertical sheets of the frame beams and the surfaces of the unloading hatch covers. The closed hatch covers were fixed with locking mechanisms, and the open hatch covers rested on the supports located on the transverse beams. The hatch cover consisted of a framework and a lining plate.

The hatch cover lining was made of Steel 10CrNiCuP in the form of roll-formed profile with six corrugations and a rear bund to avoid gaps between the cover and the T-profile of the center sill when the hatch covers were opened. The elements of a cover framework were made of Steel 09G2D.

The locking mechanism for the hatch covers consisted of door drop latches and turning sectors suspended to the bottom cord of a side wall through bearings. A torsional mechanism was used to facilitate the opening of a hatch cover; it accumulated the elastic energy generated when the hatch cover closed down and released it when the hatch cover opened up.

The torsion was mounted on the cover in the supports and it was pivotally-connected to the lever linked with the center sill.

A spatial model in SolidWorks software was built to investigate the strength of an open car body in terms of interaction with reusable lashing devices during ferry transportation (Figure 2.21).

a)

b)

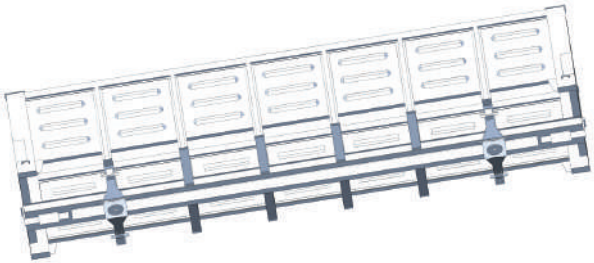

Figure 2.21 – Carrying structure of an open car body:
a) side view; b) bottom view

The model included only the elements rigidly connected (welded or riveted). As far as the hatch covers were not connected to the body frame rigidly but pivotally and acted as the elements transferring loading to the frame elements rigidly connected, they were disregarded in the model.

The design model disregarded longitudinal forces to the open car body through an automatic coupler, as they were restricted by a buffer stop installed on the end of a car batch with by brake shoes. Fixation of an open car body was simulated by additional links in the zones where the body rested on the center plates of bogies, plungers and support jacks. The research studies the least stable fixation of an open car on the deck (Figure 2.22).

Figure 2.22 – Fixation of an open car on the ferry deck

The design diagram of an open car body (Figures 2.23 and 2.24) involved such forces: vertical static $P_v^{(st)}$, pressure from bulk freight P_p, dynamic P_i, wind force and forces on the open car body through the chain binders P_{ch}.

Due to spatial location of a chain binder, the force through it to the carrying structure of an open car body was decomposed (Figure 2.25).

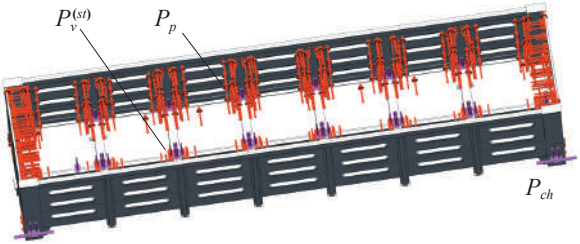

Figure 2.23 – Design diagram of the carrying structure of an open car body at angular displacements relative to transverse axle

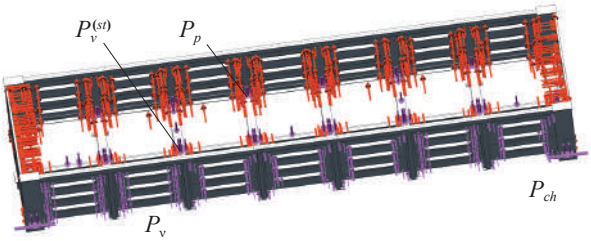

Figure 2.24 – Design diagram of the carrying structure of an open car body at angular displacements relative to the transverse axle

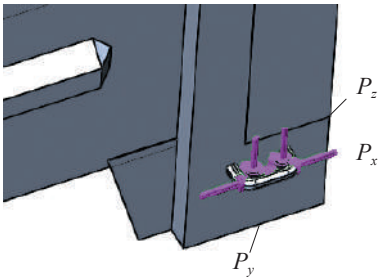

Figure 2.25 – Diagram of forces through the chain binders

The finite element model (Figure 2.26) used isoparametrical tetrahedrons the optimal number of which was defined by the graphic analytical method. The number of elements in a mesh was 494 440, the number of nodes – 160 329, the maximum element size – 80 mm, the minimum element size – 16 mm, the maximum element side ratio – 550.85; the percentage of elements with a side ratio of less than three – 27.3; and more than ten – 0.212. The element size gain ratio was 1.7. The number of elements in a circle was 9.

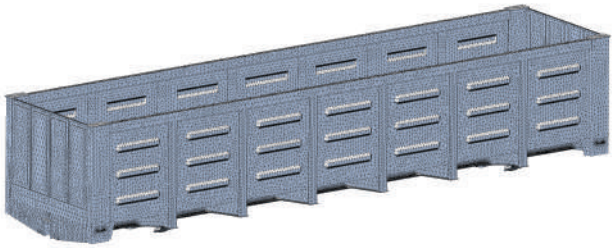

Figure 2.26 – Finite element model of the carrying structure of a flat car

Black coal was taken as bulk freight as one of the most popular type of freight transported in open cars by sea.

The pressure from the bulky freight to the walls of an open car body was determined by the method based on Coulomb's law used for calculation of support walls with Sinelnicov's adjustment [106–110]. The calculation also included the value of acceleration on the car body.

And the formula for determining the pressure from the bulk freight looks like [36–38]:

$$p = \gamma' h' \frac{\cos^2(\rho' + \alpha')}{\left[1 + \sqrt{\frac{\sin\rho' \sin(\rho' \pm \alpha')}{\cos\alpha'}}\right]^2 \cos\alpha'} g \pm F_{pr}^{\theta}, \qquad (2.25)$$

where γ' – volumetric mass of freight;

h' – height of an open car body;
ρ' – internal friction angle (for ideal bulky freight it equals the angle of natural slope);
α' – tilt angle of an open car relative to longitudinal axle;
F_{pr}^{θ} – additional pressure conditioned by the dynamic component on the bulky freight at angular displacements of a train ferry relative to the longitudinal axle.

On the basis of the calculation at $\alpha' = 12{,}2°$ the authors obtained the maximum value of pressure from the bulk freight to the side wall of an open car body of about 15 kPa.

The calculated values of the forces on the open car body in train ferry transportation are given in Table 2.5.

The strength calculation for an open car was made with the finite element method in CosmosWorks software.

The results of the calculation are given below.

Figure 2.27 – Stress state of an open car body at angular displacements relative to the transverse axle

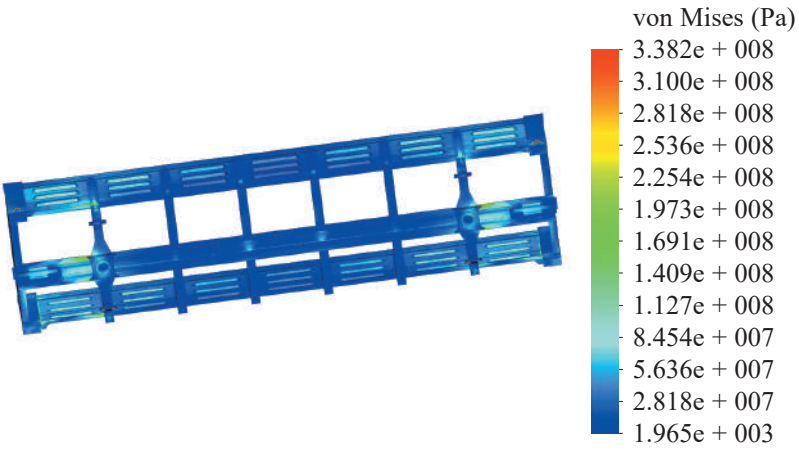

Figure 2.28 – Stress state of an open car body at angular displacements relative to the longitudinal axle

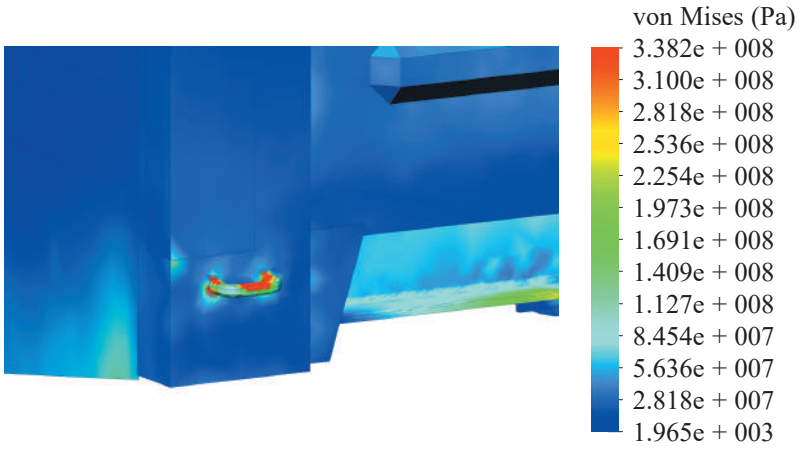

Figure 2.29 – Stress state of an open car body at angular displacements relative to the transverse axle

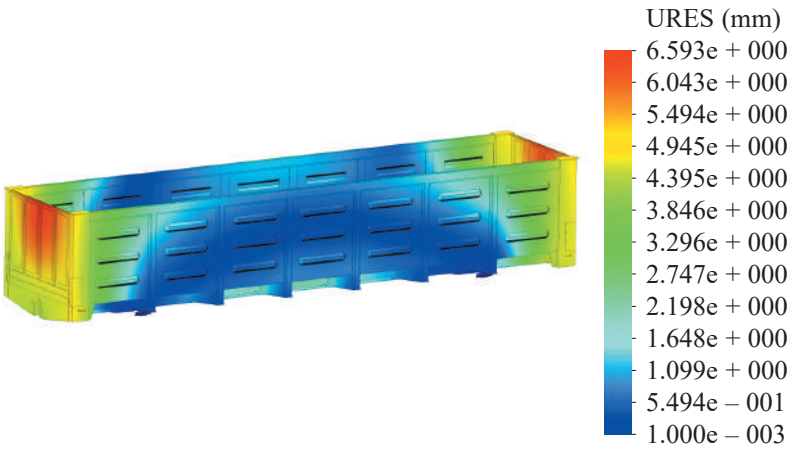

Figure 2.30 – Displacements in the units of an open car bogy at angular displacements relative to the transverse axle

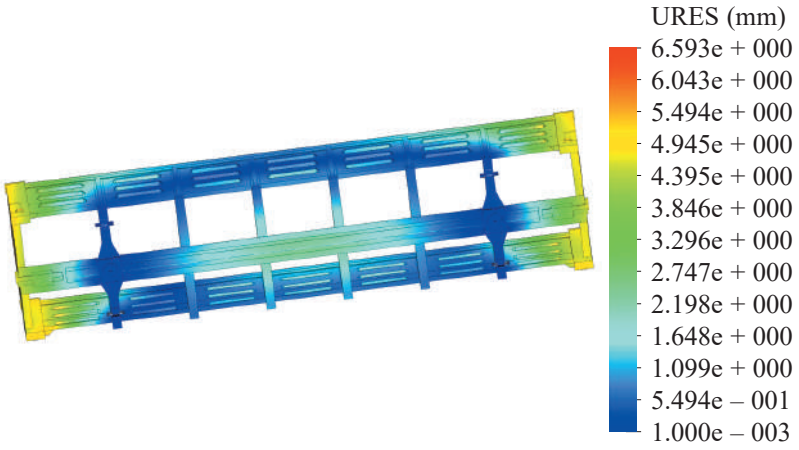

Figure 2.31 – Displacements in the units of an open car body at angular displacements relative to the longitudinal axle

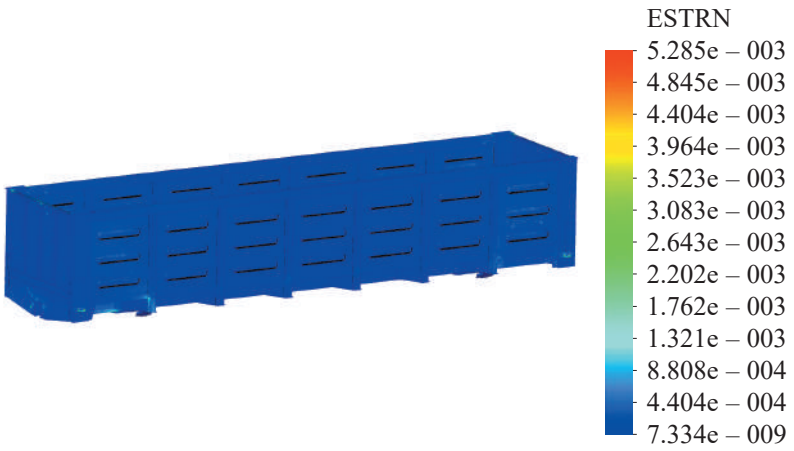

Figure 2.32 – Deformations in the open car body at angular displacements relative to the transverse axle

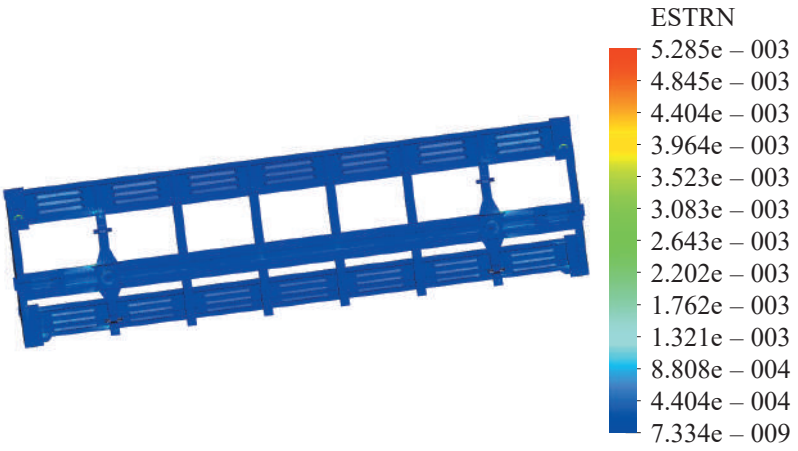

Figure 2.33 – Deformations in the open car body at angular displacements relative to the longitudinal axle

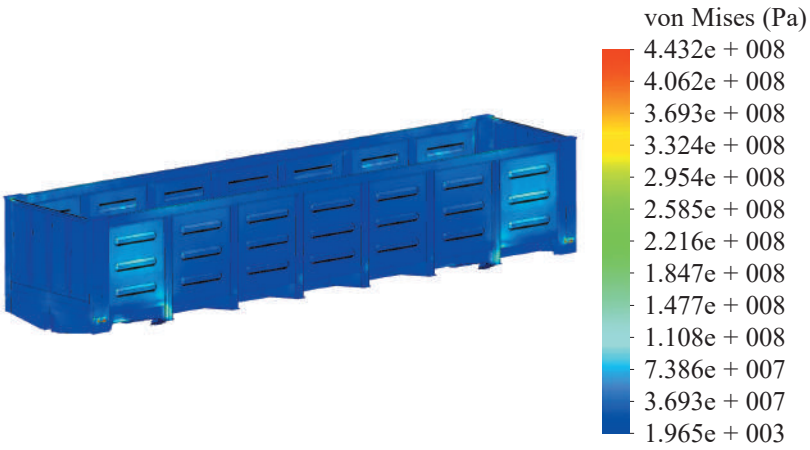

Figure 2.34 – Stress state of an open car body at angular displacements relative to the longitudinal axle

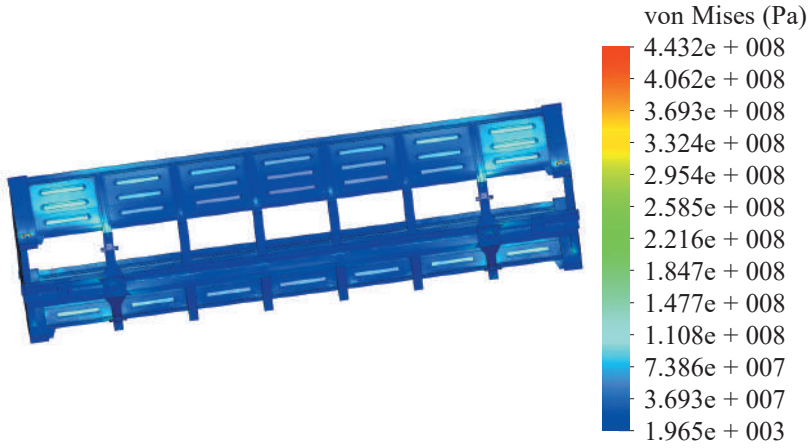

Figure 2.35 – Stress state of an open car body at angular displacements relative to the transverse axle

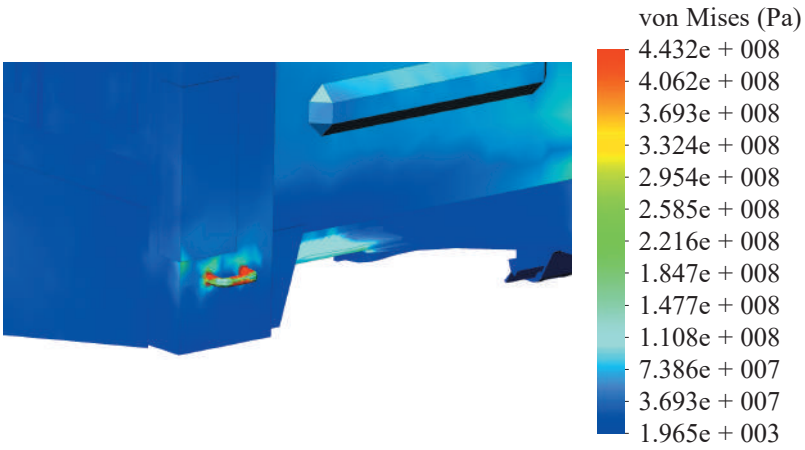

Figure 2.36 – Stress state of an open car body at angular displacements relative to the longitudinal axle

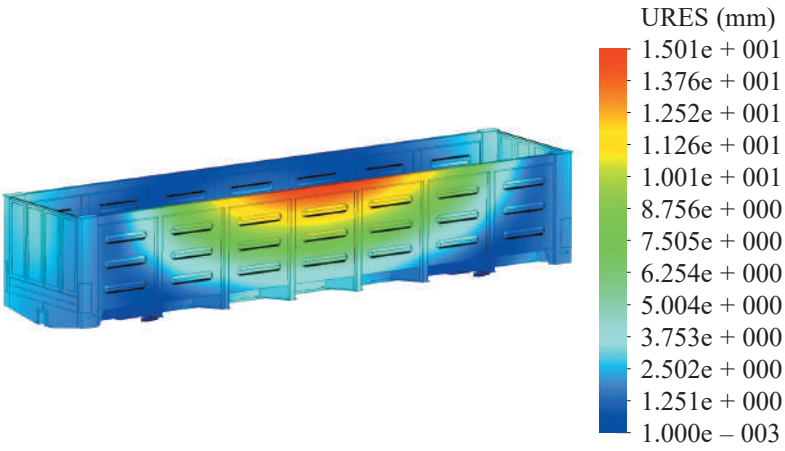

Figure 2.37 – Displacements in the units of an open car body at angular displacements relative to the longitudinal axle

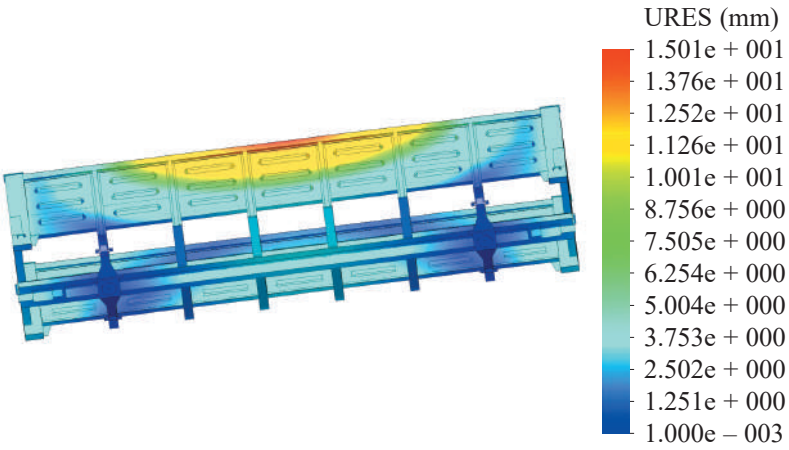

Figure 2.38 – Displacements in the units of an open car body at angular displacements relative to the longitudinal axle

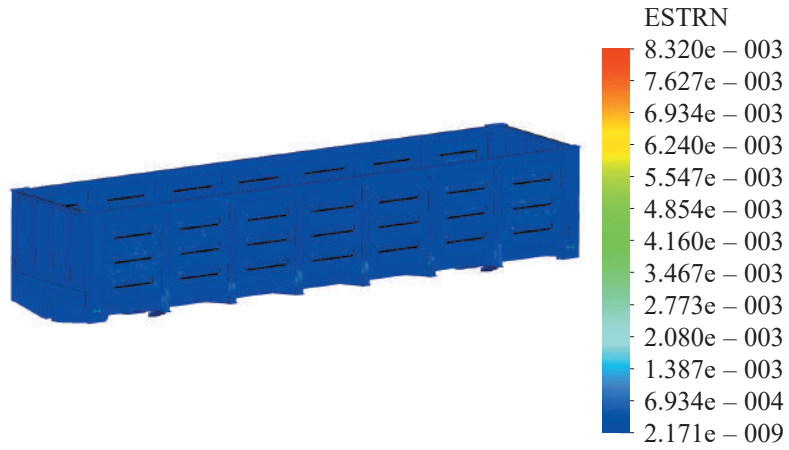

Figure 2.39 – Deformations in the open car body at angular displacements relative to the longitudinal axle

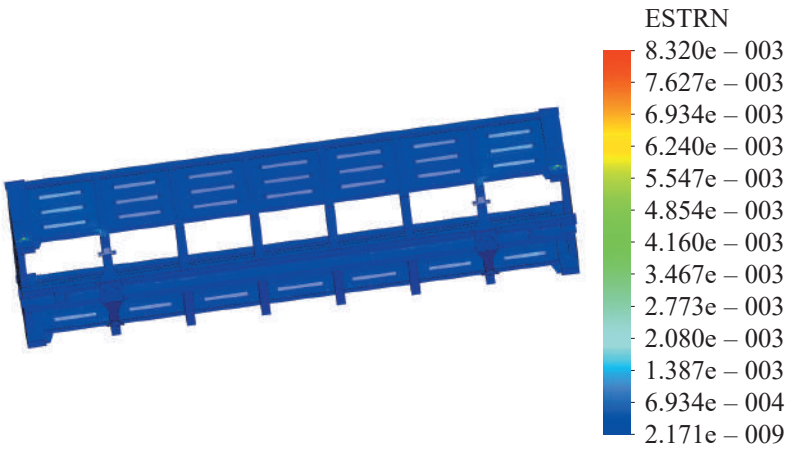

Figure 2.40 – Deformations in the open car body at angular displacements relative to the longitudinal axle

The results of the calculation demonstrated that the maximum equivalent stresses in the body of an open car appeared at angular displacements of a train ferry about the longitudinal axle and accounted for about 440 MPa. The maximum displacements were in the side wall of an open car body and they were 15 mm. The maximum deformations were $8.3 \cdot 10^{-3}$.

At angular displacements of an open car body relative to the transverse axle the maximum equivalent stresses equaled 338.2 MPa. The maximum displacements were 6.6 mm, and the maximum deformations were $5.3 \cdot 10^{-3}$.

Thus, with consideration of a typical fixation pattern for an open car on the deck, the maximum equivalent stresses in the body elements exceeded the admissible values. It can cause damage of lashing devices used for an open car body, break of the devices and loss of stability by the car on the deck.

2.4.2 Determination of strength characteristics for the carrying structure of a tank car in ferry transportation

The strength characteristics of the carrying structure of a tank car in ferry transportation were determined for a 15-1443 model taken as the base model.

A four-axle tank car with loading capacity of 60 tons had a barrel with capacity of 71.7 m^3 and total capacity of 71.3 m^3 (Figure 2.41). The internal diameter of the barrel was 3000 mm. The bottom sheet depth was 11 mm, the depth of upper and side sheets – 9 mm, and the depth of the lower sheet – 10 mm. All sheets and bottoms were welded by butt-joints. The tare of a tank car was 23.2 tons.

Figure 2.41 – Tank car of model 15-1443

The frame had light-weighted end and side beams, the latter ones were left only in the end parts of the frame. There were no middle and transverse beams.

The barrel was fixed on the frame in the middle and end parts. The shaped feet were welded to the middle part of the bottom plate, bolted through the adjusted slots to the support planes welded to the center sill of the frame.

On their ends the barrel rested on wooden blocks fastened through grooves, cotter bolts and middle frames to the bolster beams and center sills of the frame.

The barrel was tightened to the end posts with tension bends used for avoiding its vertical and transverse displacements relative to the frame. The length of the tension bends was regulated by sleeve nuts.

The tank car was equipped with external stairs with areas near the dome, universal drain valve and a safety-input valve. The complete freight discharge was provided by a special form of the bottom plate which gave a slope to a drainage valve.

The spatial model of the carrying structure of a tank car was built in SolidWorks software (Figure 2.42).

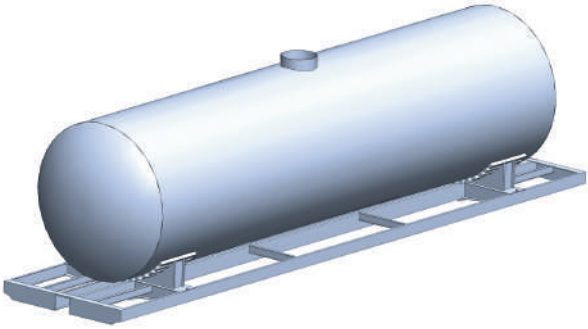

Figure 2.42 – Carrying structure of a tank car

The finite element model of the carrying structure of a tank car is given in Figure 2.43.

The finite element model was built with isoparametrical tetrahedrons. The optimal number of elements in a mesh was determined with the graphic analytical method. The number of elements in a mesh was 778 286, the number of nodes – 253 823. The maximum element size in a mesh was 40.0 mm, the minimum size – 8.0 mm, the maximum element side ratio – 105.21; the percentage of elements with a side

ratio of less than three – 18.4, and more than ten – 0.371. The minimum number of elements in a circle was 9 and the element size gain ratio in a mesh was 1.7.

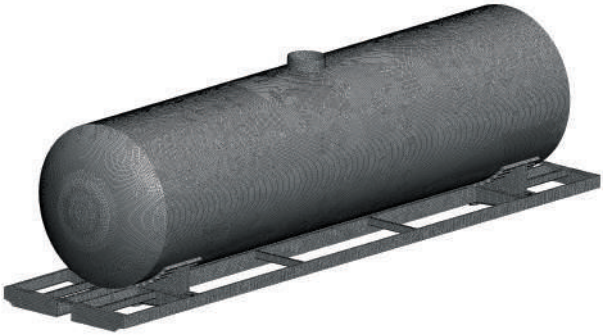

Figure 2.43 – Finite element model of the carrying structure of a tank car

The pressure to the barrel's interior wall was defined on the basis of the hydrostatic dependency [111]:

$$p = p_{st} + \rho \cdot \alpha_{eq} \cdot h, \tag{2.26}$$

where p_{st} – saturated steam pressure;
ρ – bulk freight density;
p_{eq} – equivalent acceleration of liquid freight;
α_{eq} – distance from a point on the barrel's interior surface to the free surface area.

The least stable fixation of a tank car on the deck was taken into account (Figure 2.44).

Figures 2.45 and 2.46 present the diagrams of forces to the carrying structure of a tank car during train ferry transportation. The calculated values of the forces on the carrying structure of a tank car in train ferry transportation are given in Table 2.6.

The results of the calculation are given in Figure 2.47–2.54.

Figure 2.44 – Fixation pattern of a tank car on the train ferry deck

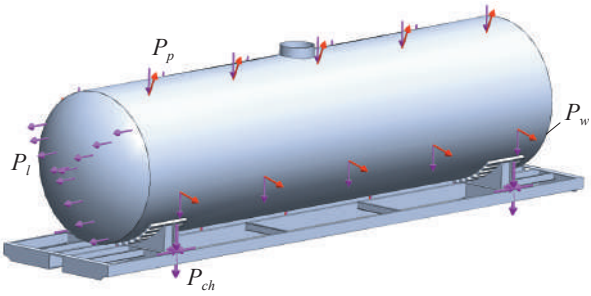

Figure 2.45 – Design diagram of the carrying structure of a tank car at angular displacements about the transverse axle

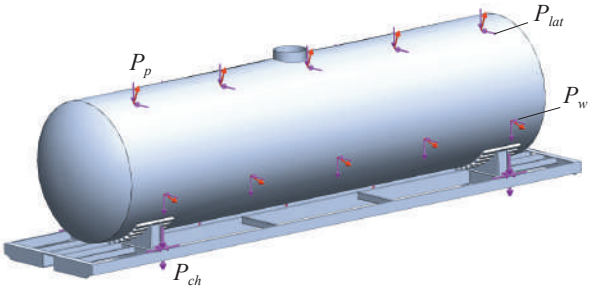

Figure 2.46 – Design diagram of the carrying structure of a tank car at angular displacements about the longitudinal axle

Table 2.6 – Forces on the carrying structure of a tank car symmetrically fixed on the deck in train ferry transportation

Displacements of car body	Forces on car body				Force components on car body through chain binders									
	Vertical static force, kN	Wind force, kN	Pressure from freight, kPa	Tensile force through chain binders, kN	Dynamic force, kN			Wind force, kN			Tension forces through chain binders, kN			
					XY	YZ	XZ	XY	YZ	XZ	XY	YZ	XZ	
Angular forces relative to the transverse axle	p_x=46.34 p_z=723.3	10.4	172.8	54	p_x=5.79 p_y=10.03	p_y=5.79 p_z=10.03	p_x=5.79 p_z=10.03	p_x=1.3 p_y=2.25	p_y=1.3 p_z=2.25	p_x=1.3 p_z=2.25	p_x=27 p_y=47	p_y=27 p_z=47	p_x=27 p_z=47	
Angular forces relative to longitudinal axle	p_y=137.2 p_z=634.7	74.57	190	54	p_x=17.15 p_y=29.7	p_y=17.15 p_z=29.7	p_x=17.15 p_z=29.7	p_x=9.32 p_y=16.14	p_y=9.32 p_z=16.14	p_x=9.32 p_z=16.14	p_x=27 p_y=47	p_y=27 p_z=47	p_x=27 p_z=47	

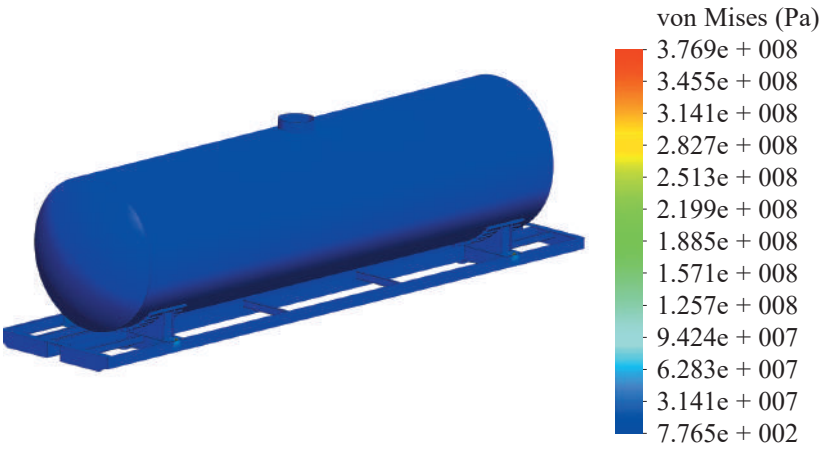

Figure 2.47 – Stress state of the carrying structure of a tank car at angular displacements relative to the transverse axle

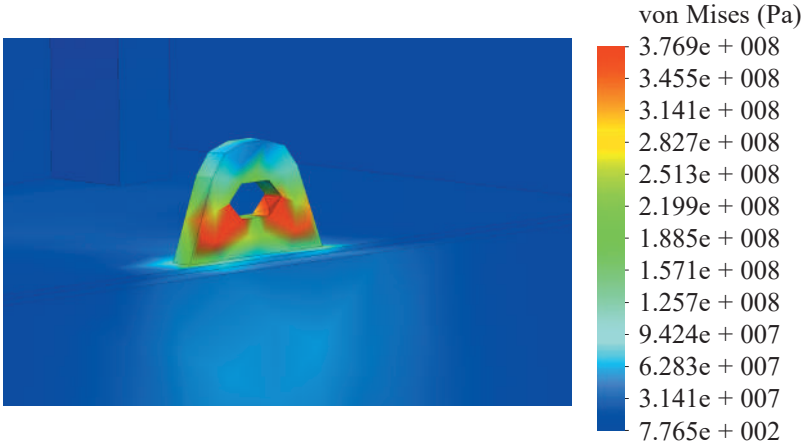

Figure 2.48 – Stress state of the carrying structure of a tank car at angular displacements relative to the transverse axle

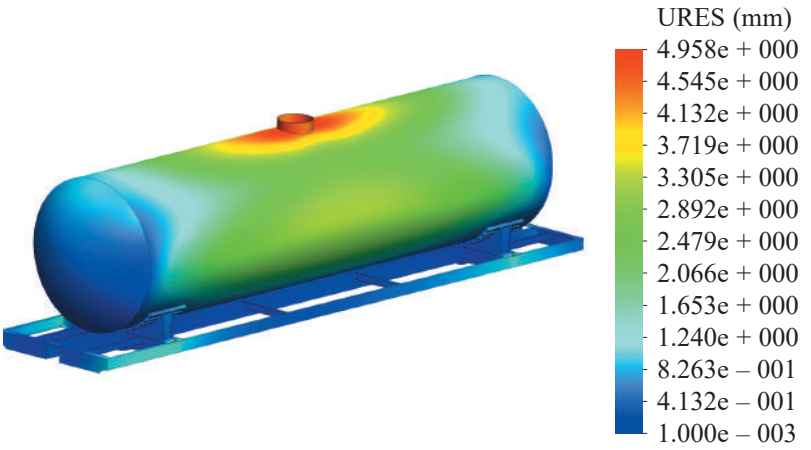

Figure 2.49 – Displacements in the units of the carrying structure of a tank car at angular displacements relative to the transverse axle

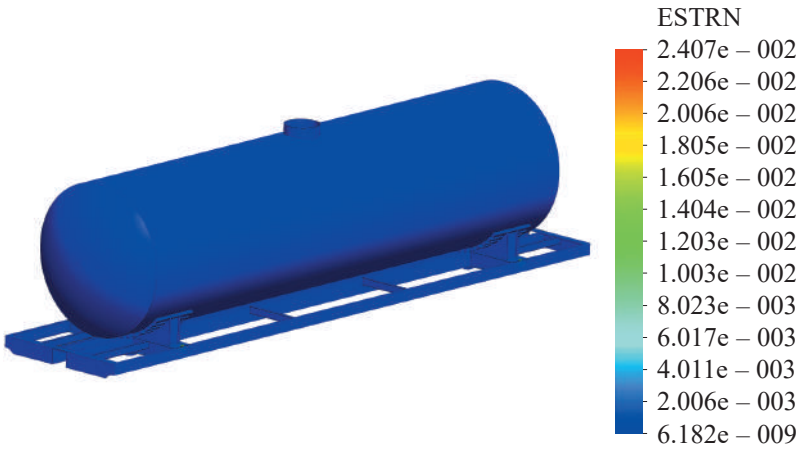

Figure 2.50 – Deformations in the carrying structure of a tank car at angular displacements relative to the transverse axle

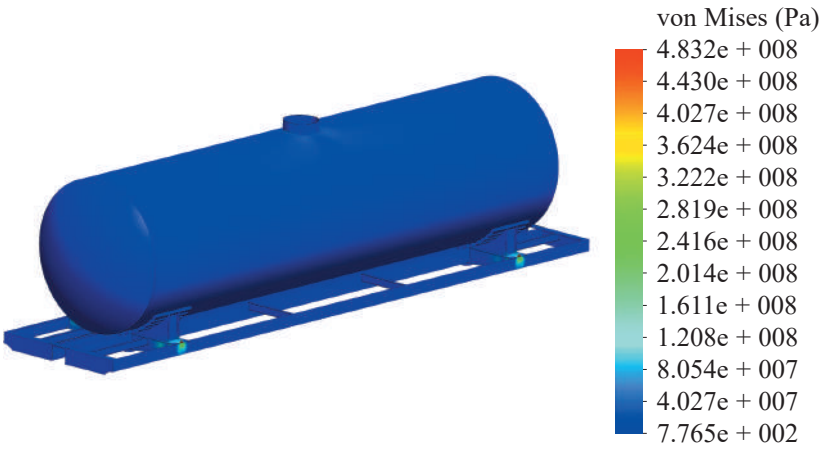

Figure 2.51 – Stress state of the carrying structure of a tank car at angular displacements relative to the longitudinal axle

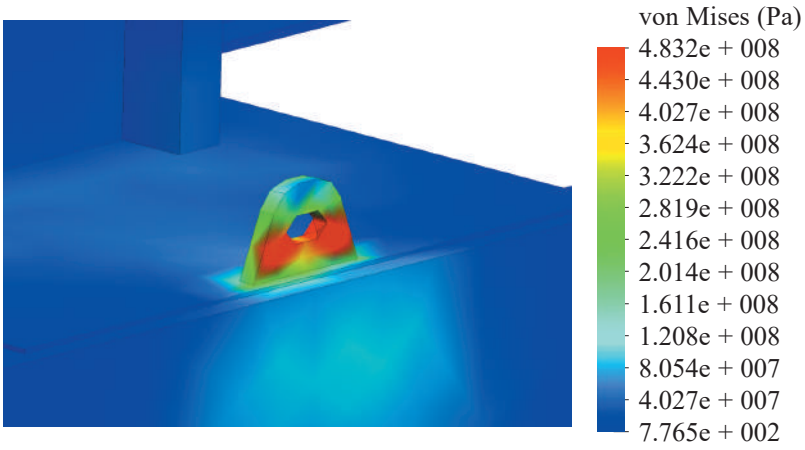

Figure 2.52 – Stress state of the carrying structure of a tank car at angular displacements relative to the longitudinal axle

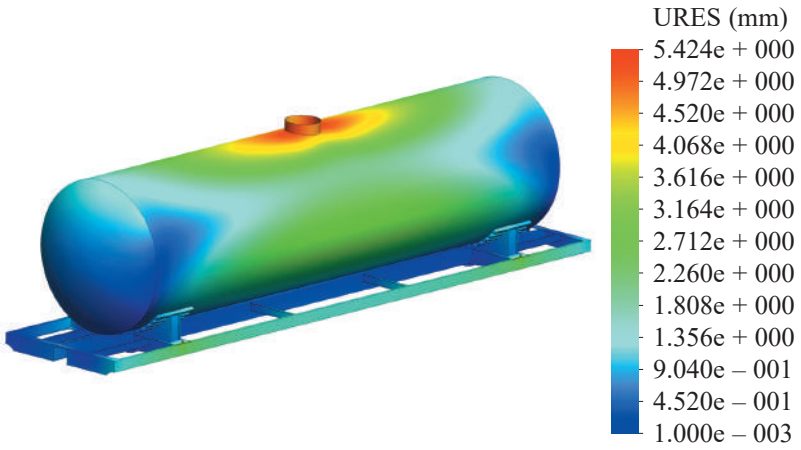

Figure 2.53 – Displacements in the units of the carrying structure of a tank car at angular displacements relative to the longitudinal axle

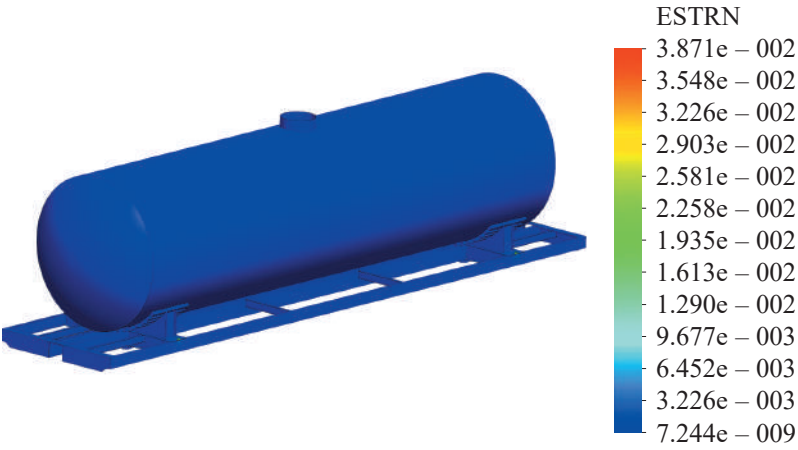

Figure 2.54 – Deformations in the carrying structure of a tank car at angular displacements relative to the longitudinal axle

The results of calculation demonstrated that the maximum equivalent stresses in the carrying structure of a tank car appeared at angular displacements of a train ferry about the longitudinal axle and accounted for about 480 MPa. The maximum displacements emerged around unloading hatches and accounted for 5.4 mm. The maximum deformations were $3.8 \cdot 10^{-2}$.

At angular displacements of the carrying structure of a tank car relative to the transverse axle, the maximum equivalent stresses were equal to about 380 MPa. The maximum displacements were about 5.0 mm, and the maximum deformations were $2.4 \cdot 10^{-2}$.

The values of maximum equivalent stresses obtained exceeded the admissible values for the given metal structure grade used for a tank car. Therefore, the typical fixation pattern of a tank car did not ensure stability of the carrying structure in train ferry transportation and endanger the safety.

2.4.3 Determination of strength characteristics of the carrying structure of a boxcar in ferry transportation

The strength characteristics of the carrying structure of a boxcar transported by train ferry were defined for a 11-217 model taken as the base model (Figure 2.55).

Boxcars are intended for transporting freight requiring weather protection [80, 112, 113]. Their bodies have sliding doors and ventilating doors on the side walls, loading hatches in the roof, and discharge hatches in the floor of some models. The slot-type hatches in the roof are intended for loading bulk freight during movement of a car batch toward the charging hopper. It assumes special folding elements between the cars. Some car bodies have sliding wall panels for more efficient use of automatic loaders and higher speed of loading / unloading work.

The body capacity was 120 m^3. It was equipped with typical shock-traction equipment, brake devices and gearing parts. The welded frame

consisted of a center sill, two longitudinal side beams, two bolster beams and four end transverse beams.

Figure 2.55 – Boxcar of model 11-217

The top cord was made of fold angle steel, middle posts were made of a U-like profile. The door posts of side walls were of Z-like and L-like profiles. The side wall was connected to the frame through the longitudinal side beam, and to the roof – through the cord.

The end walls composed of framework and external lining. The top cord of the framework was made of special roll-formed profile with the hopper pivoted to it through the bottom cord.

The body roof was an all-metal welded structure of four loading hatches and two openings. The roof was attached to the top cords of the side walls with bolts or rivet points.

The spatial model of the carrying structure of a boxcar body is given in Figure 2.56. The graphical design was made in SolidWorks software. The model used the body elements rigidly connected; it implies that the model did not include movable self-sealing doors.

The numerical values of the forces on the boxcar in train ferry transportation are given in Table 2.7. It was assumed that the deadweight capacity of the car was loaded with conditional freight. The design diagram included vertical static force P_v^{st}, dynamic force P_d, wind force P_w, and tensile forces through the chain binders P_{ch} (Figures 2.57 and 2.58).

Figure 2.56 – Spatial model of an 11-217 boxcar body

The strength calculation was made with the finite element method in CosmosWorks software.

The finite-element model of a boxcar body is given in Figure 2.59. The optimal number of elements in a mesh was determined with the graphic analytical method. The maximum number of elements in a mesh was 637 520, the number of nodes – 225 092. The maximum element size in a mesh was 100.0 mm, the minimum element size was 20.0 mm, the maximum element side ratio was 525.19, the percentage of elements with a side ratio of less than three – 11.1, and more than ten – 46.7. The minimum number of elements in a circle was 22, an element size gain ratio was 1.8, and the simplification coefficient in rounding-off areas and openings was 0.4.

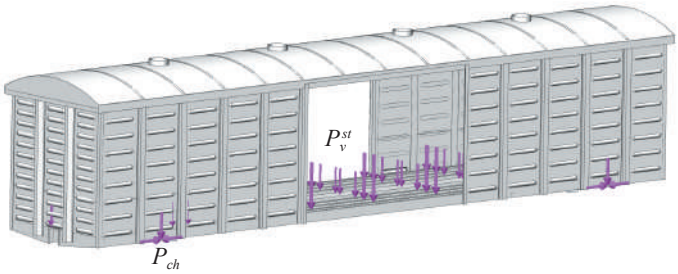

Figure 2.57 – Design diagram of the carrying structure of a boxcar body at angular displacements relative to the transverse axle

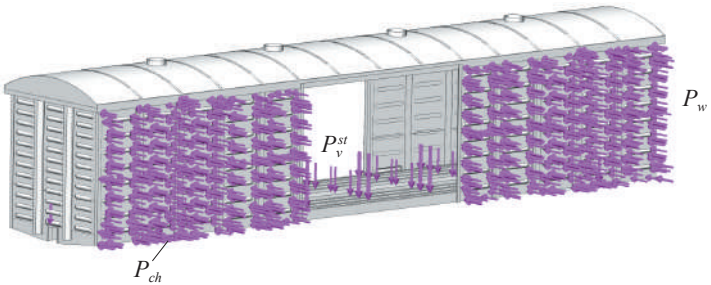

Figure 2.58 – Design diagram of the carrying structure of a a boxcar body at angular displacements relative to the transverse axle

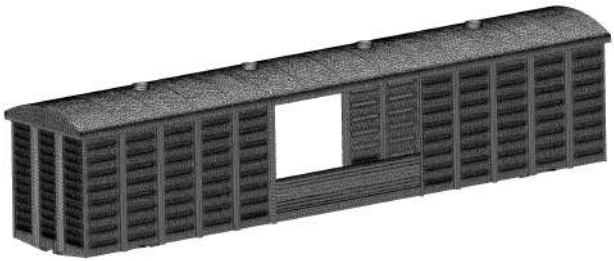

Figure 2.59 – Finite-element model of a boxcar body

The calculation used one of the least stable fixation patterns of a boxcar on the deck (Figure 2.60).

Figure 2.60 – Fixation pattern for a boxcar on the ferry deck

The results of the calculation are given below.

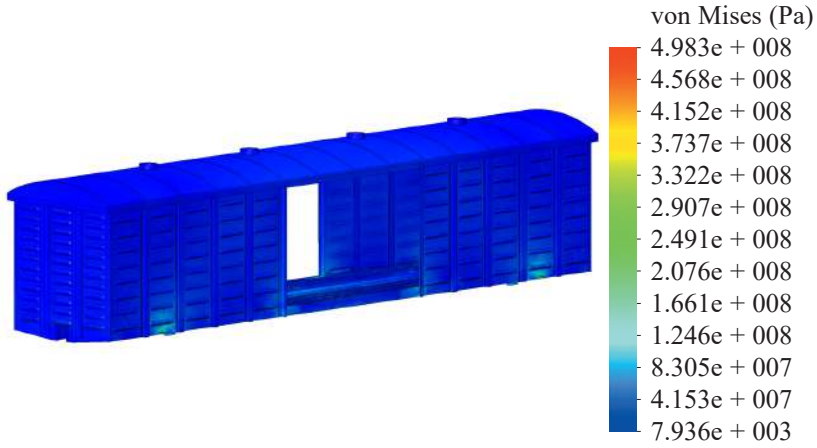

Figure 2.61 – Stress state of a boxcar body at angular displacements relative to the transverse axle

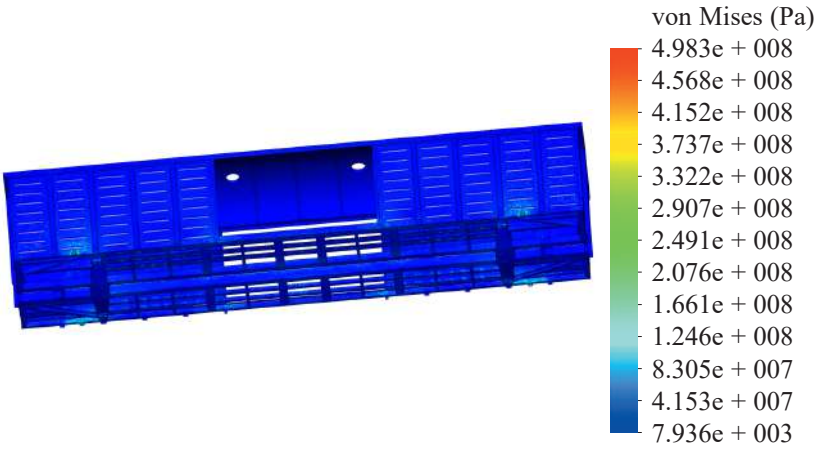

Figure 2.62 – Stress state of a boxcar body at angular displacements relative to the transverse axle

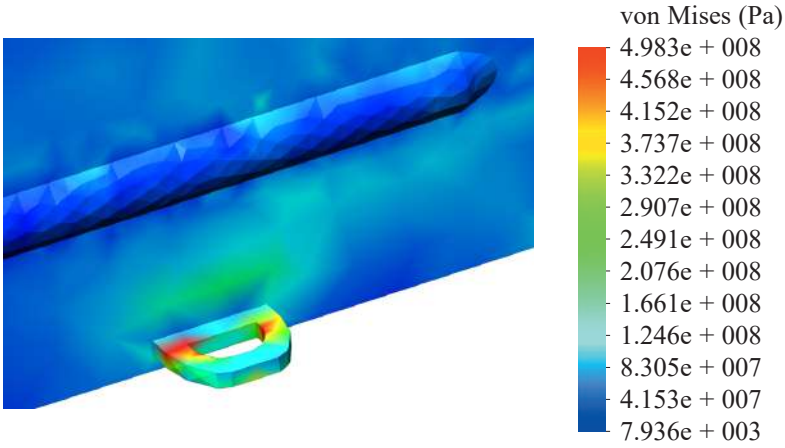

Figure 2.63 – Stress state of a boxcar body at angular displacements relative to the transverse axle

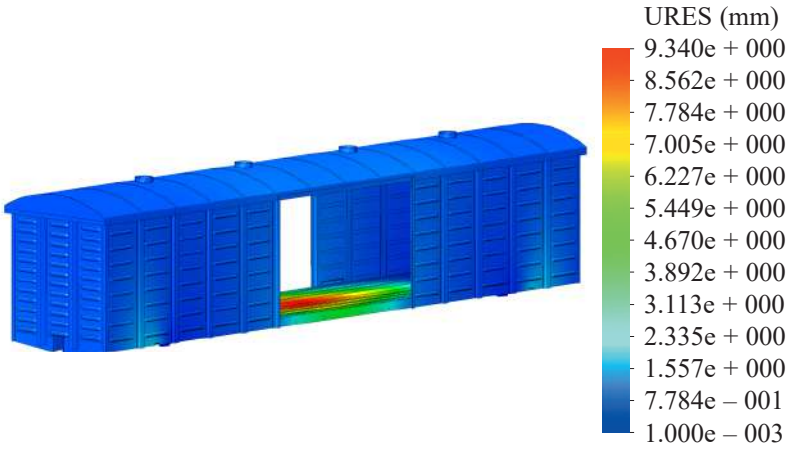

Figure 2.64 – Displacements in the units of a boxcar at angular displacements relative to the transverse axle

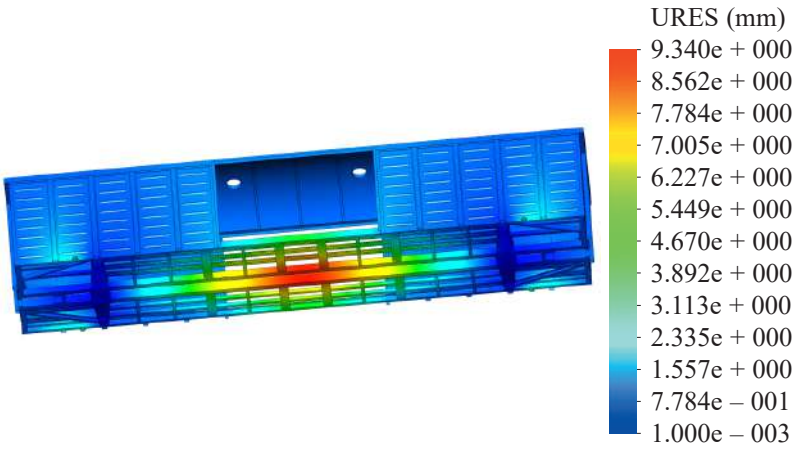

Figure 2.65 – Displacements in the units of a boxcar at angular displacements relative to the transverse axle

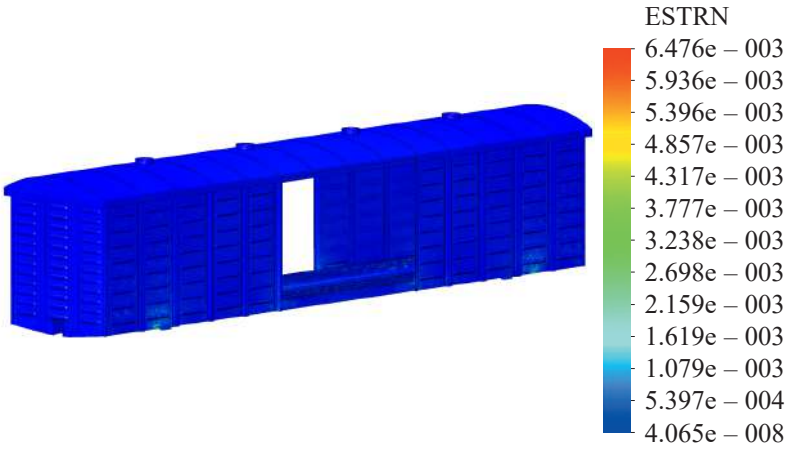

Figure 2.66 – Deformations in the open car body at angular displacements relative to the transverse axle

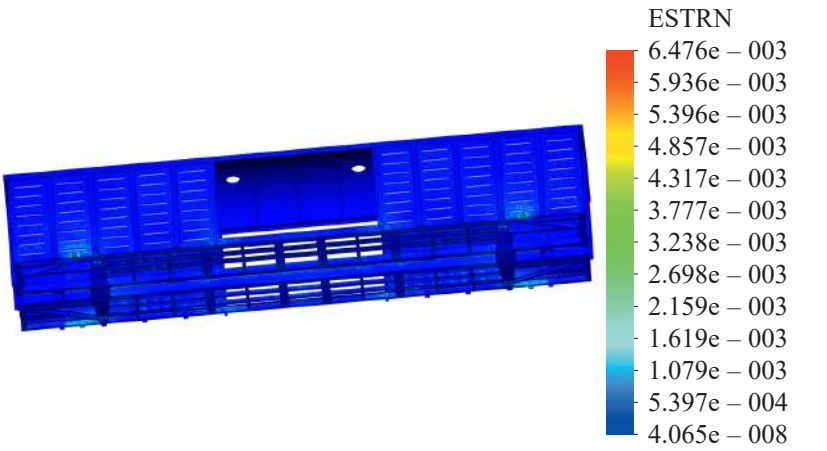

Figure 2.67 – Deformations in the boxcar body at angular displacements relative to the transverse axle

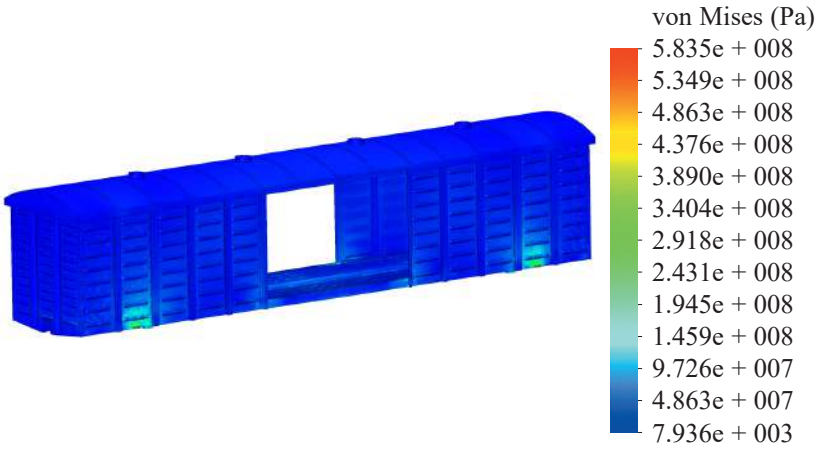

Figure 2.68 – Stress state of a boxcar body at angular displacements relative to the longitudinal axle

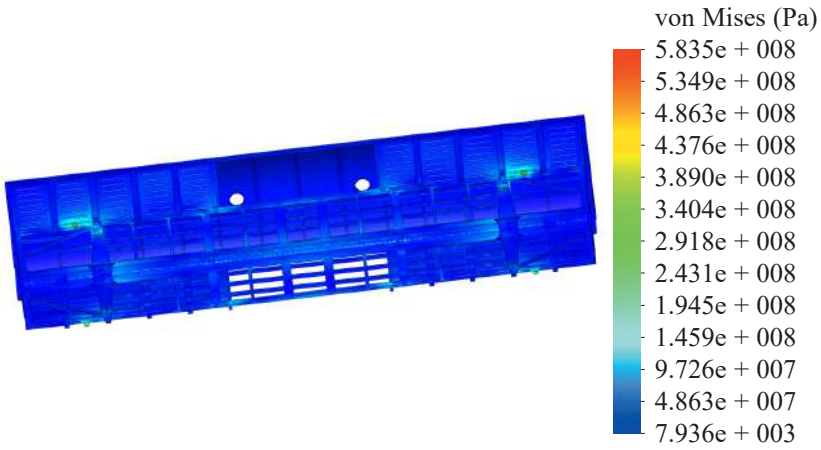

Figure 2.69 – Stress state of a boxcar body at angular displacements relative to the longitudinal axle

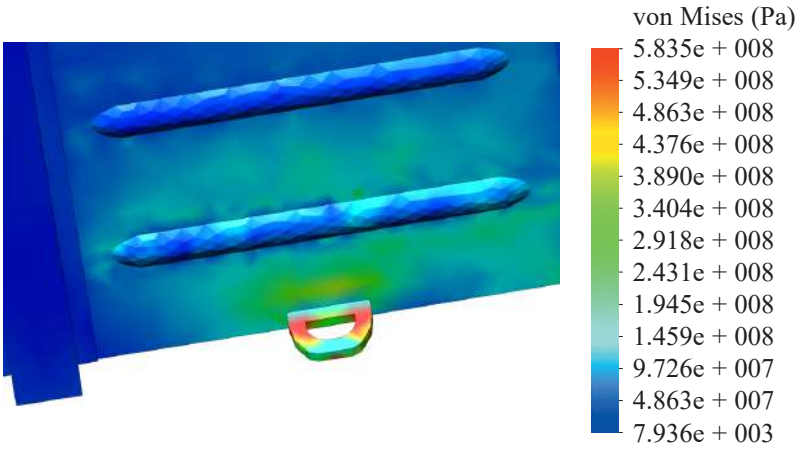

Figure 2.70 – Stress state of a boxcar body at angular displacements relative to the longitudinal axle

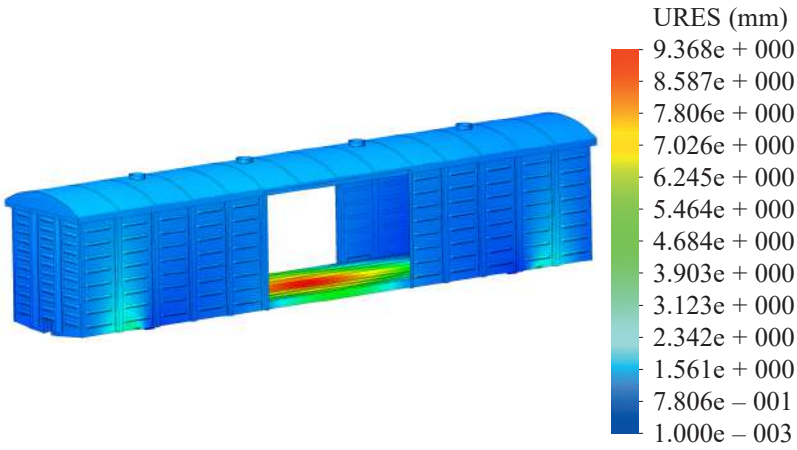

Figure 2.71 – Displacements in the units of a boxcar body at angular displacements relative to the longitudinal axle

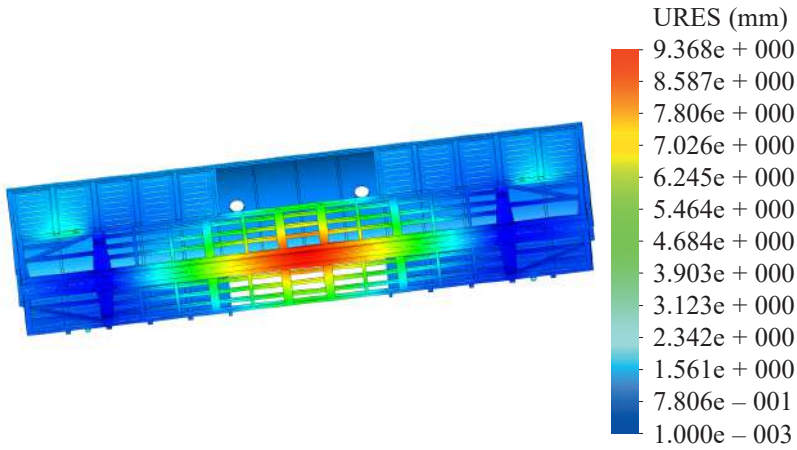

Figure 2.72 – Displacements in the units of a boxcar body at angular displacements relative to the longitudinal axle

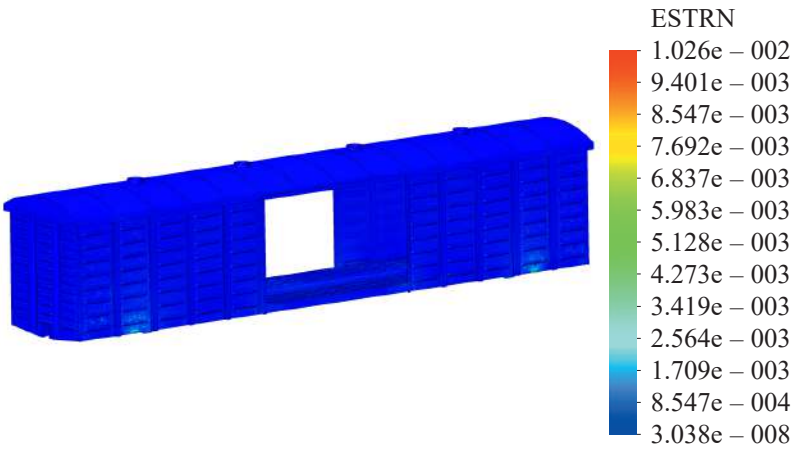

Figure 2.73 – Deformations in the boxcar body at angular displacements relative to the longitudinal axle

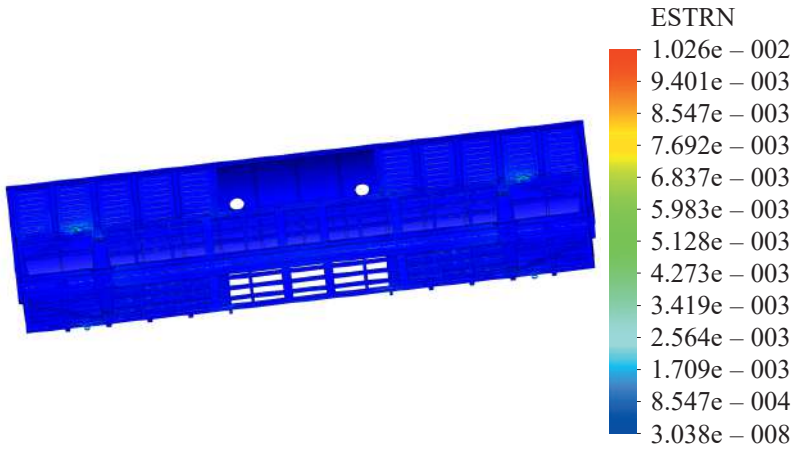

Figure 2.74 – Deformations in the boxcar body at angular displacements relative to the longitudinal axle

Table 2.7 – Forces on the carrying structure of a boxcar symmetrically fixed on the deck in train ferry transportation

Displacements of car body	Forces on car body		Force components on car body through chain binders									
	Vertical static force, kN	Wind force, kN	Tension force through chain binders, kN	Dynamic force, kN			Wind force, kN			Tension force through chain binders, kN		
				XY	YZ	XZ	XY	YZ	XZ	XY	YZ	XZ
Angular relative to transverse axle	p_x=52.3 p_z=816.4	13.1	54	p_x=6.54 p_y=11.32	p_y=6.54 p_z=11.32	p_x=6.54 p_z=11.32	p_x=1.64 p_y=2.84	p_y=1.64 p_z=2.84	p_x=1.64 p_z=2.84	p_x=27 p_y=47	p_y=27 p_z=47	p_x=27 p_z=47
Angular relative to longitudinal axle	p_y=206 p_z=798.72	55.8	54	p_x=25.75 p_y=44.6	p_y=25.75 p_z=44.6	p_x=25.75 p_z=44.6	p_x=6.98 p_y=12.1	p_y=6.98 pz=12.1	p_x=6.98 p_z=12.1	p_x=27 py=47	p_y=27 p_z=47	p_x=27 p_z=47

The results of the calculation demonstrated that the maximum equivalent stresses in the carrying structure of a boxcar body appeared at angular displacements of a train ferry about the longitudinal axle and accounted for about 580 MPa. The maximum displacements were in the middle part of the frame and accounted for 9.4 mm. The maximum deformations were $1.0 \cdot 10^{-2}$.

At angular displacements of a boxcar body relative to the transverse axle the maximum equivalent stresses equaled 500 MPa. The maximum displacements were 9.3 mm, and the maximum deformations were $6.48 \cdot 10^{-3}$.

Thus, the maximum equivalent stresses in the elements of the carrying structure of a boxcar body in ferry transportation exceeded the admissible values.

2.4.4 Determination of strength characteristics in the carrying structure of a hopper car in ferry transportation

The strength characteristics of the carrying structure of a hopper car in ferry transportation were defined for a 12-757 car taken as the base model (Figure 2.75).

Figure 2.75 – Hopper car of model 20-9749

The hopper car is intended for transportation of hot pallets and agglomerates with temperature of lower than 700°C, and bulk freight

(crashed stone, sand, coal, keramzit concrete) which does not require weather protection. The cars are discharged on both sides of the track through discharge doors [80, 112, 113].

The car body was an all-metal framework structure covered with flat sheets.

In order to prevent concentration of freight on the areas near the cords of the side walls, the top cord along the perimeter was equipped with an angle profile and the bottom cord of the side walls was equipped with a sloping plate. The end parts of the frame with the equipment located on it were protected with covers (similar to ones for hopper cars). The end valves of the discharging system were symmetrical to the brake valves on the left side of an automatic coupler.

The opening and closing of discharge doors were made with a special mechanism actuated by a remotely controlled pneumatic cylinder.

The spatial model of a hopper car was built in SolidWorks software (Figure 2.76).

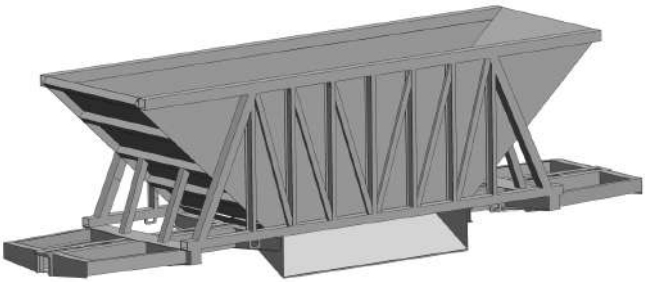

Figure 2.76 – Spatial model of the carrying structure of a hopper car body

The strength calculation used one of the least stable fixation patterns of a hopper car on the deck (Figure 2.77).

The strength calculation for the carrying structure of a hopper car was made with the finite element method in CosmosWorks software.

Figure 2.77 – Fixation pattern for a hopper car on the ferry deck

The finite element model (Figure 2.78) was built with isoparametrical tetrahedrons, the optimal number of which was defined by the graphic analytic method. The number of elements in a mesh was 376 670, the number of nodes – 126 221, the maximum element size – 60 mm, the minimum element size – 12 mm, the maximum element side ratio – 1 298.6, the percentage of elements with a side ratio of less than three – 7.43 and more than ten – 32.5. The element size gain ratio in a mesh was 1.7. The number of elements in a circle was 9.

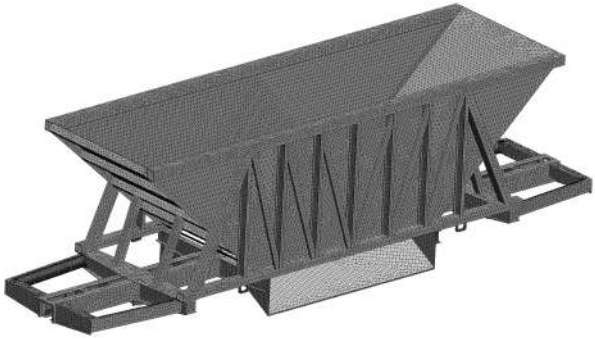

Figure 2.78 – Finite element model of the carrying structure of a hopper car

The design diagram of a hopper car body (Figures 2.79 and 2.80) included the following forces: vertical static P_v^{st}, pressure from the bulk freight P_p, dynamic P_d, wind force P_w and the forces on the car body through the chain binders P_{ch}.

The calculated values of forces on the carrying structure of a hopper car with consideration of interaction with reusable lashing devices during sea disturbance are given in Table 2.8.

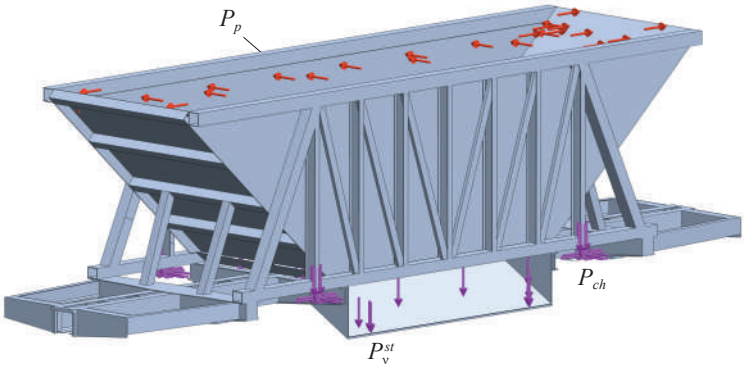

Figure 2.79 – Design diagram of the carrying structure of a hopper car at angular displacements relative to the transverse axle

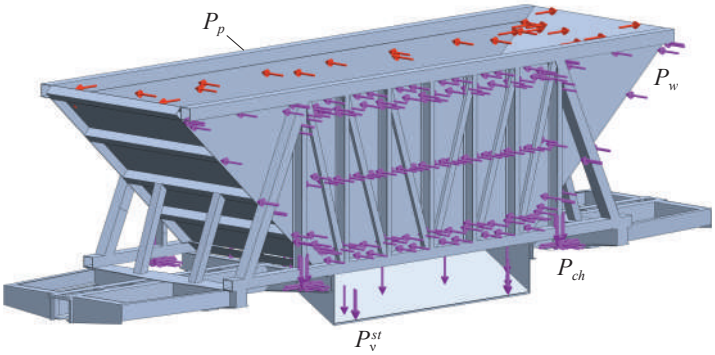

Figure 2.80 – Design diagram of the carrying structure of a hopper car at angular displacements relative to the longitudinal axle

The results of the calculation are given below.

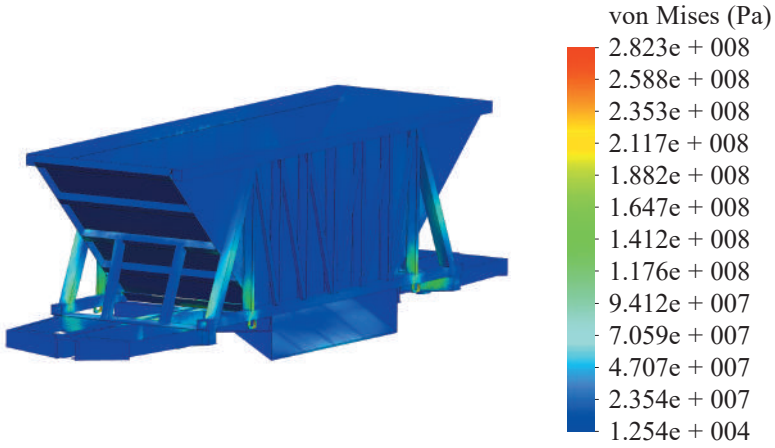

Figure 2.81 – Stress state of a hopper car at angular displacements relative to the transverse axle

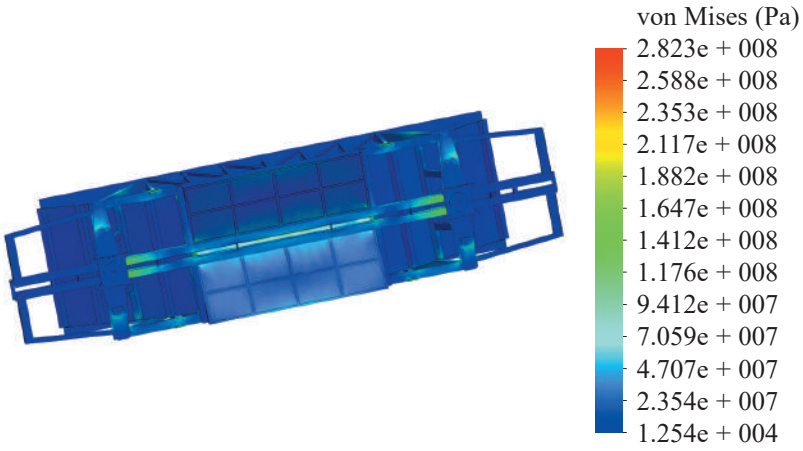

Figure 2.82 – Stress state of a hopper car body at angular displacements relative to the transverse axle

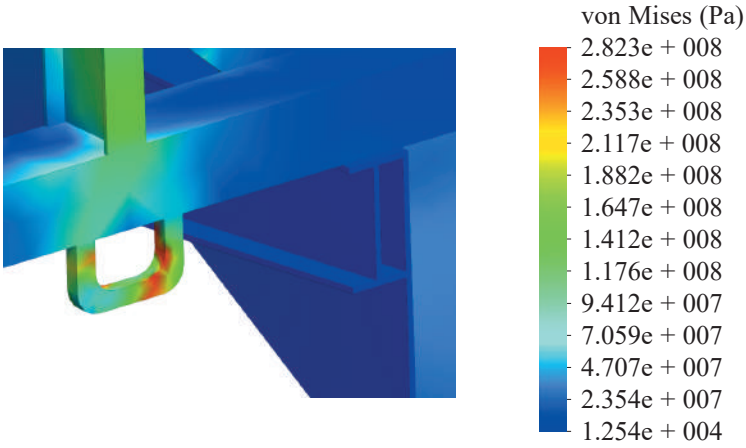

Figure 2.83 – Stress state of a hopper car at angular displacements relative to the transverse axle

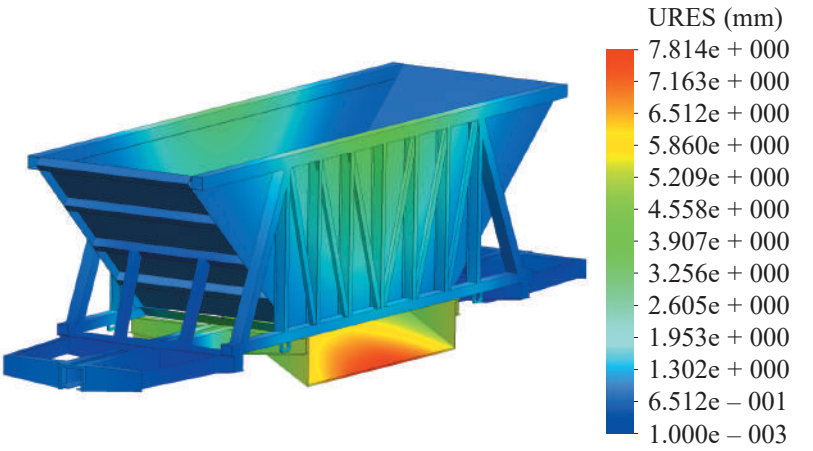

Figure 2.84 – Displacements in the units of a hopper car at angular displacements relative to the transverse axle

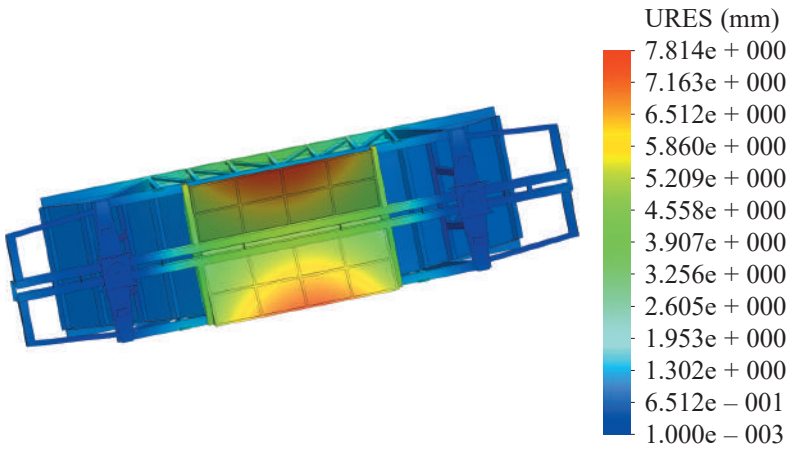

Figure 2.85 – Displacements in the units of a hopper car at angular displacements relative to the transverse axle

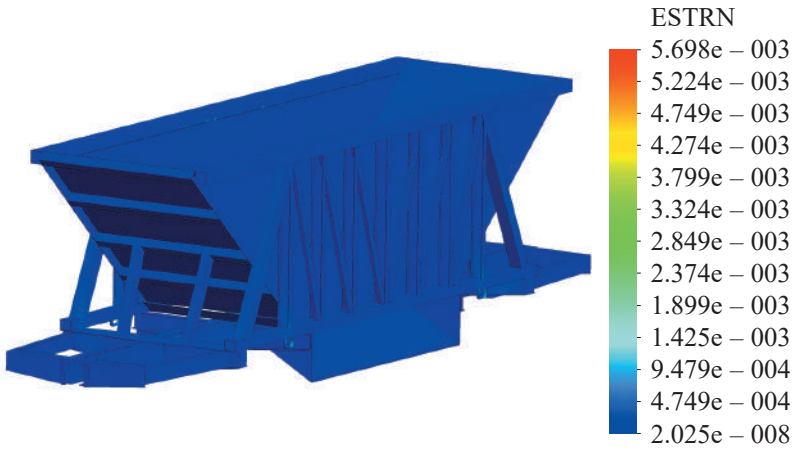

Figure 2.86 – Deformation in the carrying structure of a hopper car body at angular displacements relative to transverse axle

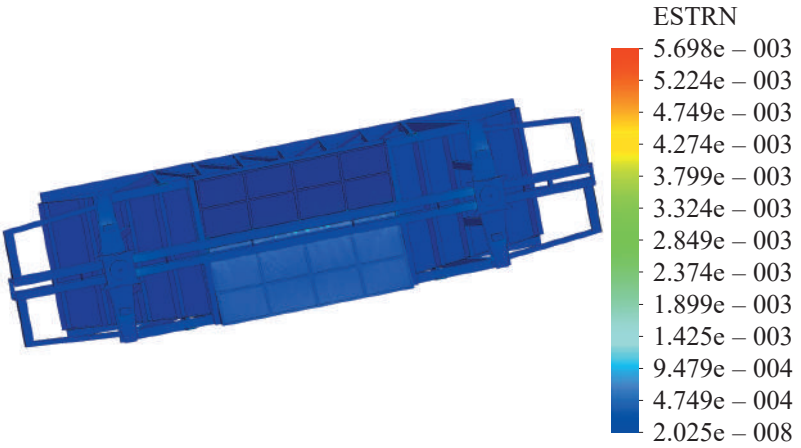

Figure 2.87 – Deformations in the carrying structure of a hopper car body at angular displacements relative to transverse axle

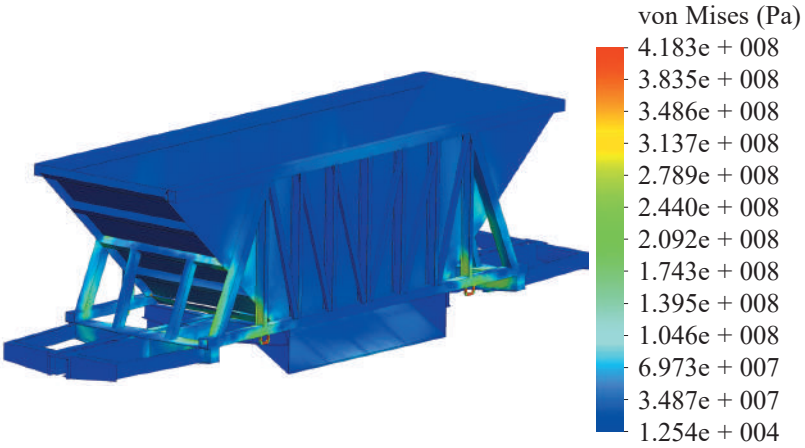

Figure 2.88 – Stress state of a hopper car at angular displacements about the longitudinal axle

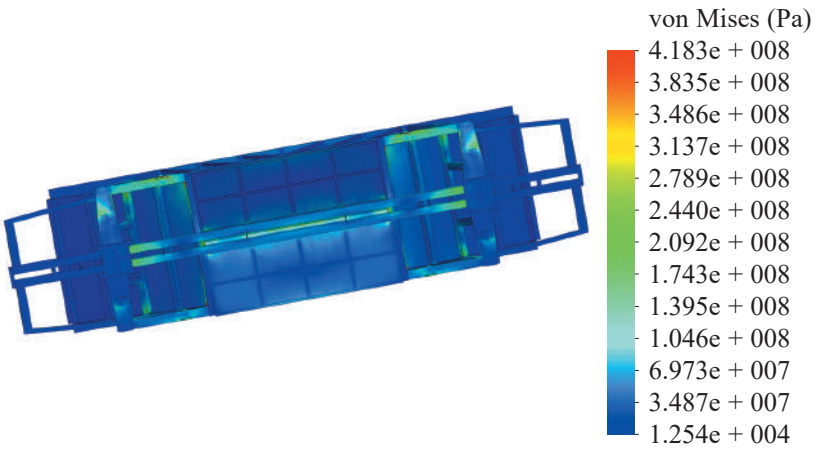

Figure 2.89 – Stress state of a hopper car at angular displacements about the longitudinal axle

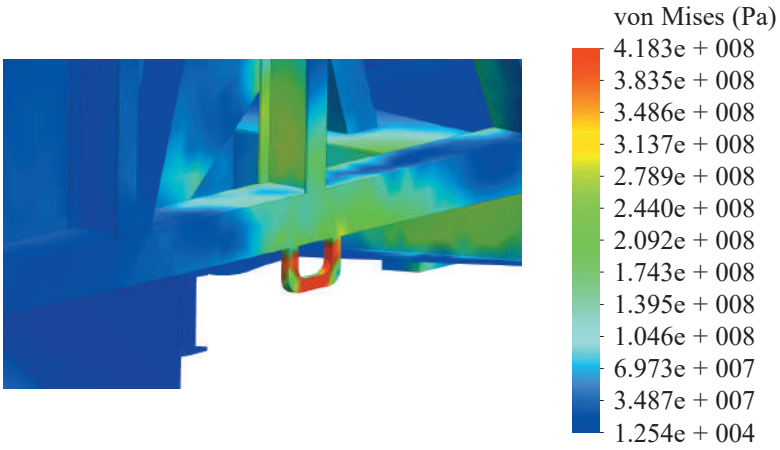

Figure 2.90 – Stress state of a hopper car body at angular displacements about the longitudinal axle

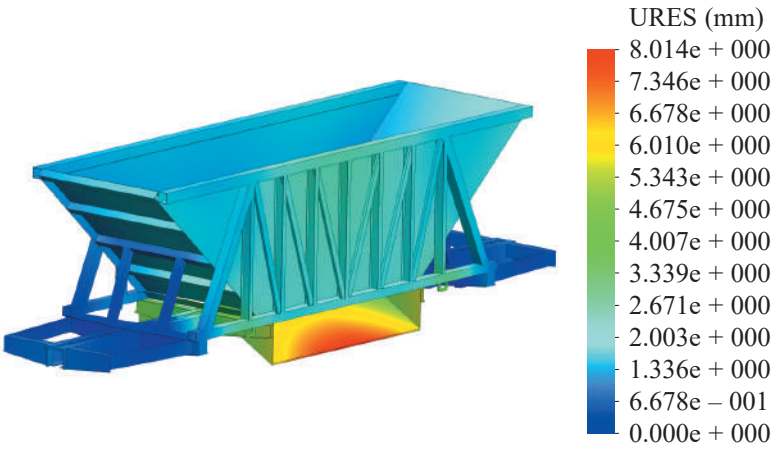

Figure 2.91 – Displacements in the units of a hopper car at angular displacements about the longitudinal axle

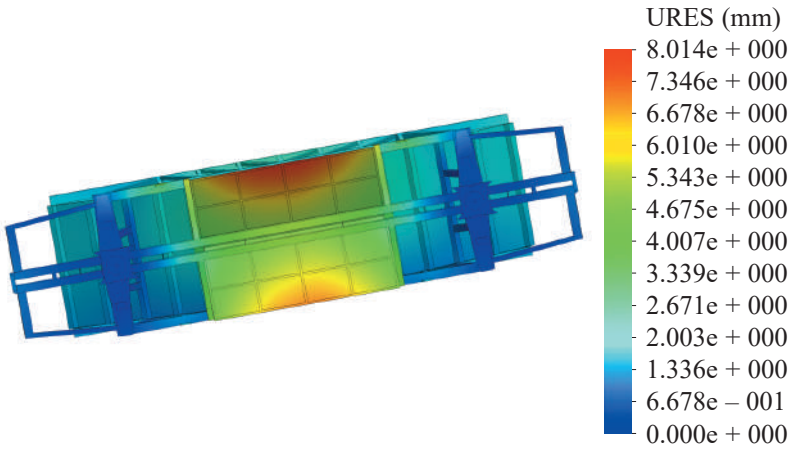

Figure 2.92 – Displacements in the units of a hopper car body at angular displacements about the longitudinal axle

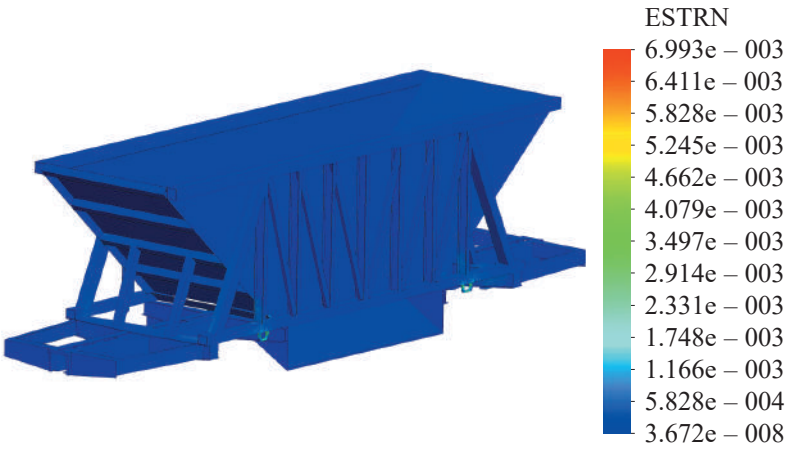

Figure 2.93 – Deformations in the carrying structure of a hopper car body at angular displacements about the longitudinal axle

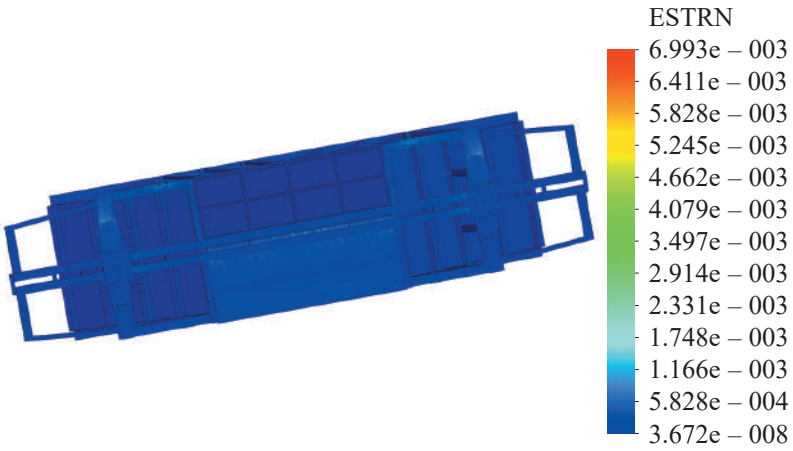

Figure 2.94 – Deformations in the carrying structure of a hopper car body at angular displacements about the longitudinal axle

Table 2.8 – Forces on the carrying structure of a hopper car symmetrically fixed in train ferry transportation

Displacements of car body	Forces on car body				Force components on car body through chain binders							
	Vertical static force, kN	Wind force, kN	Pressure from bulk freight, kPa (on tilt side)	Forces through chain binders, kN	Dynamic force, kN		Wind force, kN			Tension force through chain binders, kN		
					XY	YZ	XZ	XY	YZ	XZ	XY	YZ	XZ
Angular relative to transverse axle	p_x=53.2 p_z=829.13	11.12	7.63	54	p_x=6.65 p_y=11.52	p_y=6.65 p_z=11.52	p_x=6.65 p_z=11.52	p_x=1.4 p_y=2.42	p_y=1.4 pz=2.42	p_x=1.4 p_z=2.42	p_x=27 p_y=47	p_y=27 p_z=47	p_x=27 p_z=47
Angular relative to longitudinal axle	p_y=209.22 p_z=811.18	23.1	10.15	54	p_x=26.16 p_y=45	p_y=26.16 p_z=45.3	p_x=26.16 p_z=45.3	p_x=2.89 p_y=5.0	p_y=2.89 p_z=5.0	p_x=2.89 p_z=5.0	p_x=27 p_y=47	p_y=27 p_z=47	p_x=27 p_z=47

The results of the calculation demonstrated that the maximum equivalent stresses in the carrying structure of a hopper car emerged at angular displacements of a train ferry about the longitudinal axle and accounted for about 420 MPa. The maximum displacements were in the discharging hoppers and they accounted for 8.0 mm. The maximum deformations were $7.0 \cdot 10^{-3}$.

At angular displacements of the carrying structure of a hopper car about the transverse axle the maximum equivalent stresses were 280 MPa. The maximum displacements were 7.8 mm, and the maximum deformations were $5.7 \cdot 10^{-3}$.

Therefore, at a typical fixation pattern for a hopper car on the ferry deck the maximum equivalent stresses in the elements of the carrying stricture exceeded the admissible values.

2.4.5 Determination of strength characteristics of the carrying structure of a frat car in ferry transportation

The strength characteristics of the carrying structure of a flat car were defined for a 13-401 flat car taken as the base model.

Figure 2.95 – Universal flat car of model 13-401

The body of a flat car does not have walls and roof, and it is intended for transporting long freight, metal structures, containers, wheel and caterpillar machines, packaged freight and other types of freight which do not require weather protection.

Railways of CIS countries operate different models of flat cars of various technical characteristics and structural peculiarities.

The body of a four-axle universal flat car consisted of a frame made of eight longitudinal and two end-side walls. The welded frame had a tight center sill consisting of two T-profiles with adjustable height. The side longitudinal beams were made of T-profiles, and the bolster beams had the closed cross-section. The intersections of the center sill and the bolster beam had center plates reinforced with diaphragms. The end parts of the center sill had rear and front draft attachments connected to the coupler's striker. Besides, the end parts of the center sill had guard strips to protect the vertical walls of T-profiles from wearing. The bottom sheet of the bolster beams had slides with stiffness ribs above.

The brackets to support the end walls in the open position were mounted on the end beams.

The main transverse beams in the frame were of adjustable height, and the middle beams had constant T-profile section. The upper plane of the transverse beams was lower than the floor level by a width of additional longitudinal beams.

The floor covering was combined: metal – in the middle part and wooden – on the sides. From their one end the floor boards entered the S-like beam, and from their other end they were attached to the longitudinal side beams with a special roll-formed element. The side longitudinal beams of the frame had stake pockets, bearings, and retainers of wedge locks mounted on the longitudinal walls. The end walls, which were lower than the longitudinal side walls, were vertically fixed with the wedge locks.

The strength characteristics of a universal flat car in train ferry transportation were determined by the spatial model built in SolidWorks software (Figure 2.96).

The calculation involved the least stable fixation pattern of a flat car on the deck (Figure 2.97).

Figure 2.96 – Carrying structure of a 13-401 flat car

Figure 2.97 – Fixation pattern for a flat car on the ferry deck

The strength calculation for the carrying structure of a flat car was made by the finite element method in CosmosWorks software.

The finite element model designed (Figure 2.98) used isoparametrical tetrahedrons the optimal number of which was defined by the graphic analytic method. The number of elements in a mesh was 278 138, the number of nodes – 94 750, the maximum element

size – 236 mm, the minimum element size – 47.2 mm, the maximum element side ratio – $1.36 \cdot 10^5$, the percentage of elements with a side ratio less than three – 7.44; and with more than ten – 40.7. The element gain ratio in a mesh was 1.8. The number of elements in a circle was 9.

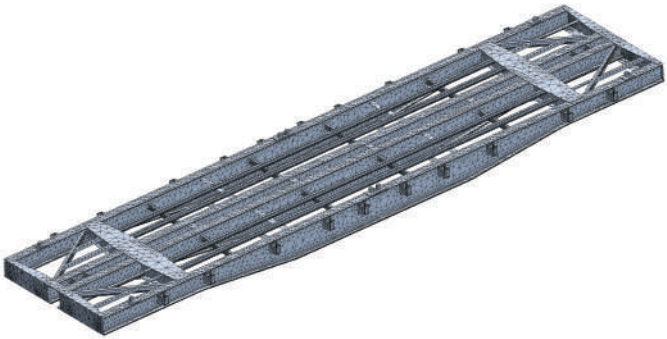

Figure 2.98 – Finite element model of the carrying structure of a flat car

The design diagram of the carrying structure of a flat car included such forces: vertical static P_v^{st}, dynamic P_d and forces on the frame through the chain binders P_{ch} (Figure 2.99).

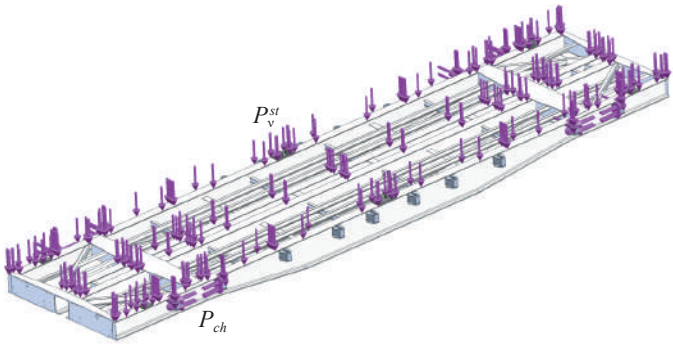

Figure 2.99 – Design diagram of the carrying structure of a flat car

The calculated values of forces on the carrying structure of a flat car with consideration of interaction with reusable lashing devices are given in Table 2.9. The results of the calculation are presented below.

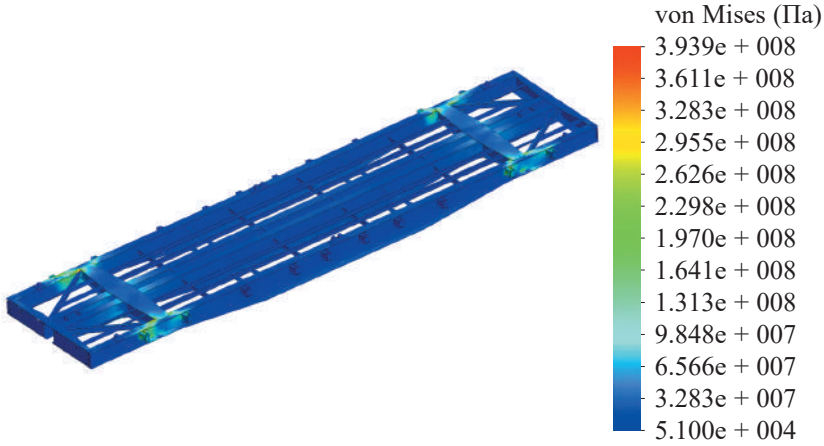

Figure 2.100 – Stress state of the carrying structure of a flat car at angular displacements relative to the transverse axle

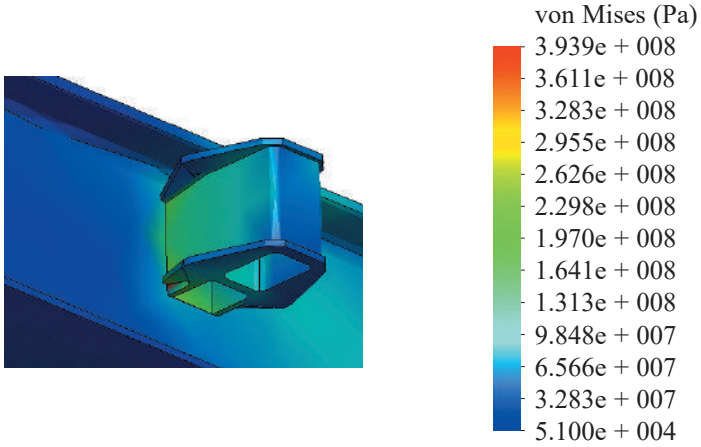

Figure 2.101 – Stress state of the stake buckle of a flat car at angular displacements about the transverse axle

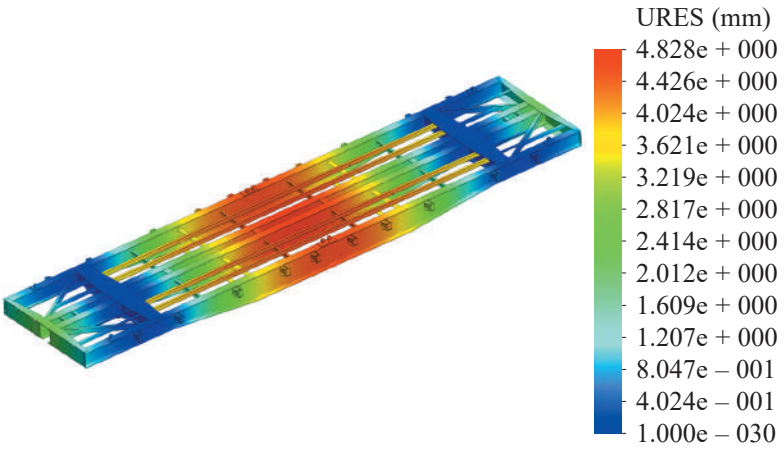

Figure 2.102 – Displacements in the units of the carrying structure of a flat car at angular displacements relative to the transverse axle

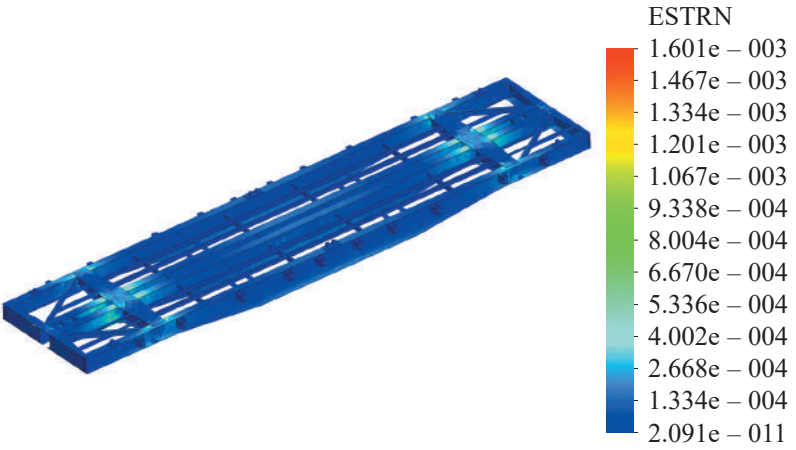

Figure 2.103 – Deformations in the carrying structure of a flat car at angular displacements relative to the transverse axle

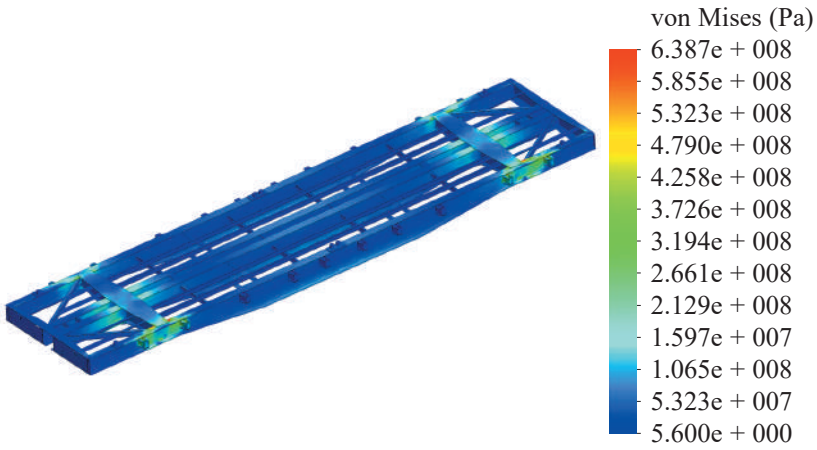

Figure 2.104 – Stress state of the carrying structure of a flat car at angular displacements about the transverse axle

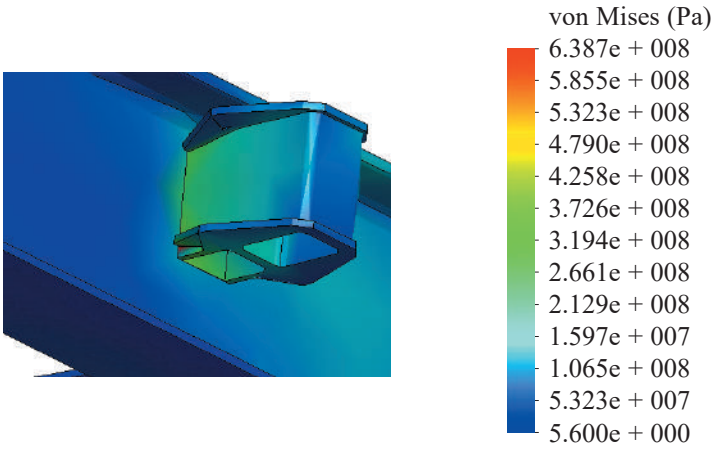

Figure 2.105 – Stress state of the stake buckle of a flat car at angular displacements relative to the transverse axle

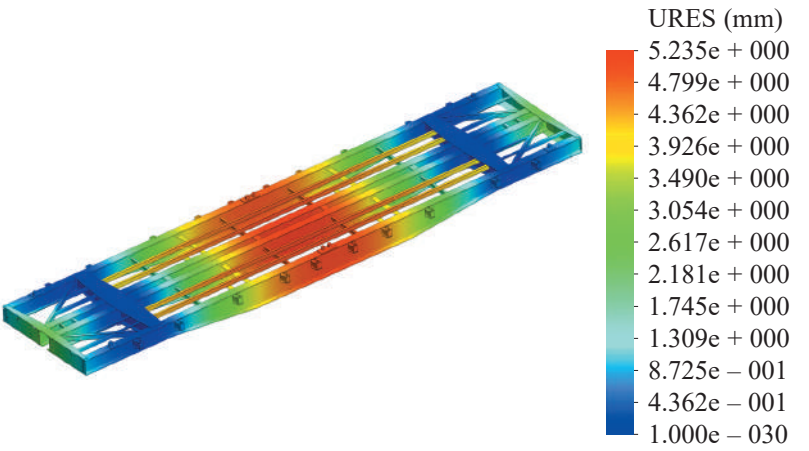

Figure 2.106 – Displacements in the units of the carrying structure of a flat car at angular displacements relative to the transverse axle

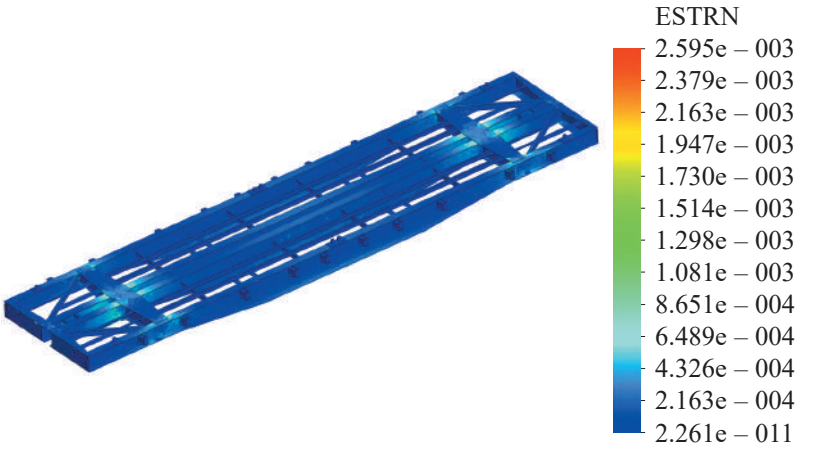

Figure 2.107 – Deformations in the carrying structure of a flat car at angular displacements relative to the transverse axle

Table 2.9 – Forces on the carrying structure of a flat car symmetrically fixed on the deck in train ferry transportation

Displacements of car body	Force on open car body		Force components on car body through chain binders					
	Vertical static force, kN	Tensile forces through chain binders, kN	Dynamic force, kN			Tension force through chain binders, kN		
			XY	YZ	XZ	XY	YZ	XZ
Angular relative to transverse axle	p_x=51.19 p_z=798.85	54	p_x=6.4 p_y=11.1	p_y=6.4 p_z=11.1	p_x=6.4 p_z=11.1	p_x=27 p_y=47	p_y=27 p_z=47	p_x=27 p_z=47
Angular relative to longitudinal axle	p_y=201.61 p_z=781.65	54	p_x=25.2 p_y=43.65	p_y=25.2 p_z=43.65	p_x=25.2 p_z=43.65	p_x=27 p_y=47	p_y=27 p_z=47	p_x=27 p_z=47

From the calculation made we can conclude that the maximum equivalent stresses were in the carrying structure of a flat car at angular displacements about the longitudinal axle and account for about 640 MPa. The maximum displacements were in the middle part of the frame and accounted for 5.2 mm. The maximum deformations were $2.6 \cdot 10^{-3}$.

At angular displacements of the carrying structure of a flat car about the transverse axle the maximum equivalent stresses were 394 MPa, the maximum displacements – 4.8 mm, and deformations – $1.6 \cdot 10^{-3}$.

The results obtained demonstrate that the maximum equivalent stresses in the carrying structure of a flat car exceeded the admissible values.

2.4.6 Determination of strength characteristics of the carrying structure of a passenger car in ferry transportation

At present train ferries are equipped with special fastening brackets for passenger car bodies (Figure 2.108). Each body has six such brackets (three at each side).

a) b)

Figure 2.108 – Brackets for fixation of a passenger car body on the train ferry deck:
a) front view; b) side view

The research deals with strength calculation of the carrying structure of a passenger car made by the finite element method in CosmosWorks software.

The spatial model of a passenger car body is given in Fig. 2.109. The model used the elements rigidly connected by welding or riveting. The finite element model (Figure 2.110) was built with spatial isoparametrical tetrahedrons. The optimal number of elements was determined with the graphic analytical method. The model consisted of 183 393 units and 520 475 elements. The maximum element size was 80 mm, and the minimum one – 16 mm. The percentage of elements with a side ratio of less than three was 15.1, and more than ten – 56. The minimal number of elements in a circle was 12; the element size gain ratio in a mesh was 1.8.

a)

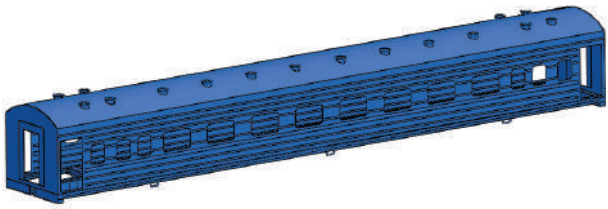

b)

Figure 2.109 – Spatial model of a passenger car body:
a) side view; b) bottom view

The strength model used the following forces on the car body: vertical static force P_v^{st}, wind force P_w, and forces through the chain

binders P_{ch} (Figure 2.111). Owing to the spatial location of chain binders, the force on the car body through them was decomposed [118, 153].

The design values of forces on the carrying structure of a passenger car body with consideration of interaction with reusable lashing devices are given in Table 2.10.

The model was fastened in the areas where the body rested on the running gears of a car, and in the areas where support jacks were installed. Carbon Steel St.3 was used as the structural material for the car body.

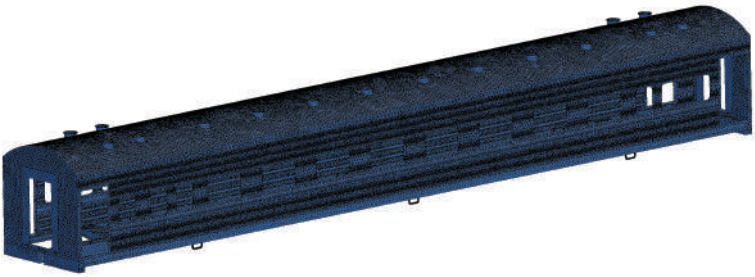

Figure 2.110 – Finite element model of a passenger car body

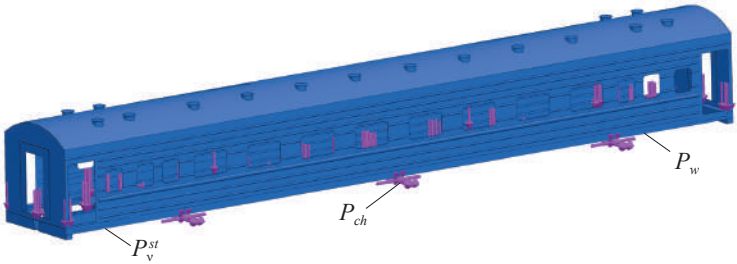

Figure 2.111 – Design diagram of a passenger car body

The results of the calculation are given below.

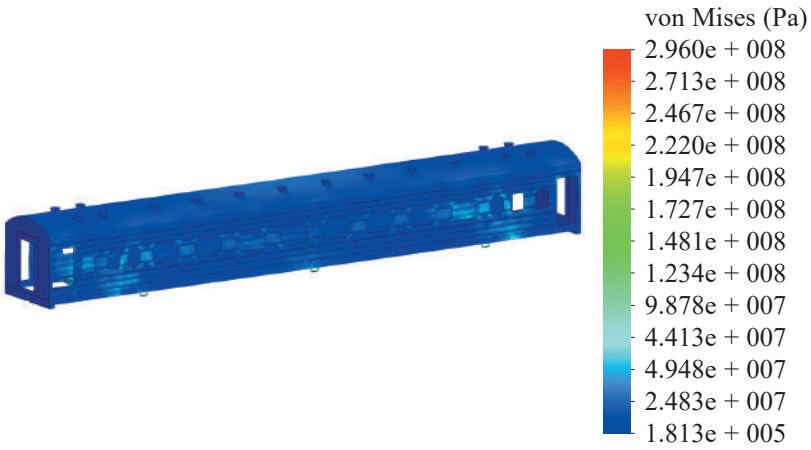

Figure 2.112 – Stress state of a passenger car at angular displacements relative to the transverse axle

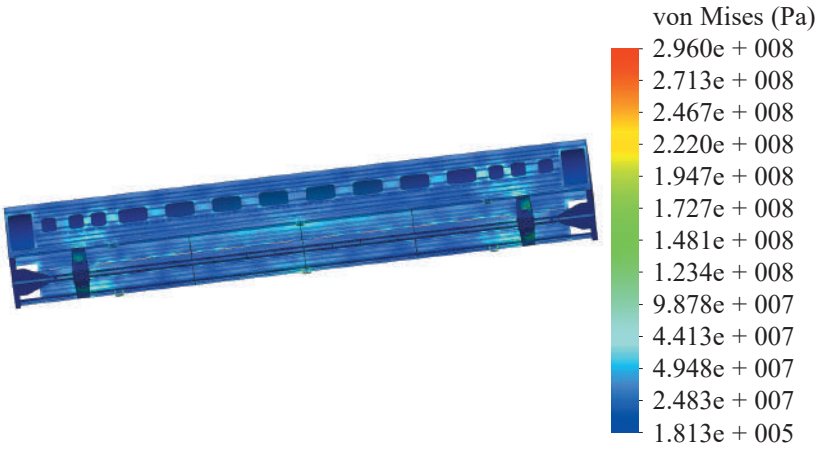

Figure 2.113 – Stress state of a passenger car body at angular displacements relative to the transverse axle

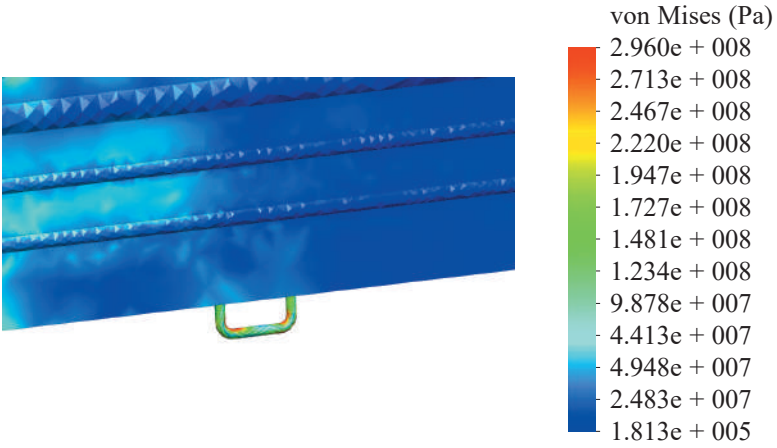

Figure 2.114 – Stress state of a passenger car body at angular displacements about the transverse axle

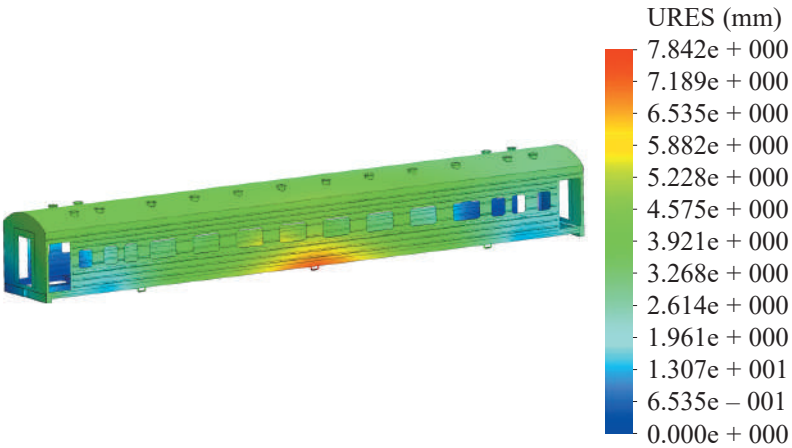

Figure 2.115 – Displacements in the units of a passenger car body at angular displacements relative to the transverse axle

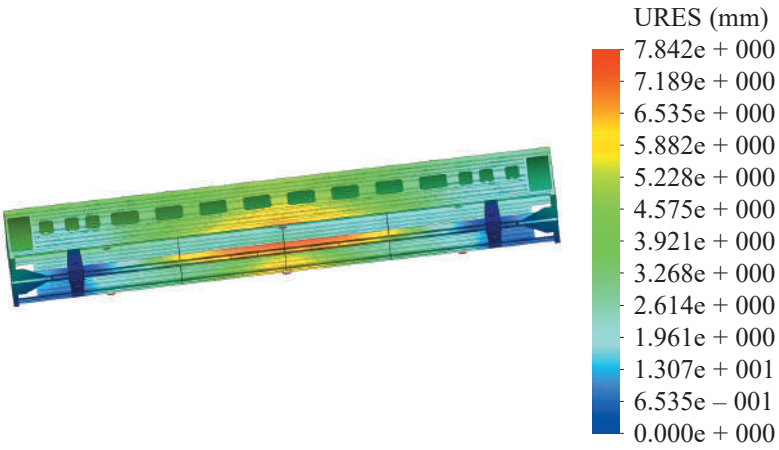

Figure 2.116 – Displacements in the units of a passenger car body at angular displacements relative to the transverse axle

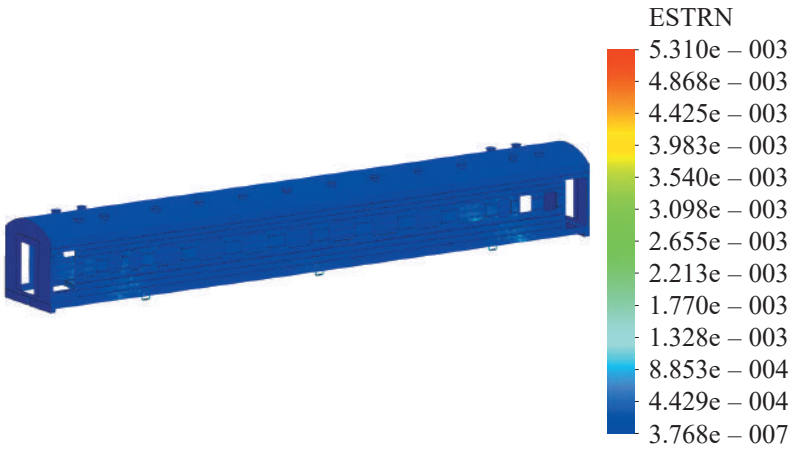

Figure 2.117 – Deformations in the passenger car body at angular displacements relative to transverse axle

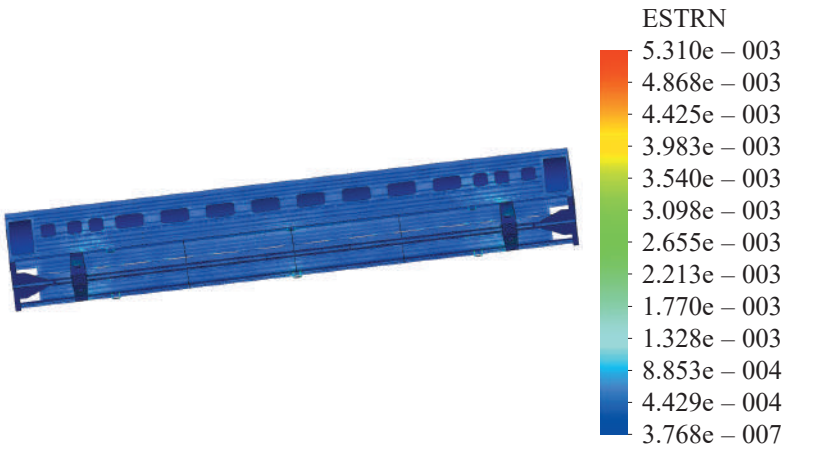

Figure 2.118 – Deformations in the passenger car body at angular displacements relative to the transverse axle

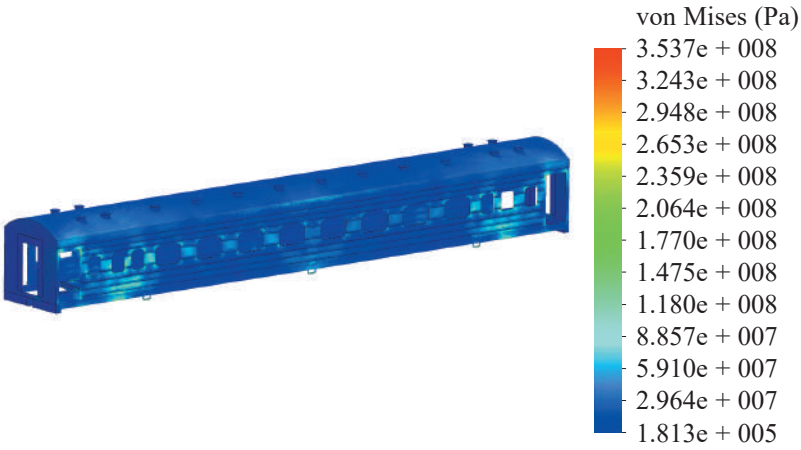

Figure 2.119 – Stress state of a passenger car body at angular displacements relative to the longitudinal axle

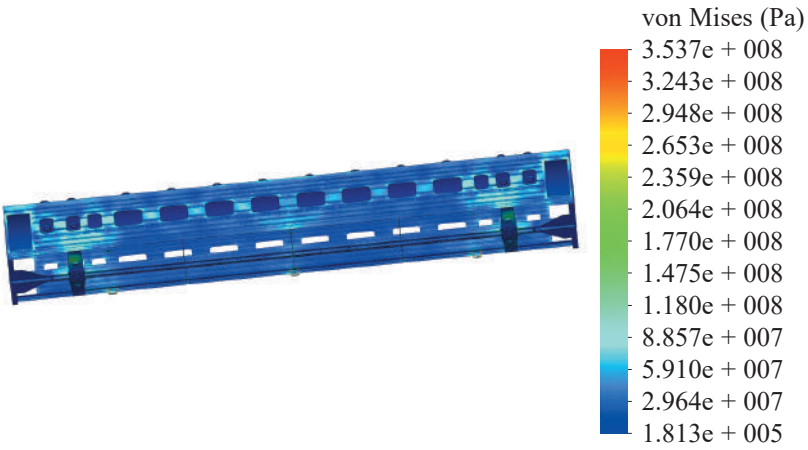

Figure 2.120 – Stress state of a passenger car body at angular displacements relative to the longitudinal axle

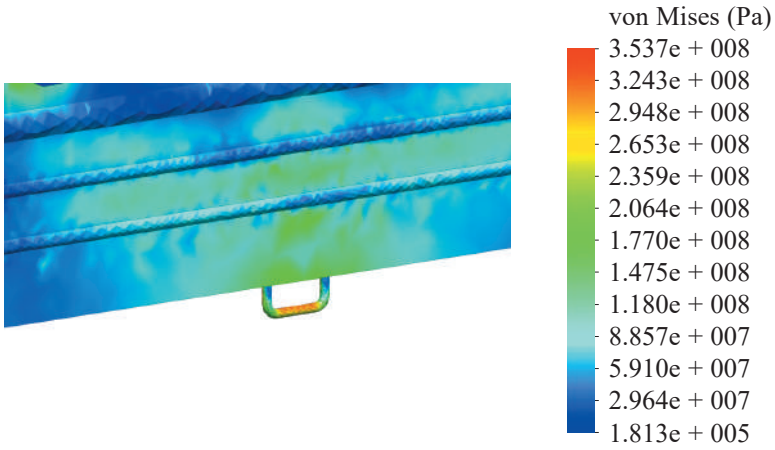

Figure 2.121 – Stress state of a passenger car body at angular displacements relative to the longitudinal axle

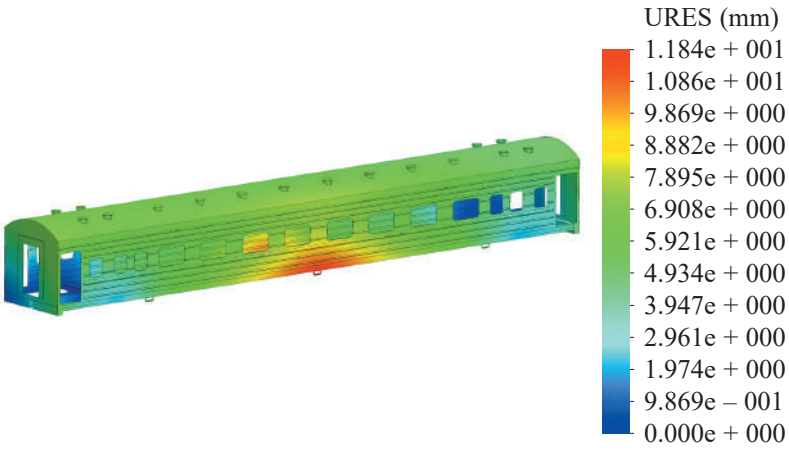

Figure 2.122 – Displacements in the units of a passenger car body at angular displacements relative to the longitudinal axle

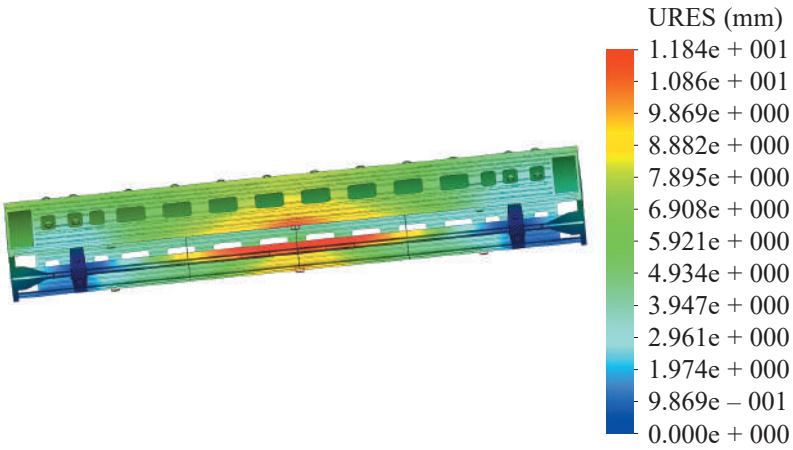

Figure 2.123 – Displacements in the units of a passenger car body at angular displacements about the longitudinal axle

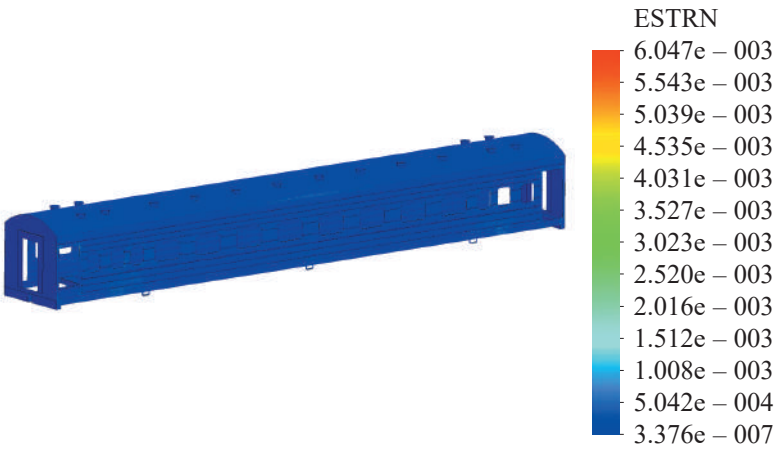

Figure 2.124 – Deformations in the passenger car body at angular displacements about the longitudinal axle

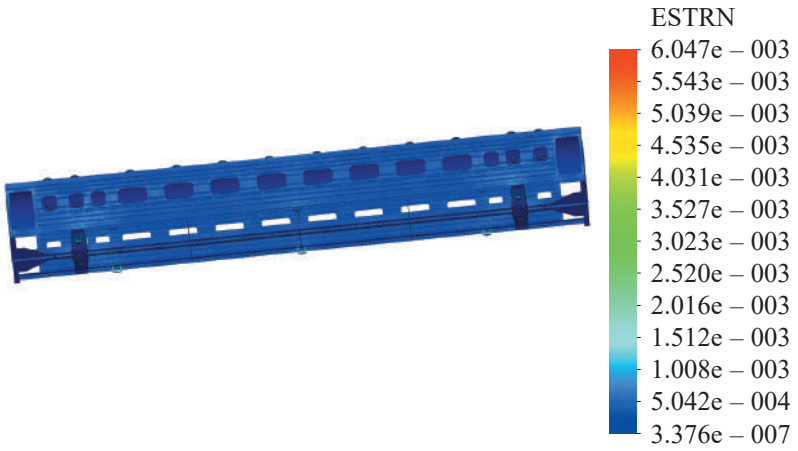

Figure 2.125 – Deformations in the passenger car body at angular displacements about the longitudinal axle

Table 2.10 – Forces on the carrying structure of a passenger car symmetrically fixed on the deck in train ferry transportation

Displacements of car body	Force on car body		Force components on car body through chain binders									
	Vertical static force, kN	Wind force, kN	Forces from chain binders, kN	Dynamic force, kN		Wind force, kN			Tension force through chain binders, kN		
				XY	YZ	XZ	XY	YZ	XZ	XY	YZ	XZ
Angular relative to transverse axle	p_x=23.73 p_z=370.47	11.31	54	p_x=2.0 p_y=3.46	p_y=2.0 p_z=3.46	p_x=2.0 p_z=3.46	p_x=0.94 p_y=1.63	p_y=0.94 p_z=1.63	p_x=0.94 p_z=1.63	p_x=27 p_y=47	p_y=27 p_z=47	p_x=27 pz=47
Angular relative to longitudinal axle	p_y=93.48 p_z=362.44	84.04	54	p_x=7.82 p_y=13.49	p_y=7.82 p_z=13.49	p_x=7.82 p_z=13.49	p_x=7.0 p_y=6.06	p_y=7.0 p_z=6.06	p_x=7.0 p_z=6.06	p_x=27 p_y=47	p_y=27 p_z=47	p_x=27 p_z=47

It was established that the maximum equivalent stresses were in the body of a passenger car at angular displacements relative to the longitudinal axle and accounted for 350 MPa. The maximum displacements were in the middle part of the center sill and accounted for 11.8 mm. The maximum deformations were $6.05 \cdot 10^{-3}$.

At angular displacements of the carrying structure of a passenger car body about the transverse axle the maximum equivalent stresses were 296 MPa, the maximum displacements – 7.8 mm, and deformations – $5.3 \cdot 10^{-3}$.

Thus, the maximum equivalent stresses in the body elements of a passenger car exceeded the admissible values.

Conclusions to Part 2

1. The research describes the basic forces on the car body in train ferry transportation: vertical forces, side (transverse) forces and longitudinal forces conditioned by the train ferry oscillations. Besides, the research indicates a special impact of the forces on the carrying structure of cars through chain binders. The authors defined irregular coefficients in fixation of chain binders, which should be taken into account in calculation of the actual values of forces on the car body.

It was established that location of a car body on the deck in train ferry transportation considerably impacts the force value.

2. The study presents the mathematical modelling of forces on the car body in train ferry transportation. The cases of the most harmful oscillations which cause significant loss of stability by a car and the cargo in ferry transportation were also studied. It revealed the maximum accelerations on the car body in train ferry transportation for different patterns of interaction with lashing devices on the decks. Besides, the authors defined the accelerations on the cars transported on basic

rail / ferry routes with consideration of the technical characteristics of ferries servicing them.

3. The computer modelling of dynamic loads on the freight car bodies during train ferry transportation was made in CosmosWorks software. The train ferry *Geroi Shipki* was used for the research. The study determined the acceleration distribution fields on the carrying structure of the cars located on the train ferry decks. The results obtained were checked for the adequacy with an F-test.

4. The study determined the strength characteristics of the carrying structure of a car body in train ferry transportation. The calculation was made with the finite element method. A peculiar feature of the design diagrams is the involving of the forces on the car body through chain binders. The least stable fixation patterns for cars on the ferry deck taken from the full-scale research were also included.

From the results obtained we can conclude that the maximum equivalent stresses for all types of the cars under research exceeded the admissible values. It may cause damage in the carrying structure and can lead to a loss of stability on the deck. Therefore, there is a need to improve the carrying structure of a car for guaranteeing its strong interaction with lashing devices on the train ferry deck.

PART 3
IMPROVEMENTS IN THE CARRYING STRUCTURE OF A CAR BODY FOR MORE RELIABLE FIXATION ON THE FERRY DECKS

3.1 Design of the structural unit of a car body for reliable fixation on the ferry deck

The location of chain binders relative to the planes of bodies and their fixation considerably affect the strength of the carrying structure of a car transported by a ferry.

On the basis of the research into actual typical fixation patterns used for the cars on the decks of Ukraine's ferries the authors revealed that the structural elements most frequently used for fixation are intended for drawing cars during shunting operations, rather than for interaction with reusable devices of ferries. Therefore, such fixation leads to damage in these elements, as the dynamic processes in the cars on the deck during sea disturbance differ from typical shunting operations and include the multi-directional forces (complex stress state), rather than one-directional force.

There are some cases when adaptation of cars for sea transportation included formation of a special car fleet involved in international rail / sea transportation. Thus, there was the Agreement on Mutual Operation of Rail/Ferry Route between Illichevsk (Soviet Union) and Varna (Bulgaria) signed in 1978. The parties to the Agreement formed a rail car fleet with wheel sets for 1435/1520 mm railways [119].

It included 1500 rail cars of different types. Maintenance and current repairs were made by one of the party depending on the car location.

The overall car repairs were made by the Ministry of Transport, and repairs of car bogies for 1435 mm railways were made by Bulgaria Railways. The charges were mutually compensated.

The difficulty of coupling between Soviet and Bulgarian rail cars was solved by formation of batches with special drive cars at both ends equipped with an automatic coupler on one side and a screw coupler and buffers on the other.

Therefore, the required strength of the carrying structure of a body on the ferry deck can be guaranteed by usage of a special car fleet adopted for interaction with reusable lashing devices by means of special structural elements (units).

The geometrical parameters of these units involved the dimensions of the bolster beam of a car body and a chain binder's hook [120–123]. At the initial designing stage the unit for fixation of a chain binder's hook was taken as a frame structure of two vertical and one horizontal bars. The strength calculation was made by the finite element method. The calculation included a rectangular section of the unit's working part [70, 131]. Thus, the target function looks like:

$$F(x) \rightarrow \min. \tag{3.1}$$

The variation parameters in calculation were length, width and height of the unit's working part.

With restrictions

1. $\sigma_p \cdot n \leq [\sigma]$,

where σ_p – design stresses, MPa;
n – strength reserve of the unit;
$[\sigma]$ – admissible stresses, MPa.

The design stresses σ_p were defined as follows:

$$\sigma_p = \left(\frac{M}{W} + \frac{p}{S} \right) k_h \cdot k_b, \tag{3.2}$$

where M – bending moment on the working part of the unit, kN · m;
P – force applied to the unit for fixation of a chain binder's hook, kN;

W – moment resistance of the working part of the unit, m^3;
S – contact area between the unit and the chain binder's hook, m^2, ($S = k \cdot b$);
k_h, k_b – coefficient corresponding to the geometric irregularity of location of a chain binder along the car body height and from the deck ring to the vertical plane of a car body.

2. $l \geq l_{min}$, $b \geq b_{min}$, $h \geq h_{min}$,

where $l \geq l_{min}$, $b \geq b_{min}$, $h \geq h_{min}$ – minimal admissible length, width and height of a unit's part, which interacts with a chain binder's hook, according to the sizes of the bolster beam and the chain binder's hook, m.
For this case l_{min} = 30 mm, b_{min} = 30 mm, h_{min} = 40 mm.

3. $n \geq 2$.

The geometry of this part was taken similar to the geometry of the chain binder to provide tight interaction of the working part of the unit for fixation of a car with a chain binder on the ferry deck.

On the basis of calculation the authors obtained a structural solution presented in Figure 3.1.

Hook guide 1 completely repeated the contact profile between the hook and the chain binder; it was intended for interaction with a fixation unit. The load concentration was reduced by means of radial lug 2 in the contact area between the unit and the support part. Cylindrical element 3 ensured good interaction between the hook and the unit; its height was designed with consideration of the hook width along the coupling geometry. Prismatic part 4 was intended for joining the working part of the unit with additional reinforcing part 5. Support parts of the 6 were intended for fixation on the bolster beam of a car [70, 124, 130, 131].

The optimized mass of the unit was about 10 kg.

The stress state of the unit for fixation of the chain binder's hook to the car was studied through strength calculation based on the energy theory; the number of elements in a mesh was 8 531 and the number of nodes – 13 829.

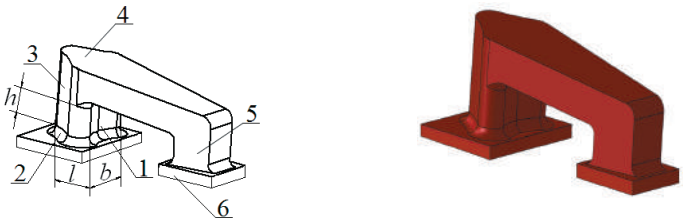

a) b)

Figure 3.1 – Unit for fixation of a chain binder:
a) spatial model; b) finite element model

The design diagram and the stress state of the unit are given in Figure 3.2.

During the strength calculation for the unit the fixation was modelled as rigid clamping by the support parts, and the loading was taken as an equally distributed force from the chain binder's hook to the unit across the contact area.

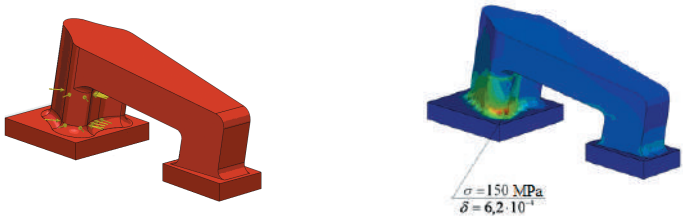

a) b)

Figure 3.2 – Unit for fixation of a chain binder to the car:
a) design diagram; b) stress state

On the basis of the calculation the authors concluded that during interaction between the chain binder's hook and the unit, i.e. when the working part of the unit (the radial guide of the chain binder's hook and the cylindrical part) was loaded, the maximum equivalent stresses could be observed in the area of the radial lug which connected

the working and the support parts. The stresses were equal to about 150 MPa, which was lower than the admissible values of the set steel grades (09G2D and 09G2C), and in the adapting and the additional parts the stresses were only 10 MPa. The maximum displacements in the unit were 0.02 mm and the deformations – $6.2 \cdot 10^{-4}$ in the area of the radial lug. The strength reserve of the structure was two.

Therefore, at the set force loads on the unit for fixation of the chain binder's hook the needed strength and stability were ensured [70].

For determination of the design lifetime of the unit for fixation of a car body on the ferry deck the following formula was used [125]:

$$T_n = \frac{\left(\sigma_{-1Д} / [n]\right)^m \cdot N_0}{B \cdot f_e \cdot \sigma_{ae}^m}, \tag{3.3}$$

where $\sigma_{-1Д}$ – average strength endurance of the unit, MPa;
n – admissible safety factor;
m – fatigue curve rate;
N_0 – number of tests;
B – coefficient characterizing a period of continuous work of the unit, sec;
f_e – effective frequency of dynamic loads, c^{-1};
σ_{ae} – amplitude of equivalent dynamic loads, MPa.

On the basis of research into the hydro meteorological characteristics of the Black Sea it was established that the annual sea disturbance period, taken into account for the calculation, was 18 days. According to the statistical data of last years it was established that the train ferry on the Chernomorsk – Varna route, chosen as the base ferry, made 50 round trips per year. The duration of a sea trip for a train ferry on the route was 18 hours; a full round trip was 36 hours. It implies that during one year the train ferry spends 1800 hours or 75 days in sea. The calculation of the design lifetime of the unit for fixation of the chain binder's hook involved the least favourable motion of a train ferry in sea, i.e. an 18-day stormy period.

The following input parameters were included in the calculation: average durability limit taken as $0{,}5\sigma_T$ of the material (steel grades 09G2D, O9G2C) – 150 MPa; test base – 10^7 cycles (recommended for steel); continuous working time for the unit – $1{,}5 \cdot 10^6$ c; effective frequency of dynamic loads determined through the excitation force parameters (for a sea wave) and for waves with a period of 9s – $0.1c^{-1}$; admissible safety factor – 2, fatigue curve rate for the welded structure (the bolster beam adopted for fixation on the ferry deck) – 4; amplitude of equivalent dynamic stresses determined on the basis of strength calculation for the bolster beam with the loads through the unit of fixation for the chain binder's hook – 140 MPa.

On the basis of the calculation the design lifetime of the unit for fixation of a car on the ferry deck accounted for about 5.2 years.

It should be mentioned that the service lifetime obtained for the unit of fixation of the carrying structure of a car body on the ferry deck is actually longer as the loads would not exceed 54 kN; it corresponds to normal operation conditions (calm sea or slight sea disturbance).

Besides, the lifetime can be prolonged with an appropriate maintenance and diagnostic system.

Higher rigidity of the section of the bolster beam for an open car can be reached with reinforcing diaphragms mounted in the areas where the unit for the binder chain's hook is fixed (Figure 3.3).

From the calculation it is possible to conclude that the reinforcing diaphragms mounted in the bolster beam can decrease stresses in the structure by about 20 % with a low increase of material capacity of the bolster beam by 6.6 kg.

The adequacy of the location angles of a chain binder on the car was checked through modelling its fixation on the body (Figure 3.4). It was established that the spatial location angles of a chain binder corresponded to the ones determined in [49, 51, 52, 70].

The results of the theoretical research conducted demonstrate that the new fixation pattern can ensure safe transportation of rail cars on the ferry decks during sea disturbance.

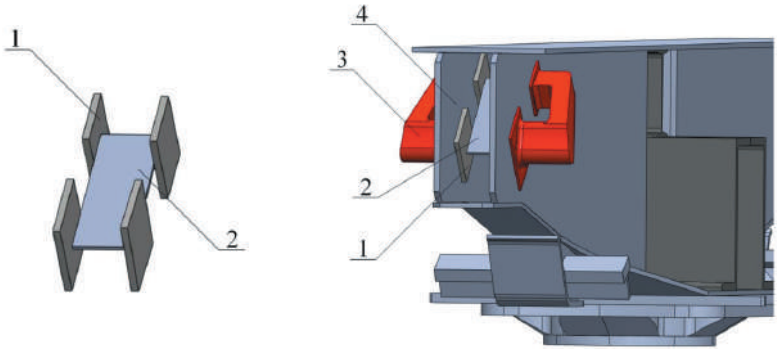

a) b)

Figure 3.3 – Reinforcement for the bolster beam section of an open car:
a) diaphragm; b) location of the reinforcing diaphragm in the bolster beam for an open car; 1 – reinforcing pad; 2 – joining pad; 3 – unit for fixation of the chain binder's hook; 4 – vertical sheet of the bolster beam

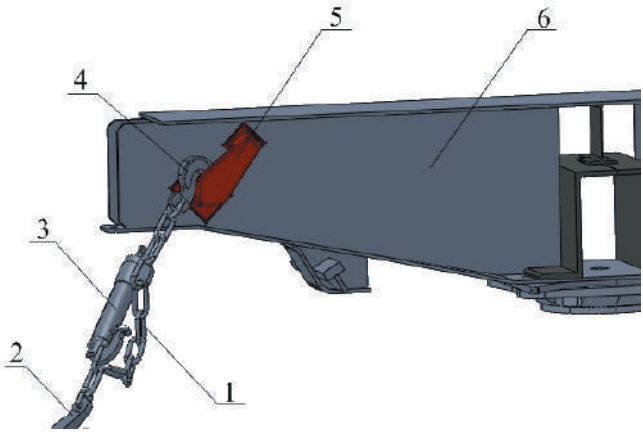

Figure 3.4 – Location of a chain binder relative to the bolster beam of an open car:
1 – chain binder; 2 – hook of a fixation ring; 3 – bottle screw; 4 – hook for fixation on the car; 5 – unit for fixation of the chain binder's hook; 6 – vertical sheet of the bolster beam

3.2 Determination of strength characteristics of the carrying structure of a car with the new fixation pattern

3.2.1 Determination of strength characteristics of the carrying structure of an open car

The strength characteristics of an open car body according to the new fixation pattern were determined through mounting the units for fixation of chain binders on the spatial model (Figure 3.5) [70, 114].

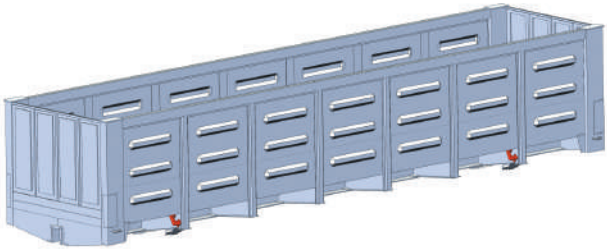

Figure 3.5 – Spatial model of the carrying structure of an open car body with units for fixation on the deck

The design model included the loads identical to those studied in 2.4.1 (Figures 3.6 and 3.7).

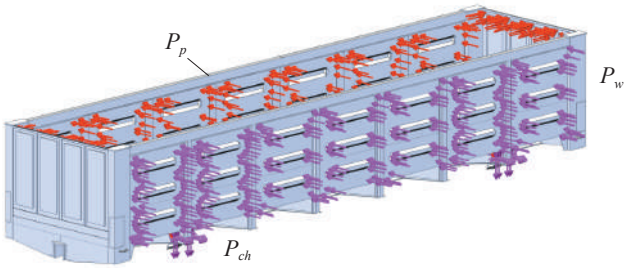

Figure 3.6 – Design diagram of the carrying structure of an open car body at angular displacements relative to the transverse axle

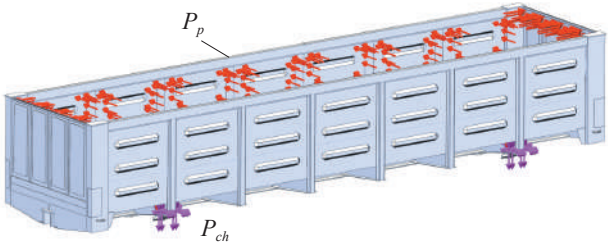

Figure 3.7 – Design diagram of the carrying structure of an open car body at angular displacements relative to the longitudinal axle

The finite element model (Figure 3.8) included isoparametrical tetrahedrons the optimal number of which was determined by the graph analytical method. The number of elements in a mesh was 509 592, the number of nodes – 164 044, the maximum element size – 80 mm; the minimum element size – 16 mm, the maximum element side ratio – 682.12, the percentage of elements with a side ratio of less than three – 27.2; and more than ten – 29.1. The element gain ratio in a mesh was 1.7. The number of elements in a circle was 9.

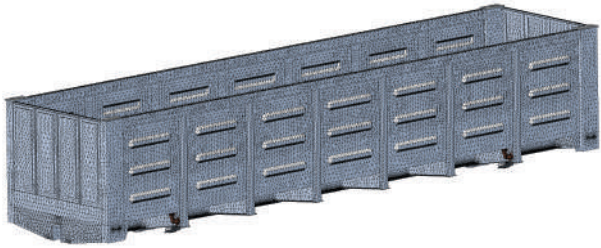

Figure 3.8 – Finite element model of the carrying structure of an open car body with units for fixation on the deck

The results of the calculation are given below.

Figure 3.9 – Stress state of an open car body at angular displacements relative to the transverse axle

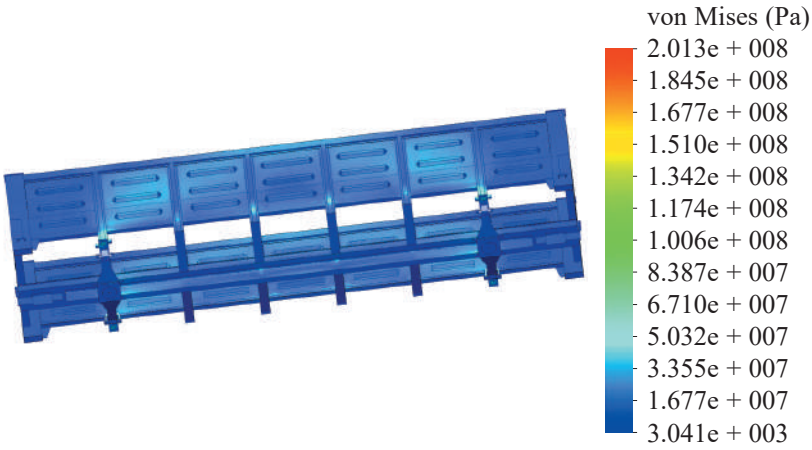

Figure 3.10 – Stress state of an open car body at angular displacements relative to the transverse axle

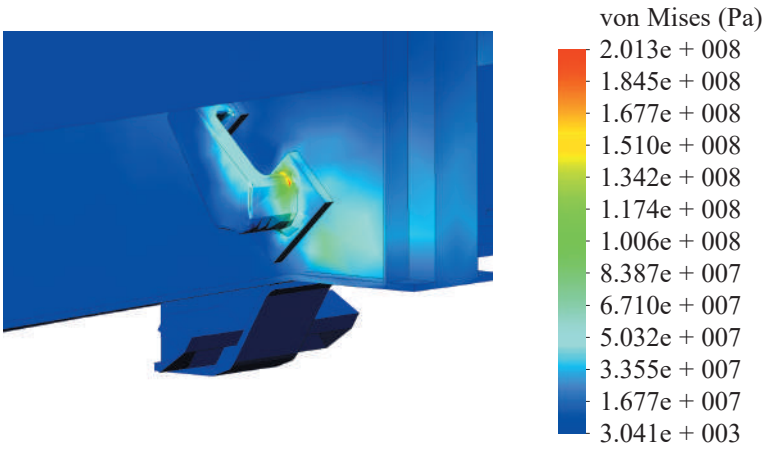

Figure 3.11 – Stress state of an open car body at angular displacements relative to the transverse axle

Figure 3.12 – Displacements in the units of an open car body at angular displacements relative to the transverse axle

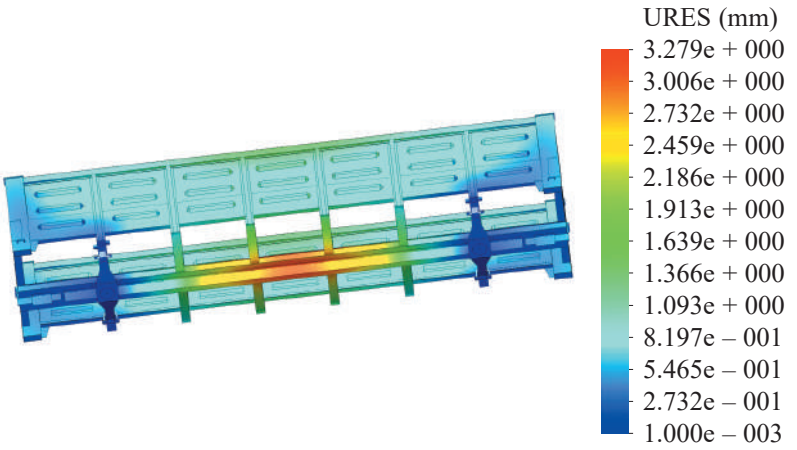

Figure 3.13 – Displacements in the units of an open car body at angular displacements relative to the transverse axle

Figure 3.14 – Deformations in the open car body at angular displacements relative to the transverse axle

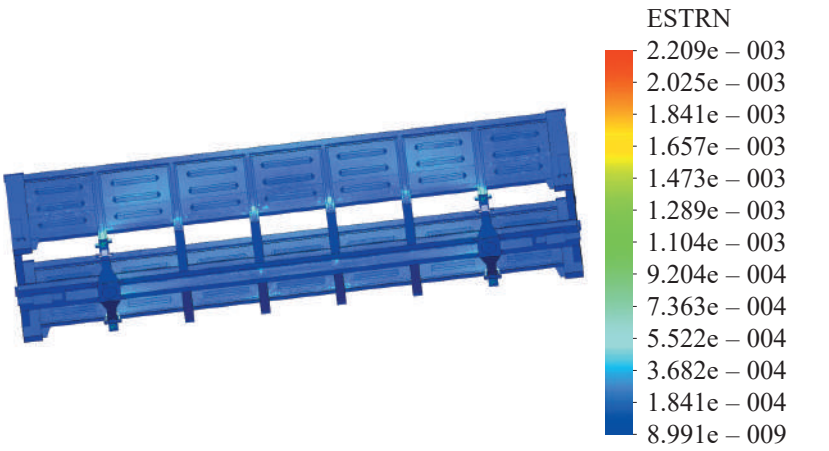

Figure 3.15 – Deformations in the open car body at angular displacements relative to the transverse axle

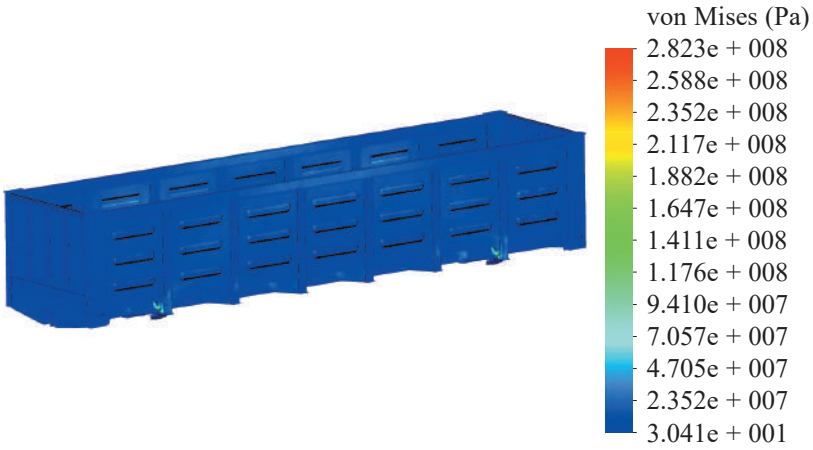

Figure 3.16 – Stress state of an open car body at angular displacements relative to the longitudinal axle

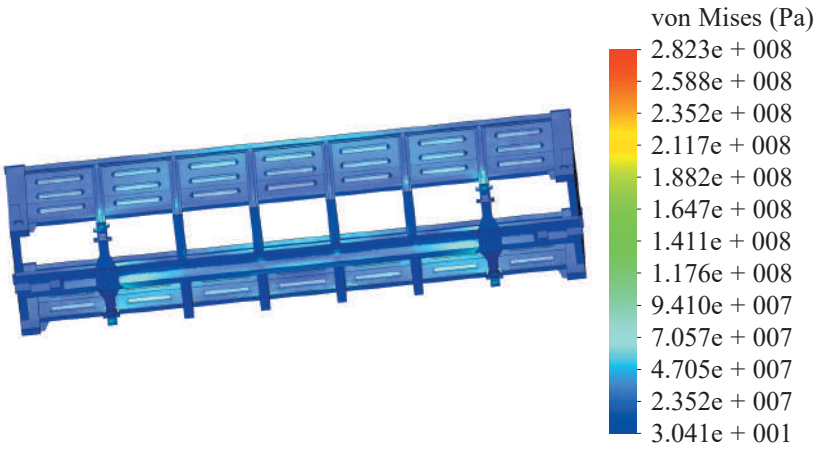

Figure 3.17 – Stress state of an open car body at angular displacements relative to the longitudinal axle

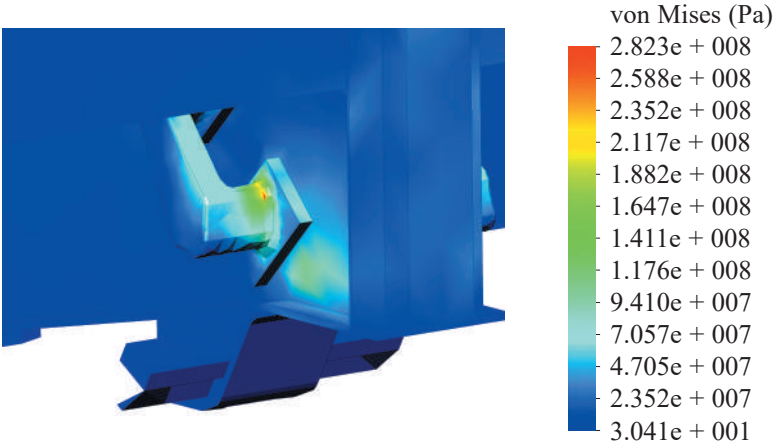

Figure 3.18 – Stress state of an open car body at angular displacements relative to the longitudinal axle

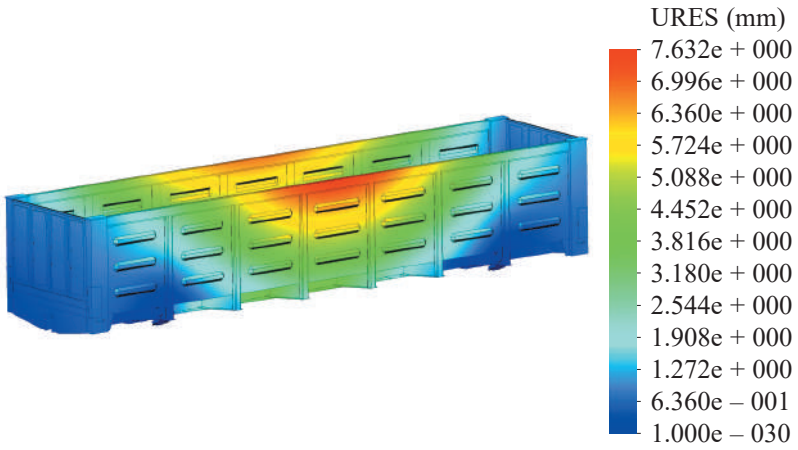

Figure 3.19 – Displacements in the units of an open car body at angular displacements relative to the longitudinal axle

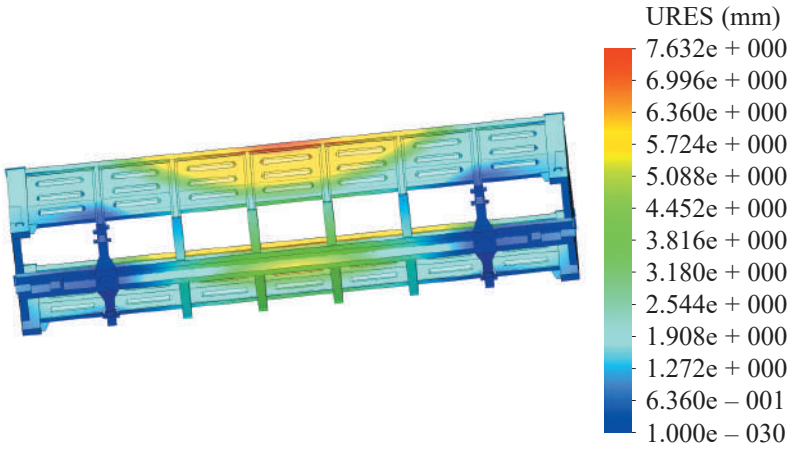

Figure 3.20 – Displacements in the units of an open car body at angular displacements relative to the longitudinal axle

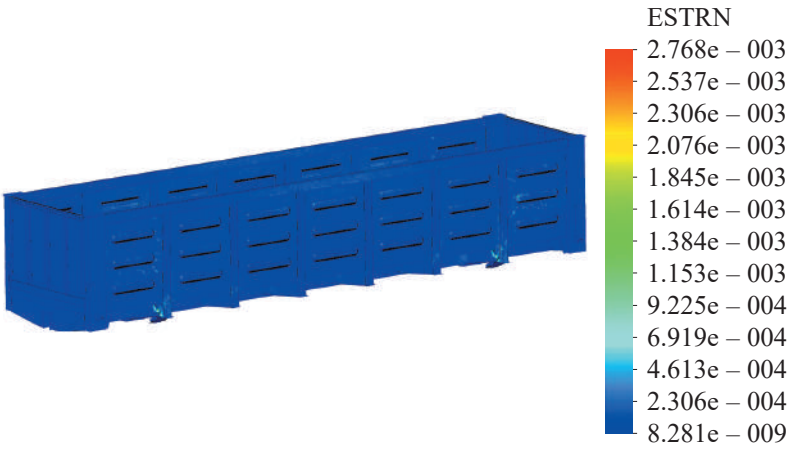

Figure 3.21 – Deformations in the open car body at angular displacements relative to the longitudinal axle

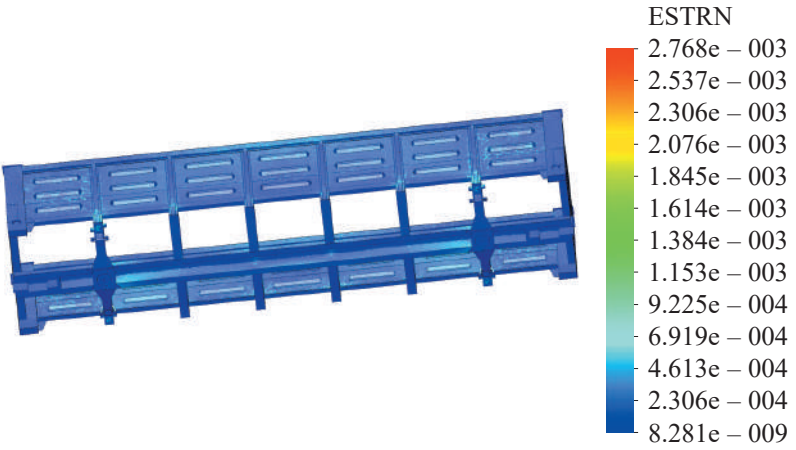

Figure 3.22 – Deformations in the open car body at angular displacements relative to the longitudinal axle

The maximum equivalent stresses in the open car body were generated at angular displacements of a train ferry about the longitudinal axle; they accounted for about 280 MPa. The maximum displacements were in the side wall of an open car body and equalled 7.6 mm. The maximum deformations were $2.8 \cdot 10^{-3}$.

At angular displacements of an open car body about the transverse axle the maximum equivalent stresses were 200 MPa. The maximum displacements were 3.3 mm, and the maximum deformations were $2.2 \cdot 10^{-3}$.

Thus, the new fixation pattern for a car on the deck demonstrated the maximum equivalent stresses in the body elements which did not exceed the admissible values.

3.2.2 Determination of the strength characteristics of the carrying structure of a tank car

The strength characteristics of the carrying structure of a tank car according to the new fixation pattern were determined by means of mounting the units for fixation of chain binders on the spatial model (Figure 3.23) [114].

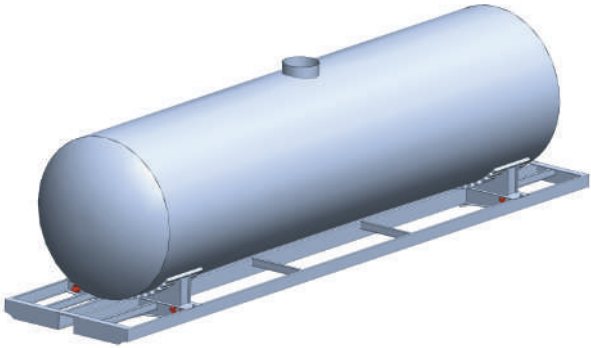

Figure 3.23 – Spatial model of the carrying structure of a tank car with units for fixation on the deck

The design model included the loads identical to those studied in 2.4.2 (Figures 3.24 and 3.25).

The finite element model (Figure 3.26) included isoparametrical tetrahedrons the optimal number of which was determined by the graph analytical method. The number of elements in a mesh was 854 729, the number of nodes – 272 478, the maximum element size – 40 mm; the minimum element size – 8 mm, the maximum element side ratio – 169.25, the percentage of elements with a side ratio of less than three – 24.5 and more than ten – 0.571. The element gain ratio in a mesh was 1.7. The number of elements in a circle was 9.

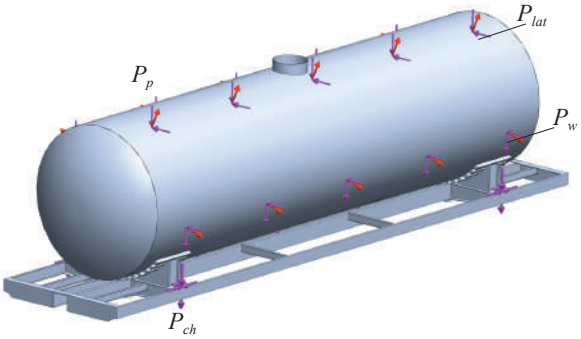

Figure 3.24 – Design diagram of the carrying structure of a tank car at angular displacements about the transverse axle

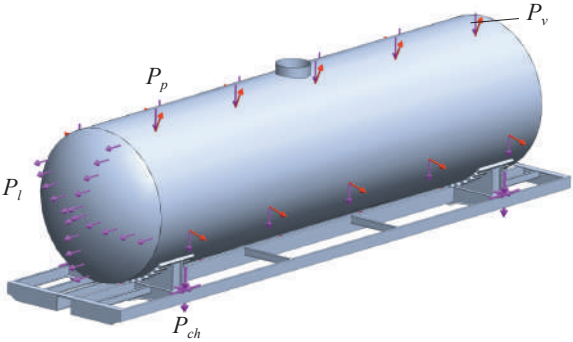

Figure 3.25 – Design diagram of the carrying structure of a tank car at angular displacements about the transverse axle

Figure 3.26 – Spatial model of the carrying structure of a tank car with units for fixation on the deck

The results of the calculation are given below.

Figure 3.27 – Stress state of the carrying structure of a tank car at angular displacements relative to the transverse axle

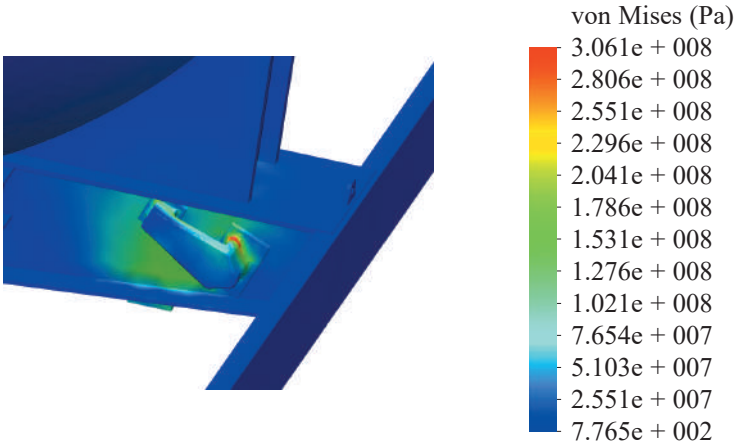

Figure 3.28 – Stress state of the carrying structure of a tank car at angular displacements relative to the transverse axle

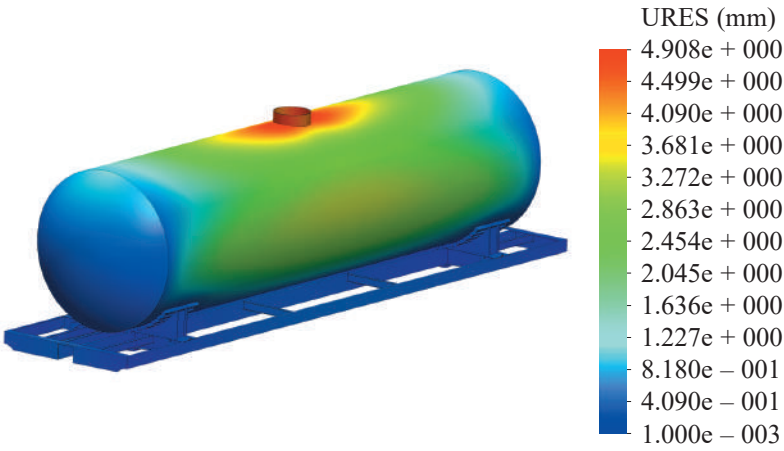

Figure 3.29 – Displacements in the units of the carrying structure of a tank car at angular displacements relative to the transverse axle

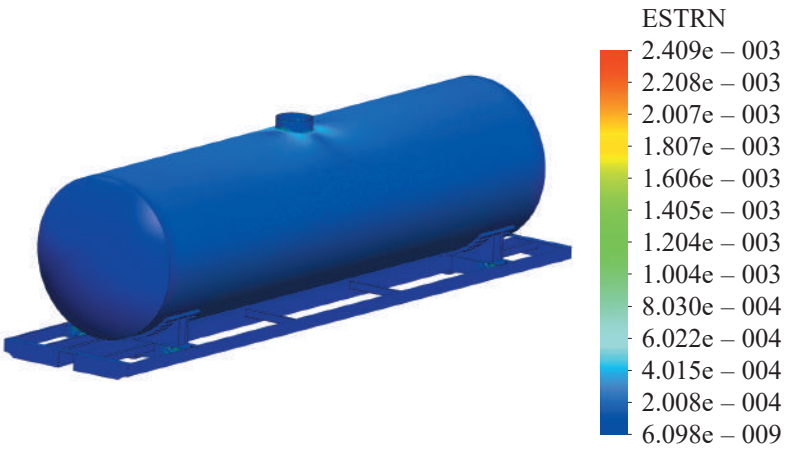

Figure 3.30 – Deformations in the carrying structure of a tank car at angular displacements relative to the transverse axle

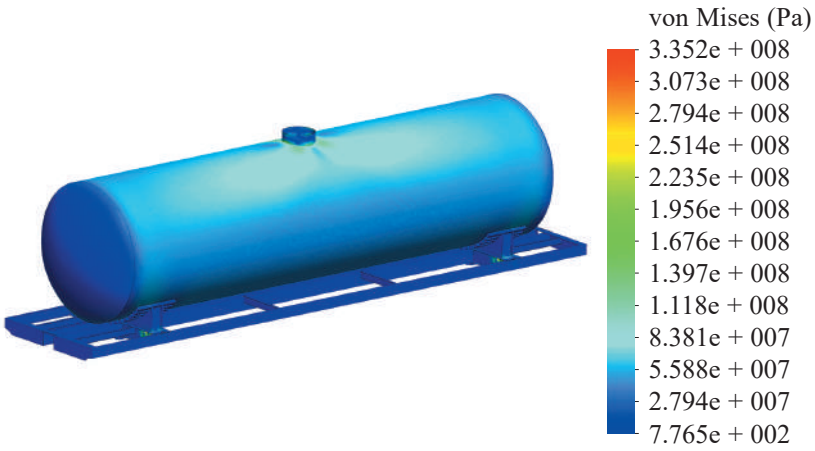

Figure 3.31 – Stress state of the carrying structure of a tank car at angular displacements relative to the longitudinal axle

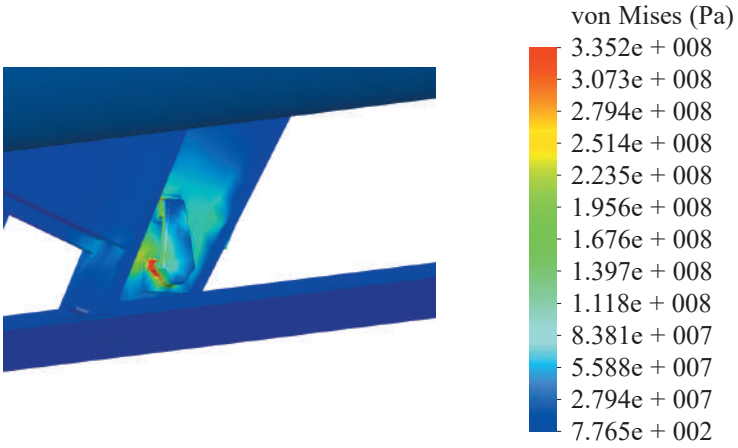

Figure 3.32 – Stress state of the carrying structure of a tank car at angular displacements relative to the longitudinal axle

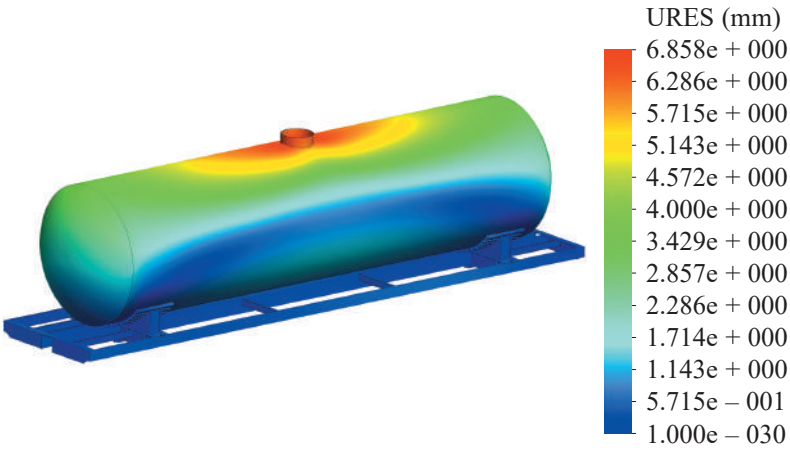

Figure 3.33 – Displacements in the units of the carrying structure of a tank car at angular displacements relative to the longitudinal axle

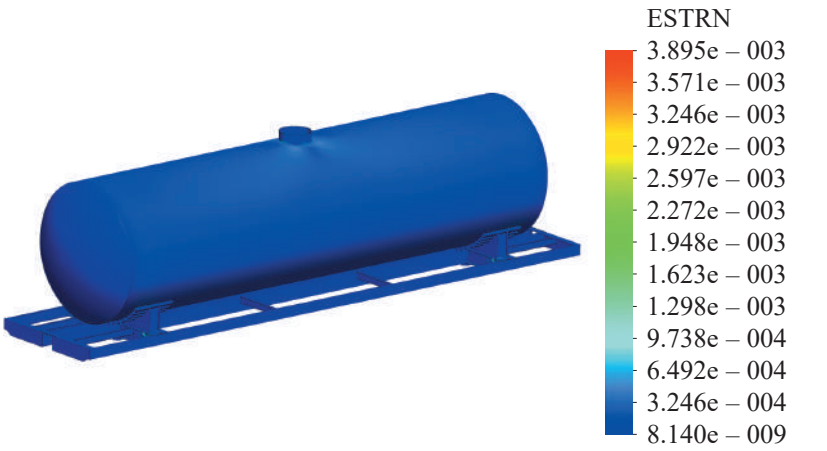

Figure 3.34 – Deformations in the carrying structure of a tank car at angular displacements relative to the longitudinal axle

The results of the calculation demonstrated that the maximum equivalent stresses in the carrying structure of a tank car were generated at angular displacements of a train ferry about the longitudinal axle and accounted for about 335 MPa. The maximum displacements were in the zones of loading hatches and accounted for 6.9 mm. The maximum deformations were $3.9 \cdot 10^{-3}$.

At angular displacements of the carrying structure of a tank car about the transverse axle the maximum equivalent stresses equalled about 300 MPa. The maximum displacements were 4.9 mm, and the deformations were $2.4 \cdot 10^{-3}$.

Thus, the new fixation pattern for cars on the deck demonstrated the maximum equivalent stresses in the body elements which did not exceed the admissible values.

3.2.3 Determination of the strength characteristics of the carrying structure of a boxcar

The strength characteristics of the carrying structure of a boxcar according to the new fixation pattern were determined through mounting the units for fixation of chain binders on the spatial model (Figure 3.5) [114].

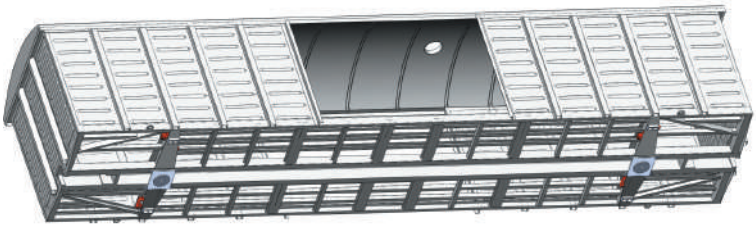

Figure 3.35 – Carrying structure of a boxcar with units for fixation on the deck

The design model included the loads identical to those described in 2.4.3 (Figures 3.36 and 3.37).

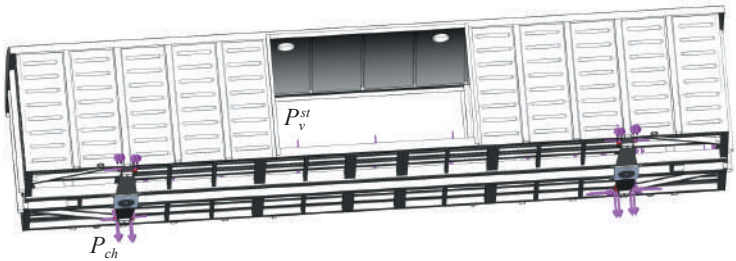

Figure 3.36 – Design diagram of the carrying structure of a boxcar at angular displacements relative to the transverse axle

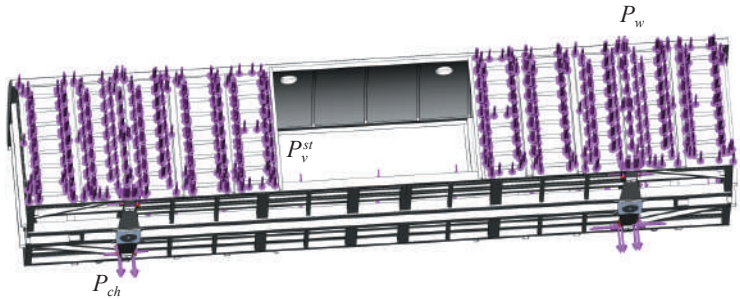

Figure 3.37 – Design diagram of the carrying structure of a boxcar at angular displacements relative to longitudinal axle

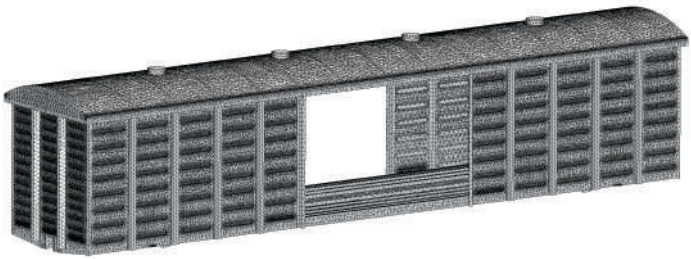

Figure 3.38 – Finite element model of the carrying structure of a boxcar with units for fixation on the deck

The finite element model (Figure 3.38) included isoparametrical tetrahedrons the optimal number of which was determined by the graph analytical method. The number of elements in a mesh was 876 083, the number of nodes – 314 193, the maximum element size – 80 mm; the minimum element size – 16 mm, the maximum element side ratio – 1 609.9; the percentage of elements with a side ratio of less than three – 12.6 and more than ten – 40.5. The element gain ratio in a mesh was 1.9. The number of elements in a circle was 22.

The results of the calculation are given below.

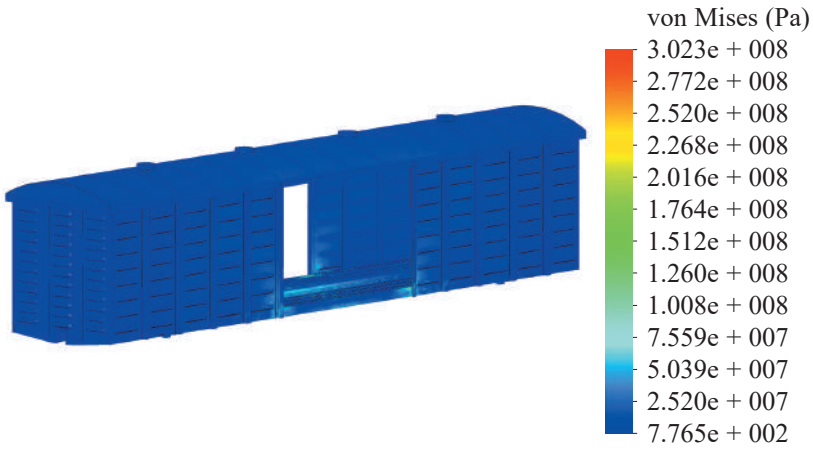

Figure 3.39 – Stress state of the carrying structure of a boxcar at angular displacements relative to the transverse axle

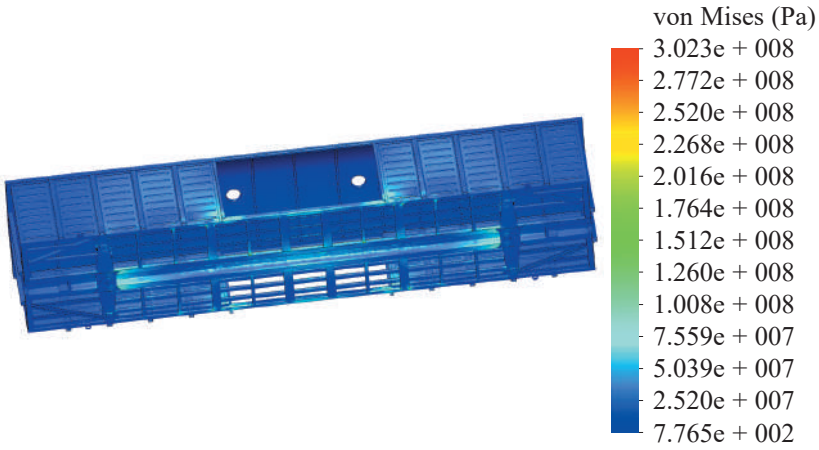

Figure 3.40 – Stress state of the carrying structure of a boxcar at angular displacements relative to the transverse axle

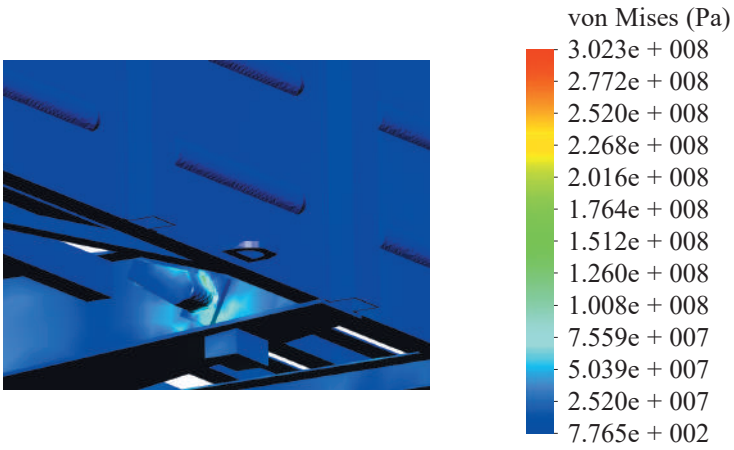

Figure 3.41 – Stress state of the carrying structure of a boxcar at angular displacements relative to the transverse axle

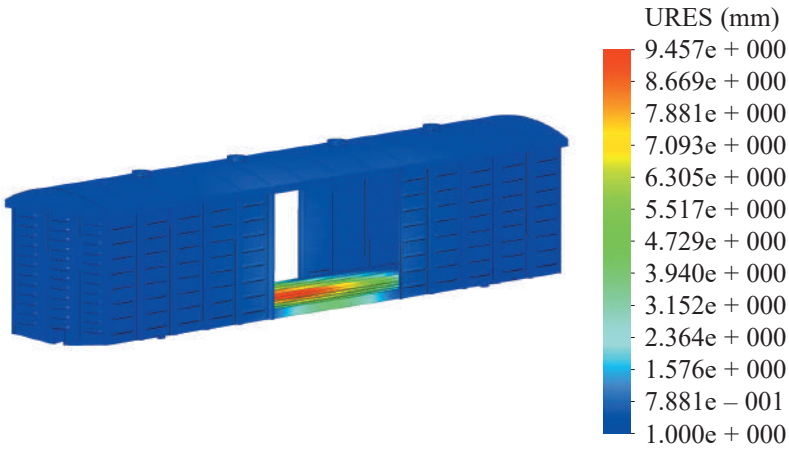

Figure 3.42 – Displacements in the units of the carrying structure of a boxcar at angular displacements relative to the transverse axle

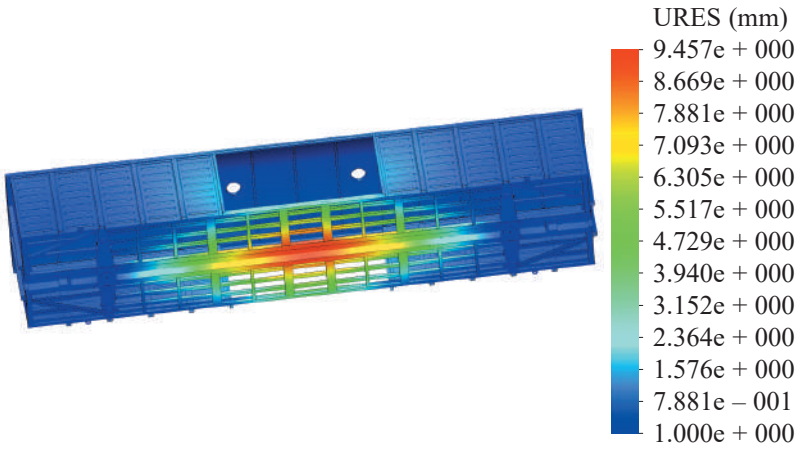

Figure 3.43 – Displacements in the units of the carrying structure of a boxcar at angular displacements relative to the transverse axle

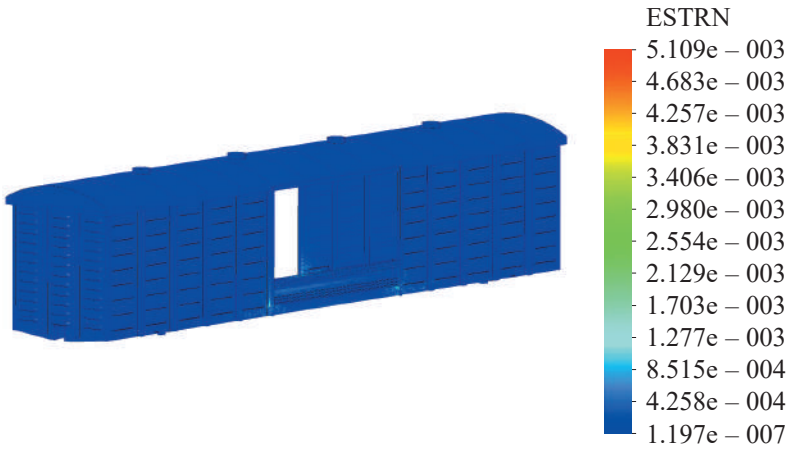

Figure 3.44 – Deformations in the carrying structure of a boxcar at angular displacements relative to the transverse axle

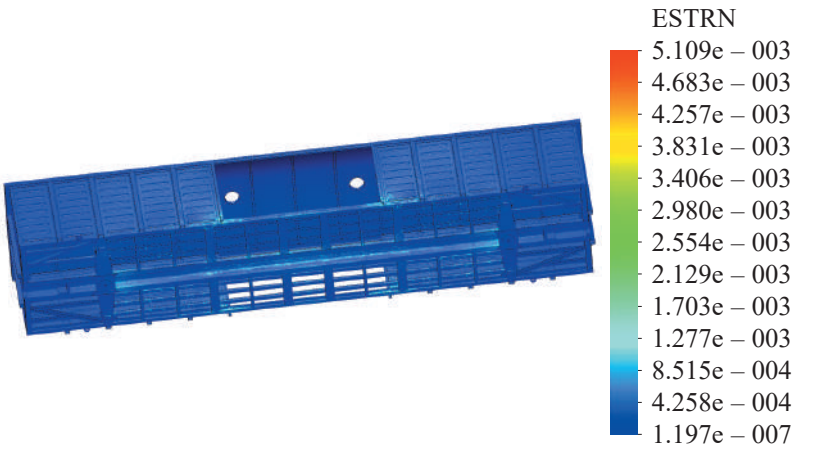

Figure 3.45 – Deformations in the carrying structure of a boxcar at angular displacements relative to the transverse axle

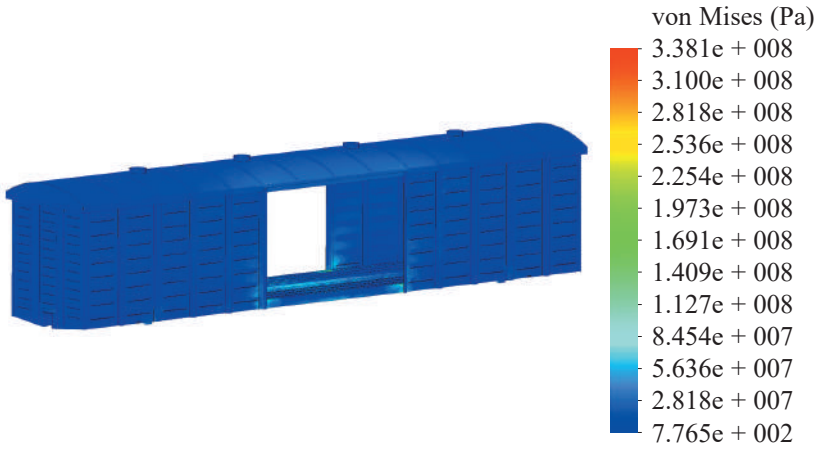

Figure 3.46 – Stress state of the carrying structure of a boxcar at angular displacements relative to the longitudinal axle

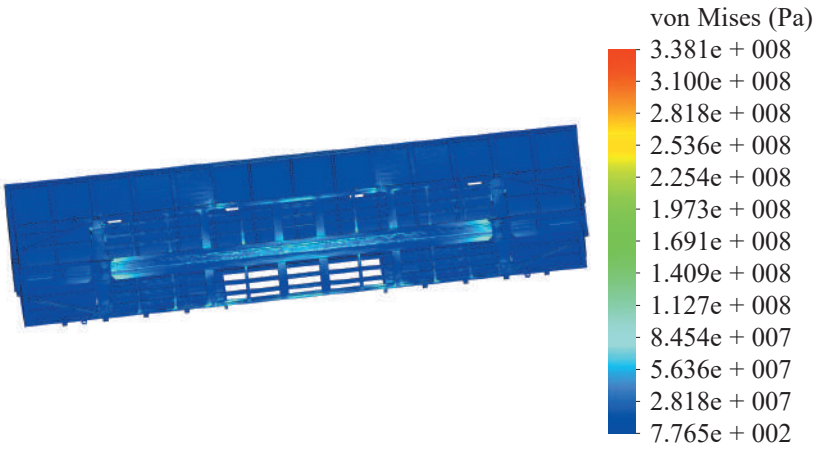

Figure 3.47 – Stress state of the carrying structure of a boxcar at angular displacements relative to the longitudinal axle

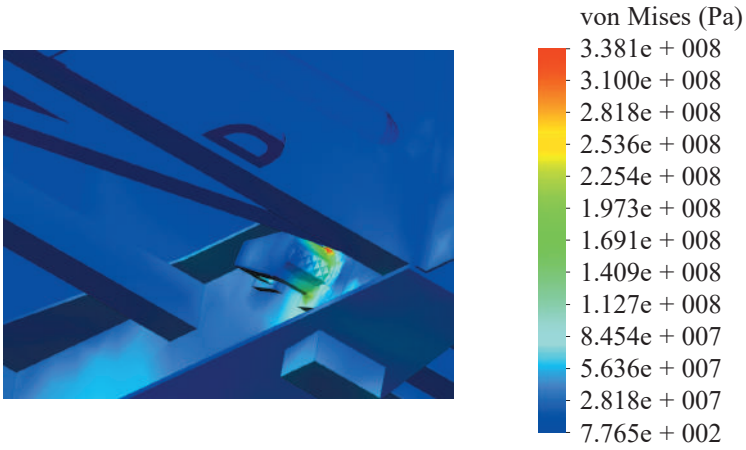

Figure 3.48 – Stress state of the carrying structure of a boxcar at angular displacements relative to the longitudinal axle

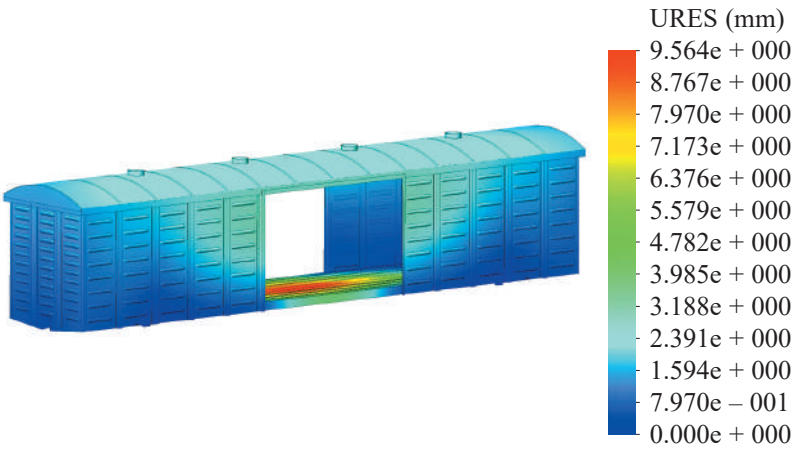

Figure 3.49 – Displacements in the units of the carrying structure of a boxcar at angular displacements relative to the longitudinal axle

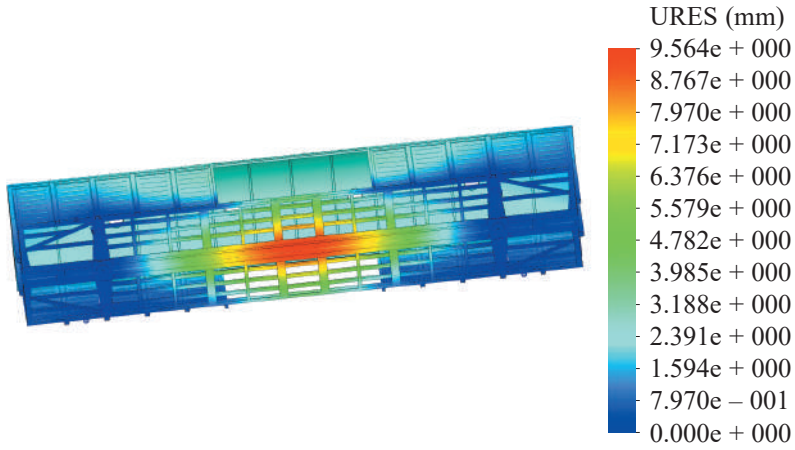

Figure 3.50 – Displacements in the units of the carrying structure of a boxcar at angular displacements relative to the longitudinal axle

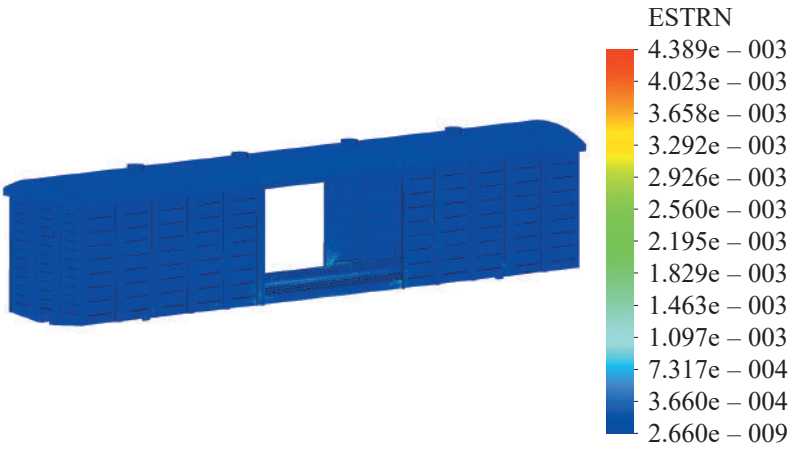

Figure 3.51 – Deformations in the carrying structure of a boxcar at angular displacements relative to the longitudinal axle

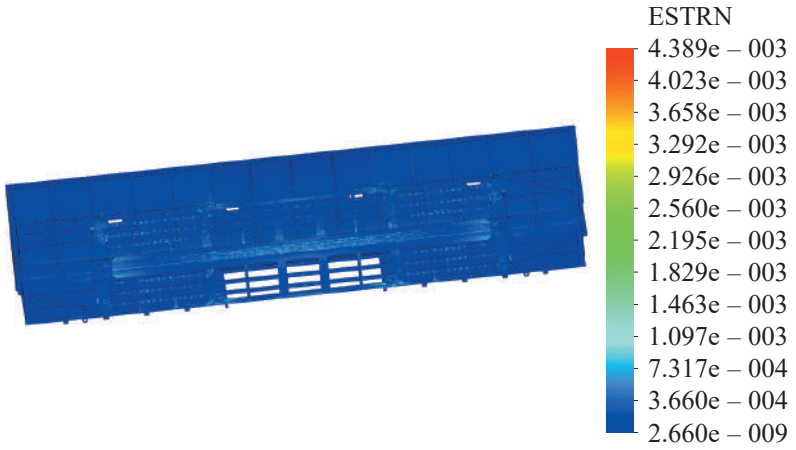

Figure 3.52 – Deformations in the carrying structure of a boxcar at angular displacements relative to the longitudinal axle

The results of the calculation demonstrated that the maximum equivalent stresses in the carrying structure of a boxcar were generated at angular displacements of a train ferry about the longitudinal axle and accounted for about 340 MPa. The maximum displacements were in the middle part of the center sill and accounted for 9.6 mm. The maximum deformations were about $4.4 \cdot 10^{-3}$.

At angular displacements of a boxcar body about the transverse axle the maximum equivalent stresses equalled 300 MPa. The maximum displacements were 9.5 mm, and the deformations were $5.1 \cdot 10^{-3}$.

Thus, the new fixation pattern for a boxcar on the deck demonstrated that the maximum equivalent stresses in the body elements did not exceed the admissible values.

3.2.4 Determination of the strength characteristics of the carrying structure of a hopper car

The strength characteristics of the carrying structure of a hopper car according to the new fixation pattern were determined by mounting the units for fixation of chain binders on the spatial model (Figure 3.53) [114].

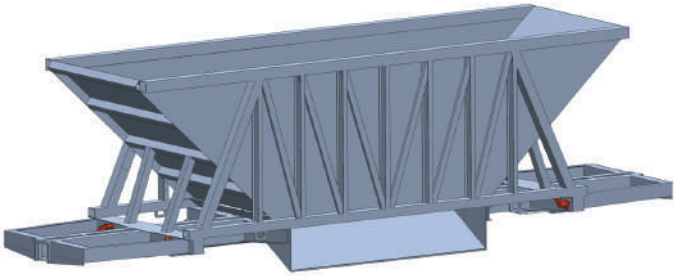

Figure 3.53 – Carrying structure of a hopper car with units for fixation on the deck

The design model included the loads identical to those described in 2.4.4 (Figures 3.54 and 3.55).

The finite element model (Figure 3.56) included isoparametrical tetrahedrons the optimal number of which was determined by the graph analytical method. The number of elements in a mesh was 420 212, the number of nodes – 137 878, the maximum element size – 60 mm; the minimum element size – 12 mm, the maximum element side ratio – 803.59, the percentage of elements with a side ratio of less than three – 14.4 and more than ten – 30.3. The element gain ratio in a mesh was 1.8. The number of elements in a circle was 12.

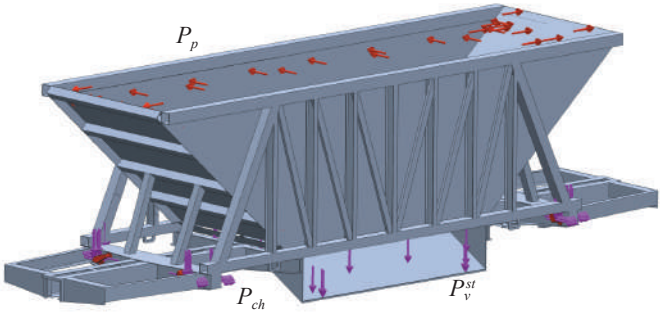

Figure 3.54 – Design diagram of the carrying structure of a hopper car at angular displacements relative to the transverse axle

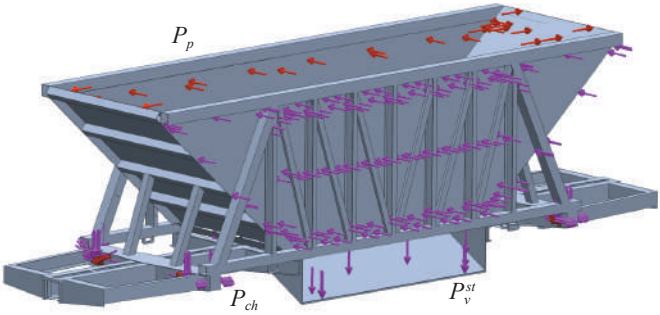

Figure 3.55 – Design diagram of the carrying structure of a hopper car at angular displacements relative to the longitudinal axle

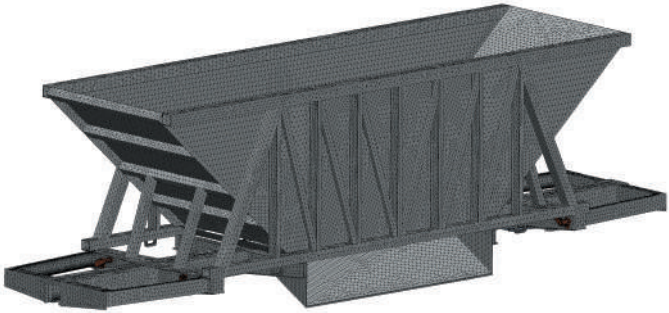

Figure 3.56 – Finite element model of the carrying structure of a hopper car with units for fixation on the deck

The results of the calculation are given below.

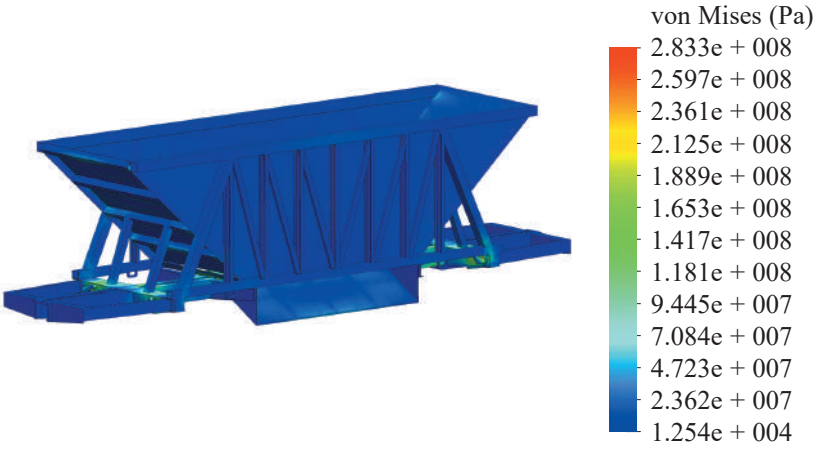

Figure 3.57 – Stress state of the carrying structure of a hopper car at angular displacements relative to the longitudinal axle

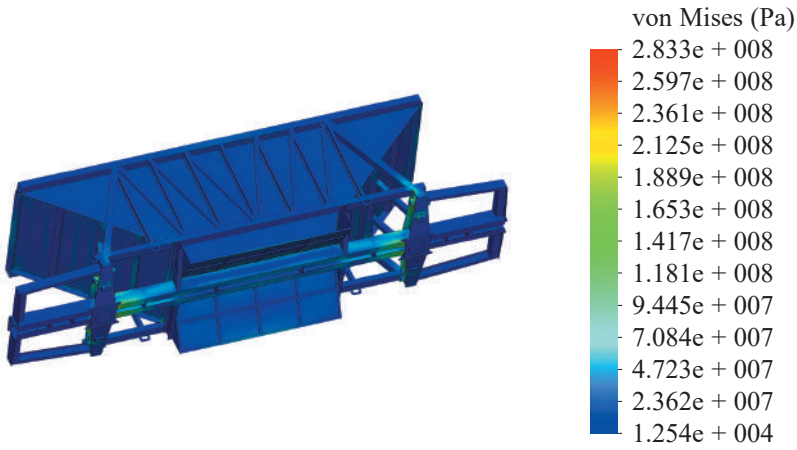

Figure 3.58 – Stress state of the carrying structure of a hopper car at angular displacements relative to the longitudinal axle

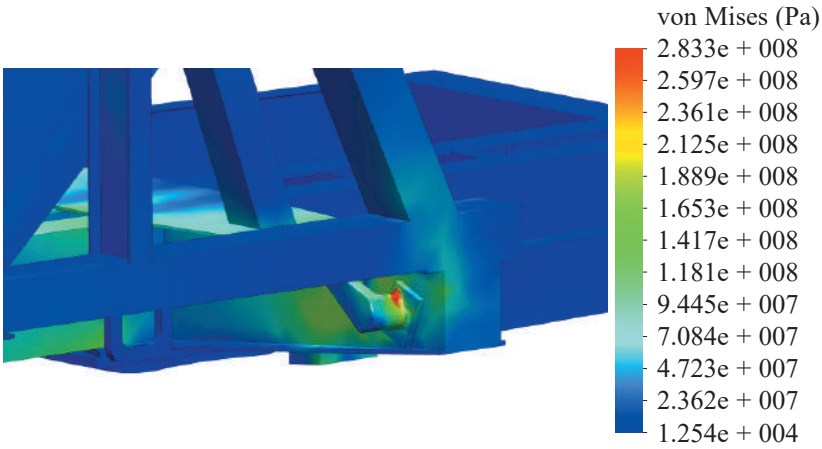

Figure 3.59 – Stress state of the carrying structure of a hopper car at angular displacements relative to the longitudinal axle

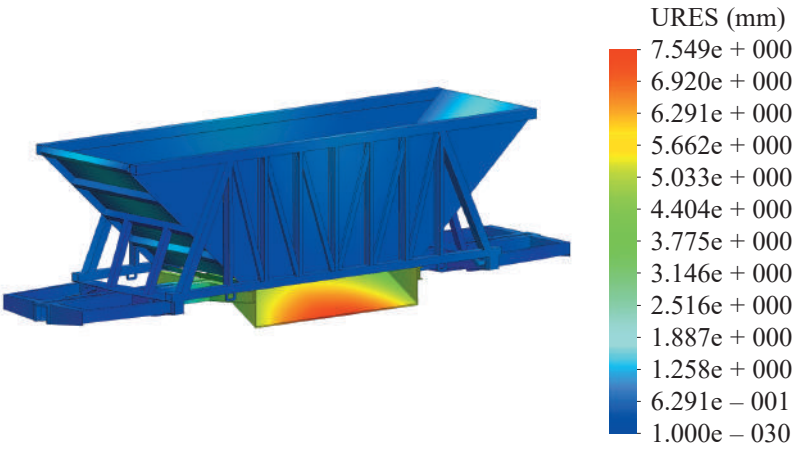

Figure 3.60 – Displacements in the units of the carrying structure of a boxcar at angular displacements relative to the transverse axle

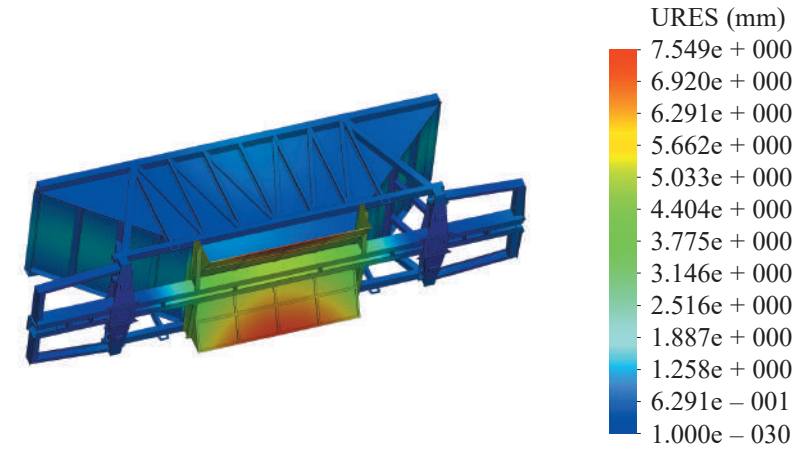

Figure 3.61 – Displacements in the units of the carrying structure of a hopper car at angular displacements relative to the transverse axle

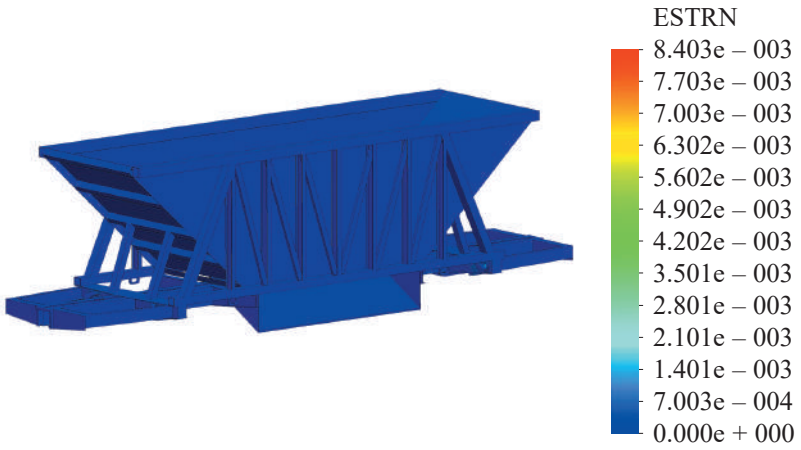

Figure 3.62 – Deformations in the carrying structure of a hopper car at angular displacements relative to the transverse axle

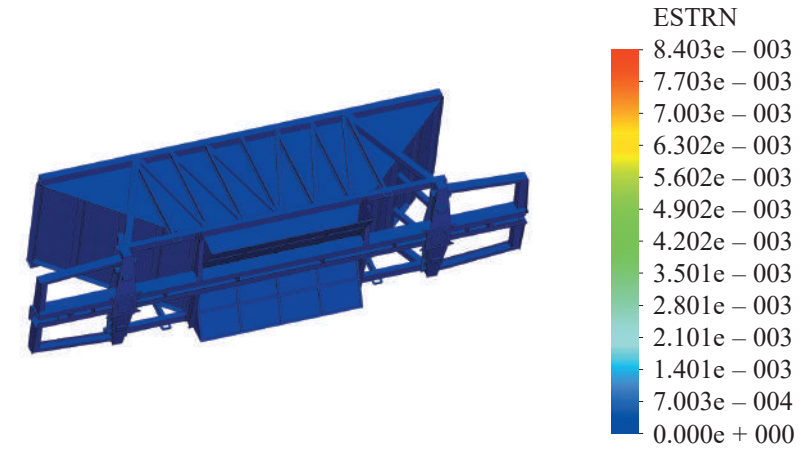

Figure 3.63 – Deformations in the carrying structure of a hopper car at angular displacements relative to the transverse axle

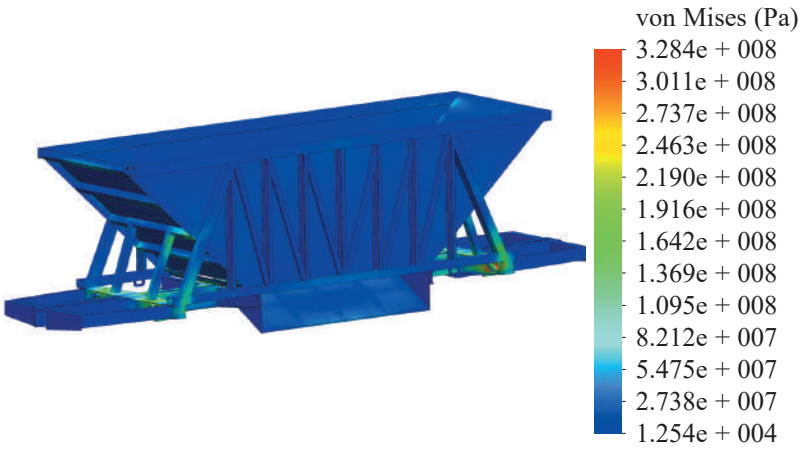

Figure 3.64 – Stress state of the carrying structure of a hopper car at angular displacements relative to the longitudinal axle

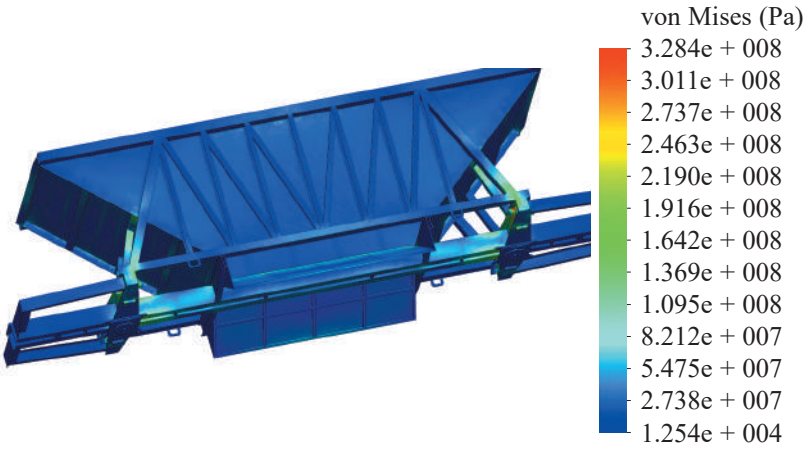

Figure 3.65 – Stress state of the carrying structure of a hopper car at angular displacements relative to the longitudinal axle

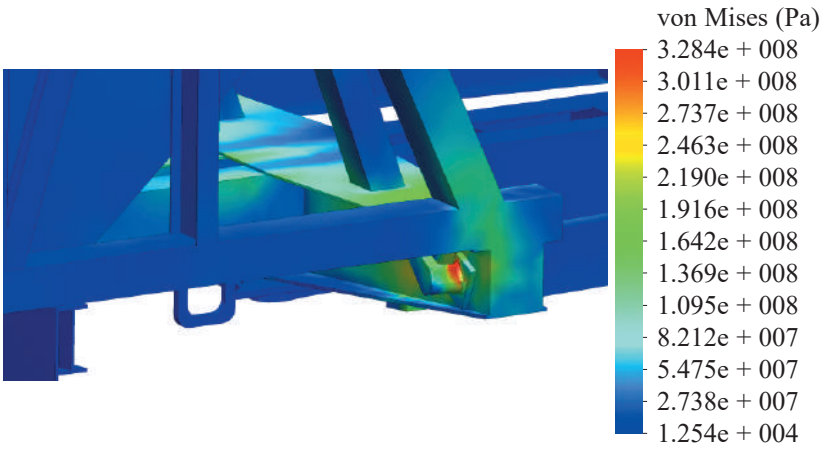

Figure 3.66 – Stress state of the carrying structure of a hopper car at angular displacements relative to the longitudinal axle

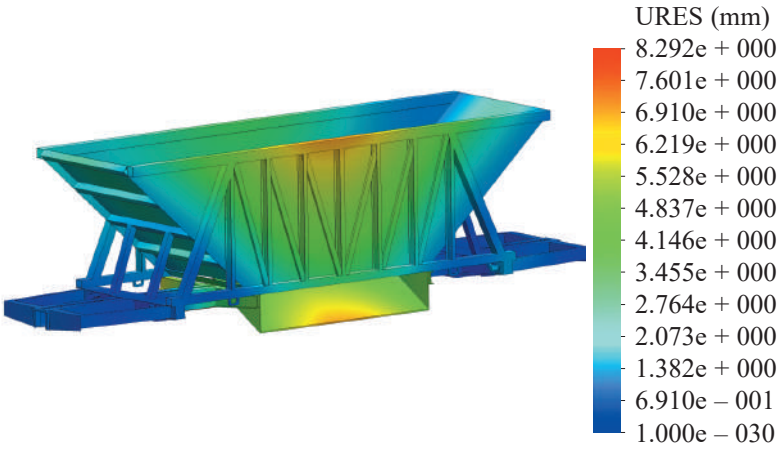

Figure 3.67 – Displacements in the units of the carrying structure of a hopper car at angular displacements relative to the longitudinal axle

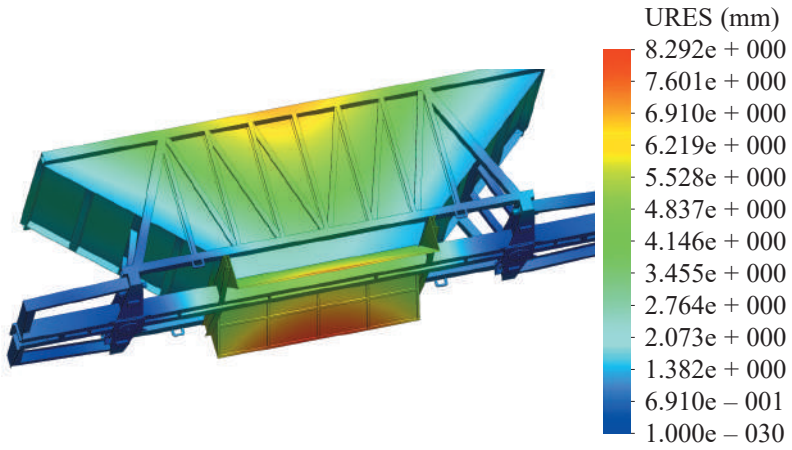

Figure 3.68 – Displacements in the units of the carrying structure of a hopper car at angular displacements relative to the longitudinal axle

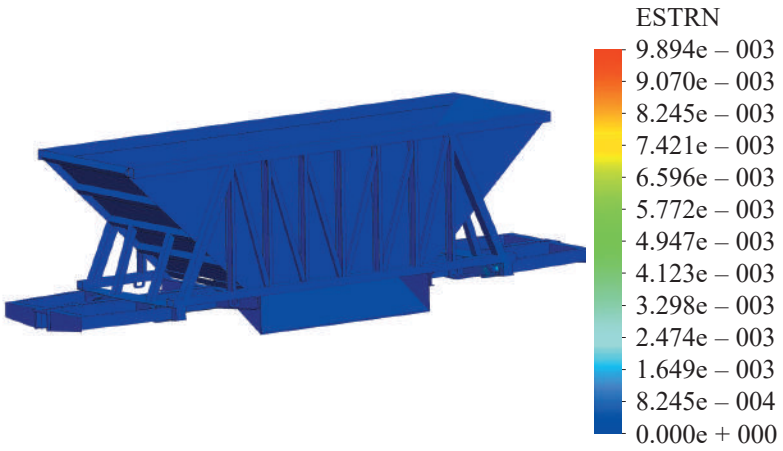

Figure 3.69 – Deformations in the carrying structure of a hopper car at angular displacements relative to the longitudinal axle

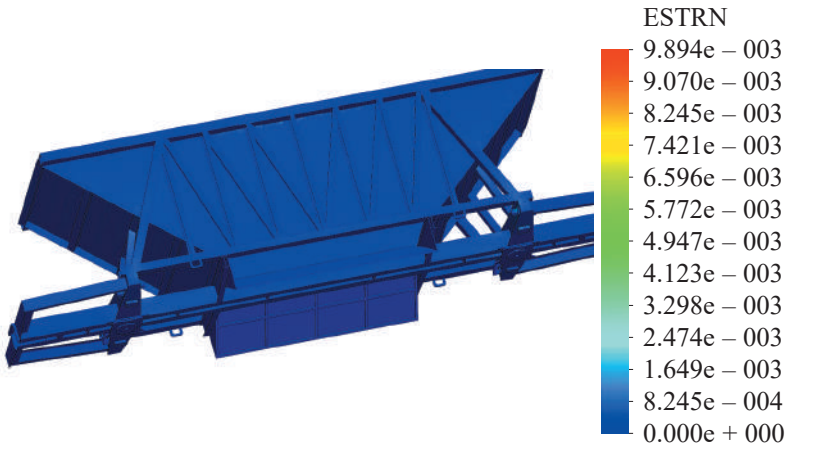

Figure 3.70 – Deformations in the carrying structure of a hopper car at angular displacements relative to the longitudinal axle

The results of the calculation demonstrated that the maximum equivalent stresses in the body of a hopper car were generated at angular displacements of a train ferry about the longitudinal axle and accounted for about 330 MPa. The maximum displacements were in the discharge hoppers and accounted for about 8.0 mm. The maximum deformations were nearly $9.9 \cdot 10^{-3}$.

At angular displacements of a hopper car body about the transverse axle the maximum equivalent stresses equalled 280 MPa. The maximum displacements were 7.5 mm, and the deformations were $8.4 \cdot 10^{-3}$.

Thus, the new fixation pattern for a hopper car on the deck demonstrated that the maximum equivalent stresses in the body elements did not exceed the admissible values.

3.2.5 Determination of the strength characteristics of the carrying structure of a flat car

As far as due to the structural features of a universal flat car it is impossible to fasten chain binders on the wall, the authors designed some adaptation measures for transportation of flat cars by ferries. Thus, they suggest additional elements installed on the flat car to be used for mounting the units to interact with a chain binder's hook (Figure 3.71) [131, 132].

These elements are box-section superstructures with reinforcing diaphragms; the location areas of the support zones of the units for fixation of chain binder's hooks are equipped with reinforcing pads.

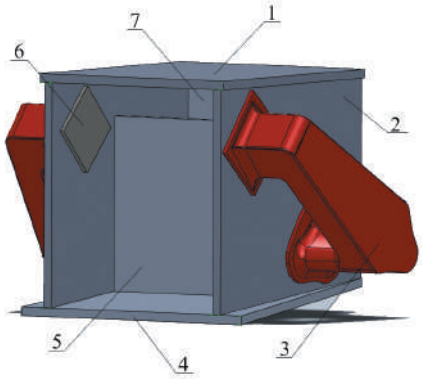

Figure 3.71 – Superstructure for units for fixation of chain binders on the flat car:
1 – upper plate; 2 – vertical plate; 3 – unit for fixation of the chain binder's hook; 4 – bottom plate; 5 – reinforcing diaphragm; 6 – reinforcing pads; 7 – front plate

Figure 3.72 presents a 13-401 universal flat car re-equipped for ferry transportation.

The supper structure of a flat car was calculated for strength. The results of the calculation proved the efficiency of the solutions taken.

The strength characteristics of the carrying structure of a flat car according to the new fixation pattern were determined by mounting the units for fixation of chain binders on the spatial model (Figure 3.72).

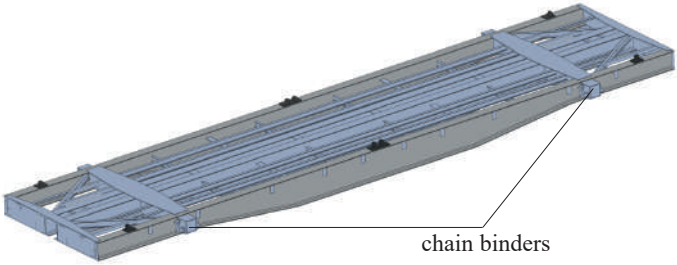

Figure 3.72 – Carrying structure of a flat car with units for fixation on the deck

The design model included the loads identical to those described in 2.4.5 (Figure 3.73). The finite element model (Figure 3.74) included isoparametrical tetrahedrons the optimal number of which was determined by the graph analytical method. The number of elements in a mesh was 141729, the number of nodes – 46552, the maximum element size – 492.0 mm, the minimum element size – 98.0 mm, the maximum element side ratio – $6.53 \cdot 10^5$, the percentage of elements with a side ratio of less than three – 1.9, and more than ten – 73.1. The element gain ratio in a mesh was 1.6. The number of elements in a circle was 8.

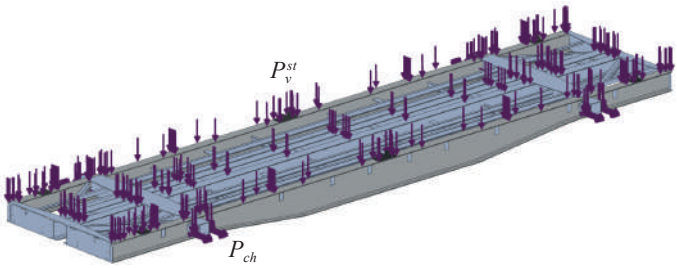

Figure 3.73 – Design diagram of the carrying structure of a flat wagon

Figure 3.74 – Finite element model of the carrying structure of a flat car with units for fixation on the deck

The results of the calculation are given below.

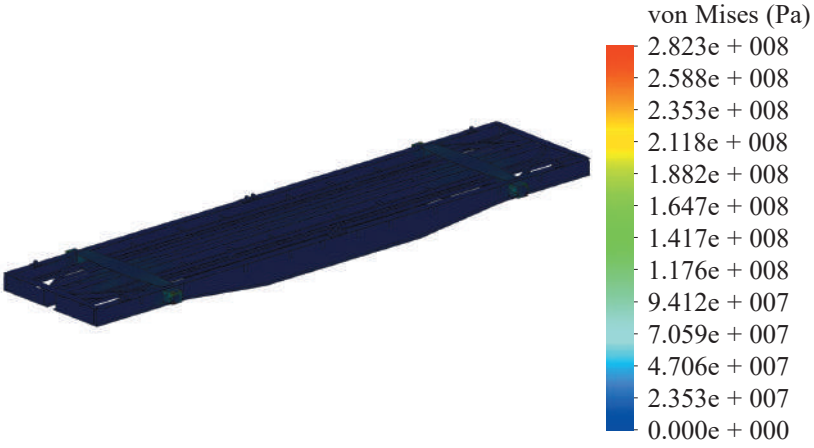

Figure 3.75 – Stress state of the carrying structure of a flat car at angular displacements about the transverse axle

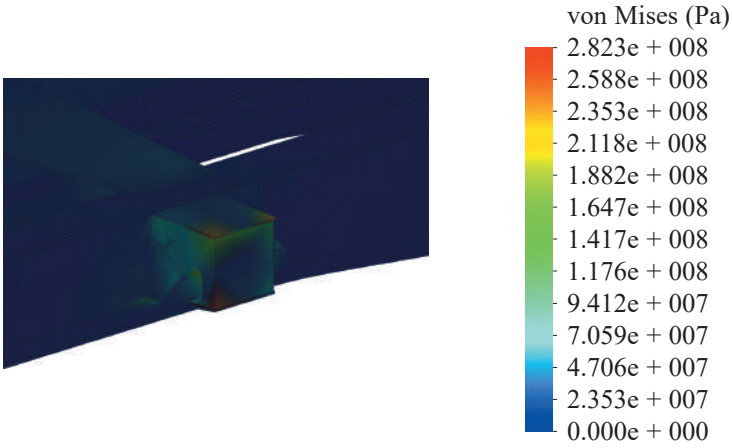

Figure 3.76 – Stress state of the carrying structure of a flat car at angular displacements about the transverse axle

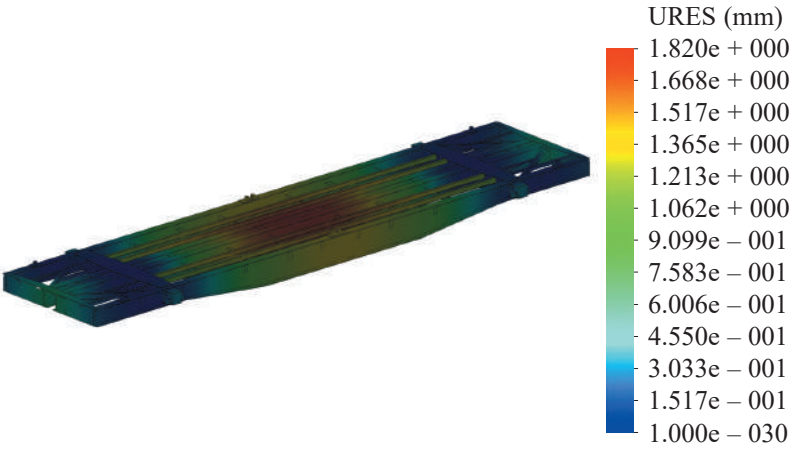

Figure 3.77 – Displacements in the units of the carrying structure of a flat car at angular displacements about the transverse axle

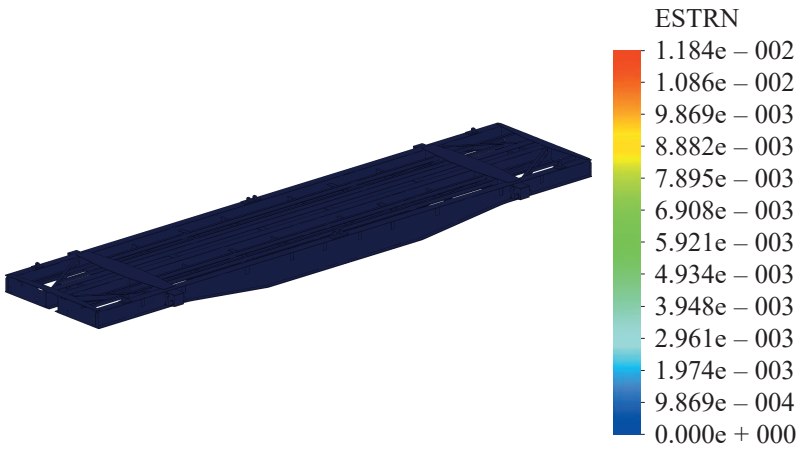

Figure 3.78 – Deformations in the carrying structure of a flat car at angular displacements about the transverse axle

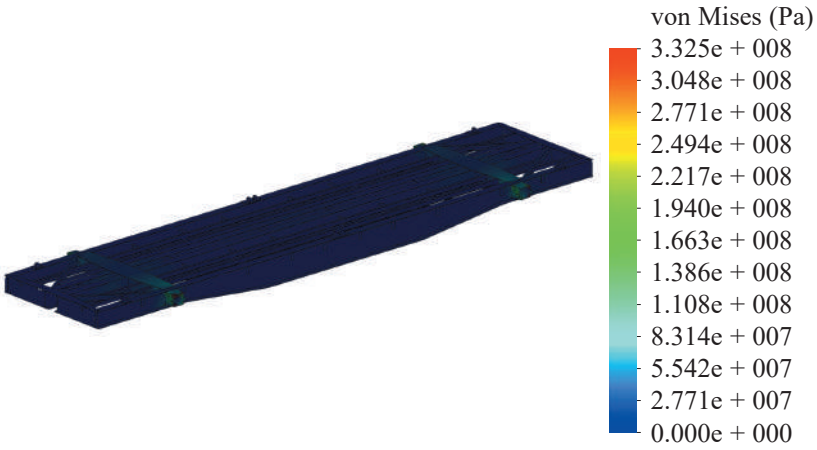

Figure 3.79 – Stress state of the carrying structure of a flat car at angular displacements about the longitudinal axle

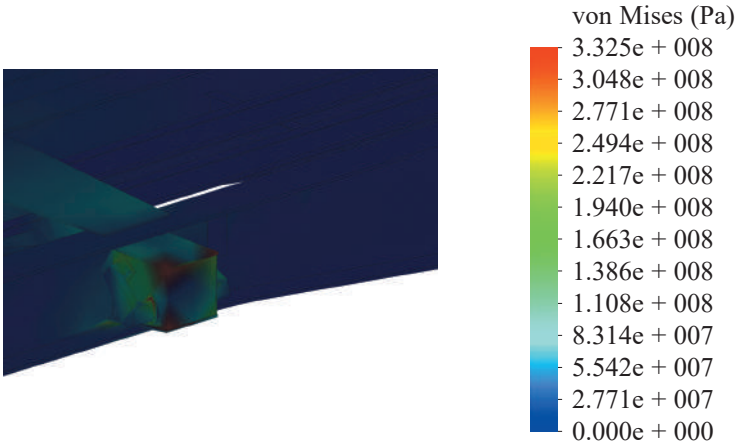

Figure 3.80 – Stress state of the carrying structure of a flat car at angular displacements about the longitudinal axle

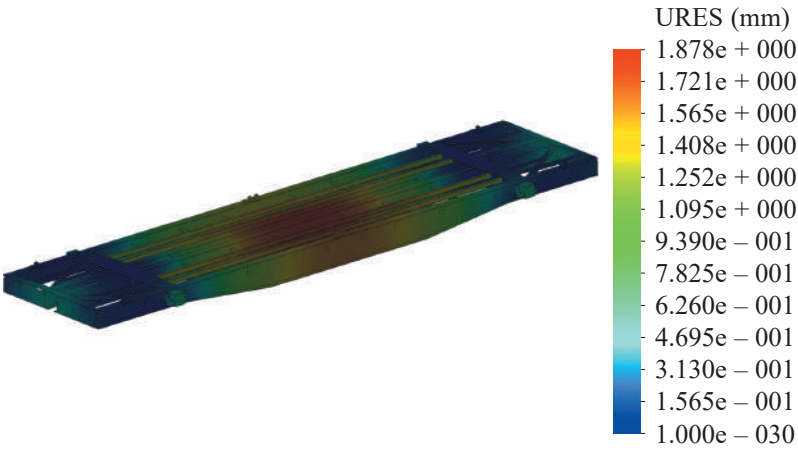

Figure 3.81 – Displacements in the units of the carrying structure of a flat car at angular displacements about the longitudinal axle

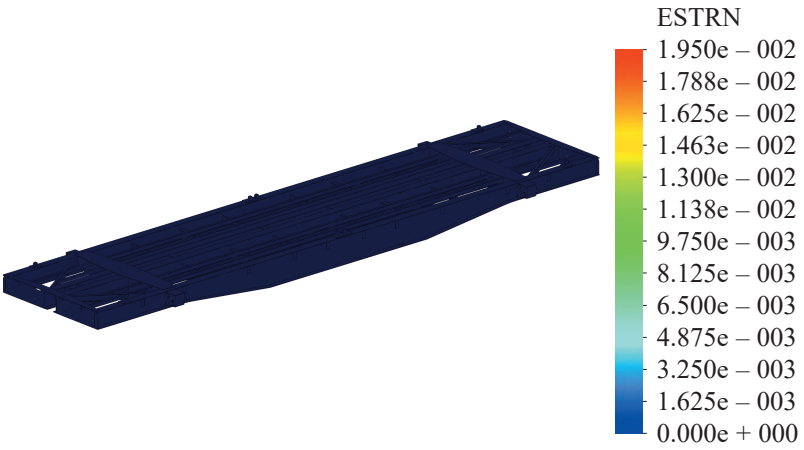

Figure 3.82 – Deformations in the carrying structure of a flat car at angular displacements about the longitudinal axle

From the calculation we can conclude that the maximum equivalent stresses were generated in the carrying structure of a flat car at angular displacements of a train ferry about the longitudinal axle and account for about 330 MPa. The maximum displacements were in the middle part of the frame and accounted for 1.8 mm. The maximum deformations were $2.0 \cdot 10^{-2}$.

At angular displacements of the carrying structure of a flat car about the transverse axle the maximum equivalent stresses equalled about 290 MPa. The maximum displacements were 1.8 mm, and the deformations were $1.18 \cdot 10^{-2}$.

Thus, with consideration of a typical fixation pattern for a flat car on the deck, the maximum equivalent stresses in the body elements did not exceeded the admissible values.

3.2.6 Determination of the strength characteristics of the carrying structure of a passenger car

The strength characteristics of the carrying structure of a passenger car fixed with the new fixation pattern were determined by mounting the units for fixation of chain binders on the spatial model (Figure 3.83) [114].

Figure 3.83 – Carrying structure of a passenger car with units for fixation on the deck

The design model included the loads identical to those described in 2.4.6 (Figures 3.84 and 3.85).

The finite element model (Figure 3.86) included isoparametrical tetrahedrons the optimal number of which was determined by the graph analytical method. The number of elements in a mesh was 462 129, the number of nodes – 159 352, the maximum element size – 80 mm; the minimum element size – 16 mm, the maximum element side ratio was 742,75, the percentage of elements with a side ratio of less than three – 12.7, and more than ten – 58. The element gain ratio in a mesh was 1.8. The number of elements in a circle was 10.

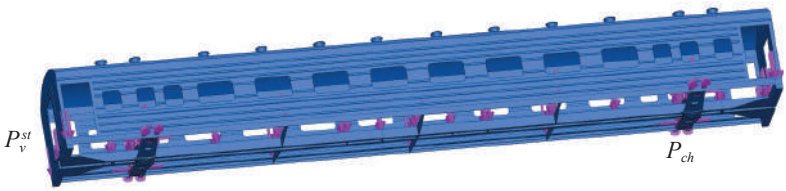

Figure 3.84 – Design diagram of the carrying structure of a passenger car at angular displacements relative to the transverse axle

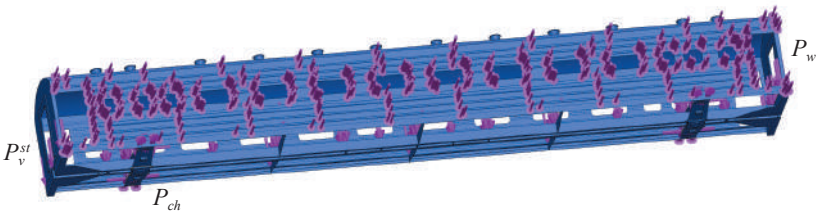

Figure 3.85 – Design diagram of the carrying structure of a passenger car body at angular displacements relative to the longitudinal axle

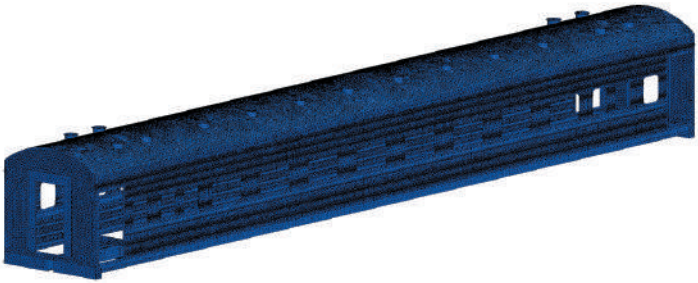

Figure 3.86 – Finite element model of the carrying structure of a passenger car with units for fixation on the deck

The results of the calculation are given below.

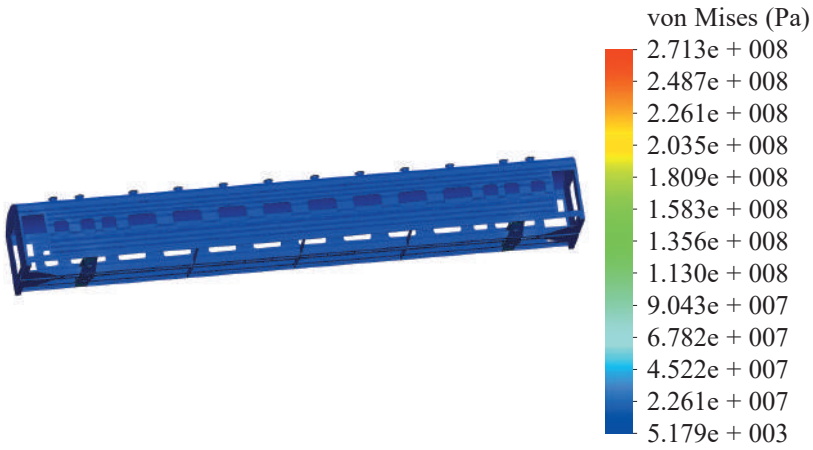

Figure 3.87 – Stress state of the carrying structure of a passenger car at angular displacements relative to the transverse axle

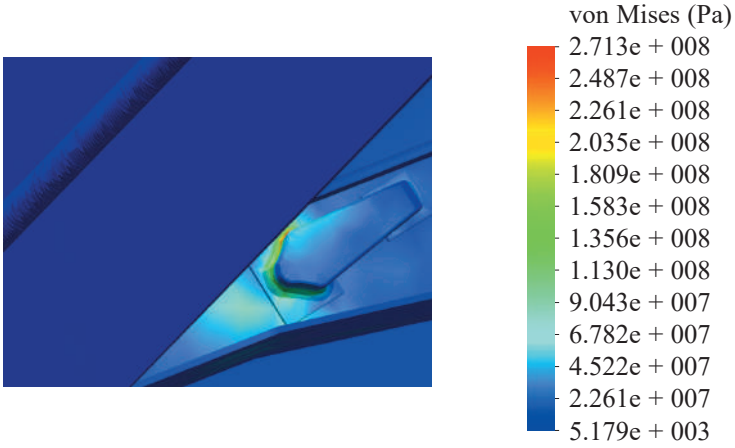

Figure 3.88 – Stress state of the carrying structure of a passenger car at angular displacements relative to the transverse axle

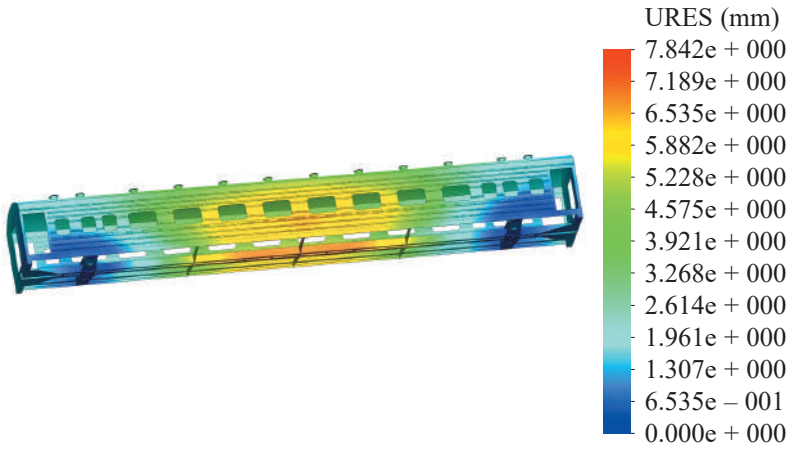

Figure 3.89 – Displacements in the units of the carrying structure of a passenger car at angular displacements relative to the transverse axle

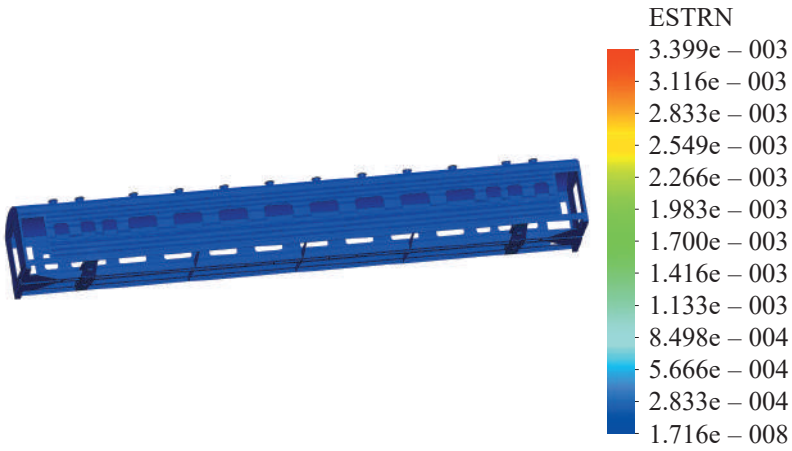

Figure 3.90 – Deformations in the carrying structure of a passenger car at angular displacements relative to the transverse axle

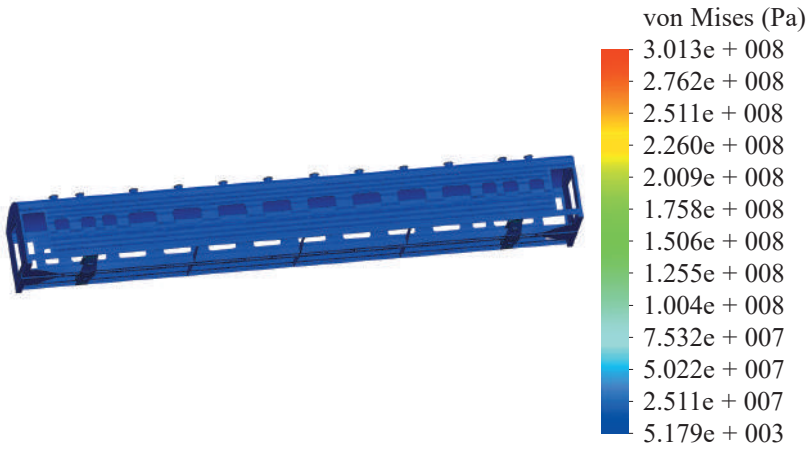

Figure 3.91 – Stress state of the carrying structure of a passenger car at angular displacements relative to the longitudinal axle

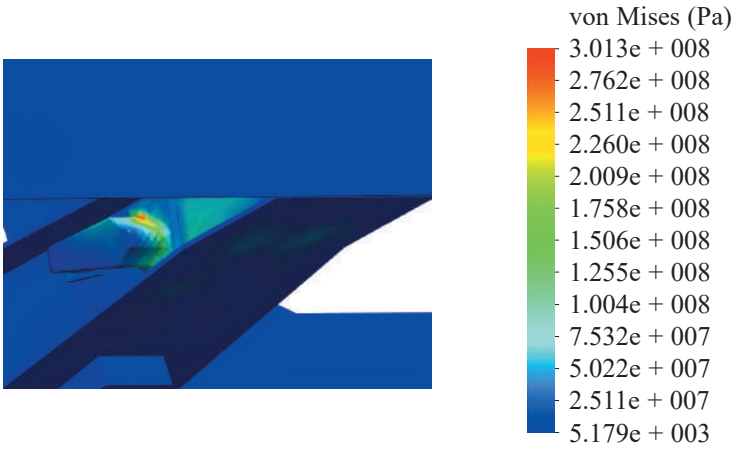

Figure 3.92 – Stress state of the carrying structure of a passenger car at angular displacements relative to the longitudinal axle

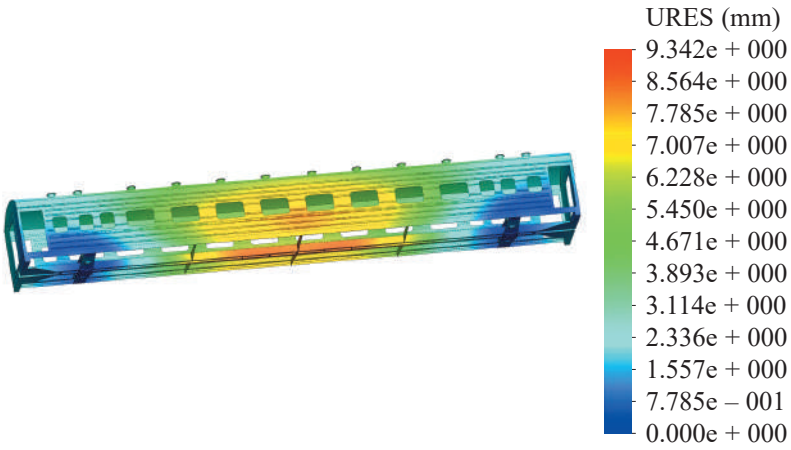

Figure 3.93 – Displacements in the units of the carrying structure of a passenger car at angular displacements relative to the longitudinal axle

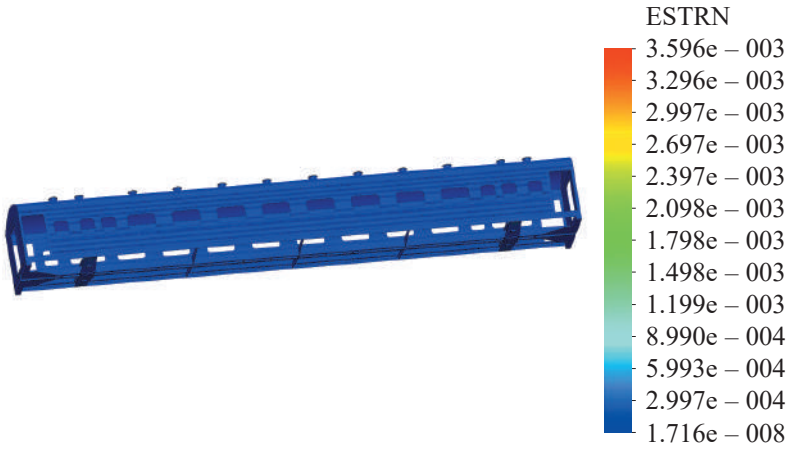

Figure 3.94 – Deformations in the carrying structure of a passenger car at angular displacements relative to the longitudinal axle

The results of the calculation demonstrated that the maximum equivalent stresses in the passenger car body were generated at angular displacements of a train ferry about the longitudinal axle and accounted for about 300 MPa. The maximum displacements were in the middle part of the center sill and accounted for 9.3 mm. The maximum deformations were $3.6 \cdot 10^{-3}$.

At angular displacements of a passenger car body about the transverse axle the maximum equivalent stresses equalled about 270 MPa. The maximum displacements were 7.8 mm, and the deformations were $3.4 \cdot 10^{-3}$.

Thus, the new fixation pattern for a passenger car on the deck demonstrated that the maximum equivalent stresses in the body elements did not exceed the admissible values.

3.3 Improvements in the pattern of interaction between the car body and the ferry deck

3.3.1 Structural peculiarities of the unit for fixation of cars on the deck

The loads from the chain binders to the car bodies can be reduced by applying a viscous link in the form of special dampers between the car body and the deck (Figure 3.95) [133, 134].

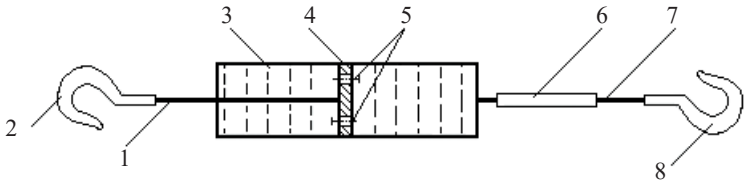

Figure 3.95 – Lashing device for fixation of a car on the deck:
1 – rod; 2 – hook for fixation of a body; 3 – body; 4 – piston; 5 – throttle openings; 6 – connector with bent threads 7 – rigid rod; 8 – hook for fixation by a deck ring

The lashing device for fixation of a car on the train ferry deck consists of rigid rod 1 with hook 2 at the end for fixation by a car body. The hydraulic damper with body 3 is the actuating part of the device. Piston 4 with throttle openings 5 is located inside the body. The bottom part of the device composes of adopter 6 with threats for regulating the length, rigid rod 7 and hook 8 for fixation by a deck ring.

The fixation pattern of an open car body with the proposed device on the deck is given in Figure 3.96.

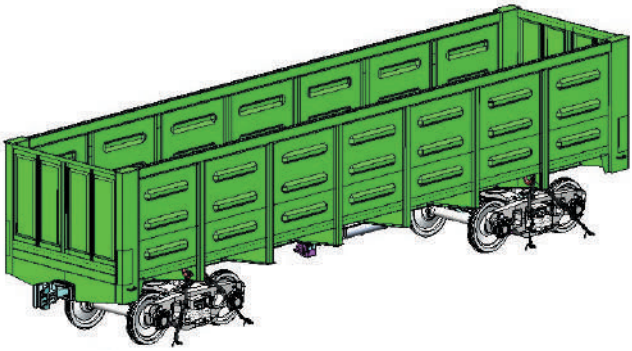

Figure 3.96 – Fixation pattern of an open car body on the deck with consideration of the proposed device

Eight devices (four at each side) are needed for fixation of one car on the deck.

3.3.2 Mathematical modelling of dynamic loads on the open car body in ferry transportation

The accelerations of an open car body fixed on the deck with the proposed devise were determined through mathematic modelling based on the design diagram of the car body located on the train ferry (Figure 3.97).

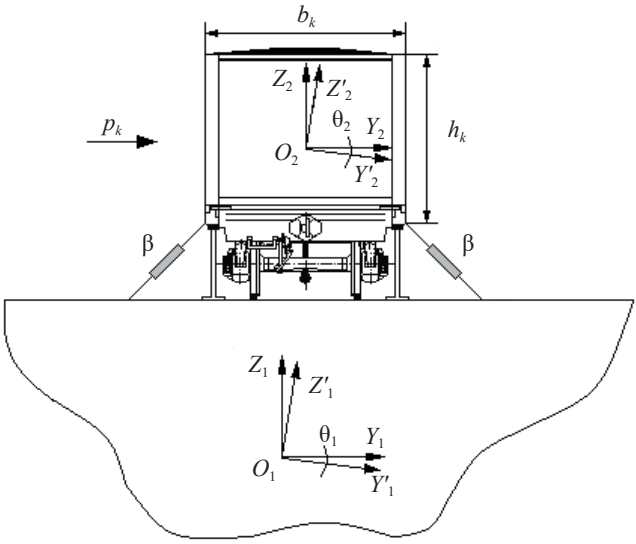

Figure 3.97 – Design diagram for determination of the dynamic loads on the open car body

The system of differential equations (3.4) included the angular displacements of a train ferry relative to the longitudinal axle, and those of a car body relative to the deck.

$$\begin{cases} \dfrac{D}{12\cdot g}\cdot\left(B^2+4\cdot z_g^2\right)\cdot\ddot{q}_1+\left(\Lambda_\theta\cdot\dfrac{B}{2}\right)\cdot\dot{q}_1=p'\cdot\dfrac{h}{2}+\Lambda_\theta\cdot\dfrac{B}{2}\cdot\dot{F}(t), \\ I_k\cdot\ddot{q}_2+\beta\cdot\dfrac{e}{2}\cdot\dot{q}_2=p_k\cdot\dfrac{h_k}{2}+F_\beta, \end{cases} \tag{3.4}$$

where q_1, q_2 – generalized coordinates corresponding to the angular displacements around the longitudinal axis X of a train ferry and a car body, respectively.

For a train ferry:

D – weight displacement; B – width; h – moulded height; Λ_θ – oscillation damping coefficient; z_g – coordinate of the

center of gravity; p' – wind force; $F(t)$ – law of action making a train ferry loaded with cars on the deck move.

For a car body:

I_k – inertia moment relative to the longitudinal axis; β – viscous resistance coefficient of an element; $в_k$ – body width; p_k – wind force to a side wall; *hk* – height of a side wall; F_β – moment of forces between the body and the deck.

The system of differential equations of motion (3.4) was solved in Mathcad software [77, 78] with the Runge–Kutta method.

The system of differential equations of the second order was transferred to the system of differential equations of the first order, the right part of which was written as a vector for standard solution algorithms with the function *rkfixed* MATHCAD.

Figures 3.98 and 3.99 present graphical dependencies of accelerations on the open car body at angular displacements of a train ferry relative to the longitudinal axle.

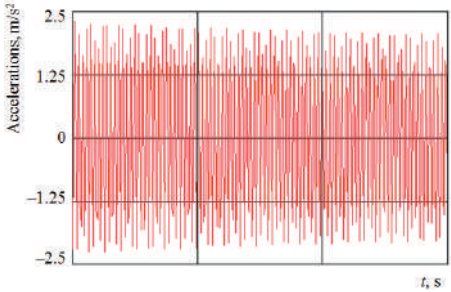

Figure 3.98 – Accelerations on the open car body with a typical interaction pattern on the deck

Figure 3.98 presents the accelerations on an open car body with a typical interaction pattern of the deck, and Figure 3.99 presents it

with a viscous pattern. The accelerations are given for a course wave angle of $\chi = 0°$ relative to the train ferry body loaded with cars.

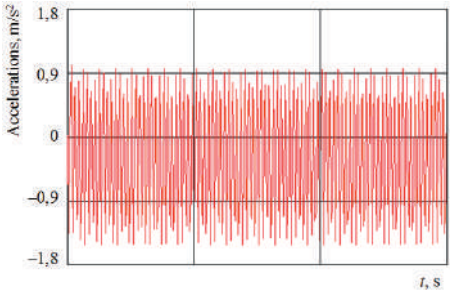

Figure 3.99 – Accelerations on the open car body with a viscous pattern of interaction on the deck

The figures demonstrate that viscous interaction between the body and the deck can decrease the values of acceleration on the carrying structure of a body by 30 %.

It should be mentioned that the coefficient of viscous resistance of the working fluid creating viscous resistance between the body and the deck should be within a range from 1.8 kN·s/m to 4.2 kN·s/m.

3.3.3 Computer modelling of dynamic loads on the open car body in ferry transportation

The accelerations on the open car body during viscous interaction with the deck were defined by computer modelling in CosmosWorks software by the finite element method.

A 12-757 open car was taken as the prototype. Isoparametric tetrahedrons were taken as finite elements. The optimal number of elements for the continuous model was defined with the graph analytical method. The basic characteristics of the model are given in Table 3.1.

Table 3.1 – Characteristics of the continuous model for an open car body

Number of elements	494489
Number of units	160639
Maximum size of an element, mm	80.0
Minimum size of an element, mm	16.0
Maximum element side ratio	1000.9
Percentage of elements with a side ratio of less than three	26.9
Percentage of elements with a side ratio of more than ten	26.2
Minimum number of elements in a circle	9
Element size gain ratio	1.7

The strength model of the carrying structure of an open car at angular displacements about the longitudinal axle is given in Figure 3.100. The model included the following forces on the open car body: vertical static force P_v^{st}, forces from the bulk freight P_p, dynamic force, and forces through lashing devices on the deck P_{ch}. As far as the device for fixation of a car has spatial location, the forces through them to the body were decomposed (Figure 3.101). Black coal was taken as one of the most popular type of freight transported in open cars.

a)

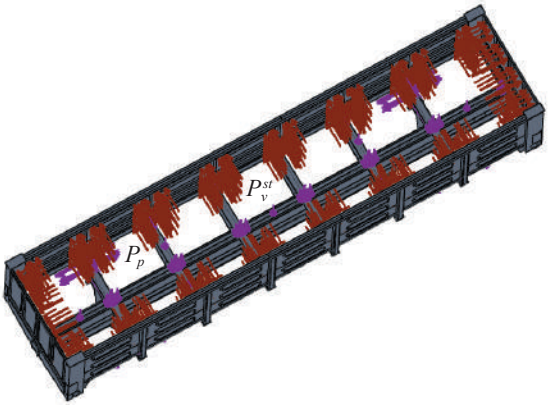

b)

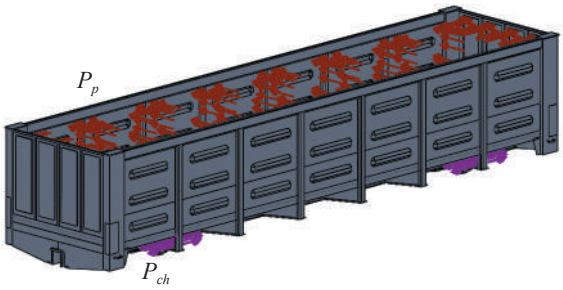

Figure 3.100 – Strength model of the carrying structure of an open car body:
a) top view; b) side view

The viscous element between the body and deck was presented as pads on the bolster beams; the material of the pads had a coefficient of viscous resistance of 3.5 kN·s/m.

The results of the calculation demonstrated that the maximum acceleration of an open car body were generated in the middle parts of the side walls (about 1.4 m/s^2), and in the end parts of the frame (1.7 m/s^2) (Figures 3.102 and 3.103).

Figure 3.101 – Modelling forces through the device for fixation of a body on the deck

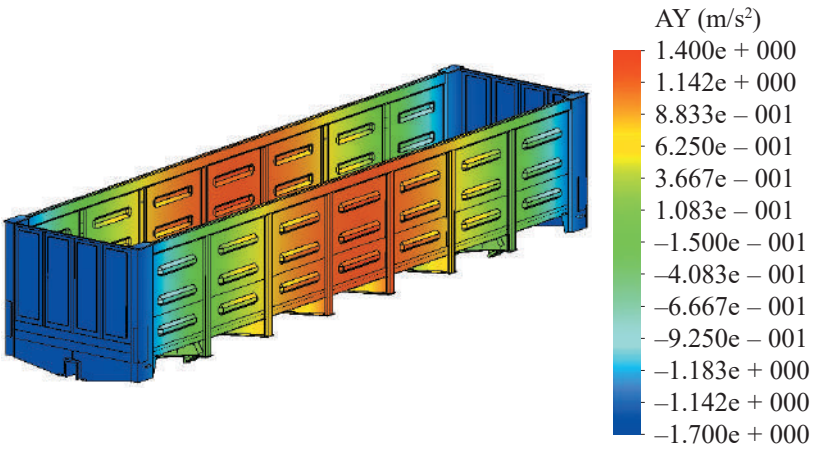

Figure 3.102 – Distribution of acceleration fields on the carrying structure of an open car body during viscous interaction with the ferry deck (side view)

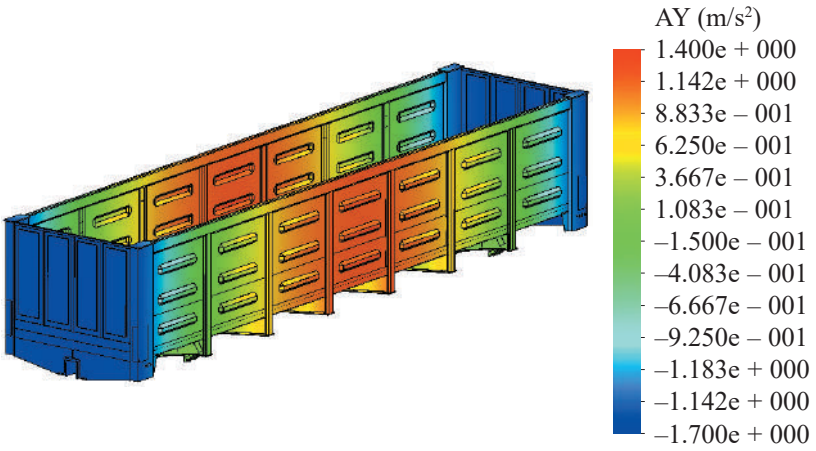

Figure 3.103 – Distribution of acceleration fields on the carrying structure of an open car body during viscous interaction with the ferry deck (bottom view)

The smallest acceleration value was observed in the zones where an open car body rested on the bogies.

3.3.4 Verification of dynamic loading models of on open car body

The models were verified with an F-test. The roll angle of a train ferry was taken as the variation parameter. From the calculation conducted the authors obtained the accelerations on the car body during train ferry oscillations (Figure 3.104).

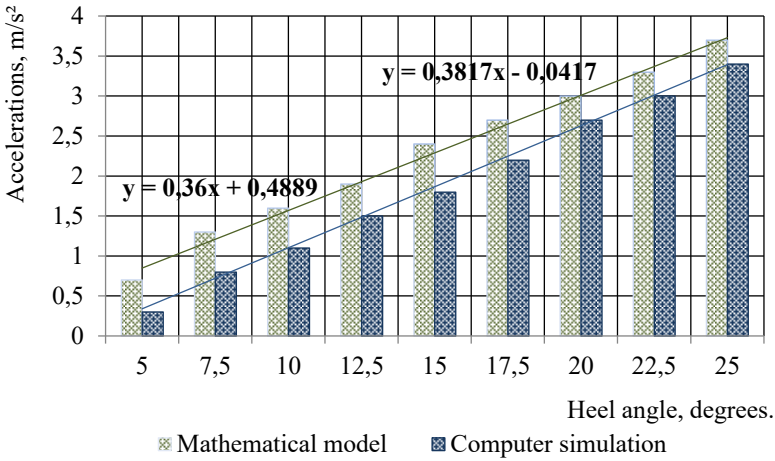

Figure 3.104 – Accelerations on the open car body in train ferry transportation

It was established that with the dispersion of restoration $S_r^2 = 0.98$ and the dispersion of adequacy $S_{ad}^2 = 1.1$, the actual value of an F-test was $F_p = 1.12$ which was lower than the tabular value $F_t = 3.29$. It implies that the hypothesis on adequacy was not rejected.

3.4 Improved structure of a passenger car body for stable securing on the ferry deck

3.4.1 Structural peculiarities of the device for fixation of a passenger car body on the deck

The authors propose installation of special units on the bolster beams for stable securing of passenger car bodies on the ferry decks (Figure 3.105). The principle of action of such a unit is based on that of a hydraulic damper; it allows reducing the dynamic loads on the body.

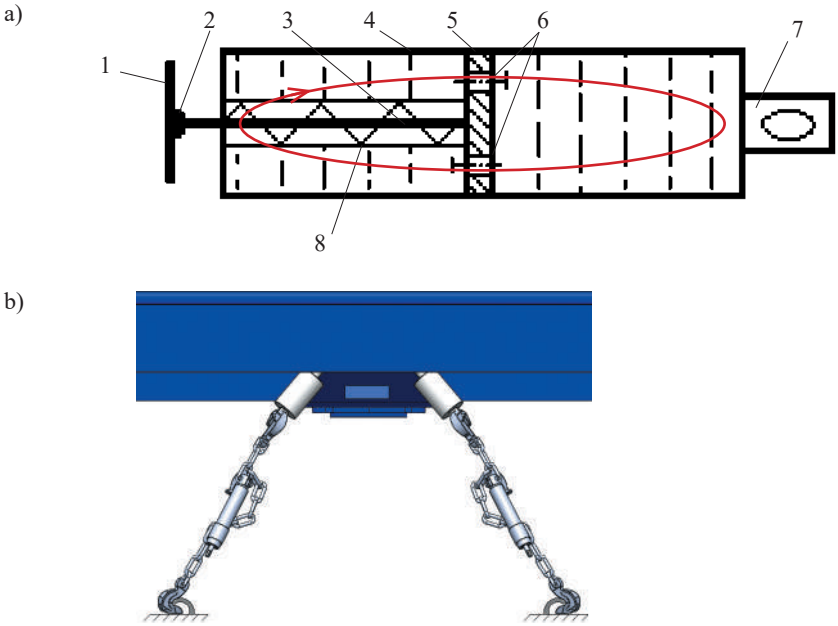

Figure 3.105 – Unit for fixation of a car body on the deck:
a) unit structure; b) fixation pattern for a body:
1 – support part; 2 – hinge; 3 – rod; 4 – body; 5 – piston; 6 – throttle openings;
7 – eyelet for fixation of a chain binder's hook; 8 – brake spring

When the force is transmitted through eyelet 7 to the unit from the chain binder's hook, piston 5 and rod 3 move relative to body 4. The working liquid flows through the throttle opening and develops resistance to motion of the piston. Brake spring 8 is pressed. Piston 5 travels to its initial position due to brake spring 8. At a backward run of piston 5 the overflow goes through another throttle opening. The energy generated dissipates into the environment.

The area where rod 3 interacts with the unit's support 1, fixed to the vertical plate of the bolster beam, has pivot connection 2. If there is no need to use it, the unit can be shifted to the horizontal position (Figure 3.106).

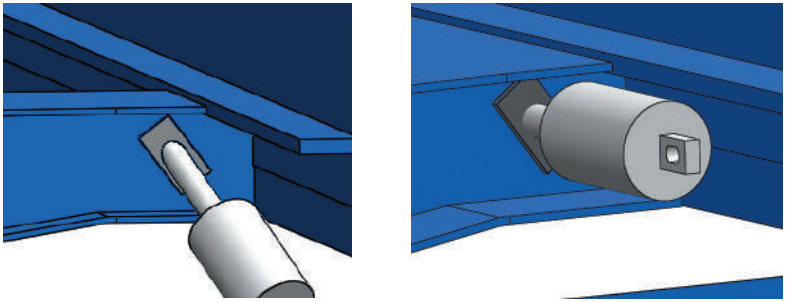

a) b)

Figure 3.106 – Position of the unit for fixation of a car body on the deck:
a) with a car body fixed; b) without fixation

3.4.2 Determination of dynamic loads on the improved passenger car body in ferry transportation

The numerical values of the dynamic loads on the car body located on the deck with application of the new fixation pattern were determined with a mathematical model (3.4).

The technical characteristics of a train ferry and a passenger car body, as well as the hydro meteorological characteristics of the cruising area were taken as the input parameters of the model. The calculation

was made for the train ferry *Mukran* operating on the Baltic Sea. The hydro meteorological characteristics of the sea were taken from [66].

The accelerations on the car body with the new fixation pattern are given in Fig. 3.107. The research demonstrated that the maximum accelerations on the car body at a wave angle to the ferry body of 60° and 120° accounted for about 1.3 m/s^2.

It should be mentioned that the viscous resistance coefficient of the working fluid developing viscous resistance between the body and the deck should be within a range from 2 kN·s/m to 4.2 kN·s/m.

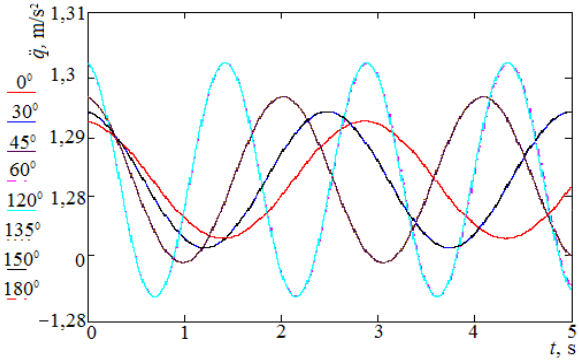

Figure 3.107 – Accelerations on the car body during viscous interaction with the deck

Thus, taking into account the proposed solution, the authors determined that the maximum accelerations on the car body decreased by 30 % in comparison with those for a typical fixation pattern [81, 82].

3.4.3 Strength calculation for the improved passenger car body in ferry transportation

The strength of the improved passenger car body was calculated with the finite element method in CosmosWorks software.

The model included the elements rigidly welded or riveted.

The finite element model was built of spatial isoparametrical tetrahedrons. The optimal number of the elements was determined with the graph analytical method. The model consisted of 152967 nodes and 434641 elements. The maximum element size was 80 mm, and the minimum size – 16 mm. The percentage of elements with a side ratio of less than three was 12, and more than ten – 59.9. The minimum number of elements in a circle was 10, and the element size gain ratio was 1.8.

The strength model involved vertical static force $P_в^{cm}$, wind force $P_в$, and forces through the chain binders $P_{лс}$ (Figure 3.108). Due to a spatial location of chain binders the force on the car body through them was decomposed and applied to the unit's support part located on the vertical plate of the bolster beam.

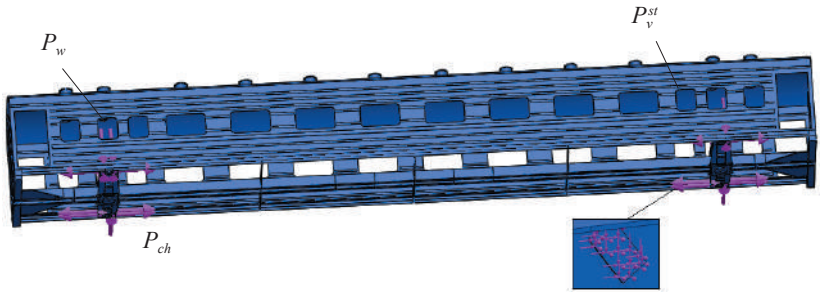

Figure 3.108 – Strength modelling for a passenger car body

The model was fixed in the areas where the body rested on the running gears of the car, and in the areas where the stop-jacks were installed. Carbon Steel St.3 was used for the body structure.

The results of the calculation are given in Fig. 3.109.

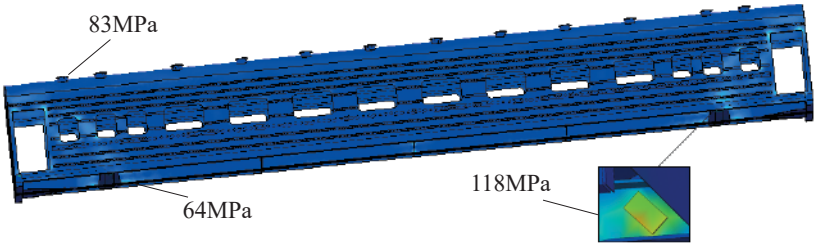

Figure 3.109 – Stress state of a passenger car body

The maximum equivalent stresses were generated in the pad simulating the unit's support part; they accounted for 120 MPa, thus, they did not exceed the admissible values [81, 82].

The maximum displacements were fixed in the center sill of a car and accounted for 1.47 mm. The maximum deformations were $1.01 \cdot 10^{-3}$.

Conclusions to Part 3

1. The research deals with the unit for strong fixation of a car body on the ferry deck. Higher rigidity of the bolster beam in the areas of installation of the unit can be provided with reinforcing diaphragms; this can decrease stresses in the bolster beam;

The unit design involves the geometrical parameters of a chain binder's hook. It was established that application of the unit for fastening rail cars on the deck is in full conformance with requirements for the spatial location of chain binders. The authors recommend the formation of a specialized fleet of rail cars equipped with units for fixation on the deck.

2. The designed finite element models were built for basic types of cars equipped with units for fixation on the decks in sea transportation. The estimation of the stress strain state of the carrying structure of a rail car demonstrated that the maximum equivalent

stresses did not exceed the admissible values. For an open car at angular displacements of a train ferry relative to the transverse axle the maximum equivalent stresses were 201.3 MPa, displacements in units – 3.28 mm, deformations – $2.209 \cdot 10^{-3}$; at angular displacements relative to the longitudinal axle these values were 282.3 MPa, 7.63 mm and $2.768 \cdot 10^{-3}$, respectively.

For a tank car at angular displacements of a train ferry relative to the transverse axle the maximum equivalent stresses were 201.3 MPa, displacements in units – 3.28 mm, deformations – $2.209 \cdot 10^{-3}$; at angular displacements relative to the longitudinal axle – 335.2 MPa, 6.86 mm and $3.895 \cdot 10^{-3}$, respectively.

For a boxcar at angular displacements of a train ferry relative to the transverse axle the maximum equivalent stresses were 302.3 MPa, displacements in the units – 9.46 mm, deformations – $5.109 \cdot 10^{-3}$; at angular displacements relative to the longitudinal axle – 338.1 MPa, 9.56 mm and $4.389 \cdot 10^{-3}$, respectively.

For a hopper car at angular displacements of a train ferry relative to the transverse axle the maximum equivalent stresses were 283,3 MPa, displacements in the units – 7.55 mm, deformations – $8.403 \cdot 10^{-3}$; at angular displacements relative to the longitudinal axle – 328.4 MPa, 8.29 mm and $9.89 \cdot 10^{-3}$, respectively.

For a flat car at angular displacements of a train ferry relative to the transverse axle the maximum equivalent stresses were 282,3 MPa, displacements in the units – 3.28 mm, deformations – $1.184 \cdot 10^{-2}$; at angular displacements relative to the longitudinal axle – 332.5 MPa, 1.88 mm and $1.95 \cdot 10^{-2}$, respectively.

For a passenger car at angular displacements of a train ferry relative to the transverse axle the maximum equivalent stresses were 271,3 MPa, displacements in units –7.84 mm, deformations – $3,4 \cdot 10^{-3}$; at angular displacements relative to the longitudinal axle – 301.3 MPa, 9.34 mm and $3.596 \cdot 10^{-3}$, respectively.

3. The forces through the chain binders to the car body can be decreased by means of viscous interaction by mounting a special damper between the body and the deck. This can decrease the

accelerations on the carrying structure by 30 % in comparison with the acceleration values with the standard fixation pattern.

It should be mentioned that the coefficient of viscous resistance of the working fluid which develops the viscous resistance between the body and the deck should be within a range from 1.8 kN·s/m to 4.2 kN·s/m.

4. The authors suggest mounting the special units on the bolster beams; this should provide tight fixation of passenger car bodies on the deck. The principle of action of such a unit is based on operation of a hydraulic damper which reduces the dynamic loads on the body.

Thus, owing to this unit, the maximum accelerations on the car body were reduced by 30 % in comparison with those with the standard fixation pattern; It should be noted that the coefficient of viscous resistance of the working fluid which develops the viscous resistance between the body and the deck should be within a range from 2 kN·s/m to 4.2 kN·s/m.

The proposed solution was proved through calculation. The maximum equivalent stresses were generated in the pad simulating the unit's support part; they accounted for about 120 MPa, thus they did not exceed the admissible values.

PART 4
DETERMINATION OF DYNAMIC LOADS AND STRENGTH OF CONTAINERS IN THE COMBINED TRAIN TRANSPORTED BY A FERRY

4.1 Modelling the dynamic loads on a dry-cargo container in the combined train in ferry transportation

For European and Asian countries maritime transport continues to play an important role; that requires the introduction of new transportation routes. One of these routes is the international transport link between European and Asian countries. It was launched at the beginning of last year with the first combined train across the Black Sea to China (Figure 4.1).

a) b)

Figure 4.1 – Flat cars loaded with containers before transportation by train ferries:
a) flat cars loaded with containers run to the rail yard;
b) rolling-on flat cars on the ferry

Safe transportation of combined trains by ferries should be based on the research into the dynamic loading and stability of containers relative to the flat car frames [135].

The dynamic loads on the carrying structure of a container in the combined train during ferry transportation were determined by means of a mathematical model (2.10) [136–138]. The calculation was based on absence of the own displacements of the carrying structure of a flat car relative to the deck due to the lasing devices applied (Figure 4.2, *a*).

The angular displacements of a flat car loaded with containers about the longitudinal axle *X* at the angle θ (the equivalent of the oscillations is rolling in the car dynamics), taken as the maximum loads on the carrying structure of a flat car with containers, and the condition of their stability on the deck were taken into accounts.

The calculation was made for the train ferry *Geroi Shipki* operating in the Black Sea. A 13-4012 flat car and a 1CC container (with a gross weight of 24 tons) were chosen as the base models.

The initial displacements and the speed of a train ferry were taken equal to zero.

The input parameters of the mathematic model were: geometric characteristics of the train ferry, hydro meteorological characteristics of the Black Sea waters, the coordinates of cars relative to the oscillation center of a ferry.

The differential equation was solved in the program designed in Mathcad software suite, where it was reduced to a regular Cauchy problem to be integrated with the Runge–Kutta method.

Figure 4.3 shows the accelerations on the carrying structure of a flat car loaded with containers located on the farthest track from the bulwark on the upper deck of a train ferry at angular displacements about the longitudinal axle. The greatest acceleration was generated at a wave angle to the train ferry body of $\chi = 120°$.

The acceleration values given do not include the horizontal component of the free fall acceleration.

The total acceleration on the farthest flat car with containers from the bulwark was about 0.25g.

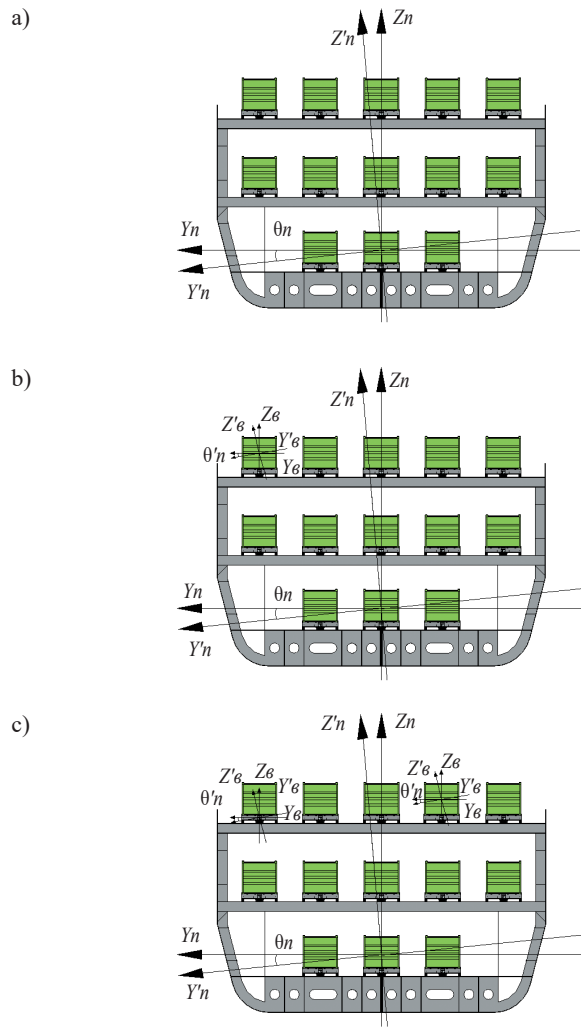

Figure 4.2 – Design diagram for research into angular displacements of a flat car loaded with containers on the ferry deck relative to the longitudinal axle:
a) without displacements of a flat car with containers relative to the deck; b) with displacements of a flat car relative to the deck and without displacements of containers relative to the flat car; c) with displacements of a flat car relative to the deck and containers relative to the flat car frame

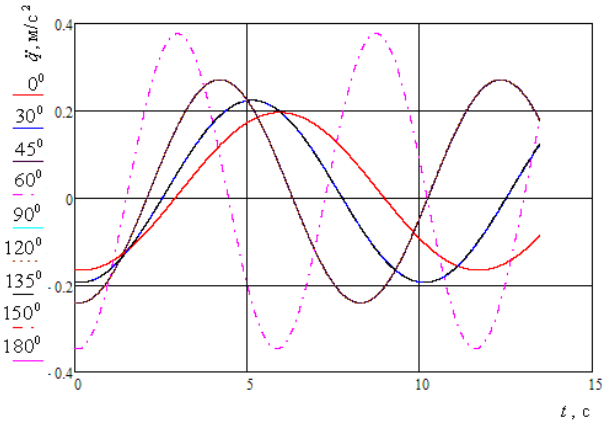

Figure 4.3 – Accelerations on the carrying structure of a flat car loaded with containers at the oscillations of a train ferry

The accelerations on the flat car loaded with containers in train ferry transportation with consideration of possible displacements of a car relative to the deck during sea disturbance (Fig. 4.2, *b*), a mathematical model was designed (4.1).

The first equation of the mathematical model describes the train ferry displacements during sea disturbance, and the second one describes the displacements of a flat car loaded with containers relative to the deck.

The mathematical model included the natural degree of freedom of a flat car on the deck:

$$\begin{cases} \left(\dfrac{D}{12\cdot g}(B^2+4z_g{}^2)\right)\ddot{q}_1+\left(\Lambda_\theta\cdot\dfrac{B}{2}\right)\dot{q}_1=p'\cdot\dfrac{h}{2}+\Lambda_\theta\cdot\dfrac{B}{2}\cdot\dot{F}(t), \\ I_\theta^C\cdot\ddot{q}_2=p'_C\cdot\dfrac{h_C}{2}+M_C^D, \end{cases} \tag{4.1}$$

where $q_1=\theta_1$ – generalized coordinate corresponding to the angular displacement of a train ferry about the longitudinal axle;

$q_2 = \theta_2$ – generalized coordinate corresponding to the angular displacement of a flat car loaded with containers about the longitudinal axle. The origin of the coordinate system was in the center of mass of a train ferry;
I_{θ}^{C} – inertia moment of a flat car loaded with containers about the longitudinal axle;
p_C' – wind force to the side projection of a flat car loaded with containers on the upper deck of a train ferry;
h_C – height of the side projection of a flat car loaded with containers;
M_C^D – moment of forces between the flat car and the train ferry deck at angular displacements about the longitudinal axle.

The initial displacement and the speed of a train ferry were taken as equal to zero; for a flat car loaded with containers the initial displacement was determined by potential flexibility of its units relative to the deck (box unit relative to the wheelset axle, bogie frame relative to the box unit axle, friction wedge relative to the side frame center, truck bolster relative to the friction wedge, center plate relative to the center bowl [80]) and accounted for 31 mm. The initial speed was taken equal to zero.

The mathematical model designed did not include the impact force of sea waves to the ferry body loaded with cars.

The results of the calculation are given in Figure 4.4. The total acceleration on the farthest flat car loaded with containers from the bulwark was about 0.3 g.

The results obtained made it possible to conclude that the value of acceleration exceeded the value of acceleration on the container located on the flat car rigidly fixed on the deck by about 20 %.

The accelerations at displacements of a flat car relative to the deck and containers relative to the flat car were determined by means of the mathematical modelling; it included the angular displacements of the system 'train ferry-flat car-container' about the longitudinal axle (Figure 4.2, *c*).

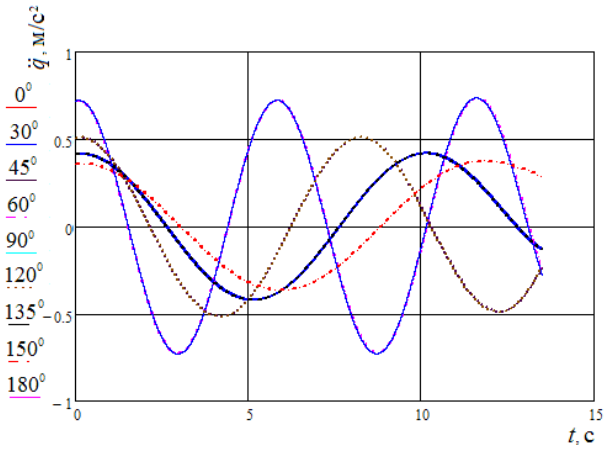

Figure 4.4 – Accelerations on the carrying structure of a flat car loaded with containers in ferry transportation with potential displacements on the deck

$$\begin{cases} \left(\frac{D}{12\cdot g}(B^2+4z_g{}^2)\right)\ddot{q}_1+\left(\Lambda_\theta\cdot\frac{B}{2}\right)\dot{q}_1=p'\cdot\frac{h}{2}+\Lambda_\theta\cdot\frac{B}{2}\cdot\dot{F}(t), & (4.2)\\ I_C^\theta\cdot\ddot{q}_2=p'_C\cdot\frac{h_C}{2}+M_C^D+M_C^c, & (4.3)\\ I_K^\theta\cdot\ddot{q}_3=p'_c\cdot\frac{h_c}{2}+M_c^C, & (4.4) \end{cases}$$

where $q_1=\theta_1$ – generalized coordinate corresponding to the angular displacement of a train ferry about the longitudinal axle;
$q_2=\theta_2$ – generalized coordinate corresponding to the angular displacement of a flat car about the longitudinal axle;
$q_3=\theta_3$ – generalized coordinate corresponding to the angular displacement of a container about the longitudinal axle. The origin of coordinate was in the center of mass of a train ferry;
M_C^c – moment of forces between the flat car and the containers under angular displacements relative to the longitudinal axle;
I_C^θ – inertia moment of a container;

h_C – height of a container side;
p'_C – wind force on the container side;
M_c^C – moment of forces between the container and the flat car at angular displacements relative to the longitudinal axle.

The longitudinal component of the gross weight with the friction forces between the car's components was included in the calculation of the moment of forces between the flat car and the deck. The horizontal component of the gross weight of a container, the friction forces between the fitting stop and the fitting, and the geometry of the fitting stop were included in the determination of the moment of forces between the flat car and the container.

It was assumed that at angular displacements about the longitudinal axle a flat car had its natural degree of freedom until the moment when the friction force F_{FR} took on the values smaller than those of the dynamic force P_d. In this case the body moved at the value of potential horizontal displacements of the structural elements [80] and would reiterate the movement pattern of a train ferry. This was included in the mathematical model by means of the following: if $t = n$, then $q_2 = q_1$, where n – moment of time, when $F_{fr} < P_d$. The same was true about a container, potential displacements of which were conditioned by a technological gap between the fitting stop and the fitting [126–128]. Thus, the flat car had its natural degree of freedom restricted by the value of potential displacements in the structural elements; therefore, it repeated the movement pattern of a train ferry. The container had its natural degree of freedom until the moment when a vertical side of a fitting rested against the fitting stop.

From the calculation conducted it was found that the greatest values of accelerations were generated at wave angles relative to the train ferry body of $\chi = 60°$ and $\chi = 120°$. The results of the calculation are given in Figures 4 and 5.

The maximum accelerations of a container were about 2.5 m/s^2, and those of a flat car – 1.8 m/s^2.

The numerical values of the accelerations are given without the free fall component.

The total value of the acceleration on the farthest flat car from the bulwark was about 0.4 g, and on the containers located on it was about 0.47 g.

The results obtained made it possible to conclude that the value of the acceleration exceeded the acceleration on the container located on the flat car rigidly fixed on the deck by about 50 %, and with displacements of a flat car relative to the deck and without displacements of containers relative to the frame – by 35 %.

The stability of a container relative to the flat car frame was evaluated with the equilibrium stability coefficient k_c at angular displacements of a train ferry relative to the longitudinal axle (Figure 4.6).

The following condition should be satisfied for the equilibrium stability of a container relative to the flat car frame [135]:

$$k_c = \frac{M_{rest}}{M_{ov}} \geq 1, \tag{4.5}$$

where M_{rest} – restoring moment;
M_{ov} – overturning moment.

$$M_{ov} = p'_c \cdot \frac{h_c}{2} + M_{br} \cdot \left(g \cdot \sin\theta + \ddot{q}_c\right) \cdot \frac{h_c}{2}, \tag{4.6}$$

$$M_{rest} = P_{br} \cdot \cos\theta \cdot \frac{B_c}{2} + n_f \cdot \left(M_{br} \cdot \left(g \cdot \sin\theta + \ddot{q}_c\right)\right) \cdot \frac{h_f}{2}, \tag{4.7}$$

where M_{br} – gross mass of a container;
$\ddot{q}_c$ – acceleration on the container at angular displacements relative to the longitudinal axle;
P_{br} – gross weight of a container;
B_c – container width;
n_f – number of fitting stops the container is rested on at angular displacements relative to the longitudinal axle,
h_f – height of a fitting stop.

Determination of the overturning moment included the maximum numerical values of the accelerations calculated by means of

mathematical modelling; they were the components of dynamic loads on the container. The stability threshold was found when the values of the restoring and overturning moments were equal.

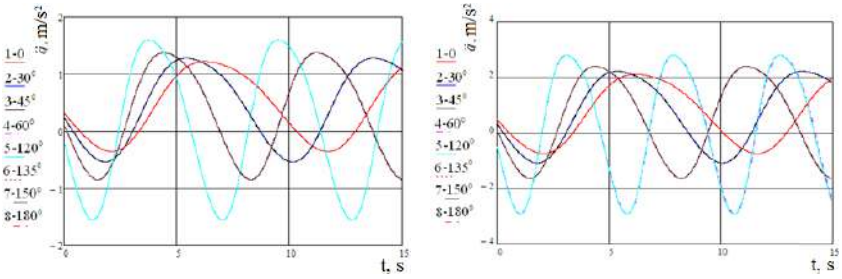

Figure 4.5 – Accelerations on the carrying structure of a flat car loaded with containers in ferry transportation with potential displacements relative to the initial position: *a) flat car; b) container*

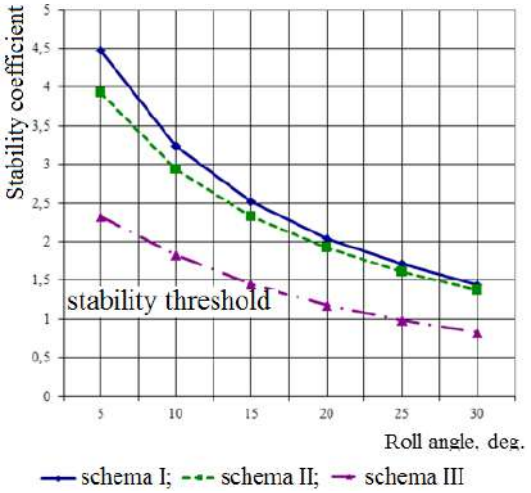

Figure 4.6 – Dependency of the stability coefficient of a container relative to the flat car frame on the roll angle of a train ferry

The research conducted made it possible to conclude that the stability coefficient of a container relative to the flat car frame was less than 1 with displacements of container's fittings relative to the fitting stops of a flat car. The container stability was ensured at roll angles of a train ferry of up to 250.

4.2 Modelling of the dynamic loads of a tank container in the combined train in ferry transportation

The dynamic loads of a tank container in ferry transportation were determined by means of a mathematical model (4.8)–(4.10). The following diagrams of interaction between the tank container and the flat car frame were taken into account [139, 140]:

– without displacements of a flat car loaded with tank containers relative to the deck. The oscillation trajectory of a train ferry is completely repeated by a flat car with tank containers on it (Figure 4.7, *a*);

– with displacements of a flat car relative to the deck and without displacements of a tank container relative to the flat car frame (Figure 4.7, *b*);

– with displacements of a flat car relative to the deck and with displacements of a tank container relative to the flat car frame (Figure 4.7, *c*);

It included angular displacements of a train ferry relative to the longitudinal axle (rolling oscillations) as the case of the maximum forces on a flat car loaded with tank containers during sea transportation.

$$\begin{cases} \left(\dfrac{D}{12\cdot g}\left(B^2+4z_g{}^2\right)\right)\ddot{\theta}_1+\left(\Lambda_\theta\cdot\dfrac{B}{2}\right)\dot{\theta}_1=p'\cdot\dfrac{h}{2}+\Lambda_\theta\cdot\dfrac{B}{2}\cdot\dot{F}(t), \\ I_{ij}\cdot\ddot{\theta}_2-m_{ij}\cdot c_{ij}\cdot l_{ij}\cdot\ddot{\theta}_1+g\cdot m_{ij}\cdot l_{ij}\cdot\theta_2=0, \end{cases} \quad (4.8)$$

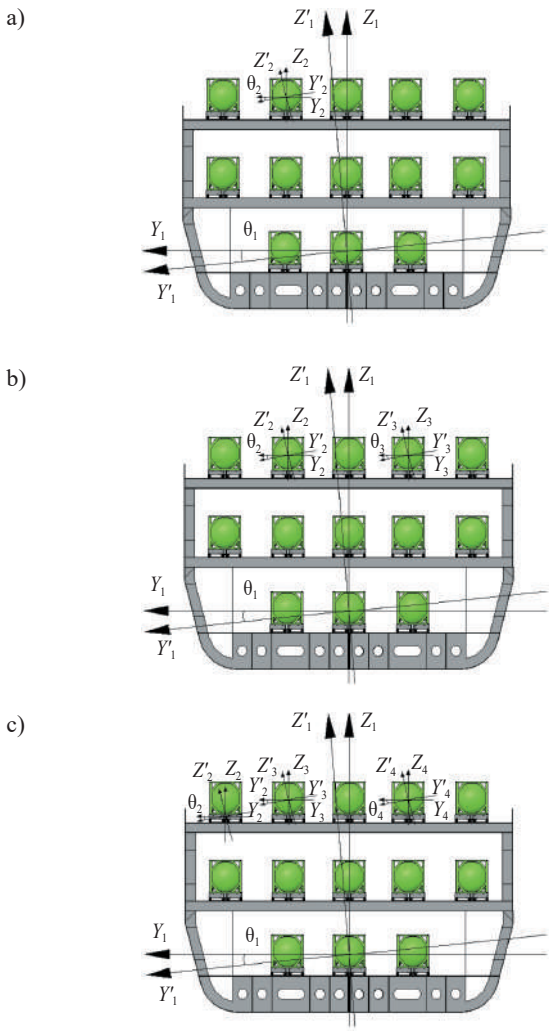

Figure 4.7 – Diagrams of displacements of tank containers in the combined trains in ferry transportation

a) without displacement of a flat car loaded with containers relative to the deck; b) with displacements of a flat car relative to the deck and without displacements of tank containers relative to a flat car frame; c) with displacements of a flat car relative to the deck and containers relative to the flat car frame

$$\begin{cases} \left(\frac{D}{12\cdot g}\left(B^2+4z_g^2\right)\right)\ddot{\theta}_1+\left(\Lambda_\theta\cdot\frac{B}{2}\right)\dot{\theta}_1=p'\cdot\frac{h}{2}+\Lambda_\theta\cdot\frac{B}{2}\cdot\dot{F}(t), \\ \left(I_{\theta i}+\sum_{j=1}^{k}m_{ij}\cdot c_{ij}^2\right)\cdot\ddot{\theta}_2+\sum_{j=1}^{k}m_{ij}\cdot c_{ij}\cdot l_{ij}\cdot\ddot{\theta}_3-g\cdot\left(m_i\cdot z_{ci}+\sum_{j=1}^{k}m_{ij}\cdot c_{ij}\right)\cdot\theta_2=M_c^C, \\ I_{ij}\cdot\ddot{\theta}_3-m_{ij}\cdot c_{ij}\cdot l_{ij}\cdot\ddot{\theta}_2+g\cdot m_{ij}\cdot l_{ij}\cdot\theta_3=0, \end{cases} \quad (4.9)$$

$$\begin{cases} \left(\frac{D}{12\cdot g}\left(B^2+4z_g^2\right)\right)\ddot{\theta}_1+\left(\Lambda_\theta\cdot\frac{B}{2}\right)\dot{\theta}_1=p'\cdot\frac{h}{2}+\Lambda_\theta\cdot\frac{B}{2}\cdot\dot{F}(t), \\ I_C\cdot\ddot{\theta}_2=p'_C\cdot\frac{h_C}{2}+M_C^D+M_C^c, \\ \left(I_{\theta i}+\sum_{j=1}^{k}m_{ij}\cdot c_{ij}^2\right)\cdot\ddot{\theta}_3+\sum_{j=1}^{k}m_{ij}\cdot c_{ij}\cdot l_{ij}\cdot\ddot{\theta}_4-g\cdot\left(m_i\cdot z_{ci}+\sum_{j=1}^{k}m_{ij}\cdot c_{ij}\right)\cdot\theta_3=M_c^C, \\ I_{ij}\cdot\ddot{\theta}_4-m_{ij}\cdot c_{ij}\cdot l_{ij}\cdot\ddot{\theta}_3+g\cdot m_{ij}\cdot l_{ij}\cdot\theta_4=0. \end{cases} \quad (4.10)$$

The origin of the coordinates was in the mass center of a train ferry.
For a train ferry:
D – weight water displacement;
B – train ferry breadth;
h – moulded depth of a train ferry;
Λ_θ – oscillation resistance coefficient;
z_g – coordinate of the center of gravity of a train ferry;
p' – wind force;
$F(t)$i – law of force which makes the train ferry loaded with cars on the deck move.
For a flat car:
I_c – inertia moment of a flat car relative to the longitudinal axle;
p'_c – wind force to the side projection of a flat car;
h_c – side projection height of a flat car;
M_C^D – moment of forces between the flat car and the train ferry deck;

M_C^c – moment of forces between the flat car and the tank container.

For a tank container with liquid freight:

I_{ij} – inertia moment of a pendulum;

m_{ij} – mass of the *j*-th pendulum in the *i*-th tank container;

c_{ij} – distance from the plane $z_1 = 0$ to the fixation point of the *j*-th pendulum in the *i*-th tank container;

l_{ij} – length of the *j*-th pendulum;

I_θ – reduced inertia moment of the *i*-th tank container and the liquid freight involved in the movement relative to the barrel;

z_{ci} – height of the gravity center of a tank container;

m_i – body mass equivalent to the i-th tank container with part of the liquid freight involved in the displacement relative to the barrel;

M_c^C – moment of forces between the tank container and the flat car.

A 13-4012M flat car was chosen as the prototype car. A 1CC tank container loaded with petrol of up to 95 % of the barrel capacity was taken for the research [116]. The research was made for the tank containers transported by the train ferry *Geroi Shipki* across the Black Sea.

The liquid freight movement was described as a set of mathematical pendulums [114].

The differential equations (4.8)–(4.9) were solved with the Runge–Kutta method in MathCad software.

The initial displacements and speeds were taken equal to zero.

The results of the calculation as dependencies of the accelerations on the tank container at roll angles to the ferry body are given in Figure 4.8. These dependencies are described with the equations given in the figure.

It was established that without displacements of a flat car and containers relative to the initial position, the total value of the acceleration on the farthest flat car loaded with containers from the bulwark was about 0.3 g.

With displacements of a flat car relative to the deck and immobility of tank containers relative to the frame, the total value of the

acceleration to the farthest tank car from the bulwark was about 0.6 g. This acceleration value exceeded that on the tank container in operation along main lines by 17 % [129].

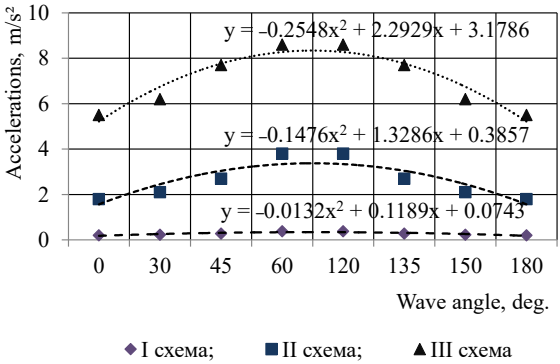

Figure 4.8 – Accelerations to the tank container during ferry transportation

With displacements of a flat car relative to the deck and a tank container relative to the frame, the total value of acceleration on the farthest tank car from the bulwark accounted for about 0.6g. It means that this acceleration value exceeded the value on the tank container in operation along main lines by 40 %.

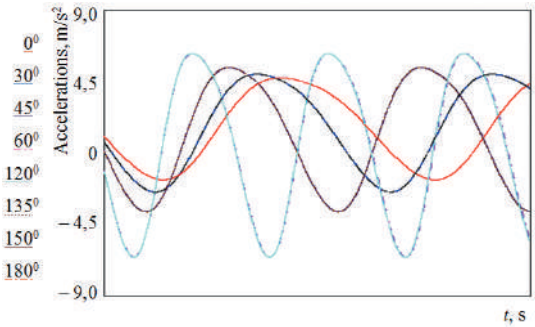

Figure 4.9 – Accelerations on the tank container of a flat car in ferry transportation

Thus, the maximum accelerations on the tank container correspond to the roll angles of sea waves relative to the ferry body of 60° and 120°.

The acceleration values obtained were included in the research into the stability of a tank container relative to the flat car frame.

It was established that the stability of a tank container in the critical loads was ensured at a roll angle of up to 10° (Figure 4.10). At the second diagram the stability of a tank container was ensured at roll angles of up to 12°, and at the third diagram – of up to 25°.

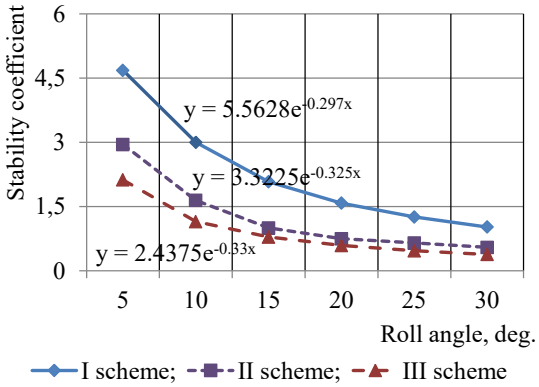

Figure 4.10 – Dependency of the stability coefficient of a tank container relative to the flat car frame on the tilt angle of a train ferry

Thus, safe maritime transportation of liquid freight in the tank containers is ensured at roll angles of a train ferry of up to 10°.

4.3 Computer modelling of the dynamic loads of containers during ferry transportation

The research into the dynamic loads of a dry freight container was made through computer modelling in CosmosWorks software.

The calculation was made with the finite element method. The design model (Figure 4.11) included the following forces on the flat car: vertical forces from the containers P_v^c, horizontal forces to the fitting stops from the fittings P_h^c (Figure 4.12), and forces to the flat car through the units of fixation for chain binders P_{ch}. Owing to the spatial location of chain binders the forces through them to the flat car frame were decomposed into three vectors with consideration of their spatial location angles.

Besides, the following forces were applied to the container: vertical static force P_v^{st} conditioned by gross weight, pressure from the bulk freight P_p to the container's side wall, and wind force P'_w [141].

The pressure from the bulk freight to the container's walls was determined with the Coulomb method with Sinelnikov's adjustment.

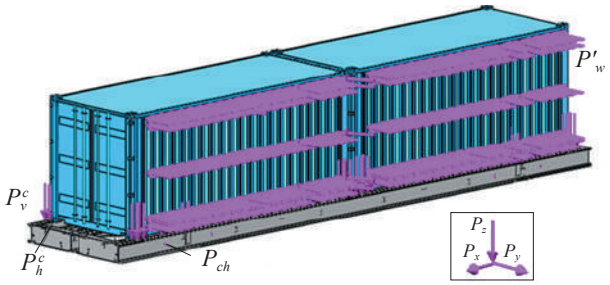

Figure 4.11 – Model for determination of the dynamic loads of a dry freight container in ferry transportation

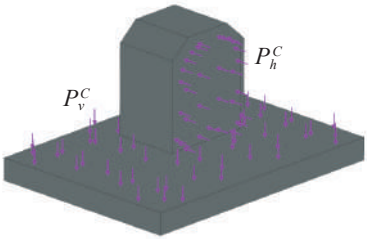

Figure 4.12 – Loads on the fitting stop of a flat car from the container's fitting during train ferry oscillations

The finite element model was built with spatial isoparametrical tetrahedrons. The optimal number of elements was determined with the graph analytical method. The characteristic of the finite element model for the carrying structure of a flat car loaded with containers in train transportation is given in the table.

Table 4.1 – Data on the finite element model of dry freight containers located on the flat car during ferry transportation

Number of elements	2010206
Number of nodes	669705
Maximum element size, mm	50
Minimum element size, mm	10
Maximum element side ratio	16258
Percentage of elements with a side ratio of less than three	47.6
Percentage of elements with a side ratio of more than ten	20.4
Minimum number of elements in a circle	8
Element size gain ratio	1.9

The tank container was fixed in the areas where the flat car rested against the fitting stops of a flat car. It was taken into account that the container had its natural degree of freedom in the horizontal plane due to the gaps between the fittings and fitting stops. Steel 09G2S was taken as the structural material for a flat car.

The results of the calculation are given in Figure 4.13. The discordance between the results of mathematical and computer modelling of the dynamic loads on the container are given in Figure 4.14.

The model was verified with an F-test. It was established that the hypothesis on adequacy is not rejected.

The calculation was made for the all above-mentioned patterns of interaction between the containers and the flat car in ferry transportation.

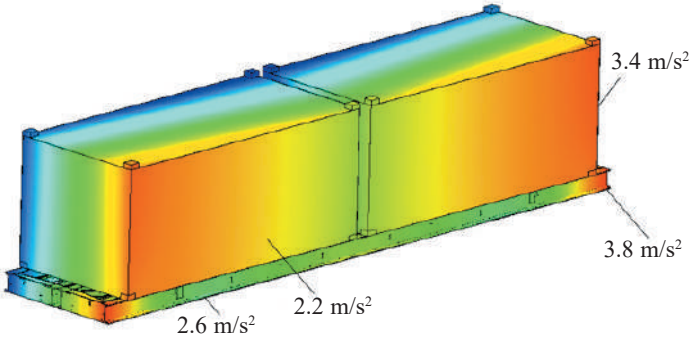

Figure 4.13 – Distribution of acceleration fields relative to the carrying structure of a dry freight container during ferry transportation

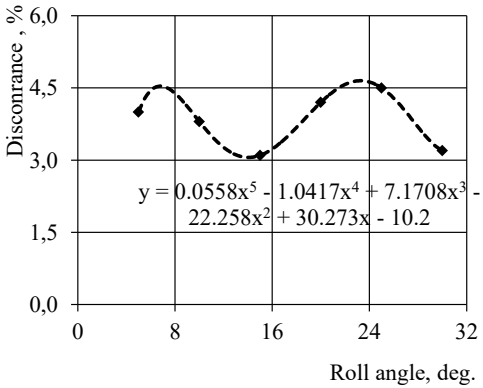

Figure 4.14 – Discordance between the results of mathematical and computer modelling of the dynamic loads on the container

The dynamic loads on the tank containers in ferry transportation were studied by means of computer modelling with the finite element method in CosmosWorks [139].

Spatial isoparametric tetrahedrons were taken as finite elements. The optimal number of elements was determined with the graph analytical method. The basic data on the finite element model of the

tank containers located on a flat car in ferry transportation are given in Table 4.2.

Table 4.2 – Data on the finite element model of the dry freight containers located on the flat car during train ferry transportation

Factor	Value
Number of Jacobian points	4
Number of units	396934
Number of elements	1192935
Maximum element size	70
Minimum element size	14
Minimum number of elements in a circle	9
Element size gain ratio	1.7
Maximum side ratio	13317
Percentage of elements with a side ratio of less than three	36.7
Percentage of elements with a side ratio of less than ten	15.4

The model used for defining the dynamic loads of a tank container located on the flat car in ferry transportation is presented in Figure 4.15. The design model included the following forces on the flat car: vertical force from the containers P_v^C located on it, horizontal force on the fitting stops P_h^C from the fittings, and forces on the flat car through the units for fixation of chain binders P_{ch}. Due to the spatial location of the chain binders the force through them to the flat car frame was decomposed into three elements which included the spatial location angles.

The flat car was fixed in the areas where it rested against the gear parts, and the working surfaces of mechanical support jacks. Therefore the main longitudinal beams of a flat car frame across the contact areas with the bolster beams were equipped with rounded pads with the diameter equal to that of the working parts of mechanical support jacks.

The calculation also included vertical static force P_v^{st}, pressure from the liquid freight P_{lf} and wind force P_w applied to the tank car.

The container was fixed in the areas where it rested against the flat car. Steel 09Mn2Cr was taken as structural material. The results of the calculation are given in Figure 4.16.

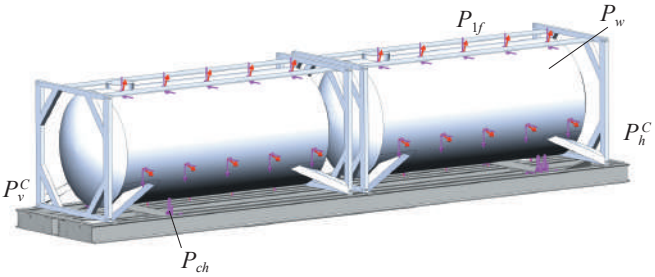

Figure 4.15 – Model for defining the dynamic loads on the dry freight container in ferry transportation

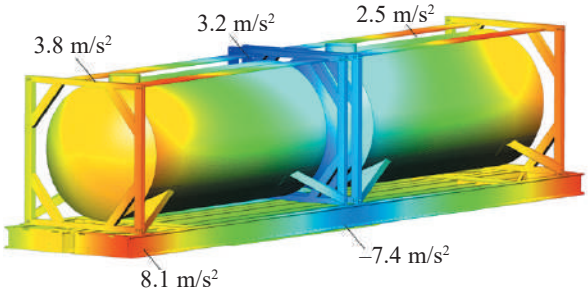

Figure 4.16 – Distribution of accelerations fields on the flat car in ferry transportation

The maximum accelerations on the tank container were concentrated in the frame from the chain binders and accounted for about 0.9 g. The accelerations in the barrel's upper part were 0.3 g.

The designed models of the dynamic loads on the tank containers in ferry transportation were verified with an F-test.

Discordance between the results of mathematical and computer modelling of the dynamic loads on the tank container in ferry transportation is shown in Figure 4.17.

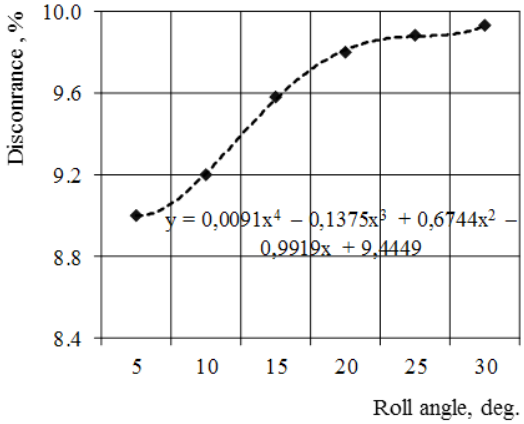

Figure 4.17 – Discordance between the results of mathematical and computer modelling of the dynamic loads on the tank container

The results of the calculation demonstrated that the hypothesis on adequacy of the models was not rejected.

Conclusions to Part 4

1. The authors studied the dynamic loads on the carrying structure of the containers located on the flat car during train ferry transportation.

It was established that without displacements of a flat car and containers relative to the initial position, the total value of acceleration on the farthest flat car loaded with containers from the bulwark was about 0.25 g.

The study demonstrated that with displacements of a flat car during train ferry oscillations and without displacements of containers relative to the frame, the total value of acceleration to the farthest flat car from the bulwark accounted for about 0.25 g.

And with displacements of a flat car relative to the deck and containers relative to the flat car frame, the total value of acceleration to the farthest flat car from the bulwark accounted for about 0.47 g.

The stability of a container was provided at roll angles of a train ferry of up to 25°.

2. The authors researched into the dynamic loads on the carrying structure of a tank container located on the flat car in ferry transportation.

The research demonstrated that without displacements of a flat car and containers relative to the initial position, the total value of the acceleration on the farthest flat car loaded with tank containers from the bulwark accounted for about 0.3 g.

And with displacements of a flat car relative to the deck and without displacements of tank containers relative to the frame, the total value of the acceleration to the farthest tank container from the bulwark was about 0.6 g.

The total value of the acceleration on the farthest tank container from the bulwark with displacements of a flat car relative to the deck and without displacements of a tank container relative to the frame accounted for about 0.9 g.

Safe maritime transportation of liquid freight in the tank container can be provided at roll angles of a train ferry of up to 10°.

3. The research also included computer modelling of the dynamic loads on the container in ferry transportation with the finite element method. The research was made at angular displacements of a flat car loaded with containers (tank containers) about the longitudinal axle and showed the distribution fields of accelerations relative to the flat car loaded with containers (tank containers) with their numerical values.

The models were verified with an F-test. It was established that the hypothesis on adequacy was not rejected.

PART 5
EXPERIMENTAL RESEARCH INTO THE STRENGTH OF AN OPEN CAR BODY DURING INTERACTION WITH REUSABLE LASHING DEVICES ON THE TRAIN FERRY

5.1 Experimental research into the strength of open car body elements in ferry transportation during sea disturbance

The purpose of the experimental research is to test the strength characteristics of open car body elements used for fixation on the ferry deck during sea disturbance, and check the adequacy of the theoretical research. The experimental research was made for the ferry *Geroi Shipki* on the Illichevsk – Poti route with a port entry to the ferry complex of the station Crimea. The full-scale research was made to test the strength of the body elements for a universal 69-ton open car located on the main deck of a train ferry, on the second track from the bulwark in the stern. The car was fully loaded with bulk freight (silica stone 3KB-97) [70, 142].

Two chain binders on the right side of a car were fastened on a bracket for tugging a car during shunting operations (Figure 5.1, *a*). and by one chain binder – on the locking sectors of hatch covers (Figure 5.1, *b*), *c*); on the left side two chain binders were fixed on the towing shackle, by ones – on the brackets used for tightening hatch covers and on the towing shackle (Figure 5.1, *d*), the location angles of chain binders relative to the car body are given in Table 5.1.

According to the logbook data it was found that the first day of the full-scale tests (August 16, 2010) had the following characteristics: wind speed – 3–5 m/s, sea disturbance – 1 point; the second day:

sea disturbance – 4–5 points, wave angle to the ferry body – 60–80°, speed and direction of the wind – 6–10 m/s and 60–80°, respectively. The roll angle of the train ferry was about 5°.

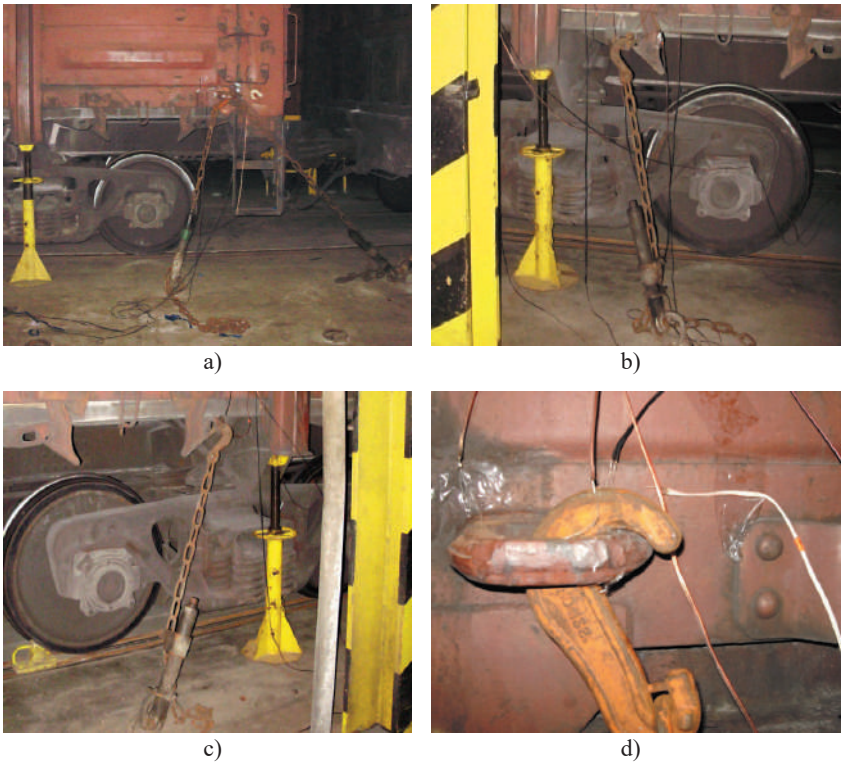

a) b) c) d)

Figure 5.1 – Fixation pattern of an open car on the train ferry deck:
a) fastening of two chain binders on the bracket used to tug a car during shunting operations; b), c) fastening of a chain binder on the locking sector of a hatch cover; d) fastening of a chain binder on the bracket used for tugging a car during shunting operations

The largest different value of the train ferry was recorded in approach to Sarych and was about 0.7 m aft (by the stern), i.e. less than 1 if expressed in the angular displacement value.

Table 5.1 – Location angles of chain binders relative to the planes of an open car with an actual fixation pattern

Location angles of chain binders relative to the car body, grad.			
	α	**β**	**γ**
1	16.2	40.6	71.3
2	16.2	18.5	49.1
3	18.5	54.2	76.4
4	18.5	35.2	64.5
5	15.9	34.8	67.7
6	15.9	19.3	50.8
7	15.9	42.5	72.7
8	18.2	54.2	76.7

The following are the technical means used for measuring forces in the contact areas between the car body and the chain binders:

1. Digital strain indicator for constructions and engineering products ВДЦ-1 (Figure 5.2).
2. Universal tester.
3. Wire strain gages with a base of 20 mm and resistance of 124 Ohm.
4. Set of mounting wires to connect the strain indicator and the wire strain gages.
5. Portative computer to store registered data during the research (Figure 5.3).

The strain measurement method was used for the experimental research into the forces in the contact areas between the car body and the chain binders [70, 143–146].

The places of installation of the strain gages on the car body were chosen in accordance with actual fixation patterns on the deck, i.e. on the contact areas between the body and the hooks of chain binders.

The strain gages were linked according to half-bridge circuit patterns in the areas under study [143–146].

Figure 5.2 – Strain indicator for constructions and engineering products ВДЦ-1

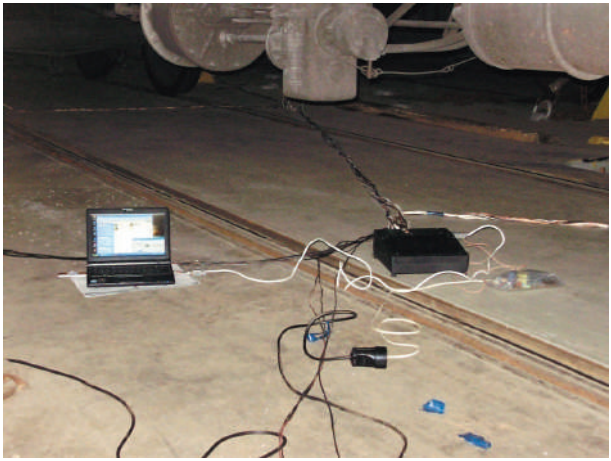

Figure 5.3 – Portable computer connected to the strain measuring station

The strain gages were mounted on the surface of the body under study with hot-setting cyanoacrylate glue. Before application of the glue, the surface of the body for mounting the strain gages was cleaned to dulling and degreased. The installation of the strain gages on the open car body elements relative to the train ferry deck is shown in Figure 5.4 [70].

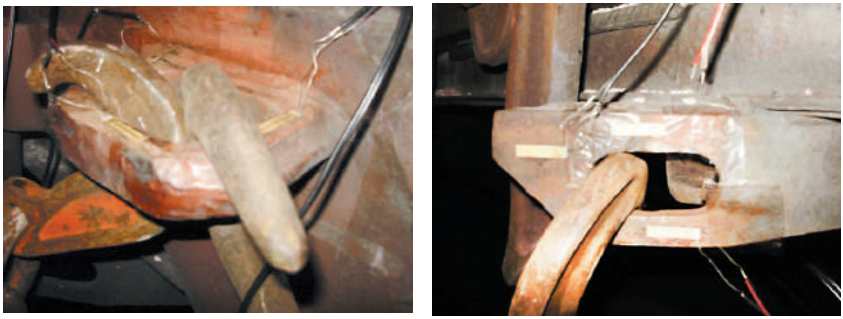

a) b)

Figure 5.4 – Location of strain resistors on the areas under study on the open car body:
a) in the area of a bracket for tugging a car during shunting operations;
b) in the area of the brackets of a hatch hook

The location diagram of the strain gages on the bracket for tugging of car during shunting operations is presented in Figure 5.5. The largest values of relative deformations in the body elements were registered by a set of strain gages mounted on the locking sectors of hatch covers and on the bracket for tugging a car provided that it held two hooks of chain brackets. These values accounted for 865 and 996 units (Figure 5.6) respectively, or 178 MPa and 203.4 MPa.

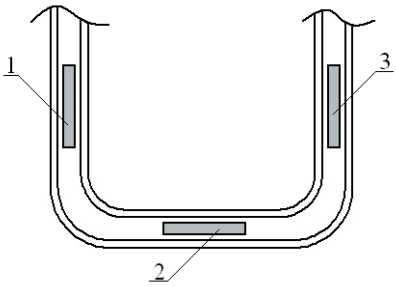

Figure 5.5 – Diagram of location of strain resistors on the bracket for tugging a car during shunting operations

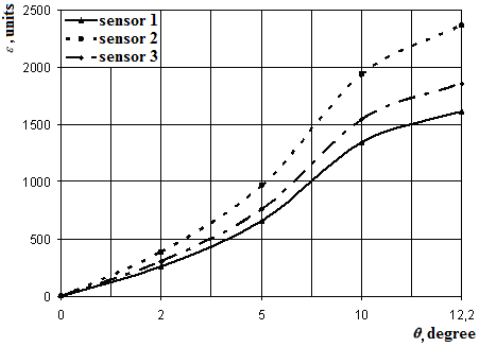

Figure 5.6 – Dependency of relative deformations in the areas of location of the strain gages on the bracket for tugging a car during shunting operations on the roll angle of a train ferry

Figure 5.7 presents a graphic dependency of relative deformations in the areas where a car was fastened on the ferry deck (towing shackle) on the sea wave parameters (length, height, frequency, etc.).

This dependency demonstrated that the relative deformations in the areas where the body was fixed on the train ferry deck were of stochastic nature and depended on the sea wave parameters.

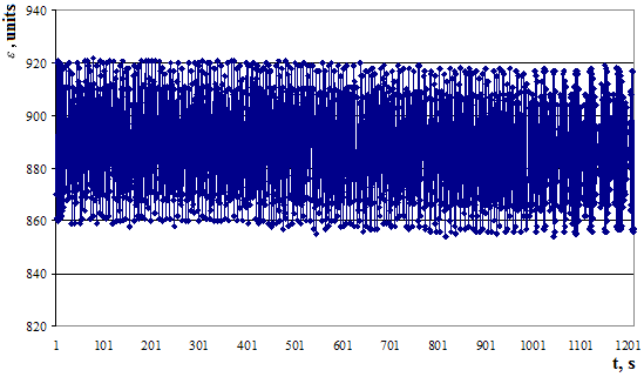

Figure 5.7 – Dependency of relative deformations in the fastening areas of an open car body on the ferry deck on time

Table 5.2 presents the results of the analysis of the experimental data on the maximum values taken by the strain resistors.

Table 5.2 – Results of statistical analysis of the maximum relative deformations of the strain gages

θ, *deg.*	**Set of measure-ments**	**№ of strain gage**	**Average**	**Min. value**	**Max. value**	**Dispersion**	**RMS**
5	3	1	512	464	514	1.2	1.1
	3	2	920.5	844	921	0.5	0.7
	7	3	612	585	641	0.68	0.82

As far as the theoretical calculation gave a roll angle of a train ferry of 12.2°, and the full-scale research – 5°, they were checked for adequacy with the correction index obtained and appropriately applied. The comparative analysis of the theoretical and full-scale results for the area where the bracket for tugging a car during shunting operations was located is presented in Tables 5.3–5.5.

The difference between the theoretical and experimental data was about 20 %, for some cases – about 40 %.

This difference was conditioned by the values of the accelerations relative to the car locations on the upper deck of a train ferry and the freight (black coal) with the appropriate physical properties which were included in the theoretical calculation.

Figures 5.8–5.10 present graphical dependencies of stress values in the areas of fastening of a car body on the roll angle of a train ferry obtained both theoretically and experimentally.

The presented dependencies demonstrated that the largest values of the relative deformation were recorded by strain register № 2. They were in the middle part of a towing shackle.

The adequacy of the strength model of an open car body with consideration with the fixation patterns on the train ferry deck was checked with an F-test.

Table 5.3 – Comparative analysis of the theoretical and experiment data on stresses in the area of location of a bracket for tugging a car during shunting operation (strain gage № 1)

Roll angle, deg.	**Stress, MPa**		**Relative difference, %**
	theoretical	**experimental**	
2	48.4	55.7	13.1
5	121	138.6	12.7
10	246	282.9	13
122	295	339.25	13
Average			12.95

Table 5.4 – Comparative analysis of theoretical and experiment results in the area of location of a bracket for tugging a car during shunting operations (strain gage № 2).

Roll angle, deg.	**Stress, MPa**		**Relative difference, %**
	theoretical	**experimental**	
2	48.4	81.4	40
5	121	203.4	41
10	246	406.8	39.5
12.2	295	496,3	40.5
Average			40.3

Figure 5.5 – Comparative analysis of theoretical and experimental data on the stresses in the area of a bracket for tugging a car during shunting operations (strain gage № 3).

Roll angle, deg.	**Stress, MPa**		**Relative difference, %**
	theoretical	**experimental**	
2	48.4	64	24.4
5	121	159.72	24
10	246	324.72	24.2
12.2	295	389.7	24.3
Average			24.2

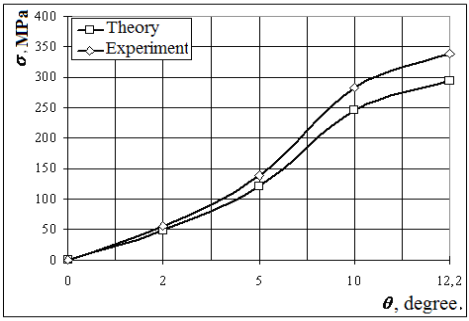

Figure 5.8 – Dependency of stresses in the areas of fixation of a car body on the roll angle of a train ferry (strain gage № 1)

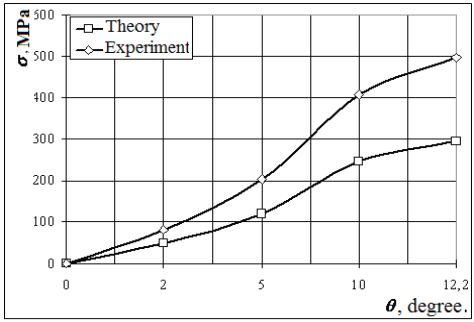

Figure 5.9 – Dependency of the stresses in the zones of fixation of a car body on the roll angle of a train ferry (strain gage № 1)

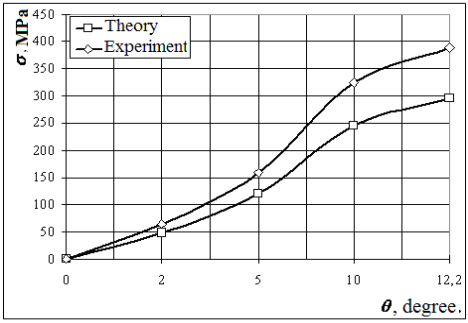

Figure 5.10 – Dependency of the stresses in the zones of fixation of a car body on the roll angle of a train ferry (strain gage № 3)

Let us take into consideration that the model under study is linear, i.e. a one-factor model which characterizes a change in the stresses in the open car body elements including its fixation on the deck during sea disturbance on the roll angle of a train ferry. Therefore, the number of degrees of freedom at $N = 5$ accounted for $f_1 = 3$.

The calculation was made for the values taken by strain resister № 1 at $\theta = 12.2°$.

On the basis of the calculation at the dispersion of renovation $S_y^2 = 6.94$, the dispersion of adequacy $S_{ao}^2 = 35.42$ and $f_2 = 5$, the authors obtained the actual Fisher's criterion value $F_p = 5.11$, which was smaller than the tabular value $F_1 = 5.41$. Thus, with the level of significance $p = 0.05$ the hypothesis on adequacy of the model designed in not rejected. In this case the approximation error was about 2 %.

The results of the experimental research made it possible to conclude that the existing technology cannot be used for fixation of a car on the deck. Therefore, there is a need to experimentally research the strength of car bodies equipped with special units for fixation of chain binders.

5.2 Experimental research into the strength of open car body elements equipped with special units for fixation of chain binders

5.2.1 Place and conditions of the research

The research objective was to test the strength characteristics of the car elements equipped with special units for fixation of chain binders mounted on the bolster beam of an open car body.

The research into the strength of the carrying structure of an open car under the forces from the chain binders through the units for fixation was made at the car depot Osnova of the Southern Railway. The authors studied the angular displacements of a train ferry relative to the longitudinal axle as the largest loading on the car structure [70, 124].

The following technique and devices were used for measuring the forces in the areas of the bolster beam of a car body equipped with special units for fixation of chain binders:

1. Strain indicator ВДЦ – 1 for constructions and engineering products.
2. Universal tester.
3. Wire strain gages with a base of 50 mm and resistance of 400 Ohm.
4. Set of mounting wires to connect the strain indicator with the strain gages.
5. Specially developed testing bench for simulating roll motion of a car as the case of the largest loading on the structure.
6. Units for fixation of chain binders were presented as steel castings.
7. Four hydraulic support jacks with capacity of 294.3 kN.
8. Metal strops with capacity of 196.2 kN.
9. Force gage with a measuring range of 20-200 kN of the 2nd accuracy class.
10. Digital camera.

The initial stage of the research included the creation of a model for fixation of chain binders. It included design and production of a detachable wooden model of the unit with subsequent casting of steel elements. The radial lugs and rounded parts on the model were formed with viscous mixture consisting of liquid glass and chock. Thus, four castings of Steel 32Cr06A (fluidity level of σ_T = 441 MPa, tensile resistance σ_B = 638 MPa, relative prolongation δ = 10 %) with Ni added, were further normalized and quenched for higher strength values. This steel grade is recommended and used for manufacturing cast pieces in car building in accordance with [147] with subsequent quenching and tempering.

The production steps of making these forms out of cold-hardening mixture to be used later for fixation of the units on the car are given in Table 5.6.

The castings were mechanically treated to nominal dimensions.

A 12-1505 open car was chosen for the experimental research into the strength of a car body in the areas of location of units for fixation of chain binders. This decision was approved by the Car Facility Department of the Southern railway.

The units were fixed on the bolster beams of a car by means of overlap welding with a double seam (Figure 5.11) calculated for strength beforehand. The units were mounted on one side of the bolster beams.

The model of chain binders included 196.2 kN wire slings one end of which was fixed on the unit, and the other end – on the staple welded to the 50-mm metal sheet (Figure 5.12).

Table 5.6 – Steps in making the forms out of cold-hardening mixture to be used for fixation of the units on the car

1	Treat the model with silver paint solution for easy removing out of the mold;
2	Put the model on the modelling plate and install the box form;
3	Prepare 10 kg of forming mixture, add hardener and mix for two minutes;
4	Mould the lower part of the form, press slightly with a hand filler;
5	After the mixture is hardened, turn the mold and shake the model to avoid aggregation;
6	Powder the disconnect line with marchalite;
7	Mount the upper part of the model and the gating system (slag trap with two feeders and two chokes). Make the upper part similar to the lower part. In the upper half-part make some punches with a diameter of 3-4 mm at a distance of 30-40 mm for gas venting;
8	Open the mold and extract chokes, gating system and models;
9	Clean out the mold from dirt;
10	Assemble the mold by dowels to avoid mismatching;
11	Load the assembled form with mass of 20 kg;
12	Pour metal of Grade 32Cr06A in the mold at temperature of 1570 °C.
13	Allow solidification;
14	Clean out the casting from padding.

Figure 5.11 – Location of a unit for fixation of a chain binder's hook on the bolster beam of an open car

The car spring suspension was relieved with 294.4 kN stationary jacks; the chain binders and the bolster beam were loaded on one side of a car. This simulated the action from the mechanical jacks of capacity of 196.2 kN to the end support parts of the bolster beams. The forces on the bolster beam were measured with a force gage with capacity of 196.2 kN.

The relative strains in the bolster beam were determined with the classic method of strain measurement [70].

Figure 5.12 – Forces to the unit for fixation of a chain binder's hook

The location of strain gages was determined in the theoretical research (in the areas of the maximum loads on the basis of the fields of stress-strain state obtained). As far as the forces on the unit for fixation of a chain binder's hook during rolls of a train ferry transferred symmetrically, the strain gages were installed on the vertical sheet of a bolster beam (Figure 5.13) [70].

Figure 5.13 – Location of strain gages on the vertical sheet of a car bolster beam

The strain gages were linked according to a Wheatstone bridge. A dummy strain gage was mounted on the homogeneous non-deflecting 09Mn2Cr plate of a car body (Figure 5.14).

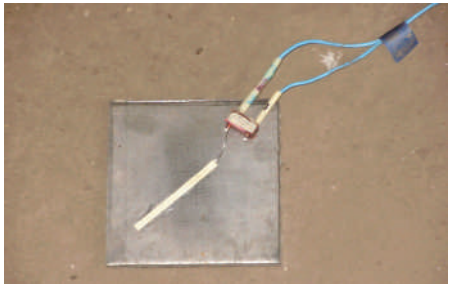

Figure 5.14 – Plate with a dummy strain gage

Wires with a diameter of 0.5 mm^2 were used for connecting the gages to the circuit.

The loading on the bolster beam led to the deformation corresponding to the forces applied: 49.1 kN – tension forces of chain binders; 98.1 kN – forces to the car body through the chain binders at small roll angles (up to 10°); 147.2 kN – forces to the car body through the chain binder at large roll angles (more than 10°) [70].

The greatest relative deformations indicated by strain gages № 2, 3, 4 and 9 (Figure 5.13) were 301.12, 308.65 and 188.2 strain rates (Figure 5.15).

On the basis of the strain rates obtained the authors calculated the stresses in corresponding areas of the bolster beam (Tables 5.7–5.10), and made the conclusion that, when the bolster beam was loaded with forces from the chain binders through the special units for fixation, the strength reserve of the structure exceeded 2.

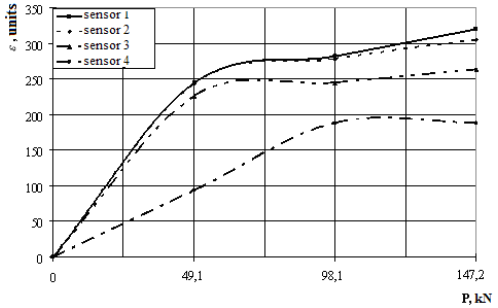

Figure 5.15 – Dependency of strain rates in the areas of a car's bolster beam on the loading through the special units for fixation of chain binders

The strength of a bolster beam in the areas of strain gages № 3 and № 4 can be increased by means of reinforcing diaphragms. The theoretical calculation for the strength of the improved open car has been presented in previous sections of the study.

It should be mentioned that the experimental research with the method of electric measuring can have an error conditioned by metrological parameters of gages, equipment, connection line, experiment conditions and measuring scheme applied [84].

Table 5.7 – Stresses in the area of location of the unit for fixation of a chain binder's hook (strain gage № 2)

Test number	Stress, MPa		
	Design load, kN		
	49.1	**98.1**	**147.2**
1	2	3	4
1	39.7	51.8	71.6
2	39.8	52	73
1	2	3	4
3	40	51.1	71.1
4	40.4	51	70.9
5	39.4	51.4	71.4
6	38.8	51	71.2
7	39.1	52.1	72.1
8	39.5	51.2	71.3
9	39.4	52.2	71.8
10	41	52.3	70.7
σ, MPa	39.7	51.6	71.5

Table 5.8 – Stresses in the area of location of the unit for fixation of a chain binder's hook (strain resistor № 3)

Test number	Stress, MPa		
	Design load, kN		
	49.1	**98.1**	**147.2**
1	34.6	46	51.6
2	34.7	46.3	51.3
3	35.1	45.7	51.1
4	34.45	46.2	51.5
5	34.4	45.8	50.3
6	34.5	46.6	52
7	37	46.1	51.4
8	34.8	45.4	50.2
9	34.9	45.3	50
10	36.9	46.8	52.1
σ, MPa	35.1	46	51

Table 5.9 – Stresses in the area of location of the unit for fixation of a chain binder's hook (strain resistor № 4)

Test number	Stress, MPa		
	Design load, kN		
	49.1	**98,1**	**147.2**
1	35.7	47	55.1
2	35.1	47.3	55.3
3	35.4	47.7	56
4	36.4	47.9	55.5
5	35.2	47.8	55.8
6	35.5	47.2	55.6
7	36.2	47.65	55.4
8	35.9	47.4	56.1
9	35.3	48	55.2
10	36.1	48.7	55.7
σ, MPa	35.7	47.65	55.6

Table 5.10 – Stresses in the area of location of the unit for fixation of a chain binder's hook (strain resistor № 9)

Test number	Stress, MPa		
	Design load, kN		
	49.1	**98.1**	**147.2**
1	2	3	4
1	7	19.7	39
2	7.1	18.9	38.6
3	7.6	19.7	38.5
4	7.2	19.7	38
5	6.9	18.8	38.3
1	2	3	4
6	7	19.2	38.2
7	6.4	19.5	38.3
8	7.1	19	38.1
9	7.2	18.8	38.4
10	6.5	19.7	38.6
σ, MPa	7	19.3	38.4

The measuring error was defined by the following formula:

$$\Delta\varepsilon = \Delta\varepsilon_c + \Delta\varepsilon_в, \tag{5.1}$$

where $\Delta\varepsilon_c$ – measurement bias;
$\Delta\varepsilon_в$ – random measurement error.

The measurement bias here is conditioned by the tolerances due to lack of parallelism and the width of a beam with equal resisting moment, and, in accordance with [151] the standard beam should have resistance of 4 %.

A random measurement error is defined by the formula:

$$\Delta\varepsilon = \frac{\varepsilon_в}{\varepsilon_e}, \tag{5.2}$$

where $\Delta\varepsilon_в$ – absolute measurement error;
$\Delta\varepsilon_c$ – error obtained in the experiments.

The random error was defined according to [151] by the following formula:

$$\Delta\varepsilon_в = \pm\left\{\left|0{,}01\cdot\tilde{I\!I}_t\cdot\varepsilon\right| + 2\sqrt{\varepsilon^2\left[\left(\frac{S_k}{\tilde{K}}\right)^2+\left(\frac{S_f}{\tilde{\Phi}}\right)^2+(0{,}01\cdot S_T)^2\right]+\left(\frac{1}{K\cdot\Phi}\right)^2\times 2\left\{2\left[\frac{S_t(t-t_n)}{t-t_0}\right]^2+\right.}\right.$$

$$+2S_d{}^2+\sigma_\xi^2+\frac{1}{2}\left(\frac{\xi}{R}\right)^2\times\left[S_r^2\left(\frac{\bar{r}}{\bar{\bar{R}}}\right)^2\times\left(\frac{\delta_{Rn}\bar{R}\cdot 10^{-2}}{2\sqrt{3}}\right)^2\right]+\left[\beta(t-t_n)\frac{1}{\bar{\bar{R}}}\times S_{(rnn1-rnn2)}\right]^2+ \tag{5.3}$$

$$\left.\left.+\left[2\frac{\bar{r}_{no}}{r}\beta(t-t_n)\right]^2\times\frac{1}{4}\left(\frac{1}{R}\right)^2\times\left[S^2_{(r1-r2)}+\left(\frac{\bar{r}}{\bar{\bar{R}}}\right)^2\left(\frac{\delta_{Rr}\bar{R}\cdot 10^{-2}}{2\sqrt{3}}\right)^2\right]\right\}\right\},$$

where S_k – RMS of sensitivity;
$\tilde{K}$, K – mathematic expectation and average sensitivity for strain gages, responsively;
S_f – average square error of the temperature to sensibility function;
$\tilde{\Phi}$, Φ – mathematic expectation and average value of the temperature to sensibility function, respectively;
S_T – RMS of creep at temperature t in time moment T;
S_t – RMS of temperature characteristics of resistance;

t – design value of temperature, °C;
t_n – temperature in the initial moment of measurement, °C;
t_0 – normal temperature value, °C;
S_d – RMS of output signal drift;
σ_ξ – RMS of an error of stain measurement equipment, m^{-1};
ξ – resistance temperature characteristic of a strain gage, m^{-1};
R – average resistance of strain gages, Ohm;
S_r – RMS of connection line resistance, Ohm;
$\bar{r}$ – average value of connection line resistance, Ohm;
δ_{Rn} – ratio between the difference of resistance boundary values of strain gages and the nominal values, %;
β – temperature resistance coefficient of connection line material, $(°C)^{-1}$;
$S_{(rnn1 - rnn2)}$ – RMS of resistance of a connection line section running through the heating zone, Ohm;
$\bar{r}_{no}$ – average resistance of a connection line chain running through the heating zone at the normal conditions, Ohm;
r – connection line resistance at the normal conditions, Ohm;
$S_{(r1 - r2)}$ – RMS of the difference in the connection line resistance of working and dummy strain gages, Ohm;
δ_{Rr} – ratio of the difference of the boundary values of strain gages in a group to the nominal resistance, %;

The values of the output parameters used for calculating the random measurement error are given in Table 5.11.

Table 5.11 – Output parameters for calculation of the random measurement error

Factor	S_k	K	S_f	Φ	S_T	S_t	t	t_0	σ_ξ
Value	0.05	2.2	0.03	3	1.5 %	10	35 C	30 C	20
Factor	ξ	R	S_r	$\bar{r}$	σ_{Rn}	β	$S_{(rnn1 - rnn2)}$	$\bar{r}_{no}$	$S_{(r1 - r2)}$
Value	800	400	0.005	1	0.2 %		0.0006	0.3	0.008

On the basis of the calculation the random error value was strain rates.

And

$$\Delta\varepsilon_{\sigma} = \frac{29.8}{338.76} \approx \pm 8.8\,\%.$$

Therefore, the total error value is:

$$\Delta\varepsilon = 4 + 8.8 = 12.8\ \%.$$

5.2.2 Determination of statistical characteristics of experimental data

The adequacy of the experimental data of the hypothesis on the distribution of the random value σ by the normal law, the most exploitable for engineering calculation, was checked with Pierson's test χ^2. Thus, the authors composed a statistical series of distributions for a random value.

And on the basis of calculation with a probability of 0.95 we could confirm that the random value σ was distributed by the normal law.

For defining the statistical characteristics of a one-factor experiment [148–150], i.e. for determining the stresses in the bolster beam under the forces through the special unit for fixation of a chain binder's hook, the following formulae of probability theory and mathematical statistic were used [91, 92, 94, 95].

The sample collection was defined by the formula [152]:

$$n = \frac{t^2_{(p,k)}\sigma^2}{\Delta^2\sigma}, \tag{5.4}$$

where $t^2_{(p,k)}$ – value of Student's test at a given probability and value of freedom.

$$\Delta\sigma = t_{\alpha}(n) \cdot \Delta S_{\bar{\sigma}}, \tag{5.5}$$

where $\Delta^2\sigma$ – absolute error of the measurement result.

On the basis the data calculated for determination of the required number of experiments, we can say that there is no need to make more

measurement, as the number of the needed tests was half as many as the factual number.

Tables 5.12–5.15 present the analysis of the experimental data from the strain gages [70].

Table 5.12 – Results of the statistical analysis of the experimental data (strain gage № 2)

P, kN	Set of measurements	Average	Min. value	Max. value	Dispersion	RSM
49.1	10	39.7	38.8	41	0.04	0.2
98.1	10	51.6	51	52.3	0.03	0.17
147.2	10	71.5	70.7	71.8	0.04	0.21

Table 5.13 – Results of the statistical analysis of the experimental data (strain resistor № 3)

P, kN	Set of measurements	Average	Min. value	Max. value	Dispersion	RMS
49.1	10	35.1	34.4	37	0.1	0.31
98.1	10	46	45.3	46.8	0.02	0.15
147.2	10	51	50	52.1	0.06	0.24

Table 5.14 – Results of the statistical analysis of the experimental data (strain resistor № 4)

P, kN	Set of measurements	Average	Min. value	Max. value	Dispersion	RMS
49.1	10	35.7	35.1	36.2	0.02	0.14
98.1	10	47.65	47	48.7	0.02	0.15
147.2	10	55.6	55.1	56.1	0.01	0.11

Table 5.15 – Results of the statistical analysis of the experimental data (strain resistor № 9)

P, kN	Set of measurements	Average	Min. value	Max. value	Dispersion	RMS
49.1	10	7	6.4	7.6	0.01	0.11
98.1	10	19.3	18.8	19.7	0.02	0.13
147.2	10	38.4	38	39	0.01	0.09

5.2.3 Comparative analysis of the theoretical and experimental data on the strength of body elements equipped with special units for fixation of chain binders

In order to check the adequacy, let us compare the theoretical data obtained in the strength calculation of the body elements equipped with special units for fixation of chain binders with the experimental data (Tables 5.16–5.19) [70].

The interpolation of the theoretical and experimental data was made with the most widespread regression analysis methods, i.e. the method of least squares (Figures 5.16–5.19).

Table 5.16 – Comparative analysis of the theoretical and experimental data on the stresses in the bolster beam of a car (strain gage № 2)

Load, kN	**Stress, MPa**		**Relative difference, %**
	theoretical	**experimental**	
49.1	38.7	39.7	2.5
98.1	50.3	51.6	2.5
147.2	61.9	71.5	13.4
Average value	6.1		

Table 5.17 – Comparative analysis of the theoretical and experimental data on the stresses in the bolster beam of a car (strain gage № 3)

Load, kN	**Stress, MPa**		**Relative difference, %**
	theoretical	**experimental**	
49.1	34.2	35.1	2.6
98.1	46.8	46	1.7
147.2	48.3	51	5.3
Average value	3.5		

Table 5.18 – Comparative analysis of the theoretical and experimental data on the stresses in the bolster beam of a car (strain gage № 4)

Load, kN	Stress, MPa		Relative difference, %
	theoretical	experimental	
49.1	34.8	35.7	2.5
98.1	46.4	47.65	2.6
147.2	46.4	55.6	16.5
Average value	7.2		

Table 5.19 – Comparative analysis of the theoretical and experimental data on the stresses in the bolster beam of a car (strain gage № 9)

Load, kN	Stress, MPa		Relative difference, %
	theoretical	experimental	
49.1	14.2	7	50.7
98.1	30.4	19.3	36.5
147.2	43	38.4	10.7
Average value	32.63		

The difference accounted for about 10 %, with the exception of some results –36.5 %; that testifies the precision between the theoretical and experimental results of the research.

The adequacy of the strength model for the bolster beam of an open car body with consideration of the adaptation measures for ferry transportation was checked with an F-test. The calculation included the measurements of strain gage № 3. On the basis of the calculation at $S_y^2 = 0.41$, $S_{ao}^2 = 1.17$, $f_1 = 8$ and $f_2 = 10$ the authors obtained the value $F_p = 2.82$, which was lower than $F_1 = 3.07$. Thus, with the level of significance $p = 0.05$, the hypothesis on adequacy of the model designed is not rejected. The approximation error accounted for about 14 %.

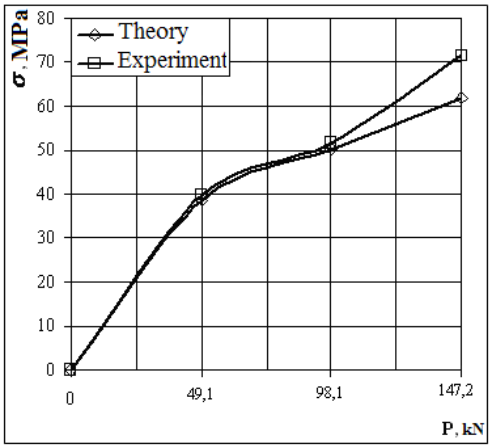

Figure 5.16 – Dependency of stresses in the vertical plane of a bolster beam on the external loads through the unit for fixation of a chain binder's hook (strain gage № 2)

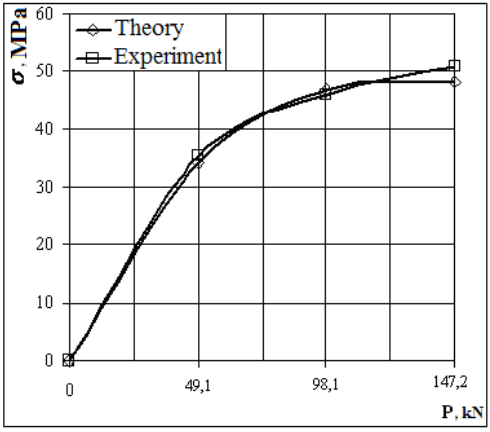

Figure 5.17 – Dependency of stresses in the vertical plane of a bolster beam on the external loads through the unit for fixation of a chain binder's hook (strain gage № 3)

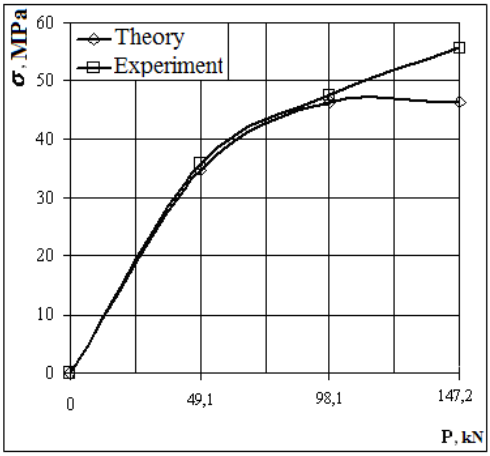

Figure 5.18 – Dependency of stresses in the vertical plane of a bolster beam on the external loads through the unit for fixation of a chain binder's hook (strain gage № 4)

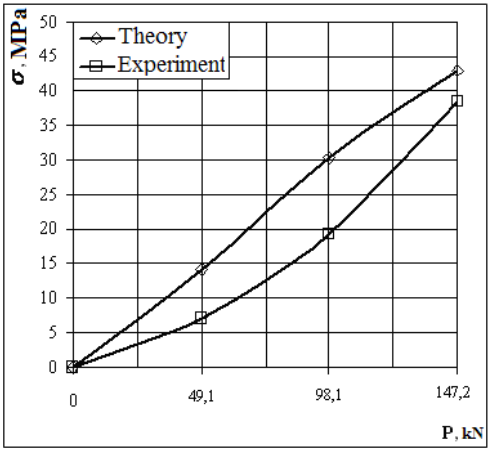

Figure 5.19 – Dependency of stresses in the vertical plane of a bolster beam on the external loads through the unit for fixation of a chain binder's hook (strain gage № 9)

Conclusions to Part 5

1. The authors made the experimental research into the stress-strain state of an open car body transported by a ferry during sea disturbance with the method of electrical strain measurement.

The experimental research was made for the ferry *Geroi Shipki* on the Illichevsk – Poti route with a port entry to the ferry complex of the station Crimea. The strength of the body elements was studies for a 69-ton universal open car. The places of installation of strain gages on the car body were chosen in accordance with actual fixation patterns on the deck, i.e. on the contact areas between the body and the hooks of chain binders.

It was established that existing technologies and technical mean applied for fixation of rail cars on the ferry decks cannot provide the required fixation during strong sea disturbance. These stresses exceed the admissible values for steel grades 09Mn2Cr and 09Mn2Cr applied in the manufacture of car bodies; they account for about 500 MPa and deformations – about 2500 strain rates.

The discordance between the theoretical and experimental calculation of the stress-strain state of open car body elements was about 20 %.

2. The research was made for the stress-strain state of an open car body equipped with units for fixation in their interaction with disposable devices during bench tests.

The research was made at the Osnova depot of the Southern Railway.

The location of strain gages was determined in the theoretical research (in the areas of the maximum loads on the basis of the stress-strain state fields obtained). As far as the forces to the unit for fixation of a chain binder's hook during roll of a train ferry were symmetrical, the strain gages were installed on the vertical plate of a bolster beam (Figure 5.13) [70].

It was found that the stresses in the elements of the carrying structure of an open car body accounted for about 70 MPa. Therefore, they did not exceed the admissible values and the deformations were about 310 strain rates.

The discordance between the theoretical and experimental data on the calculation of the stress-strain state of the elements of an open car body equipped with units for fixation of chain binders were about 10 %.

3. The strength models for the carrying structure of an open car fixed on the ferry deck with consideration of the units for fixation of chain binders were checked for adequacy. It was established that the hypothesis on adequacy of the models proposed is not rejected.

REFERENCES

1. Сотников Е. А. Железные дороги мира из XX в XXI век. М. : Транспорт, 1993. 200 с.
2. Иванченко И. А., Платонов Е. В. Железнодорожные паромные переправы. М. : Государственное транспортное железнодорожное издательство, 1943.
3. Виноградов Н. А. Взаимодействие различных видов транспорта при перевозках грузов в зарубежных странах. М. : ВИНИТИ, 1960. – 89 с.
4. Рачков А. С. Паром для Каспийского моря. Судостроение. 1960. № 7 (213). С. 1–6.
5. Фрик Э. Паром «Советский Дагестан». Морской флот. 1985. № 7. С. 42–44.
6. Тунзале Касумова. Гибель «Меркурия – 2». Как это было… URL: https://www.pravda.ru/accidents/9720-parom/ (дата обращения: 01.11.2002).
7. Сдан в эксплуатацию паром «Академик Зарифа Алиева». URL: https://www.ceo.az/news/events/8187.html (дата обращения: 09.01.2008).
8. Сдан в эксплуатацию паром «Академик Зарифа Алиева». URL: https://www.baku.ru/blg-list.php?blg_id=3&id=50405&cmm_id=793&usp_id=0 (дата обращения: 18.04.2008).
9. В Махачкалу прибыл первый грузовой паром из Хорватии. URL: https://regnum.ru/news/535625.html (дата обращения: 27.10.2005).
10. Килессо А. Мощные паромы-ледоколы. Морской флот. 1945. № 5–6. С. 33–36.
11. Рачков А., Бубнов К., Евстифеев В. Морской паром «Сахалин». Морской флот. 1972. № 12. С. 41–44.
12. Рачков А. С., Бубнов К. П., Евстифеев В. А. Морской паром «Сахалин». Судостроение. 1972. № 6. С. 3–7.

13. Зарубежная хроника. Судостроение. 1973. № 6. С. 60.

14. Волков Ю. П. Железнодорожные паромы. Судостроение. 1977. № 9. С. 15–20.

15. Каракашлы Н., Шклярук А. Транспортировка железнодорожного подвижного состава на лихтере «Ишимбай». Морской флот. 1965. № 7. С. 9–10.

16. Купенский Я. И. Создание железнодорожной паромной переправы в Астрахани. Судостроение. 1988. № 2. С. 59–60.

17. Кузовкин В. Паромы для Каспия. Морской флот. 1984. № 5. С. 41–43.

18. Каргин Л. Рейс Дружбы. Морской флот. 1986. № 4. С. 14–15.

19. Каргин Л. Новая паромная трасса. Морской флот. 1988. № 4. С. 6–7.

20. Зорин Ф. Мост через Каспий. Морской флот. 1988. № 12. С. 16–17.

21. Кирсанов Б. А. Железнодорожно-пассажирский паром «Советский Дагестан». Судостроение. 1985. № 4. С. 3–6.

22. Ершов Б. Дела паромные… Морской флот. 1978. № 9. С. 10–16.

23. Кузовкин В. Паромы для Каспия. Морской флот. 1984. № 5. С. 41–43.

24. Толстов Ю. Г. Железнодорожная паромная переправа через Байкал. Железнодорожный транспорт. 2001. № 7. С. 38–39.

25. Числав Воевудка. Паромное судоходство ПНР. Морской флот. 1979. № 10. С. 42–43.

26. Хаджимурад Гаджиев. Паромы для Махачкалы. Порты Украины. 2005. № 2. С. 70.

27. Поезда пересекают Балтику. Старые как мир паромные переправы обретают новые черты. Наука и жизнь. 1987. № 1. С. 52–55.

28. Гавриленко М. Паромная переправа Клайпеда – Мукран. Морской флот. 1984. № 5. С. 14–15.

29. Серова А. А. Железнодорожные паромные переправы. Железнодорожный транспорт. 1988. № 1. С. 73–76.

30. Балтийский мост. Морской флот. 1987. № 2. С. 18–20.

31. Шишин В. П. Морской железнодорожный паром «Мукран». Судостроение, 1986. № 12. С. 3–5.

32. Автомобильно-железнодорожный/пассажирский паром «Каунас». URL: https://www. ukrferry.com

33. Егоров Г., Кузьмин Г., Ильницкий И. Морской паром «Балтийск» вмистимостью 135 вагонов пр.CNF05. Судостроение и судоремонт. 2006. № 5–6. – С. 10–19.

34. Информационный отдел. Судостроение. 1990. № 1. С. 56–57.

35. Зарубежная информация. Судостроение. 1983. № 12. С. 54.

36. Егоров Г., Ильницкий И., Черников Д. «Линейка» паромов для Черного моря. 2014. № 1. С. 50–57.

37. Тигиранов В. Керченская паромная железнодорожная переправа. Железнодорожный транспорт. 1955. № 6. С. 75–77.

38. Недосекин А. Улучшить работу Керченской паромной переправы. Морской флот. 1956. № 2. С. 7–8.

39. Чикановский В. Возрождение железнодорожной паромной переправы «Крым – Кавказ». Порты Украины. 2004. № 4. С. 33–34.

40. Визняк Р. И., Ходько С. П., Ловская А. А., Головченко О. В. Особенности функционирования железнодорожно-паромных маршрутов Украины. Вагонный парк. 2008. № 9. С. 14–18.

41. http://forum.flot.su/showthread.php

42. Егоров Г. В. Развитие железнодорожных паромних переправ на Черном море. Судоходство. 2007. № 11. С. 25–29.

43. «Морское инженерное бюро»: реализация проектов. Судостроение и судоремонт. 2004. № 5. С. 7.

44. Егоров Г., Чистяков И., Автутов Н. Железнодорожный паром вместимостью 50 вагонов для Черного моря. Судостроение и судоремонт. 2007. № 3. С. 8–18.

45. http://www.uz.gov.ua/ci/c/bolgaria/ferry/vstupl.html – 27 k

46. http://www.ukrferry.com/rus/services/ferry.asp – 57_1

47. http://od.Ura – inform.com

48. Ефремов Н., Егоров Г. Железнодорожные паромы для Черного моря. Морской флот. 2007. № 6. С. 45–49.

49. Наставление по креплению груза для т/х «ПЕТРОВСК» ПР. № 002CNF001 – ЛМПЛ – 805. МИБ, 2005. 52 с.

50. Васильев В. Железнодорожные паромы для линии Ильичевск – Варна. Морской флот. 1976. № 12. С. 16.

51. Наставление по креплению генеральных грузов при морской перевозке для т/х «Герои Плевны». CARGO SECURING MANUAL for m/v "Geroi Plevny" № 2512.02. Мин. транспорта Украины. Гос. департамент морского и речного транспорта. Одесса, 1997. 51 с.

52. Cargo secuaring menual transocean line a/s ms "Greifswald" – Germanischer Lloyd, 2001. P. 39.

53. Михайлова В. "Vilnius Seaways" вышел на черноморские линии. Порты Украины. 2013. № 6. С. 46–48.

54. Смородин А. Н. Ледокол для железной дороги. Железнодорожный транспорт. 2013. № 6. С. 71–73.

55. Ломоносов Ю. М. Перевозка паровозов $Э^{ш}$ и $Э^{шг}$ из-за границы. Берлин, 1923.

56. Наплавные мосты, паромные и ледяные переправы / В. И. Телов, И. М. Кануков ; под ред. В. И. Телова. М. : Транспорт, 1978. 384 с.

57. Телов В. И. Наплавные мосты и паромные переправы : монография. М. : Маршрут, 2006. 423 с.

58. http://www.unece.org

59. Нейдинг М., Короткий Р. Морские паром. Наука и жизнь. – 1978. – № 8. – С. 25–28.

60. Йовчев Н. Мост дружбы. Морской флот. 1984. № 4. С. 52–53.

61. Кузьмин Г., Егоров Г. «Плавучий мост» Калининград – Усть-Луга. Морской флот. 2006. № 6. С. 59–63.

62. А. Л. Суда для перевозки тяжеловесов. Морской флот. 1943. № 5–6. С. 35–36.

63. 2016. Морской железнодорожно-автомобильно-пассажирский паром "Petersburg" [onlinecit.: 2016-02-03]. Available from: http://www.korabli.eu/galleries/oboi/grazhdanskie-suda/petersburg

64. 2006. Вчера в Балтийске успешно проведены испытания подъемно-переходного моста и пробная накатка вагонов на железнодорожный паром на железнодорожно-автомобильном паромном комплексе [onlinecit.: 2006-06-16]. Available from: https://www.mintrans.ru/press-center/news/2296

65. Клоченко Н. Паром «Клайпеда», Морской флот. 1988. № 5. С. 27–31.

66. Ветер и волны в океанах и морях: справочные данные / под. ред. И. Н. Давидана. Л. : Транспорт, 1974. 360 с.

67. Благовещенский С. Н. Справочник по статике и динамике корабля. В двух томах. Изд. 2-е. перераб. и доп. Том 2. Динамика (качка) корабля / С. Н. Благовещенский, А. Н. Холодилин. Л. : Судостроение, 1975. 176 с.

68. Забезпечення надійності роботи та збереження пасажирських і вантажних вагонів при перевезенні на поромах. Звіт з НДР. № держ. р. 0107U000340. 2008. 176 с.

69. Візняк Р. І. Підвищення ефективності взаємодії залізничного і морського транспорту в умовах міжнародних поромних перевезень. Грант Президента України для підтримки наукових досліджень молодих учених.-дог. Ф 26/424–2008 від 31.07.08. № держ. р. 0108U088652. 2008. 104 с.

70. Ловська А. О. Удосконалення несучих конструкцій кузовів напіввагонів для підвищення надійності їх кріплення на залізничних поромах : дис. на здобуття наукового ступеня канд. техн. наук : спец. 05.22.07 – рухомий склад залізниць та тяга поїздів. Харків, 2013. 209 с.

71. Крылов А. Н. Качка корабля. М. : Воениздат, 1938.

72. Шиманский Ю. А. Динамический расчет судовых конструкций. Л. : Государственное издательство судостроительной промышленности, 1963. 444 с.

73. Луговский В. В. Динамика моря: Избр. вопросы связ. с учением мореходности корабля : учебник для втузов по специальности «Гидроаэродинамика». Л. : Судостроение, 1976. 199 с.

74. Вершинский С. В., Данилов В. Н., Хусидов В. Д., Динамика вагона : учебник для вузов ж.-д. трансп.; под ред. С. В. Вершинского. 3-е изд., перераб. и доп. М. : Транспорт, 1991. 360 с.

75. Бекенский Б. В. Практический расчет мореходных качеств судна. М., «Транспорт», 1955. 264 с.

76. Маков Ю. Л. Качка судов. Калининград, «КГТУ», 2007. 321 с.

77. Дьяконов В. MATHCAD 8/2000 : специальный справочник. СПб. : Питер, 2000. 592 с.

78. Кирьянов Д. В. Mathcad 13 [Текст]. СПб. : БХВ – Петербург, 2006. 608 с.

79. Землезин И. Н. Методика расчета и исследования сил, действующих на вагон при транспортировке на морских паромах. М. : Транспорт, 1970. 104 с.

80. Лукин В. В. Шадур Л. А., Котуранов В. И., Хохлов А. А., Анисимов П. С. Конструирование и расчет вагонов. М. : УМК МПС России, 2000. 731 с.

81. ДСТУ 7598:2014. Вагони вантажні. Загальні вимоги до розрахунків та проектування нових і модернізованих вагонів колії 1520 мм (несамохідних). Київ, 2015. 162 с.

82. EN 12663–2. Railway applications - structural requirements of railway vehicle bodies. Part 2: Freight wagons. B., 2010. 54 c.

83. Визняк Р. И., Ловская А. А. Уточнение величин усилий, которые действуют на кузова вагонов при их перевозке железнодорожными паромами. Вестник ВНИИЖТа, 2013. № 2. С. 20–27.

84. Рачков А., Бубнов К., Евстифеев В. Морской паром «Сахалин». Морской флот. 1972. № 12. С. 41–44.

85. Судовой типовой паспорт для железнодорожных паромов. Верфь им. Матиаса Тезена. Висмар. 1987. С. 29.

86. Візняк Р. І., Ловська А. О. Визначення динамічних зусиль, які діють на кузова вагонів при перевезенні залізничним поромом в умовах хвилювання моря. 2013. № 2. С. 54–58.

87. Кабатченко И. М. Моделирование ветрового волнения. Численные расчеты для исследования климата и проектирования

гидротехнических сооружений : автореф. дис. на соискание ученой степени доктора географических наук: спец. 25.00.28 «Океанология». Москва, 2006. 41 с.

88. Ловська А. О. Дослідження випадкових коливальних процесів кузова напіввагону при перевезенні залізничним поромом в умовах хвилювання моря. Збірник наукових праць УкрДАЗТ. Харків : УкрДАЗТ, 2014. Вип. 149. С. 67–71.

89. Земляновский Д. К. Устойчивость движения и рыскливость судов. М. : Транспорт, 1976. 95 с.

90. Ловська А. О. Особливості визначення зусиль, що діють на вагон при його взаємодії з багатообертовими засобами закріплення залізнично-поромних суден. Збірник наукових праць ДонІЗТ. Донецьк : ДонІЗТ, 2011. Вип. 25. С. 157–161.

91. Ван дер Варден Б. А. Математическая статистика. М. : Иностранная литература, 1960. 450 с.

92. Вентцель Е. С., Овчаров Л. А. Теория вероятностей и ее инженерные приложения : учеб. пособие для втузов. 2-е изд., стер. М. : Высш. шк., 2000. 480 с.

93. Гмурман В. Е. Теория вероятностей и математическая статистика : учеб. пособие для вузов. М. : Высшая школа, 2003. 479 с.

94. Коваленко И. Н., Филиппова А. А. Теория вероятностей и математическая статистика. М. : Высшая школа, 1982. 256 с.

95. Пугачев В. С. Теория вероятностей и математическая статистика : учеб. пособие. 2-е изд., исправл. и дополн. М. : ФИЗМАТЛИТ, 2002. 496 с.

96. Масленников А. М. Расчет строительных конструкций методом конечных элементов. Л. : ЛИСИ, 1977. 71 с.

97. Метод конечных элементов в проектировании транспортных сооружений / под ред. Городецкого А. С. М. : Транспорт, 1981. 143 с.

98. Галлагер Р. Метод конечных элементов. М. : Мир, 1984. 428 с.

99. Алямовский А. А. Solid Works / COSMOS Works 2006–2007. Инженерный анализ методом конечных элементов. М. : ДМК, 2007. 784 с.

100. Прерис А. М. SolidWorks 2005/2006. Учебный курс. Питер, 2006. 528 с.

101. Прохоренко В. П. SolidWorks 2005. Практическое руководство. М. : ООО «Бином–Пресс», 2006. 512 с.

102. Шам Тику. Эффективная работа SolidWorks 2005. Официальное руководство. Питер, 2006. 720 с.

103. Руденко В. М. Математична статистика. Киев, 2012. 304 с.

104. Кобзарь А. И. Прикладная математическая статистика. Москва, 2006. 816 с.

105. Alena Lovska. Research of dynamic loads acting on the supporting structures of car bodies in train ferries. Metallurgical and mining industry – 2016. № 4. P. 34–41.

106. Землезин И. Н. К оценке нагрузок распора сыпучих грузов в условиях транспортировки вагонов на морских паромах. Сб. «Исследование динамики вагонов». Труды ЦНИИ МПС. Вып. 307. М. : Транспорт, 1965. С. 37–63.

107. Рабинович И. М. Основы строительной механики стержневих систем. Ч. II. Госстройиздат, 1954.

108. Зенков Р. Л. Механика насыпных грузов. М. : Машиностроение, 1964. 250 с.

109. Синельников В. В. Развитие метода Кулона при определении давления сыпучего тела. Труды МИИТа. Вып. 69. Трансжелдориздат, 1946. 323 с.

110. Ловська А. О. Визначення зусиль розпору насипного вантажу на стіни кузова напіввагону при перевезенні залізничним поромом. Збірник наукових праць УкрДАЗТ. Харків : УкрДАЗТ. 2014. Вип. 143. С. 54–57.

111. Шиманский А. О., Путято А. В. Конечно-элементное моделирование нагруженности резервуаров для транспортирования нефтепродуктов. Гомель, БелГУТ, 2013. 6 с.

112. Вагоны : учеб. для ВУЗов ж.-д. трансп. / под ред. Л. А. Шадура. 3-е изд., перераб. и доп. М. : Транспорт, 1980. 139 с.

113. Шевченко В. В., Горбенко А. П. Вагоны промышленного железнодорожного транспорта. К. : Вища школа, 1980. 224 с., ил.

114. Богомаз Г. И., Мехов Д. Д., Пилипченко О. П., Черномашенцева Ю. Г. Нагруженность контейнеров-цистерн, расположенных на железнодорожной платформе, при ударах в автосцепку. Збірник наукових праць «Динаміка та керування рухом механічних систем» – Київ : АНУ, Інститут технічної механіки, 1992. С. 87–95.

115. Кривовязюк Ю. П. Оценка эквивалентной нагруженности четырехосных железнодорожных цистерн с жидкими грузами различной плотности при продольных ударах : дис. на соискание ученой степени канд. техн. наук : спец. 05.22.07 «Подвижной состав железных дорог и тяга поездов». Днепропетровск, 1986. 157 с.

116. Правила перевозок опасных грузов. К соглашению о международном железнодорожном грузовом сообщении. Том 3. ОСЖД, 2011. 531 с.

117. Шмаков М. Г. Специальные судовые устройства. Л. : Судостроение, 1975. 344 с.

118. Alyona Lovska, Oleksij Burlutski, Oleksij Fomin, Mykola Gorbunov, Gintautas Bureika, Stasys Steišūnas, Gediminas Vaičiūnas. The improved carrying structure of a passenger car for the appropriate strength in train ferry transportation // Current problems in rail vehicles – PRORAIL 2019, September 17–19, 2019. Žilina, Slovakia. P. 17–25.

119. Суколенов А. Е. Захариев Э., Гутин И. Г. и др. Международная паромная переправа Илличевск – Варна. М. : Транспорт, 1989. 103 с.

120. Банди Б. Методы оптимизации. Вводный курс / пер. с англ. М. : Радио и связь, 1988. 128 с.

121. Моисеев Н. Н., Иванилов Ю. П., Столярова Е. М. Методы оптимизации. М. : Наука, 1978. 352 с.

122. Реклейтис Г., Рейвиндран А., Рэгсдел К. Оптимизация в технике: в 2-х книгах / пер. с англ. М. : Мир, 1989.

123. Шевченко В. В., Головко В. Ф. Дослідження операцій у виробництві, ремонті та експлуатації вагонів : навчальний посібник. Харків : УкрДАЗТ, 2006. 171 с.

124. Визняк Р. И., Ловская А. А. О сохранности грузовых вагонов. Железнодорожный транспорт, 2011. № 12. С. 48–49.

125. Устич П. А., Карпыч В. А., Овечников М. Н. Надежность рельсового нетягового подвижного состава. М. : ИГ «Вариант», 1999. 415 с.

126. ГОСТ 20259–80. Контейнеры универсальные. Общие технические условия. Введ. 1982–01–01. Москва : ИПК стандартов, 2002. 17 с.

127. ГОСТ 18477–79. Контейнеры универсальные. Типы, основные параметры и размеры. Введ. 1980–01–01. Москва : ИПК стандартов, 2004. 12 с.

128. ГОСТ 20527-82. Фитинги угловые крупнотоннажных контейнеров. Конструкция и размеры. Введ. 1983–01–01. Москва : ИПК стандартов, 2004. 9 с.

129. ГОСТ 31232-2004. Контейнеры для перевозки опасных грузов. Требования по эксплуатационной безопасности. Минск, 2005. 6 с.

130. Пат. 108214 Україна, МПК[7] B63B25 / 00. Вузол несучої конструкції кузова вагона для його закріплення відносно палуби залізнично-поромного судна : Пат. 108214 Україна, МПК (2015.01), B60P 7 / 08 (2006.01), B60P 7/135 (2006.01), B60P 3/06 (2006.01), B61F 1/12 (2006.01) Візняк Р. І., Ловська А. О. (Україна); Заявл. 21.05.2012; Опубл.10.04.2015. № 7. 4 с.

131. Візняк Р. І., Ловська А. О., Кеба Є. М. Розробка заходів щодо забезпечення збереження та адаптування конструкцій вагонів до їх надійної взаємодії з багатообертовими пристроями закріплення відносно палуб залізничних поромів. Збірник наукових праць ДонІЗТ. Донецьк : ДонІЗТ, 2010. Вип. 21. С. 110–119.

132. Візняк Р. І., Ловська А. О. Дослідження напружено-деформованого стану вагонів-платформ при перевезенні залізнично-поромним судном в умовах хвилювання моря та розробка заходів щодо забезпечення їх збереження. Збірник наукових праць УкрДАЗТ. Харків : ХарДАЗТ, 2011. Вип. 99. С. 47–54.

133. Fomin O., Lovska A., Kulbovskyi I., Holub H., Kozarchuk I., Kharuta V. Determining the dynamic loading on a semi-wagon when fixing it with a viscous coupling to a ferry deck. Eastern-European Journal of Enterprise Technologies. 2019. № 2/7 (98). P. 6–12.

134. Пат. 136743 Україна, МПК[7] Пристрій для закріплення вагона відносно палуби залізничного порому : Пат. 136743 Україна, МПК (2006), B60P 7/08 (2006.01), B60P 7/135 (2006.01), B60P 3/06 (2006.01), B63B 25/00 / А. О. Ловська, О. В. Фомін, І. І. Кульбовський, В. С. Харута (Україна); Заявл. 04.04.19; Опубл. 27.08.19. № 16.

135. Ловська А. О. Визначення навантаженості контейнерів у складі комбінованих поїздів при перевезенні залізничним поромом. Наука та прогрес транспорту. Вісник Дніпропетровського національного університету залізничного транспорту імені академіка В. Лазаряна. 2017. Вип. 6 (72). С. 49–60.

136. Lovska Alyona. Simulation of loads on the carrying structure of an articulated flat car in combined transportation. International Journal of Engineering & Technology. 2018. 7 (4.3). P. 140–146.

137. Oleksij Fomin, Alyona Lovska, Václav Píštěk, Pavel Kučera. Dynamic load computational modelling of containers placed on a flat wagon at railroad ferry transportation. VIBROENGINEERING PROCEDIA. 2019. Vol. 29. P. 118–123.

138. Ловська А. О. Дослідження динамічної навантаженості вагона-платформи з контейнерами при перевезенні на залізничному поромі. Залізничний транспорт України. 2017. № 2. С. 16–20.

139. Fomin O., Lovska A., Melnychenko O., Shpylovyi I., Masliye v V., Bambura O., Klymenko M. Determination of dynamic load features of tank containers when transported by rail ferry. Eastern-European Journal of Enterprise Technologies. 2019. № 5/7 (101). P. 19–26.

140. Oleksij Fomin, Alyona Lovska, Václav Píštěk, Pavel Kučera. Dynamic load effect on the transportation safety of tank containers as part of combined trains on railway ferries. Vibroengineering Procedia. 2019. Vol. 29. P. 124–129.

141. Ловська А. О., Рибін А. В. Моделювання навантаженості контейнера типорозміру 1СС при перевезенні на залізничному

поромі. Збірник наукових праць науково-практичної конференції здобувачів вищої освіти та молодих вчених «Логістичне управління та безпека руху на транспорті», 14–16 листопада 2019 року, м. Лиман. Сєвєродонецьк, 2019. С. 96–99.

142. Візняк Р. І., Ловська А. О., Пітенко С. О., Хоменко В. С. Експериментальні дослідження міцності кузовів вагонів при взаємодії їх з багатообертовими засобами закріплення залізничнопоромних суден. Вагонный парк. 2010. № 11. С. 4–7.

143. Райков И. Я. Испытания двигателей внутреннего сгорания. М. : Высш. шк., 1975. 320 с.

144. Содержание и реконструкция мостов / Под ред. Осипова В. О. М. : Транспорт, 1986. 327 с.

145. Тензометрия в машиностроении : справочное пособ. / Под ред. Р. А. Макарова. М. : Машиностроение, 1975. 288 с.

146. Финк К., Робрах Х. Измерения напряжений и деформаций. М. : Машгиз, 1961. 535 с.

147. Отливки стальные. Общие технические условия. ГОСТ 977-88. Действителен от 01.08.2004. М. : ИПК стандартов, 2004. 35 с.

148. Ермаков С. М., Жиглявский А. А. Математическая теория оптимального эксперимента. М. : Наука, 1987. 320 с.

149. Нефедов А. Ф., Высочин Л. Н. Планирование эксперимента и моделирование при исследовании эксплуатационных свойств автомобилей. Львов : Высш. шк., 1976. 160 с.

150. Хартман К., Лецкий Э., Шеффер В. Планирование эксперимента в исследованиях технологических процессов. М. : Мир, 1977. 552 с.

151. Мороз В. І., Суранов О. В., Братченко О. В., Логвіненко О. А. Особливості виникнення погрішностей тензометрування в дослідженнях механізмів газорозподілу чотиритактних дизелів. Зб. наук. праць. Харків : ХарДАЗТ, 2001. Вип. 49. С. 85–90.

152. Космин В. В. Основы научных исследований: Учебное пособие. М. : ГОУ «Учебно-методический центр по образованию на железнодорожном транспорте», 2007. 271 с.

153. Fomin Oleksij, Lovska Alyona, Anatoliy Horban, Valentyna Radkevych, Pavel Skok, Inna Skliarenko. Investigation of the dynamic loading of a body of passenger cars during transportation by rail ferry. EUREKA: Physics and Engineering, Number 4, 2019. P. 91–100.

154. Fomin O. V., Lovska A. O., Plakhtii O. A., Nerubatskyi V. P. The influence of implementation of circular pipes in load-bearing structures of bodies of freight cars on their physico-mechanical properties. Scientific Bulletin of National Mining University. 2017. No. 6. P. 89–96.

155. Oleksij Fomin, Juraj Gerlici, Alyona Lovskaya, Kateryna Kravchenko, Pavlo Prokopenko, Anna Fomina, Vladimír Hauser. Research of the strength of the bearing structure of the flat wagon body from round pipes during transportation on the railway ferry / MATEC Web of Conferences "Horizons of Railway Transport", 10th Year of International Scientific Conference, Vol. 235, 21 November, 2018.

156. Fomin O., Lovska A., Masliyev V., Tsymbaliuk A., Burlutski O. Determining strength indicators for the bearing structure of a covered wagon's body made from round pipes when transported by a railroad ferry / Eastern-European Journal of Enterprise Technologies. 2019. № 1/7 (97). P. 33–40.

157. Oleksij Fomin, Alyona Lovska, Václav Píštěk, Pavel Kučera. Strength determination of wagon bearing structures made of round pipes at railroad ferry transportation / Vibroengineering Procedia. 2019. Vol. 29. P. 100–105.

158. Fomin O., Lovska A., Daki O., Bohomia V., Tymoshchuk O., Tkachenko V. Determining the dynamic loading on an open-top wagon with a two-pipe girder beam / Eastern-European Journal of Enterprise Technologies. 2019. № 3/7 (99) – P. 18–25.

159. Fomin O., Lovska A., Chimshir V., Bukatova O., Yarenchuk L. Peculiarities of determining the bearing structure load of the body of articulated open wagon made of round pipes / IOP Conf. Series: Materials Science and Engineering, Vol. 708, 2019, 012009. doi:10.1088/1757-899X/708/1/012009.

160. Пат. 112239 Україна, МПК[7] Залізничний вагон-платформа: Пат. 112239Україна, МПК (2016.01), B61D 3/00, B61F 1/02, (2006.01), B61F 1/00, B61F 1/08 (2006.01). О. В. Фомін, А. О. Ловська (Україна); Заявл. 17.02.2015; Опубл. 10.08.2016. № 15. 4 с.

161. Пат. 111317 Україна, МПК[7] Напіввагон глуходонний: Пат. 111317 Україна, МПК (2016.01), B61D 3/00, B61D 3/16 (2016.01), B61D 17/00, B61D 17/18 (2006.01), B61F 1/02 (2006.01), B61F 1/08 (2006.01), B61F 1/00. О. В. Фомін, А. О. Ловська (Україна); Заявл. 18.09.2015; Опубл. 11.04.2016. № 7. 4 с.

162. Пат. 111572 Україна, МПК[7] Критий вагон: Пат. 111572 Україна, МПК (2016.01), B61D 3/00, B61F 1/00, B61F 1/02 (2006.01), B61F 1/08 (2006.01), B61D 17/04 (2006.01), B61D 17/08 (2006.01), B61D 17/12 (2006.01). О. В. Фомін, А. О. Ловська (Україна); Заявл. 18.09.2015; Опубл. 10.05.2016. № 9. 4 с.

163. Патент України на винахід № 118389, МПК (2006.01) B61F 1/02 (2006.01) B61F 1/10 (2006.01) B61D 7/00 Залізничний відкритий вагон-хопер / О. В. Фомін, М. І. Горбунов, А. О. Ловська, В. В. Фомін (Україна); власник: автори. № а 2017 01810; заявка 27.02.2017; заявка 26.06.2018; публ. 10/01.2019, Бюл. № 1/2019.

164. Пат. 134913 Україна, МПК[7] Вагон-платформа для перевезення контейнерів: Пат. 134913 Україна, МПК (2006), B61D 3/08 (2006.01), B61D 3/20 (2006.01). Ловська А. О., Фомін О. В., Бурлуцький О. М., Фоміна А. М. (Україна); Заявл. 26.12.2018; Опубл. 10.06.2019. № 11.

165. Пат. 138422 Україна, МПК[7] Ударно-тяговий прилад залізничного вагону: Пат. 138422 Україна, МПК (2006), B65G 11/16 (2006.01), B60G 11/18 (2006.01). Фомін О. В., Ловська А. О., Кульбовський І. І., Мельниченко О. І. (Україна); Заявл. 23.05.19; Опубл. 25.11.19 № 22.

166. Fomin Oleksii, Alyona Lovska, Gorban Anatoly. Historical aspects of construction and operation of train ferry routes. History of science and technology. 2021. Vol. 11, Issue 2. P. 351–382. doi: 10.32703/2415-7422-2021-11-2-351-382

NOTES

Izdevniecība “Baltija Publishing”
Valdeķu iela 62 – 156, Rīga, LV-1058
E-mail: office@baltijapublishing.lv

Iespiests tipogrāfijā SIA “Izdevniecība “Baltija Publishing”
Parakstīts iespiešanai: 2023. gada 21. jūlijs
Tirāža 300 eks.